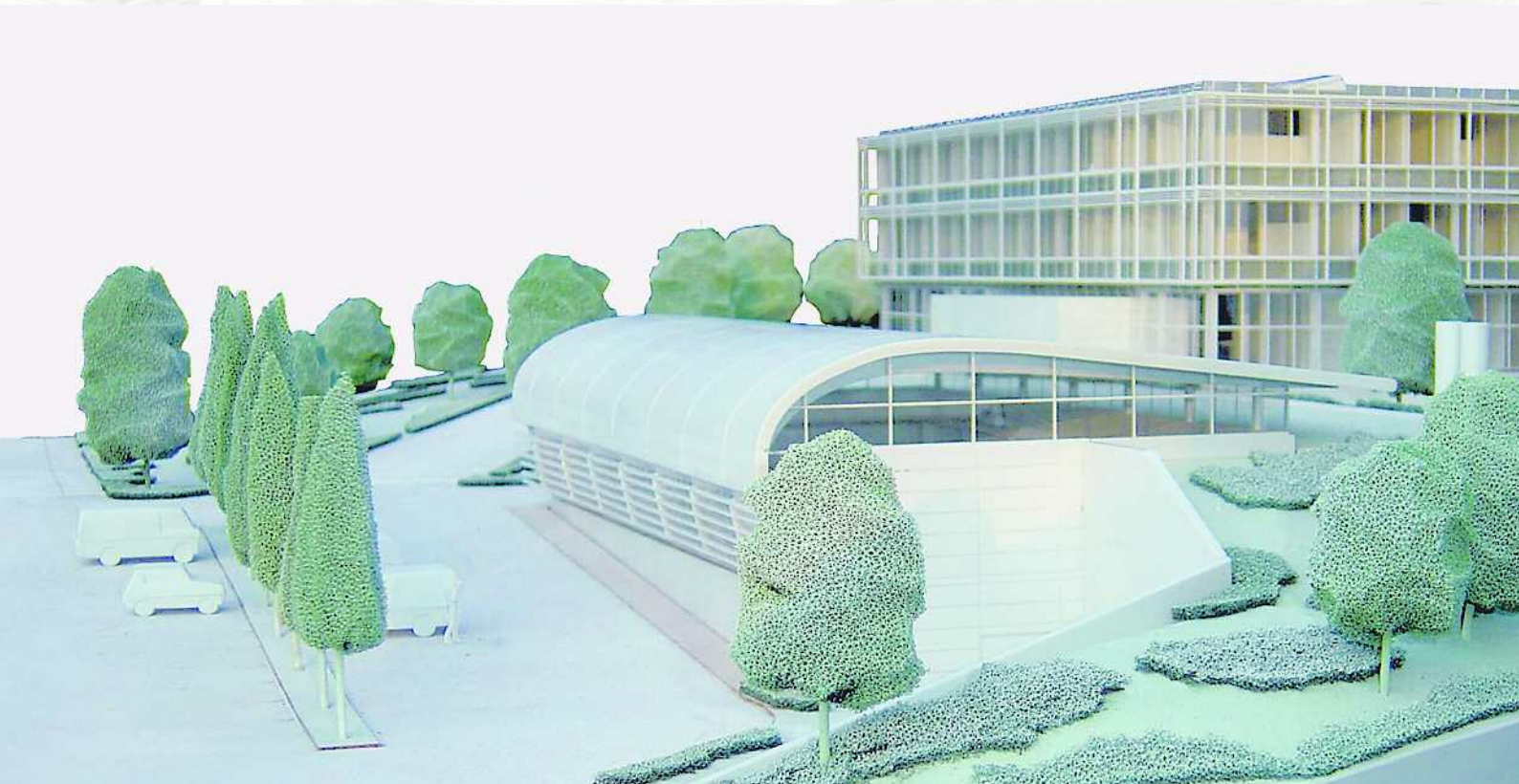




Max Planck Institute



**for Dynamics
and Self-Organization**

Research Report 2006

© Max Planck Institute for Dynamics and Self-Organization, Göttingen (www.ds.mpg.de). 2006

Editing: Dr. Kerstin Mölter
CAD-Drawings: Udo Schminke
Photos: Kai Bröking, Irene Böttcher-Gajewski, Will Brunner, Ragnar Fleischmann,
Peter Goldmann, Anna Levina, David Vincent, Stephan Weiss
Design/Layout: dauer design, Göttingen
Printed by: Goltze Druck, Göttingen

**Max Planck Institute
for Dynamics and Self-Organization
Research Report 2006**

DIRECTORS

Prof. Dr. Eberhard Bodenschatz (Managing Director)
Prof. Dr. Theo Geisel
Prof. Dr. Stephan Herminghaus

SCIENTIFIC ADVISORY BOARD

Prof. Dr. William Bialek, Princeton University, USA
Prof. Dr. David K. Campbell, Boston University, USA
Prof. Dr. Jerry P. Gollub, Haverford College, USA
Prof. Dr. Pierre C. Hohenberg, New York University, USA
Prof. Dr. Alexei R. Khokhlov, Moscow State University, Russia
Prof. Dr. Tim Salditt, Georg August University Göttingen, Germany
Prof. Dr. Boris I. Shraiman, University of California at Santa Barbara, USA
Prof. Dr. Uzy Smilansky, Weizmann Institute of Science, Israel
Prof. Dr. Sandra M. Troian, Princeton University, USA

1. Introduction 4

2. Departments

2.1 Nonlinear Dynamics

2.1.1 Overview **6**

2.1.2 People **7**

2.1.3 Projects

2.1.3.1 Pattern Formation and Self-Organization in the Visual Cortex **10**

2.1.3.2 Self-Organized Criticality in the
Activity Dynamics of Neural Networks **13**

2.1.3.3 Dynamics of Anomalous Action Potential
Initiation in Cortical Neurons **15**

2.1.3.4 Nonlinear Dynamics of Networks:
Spatio-Temporal Patterns in Neural Activity **17**

2.1.3.5 Quantum Graphs: Network Models for Quantum Chaos **20**

2.1.3.6 Random Matrix Theory and its Limitations **22**

2.1.3.7 From Ballistic to Ohmic Transport
in Semi-Conductor Nanostructures **25**

2.1.3.8 What are the Quantum Signatures of
Typical Chaotic Dynamics **28**

2.1.3.9 Topological Superdiffusion – A New Theory for
Lévy Flights in Inhomogeneous Environments **31**

2.1.3.10 Human Travel and the Spread of Modern Epidemics **34**

2.2 Dynamics of Complex Fluids

2.2.1 Overview **39**

2.2.2 People **40**

2.2.3 Projects

2.2.3.1 Wet Granular Matter and Irreversibility **42**

2.2.3.2 Statics and Dynamics of Wet Random Assemblies **44**

2.2.3.3 Wetting of Topographic Substrates **46**

2.2.3.4 Discrete Microfluidics **49**

2.2.3.5 Wetting and Structure Formation at Soft Matter Interfaces **52**

2.2.3.6 Membrane Assembly for Nanoscience **54**

2.2.3.7 Spectroscopy of Aqueous Surfaces **56**

2.2.3.8 Biological Matter in Microfluidic Environment **58**

2.2.3.9 Locomotion in Biology at Low Reynolds Number **61**

2.2.3.10 Colloids In and Out of Equilibrium **63**

2.3 Fluid Dynamics, Pattern Formation and Nanobiocomplexity

2.3.1 Overview **67**

2.3.2 People **68**

2.3.3 Projects

2.3.3.1 Particle Tracking Measurements in Intense Turbulence **70**

2.3.3.2 Development of Fluid Dynamics Measurement Techniques **72**

2.3.3.3 The Göttinger Turbulence Tunnel **75**

2.3.3.4 Polymer Solutions and Viscoelastic Flows **77**

2.3.3.5 Experiments on Thermal Convection **79**

2.3.3.6 Wax Modeling of Plate Tectonics **81**

2.3.3.7 Nonlinear Dynamics and Arrhythmia of the Heart **84**

2.3.3.8 Chemotaxis and Cell Migration **87**

2.3.3.9 The Cell Culture Laboratory –
Myocardial Tissue Engineering **91**

2.4 Associated Scientists

2.4.1 People **92**

2.4.2 Projects

2.4.2.1 Elementary Gas-Phase Reactions **93**

2.4.2.2 Mathematical Physics **95**

2.5 Publications

2.5.1 Nonlinear Dynamics (1996–2006) **98**

2.5.2 Dynamics of Complex Fluids (2003–2006) **109**

2.5.3 Fluid Dynamics, Pattern Formation and Nanobiocomplexity (2003–2006) **112**

2.5.4 Associated Scientists (2003–2006) **114**

3. Services and Infrastructure

3.1 Design and Engineering **118**

3.2 Computing Facilities and IT Service **120**

3.3 Facility Management **120**

3.4 Administration **121**

3.5 Library **121**

3.6 Outreach Activities **122**

1. Introduction

THE SELF-ORGANIZATION of systems far from equilibrium plays a key role in many fields of interest. Be it the pattern formation of a dewetting liquid film, the complex signaling of neurons in the brain, or even the collective dynamics of eddies in a thunderstorm cloud; a large number of intimately coupled entities often conspire to generate unanticipated structure and dynamics at higher levels of integration. The mission of the Max Planck Institute for Dynamics and Self-Organization (MPIDS) is the investigation of the physics of such phenomena. Founded in 2003 as the successor of the 80 year old Max Planck Institute for Fluid Dynamics, it combines expertise from fluid dynamics, soft condensed matter physics, and nonlinear dynamics. Presently, the institute has three departments, which tackle various aspects of non-equilibrium complex systems.

Considerable attention is devoted to pattern formation phenomena in media as different as convection in fluids, the visual cortex of the brain, plate tectonics of Earth, or the signaling of cell colonies. While the microscopic properties of the systems are quite disparate, certain aspects of the emerging structures are often strikingly similar. Finding the general principles underlying the communal-ity of the non-linear processes is at the center of this research.

The realm of life and biology intensively exploits such mechanisms. As a further complication, however, life is strongly influenced by discrete events (gene expression, mutations, etc.), has active components (molecu-

lar motors, transport, etc.), and operates in a stochastic or disordered environment. In addition, many biological processes evolve at the micron scale or below, where the molecular properties become important. The fluid dynamics of these systems is strongly influenced by large macromolecules or other self-assembling, often dynamical structures and components. Due to the small size, some aspects of the comparably simple continuous descriptions may break down, and molecular scale properties must be considered.

Our current research includes the application of concepts from self-organization to medicine (cellular signaling, neural brain dynamics, cardiac fibrillation, spread of epidemics), which necessitates a sometimes strongly interdisciplinary approach. The research programs of the departments are set up in collaboration with the Bernstein Center for Computational Neuroscience, the International Collaboration for Turbulence Research, and the faculties of Physics and Medicine at the University of Göttingen.

For the time being the institute is present at two separate locations. The departments of Theo Geisel and Stephan Herminghaus are located at the original campus of the MPI for Fluid Dynamics close to downtown Göttingen. The department of Eberhard Bodenschatz is accommodated at the Max Planck Institute for Biophysical Chemistry, adjacent to which the first part of our new building has already been completed. This includes the experimental hall, which will accommodate the turbulence wind tunnel and other fluid dy-

namics experiments, a computational facility, and the clean room. The latter will be instrumental for many of the micro-fluidic and nano-scale experiments, which are planned in the near future. The second (main) part of the building will provide space for all departments including services, and is scheduled for completion in 2009. It will reunite the in-

stitute in stimulating neighborhood to the Max-Planck Institute for Biophysical Chemistry and the Campus of the University.

The following pages give an introduction to the current research projects and the infrastructure of the institute.

Göttingen, May 2006

Prof. Eberhard Bodenschatz

Prof. Theo Geisel

Prof. Stephan Herminghaus

2. Departments

2.1 Nonlinear Dynamics

2.1.1 Overview

Theo Geisel

How do the myriads of neurons in our brain cooperate when we perceive an object or perform a task? How does the dynamics of networks in general depend on their topology? What are the dynamical properties of quantum mechanical networks and how can they be described semiclassically? How does the interplay of quantum mechanics and disorder shape the branching flows of the two-dimensional electron gas? Are there statistical principles underlying human travel and can they be used to forecast the geographical spread of epidemics?

Several of these questions, which among others, motivate our research address the complex dynamics of spatially extended or multicomponent nonlinear systems, which still reserve many surprises. For instance, in networks of spiking neurons we found unstable attractors, a phenomenon which would neither have been guessed nor understood without mathematical modelling and which many physicists consider an oxymoron. Under external stimulation the network can rapidly switch between these unstable attractors. They may play a functional role in the central nervous system by providing it with a high degree of flexibility to respond to frequently changing tasks.

This example illustrates the need and role of mathematical analysis for the understanding of many complex systems which nature presents us in physics and biology. The concepts and methods developed in nonlinear dynamics

and chaotic systems in recent times can now help us clarify the dynamics and function of spatially extended and multicomponent natural systems. On the other hand rigorous mathematical analysis of the dynamics of such systems often cannot rely on mainstream recipes, but poses new and substantial challenges. In particular, neural systems exhibit several features that make them elude standard mathematical treatment. These features include network communication at discrete times only and not continuously as in most cases in physics, significant interaction delays, which make the systems formally infinite-dimensional, and complex connectivities, which give rise to a novel multi-operator problem. For the latter, e.g., we devised new methods based on graph theory to obtain rigorous analytic results.

Graph theory is also applied in our work on quantum chaos, the same is true for random matrix theory, which we applied to the stability matrices of synchronized firing patterns of disordered neural networks. Neuronal spike trains may be considered as stochastic point processes and so may energy levels of quantum chaotic systems. This enumeration shows to which extent cross-fertilization among our various areas of research is possible. In fact, it has often been essential for our progress. The scientists of this department feel that the breadth of existing research activities and the opportunity of intense scientific exchange are key prerequisites for the success of our work.

They are also important for establishing and sustaining a culture of analytic rigor in theoretical work close to biological experiments.

Quite generally, theoretical studies of complex systems are most fruitful scientifically when analytical approaches to mathematically tractable and often abstract models are pursued in close conjunction with computational modeling and advanced quantitative analyses of experimental data. The department thus naturally has a strong background in computational physics and operates considerable computer resources. Research for which this is essential besides the network-dynamics mentioned above includes studies of pattern formation in the developing brain, of the dynamics of spreading epidemics, and of transport in mesoscopic systems.

When this department was created by the Max Planck Society in 1996, the focus of the institute was on mesoscopic systems. With the

opening of two new experimental departments in our institute this focus has changed; we are shifting our accents and tackling new subjects in the interest of a coherent research program. Besides, this department has initiated and hosts the federally (BMBF) funded Bernstein Center for Computational Neuroscience Göttingen, in which it cooperates with advanced experimental neuroscience labs in Göttingen. Our group is closely connected with the Faculty of Physics, it is financed to a large part by the Max Planck Society and to a smaller part by the University of Göttingen through its Institute for Nonlinear Dynamics. On the following pages we are describing some of our recent and ongoing research projects. As this department began its work already in 1996, an account of past research activities may be found in the publication list (2.5.1), which extends to the period from its creation in the year 1996 to the year 2006.

2.1.2 People



Prof. Dr. Theo Geisel

studied Physics at the Universities of Frankfurt and Regensburg, where he received his Ph.D. in 1975. He worked as a Postdoc at the MPI for Solid State Research in Stuttgart and at the Xerox Palo Alto Research Center before becoming a Heisenberg fellow in 1983. He was Professor of Theoretical Physics at the Universities of Würzburg (1988-1989) and

Frankfurt (1989-1996), where he also acted as a chairperson of the Sonderforschungsbereich Nichtlineare Dynamik. In 1996 he became director at the MPI for Fluid Dynamics (now MPI for Dynamics and Self-Organization). He also teaches as a full professor in the Faculty of Physics of the University of Göttingen and heads its Bernstein Center for Computational Neuroscience Göttingen.



Dr. Dirk Brockmann

is postdoctoral researcher in the Department of Nonlinear Dynamics. He studied theoretical physics and mathematics at Duke University, Durham N.C. and the Georg-August University in Göttingen.

Before he joined the group of Theo Geisel, where he received his doctorate in 2003, he worked in the group of Annette Zippelius at the

Institute for Theoretical Physics at the University of Göttingen.



Dr. Ragnar Fleischmann

studied physics at the Johann-Wolfgang-Goethe University in Frankfurt am Main and received his PhD in 1997. His thesis was awarded the Otto-Hahn-Medal of the Max-Planck-Society. From 1997 to 1999 he was Postdoc in the group of Theo Geisel at the Max-Planck-Institut für Strömungsforschung and from 1999 to 2000 in the group of Eric Heller at Harvard University.

Since 2000 he has worked as a scientific staff member in the Department for Nonlinear Dynamics and as deputy institute manager of the Max-Planck-Institute for Dynamics and Self-Organization.



Dr. Denny Fliegner

studied physics at the University of Heidelberg and received his doctoral degree in theoretical particle physics in 1997. From 1997 to 2000 he was a Postdoc at Karlsruhe University working on parallel computer algebra and symbolic manipulation in high energy physics. He joined the group of Theo Geisel at the Max-Planck-Institut für Strömungsforschung as an IT

coordinator in 2000. In 2003 he became head of the IT service group of the Max-Planck-Institute for Dynamics and Self-Organization.



Dr. J. Michael Herrmann

studied mathematical physics and computer science and has defended a doctoral thesis on artificial neural networks at Leipzig University. He did postdoctoral research at NORDITA (Copenhagen), RIKEN (Wako) and the Max-Planck-Institut für Strömungsforschung (Göttingen). Presently, he is Assistant Professor at the Institute of Nonlinear Dynamics of the

University of Göttingen and adjunct scientist at the Max Planck Institute for Dynamics and Self-Organization. Besides he is a member of the Center of Informatics at the University of Göttingen as well as a principal investigator at the Bernstein Center for Computational Neuroscience Göttingen.



Dr. Lars Hufnagel

received his diploma in mathematics from the University of Hagen. He studied physics at the Philipps-University in Marburg and conducted his diploma thesis at the Fritz-Haber-Institute of the Max-Planck Society in Berlin. In 1999 he joined the Max-Planck Institute for Dynamics and Self-Organization in Göttingen and received his doctorate in theoretical physics from the

Georg-August University in Göttingen. Since 2004 he has worked as a post-doctoral fellow at the Kavli-Institute for Theoretical Physics at the University of California at Santa Barbara.



Dr. Tsampikos Kottos

received his PhD in theoretical solid-state physics from the University of Crete in 1997. In 1997 he received a US European Office of Air Force Research and Development Fellowship. In the same year, he received the Feinberg Fellowship and joined the Quantum Chaos group of U. Smilansky at the Weizmann Institute of Science, Israel. In 1999 he moved to Germany as a

postdoctoral research fellow in the group of T. Geisel at the Max Planck Institute for Dynamics and Self-Organization in Göttingen. In 2005 he has become an Assistant Professor at Wesleyan University, USA and continues working with the Department of Nonlinear Dynamics as an adjunct scientist.



PD Dr. Holger Schanz

studied physics at the Technical University of Dresden and graduated in 1992. He worked towards his PhD in the groups of Werner Ebeling (Humboldt University Berlin) and Uzy Smilansky (The Weizmann Institute of Science, Rehovot, Israel) and received his doctorate from the Humboldt University in 1996. After two years as a Postdoc at the Max Planck Institute for Physics

of Complex Systems in Dresden, he joined the group of Theo Geisel at the Max-Planck-Institut für Strömungsforschung in Göttingen. Currently he is Assistant Professor at the Institute of Nonlinear Dynamics of the University of Göttingen, and adjunct scientist at the Max Planck Institute for Dynamics and Self-Organization.



Dr. Marc Timme

studied physics at the University of Würzburg, Germany, at the State University of New York at Stony Brook, USA, and at the University of Göttingen, Germany. He received an MA in physics in 1998 (Stony Brook) and a doctorate in theoretical physics in 2002 (Göttingen). After working as a postdoctoral researcher at the Max Planck Institute for Dynamics and Self-

Organization, Göttingen, from 2003 to 2005, he is currently a research scholar at the Center of Applied Mathematics, Cornell University. He is also a founding member of and a principal investigator at the Bernstein Center for Computational Neuroscience, Göttingen.



Dr. Fred Wolf

studied physics and neuroscience at the J.W.Goethe University in Frankfurt, where he received his doctorate in theoretical physics in 1999. After postdoctoral research at the MPI für Strömungsforschung (Göttingen) and the Interdisciplinary Center for Neural Computation of the Hebrew University of Jerusalem (Israel), he became a research associate at the MPI für

Strömungsforschung in 2001. Since 2001 he has participated in various research programs of the Kavli Institute for Theoretical Physics (Santa Barbara, USA). In 2004 he became head of the research group of Theoretical Neurophysics at the MPI for Dynamics and Self-Organization. He is a faculty member of the International Max Planck Research School Neurosciences and of the Center for Systems Neuroscience at Göttingen University.

pattern formation in physical systems far from equilibrium, it is natural to ask whether this process might be modeled by dynamical equations for macroscopic order parameters as often proved successful and instructive in simpler pattern formation problems.

Symmetries in visual cortical development

As a paradigmatic model system our studies are focusing on the development and the spatial structure of the pattern of contour detecting neurons in the visual cortex called the orientation preference map (OPM, see Figure 1b). Functional brain imaging has revealed that the spatial structure of OPMs is aperiodic but roughly repetitive with a characteristic wavelength in the millimeter range (see e.g. [4]) and that OPMs contain numerous singular points called pinwheel centers (see Fig. 1b).

In previous work, Wolf and Geisel demonstrated that basic symmetry assumptions imply a universal minimal initial density of pinwheel defects [3]. They also found, however,

that the defects generated initially are typically unstable and are decaying by pairwise annihilation in various models of visual cortical development. To solve the problem of pinwheel stability, subsequent studies have raised the hypothesis, that a reduced symmetry of the dynamics of visual cortical pattern formation may underlie the formation of stable pinwheel patterns [5,6]. In the proposed models of reduced symmetry, however, pinwheels generally crystallize in periodic spatial patterns that are clearly distinct from the patterns observed experimentally.

In recent work, we have therefore investigated conditions for the emergence of spatially nonperiodic OPMs theoretically. To this end, Wolf introduced an analytically tractable class of model equations [7], which was shown to possess solutions that qualitatively and quantitatively resemble the experimentally observed patterns. Its construction is based on the requirement that the visual cortex must develop detectors for contours of all orientations. Assuming a supercritical bifurcation of the pattern this turned out to be guaranteed near criticality by a novel permutation symmetry. This symmetry in addition implies the existence of a large number of dynamically degenerate solutions that are qualitatively very similar to OPMs in the visual cortex (Fig. 1a). Further analysis revealed that, judged by their pinwheel densities, these patterns even quantitatively resemble the experimentally observed OPMs (see Fig. 1c). The stability boundaries of various solutions were calculated in a generalized Swift-Hohenberg model incorporating long-range interactions, a key feature of visual cortical processing. Generically, long-range interactions were found to be essential for the stability of realistic solutions. Their existence and stability, however, turned out to be rather insensitive to full or reduced symmetries of the developmental dynamics [8].

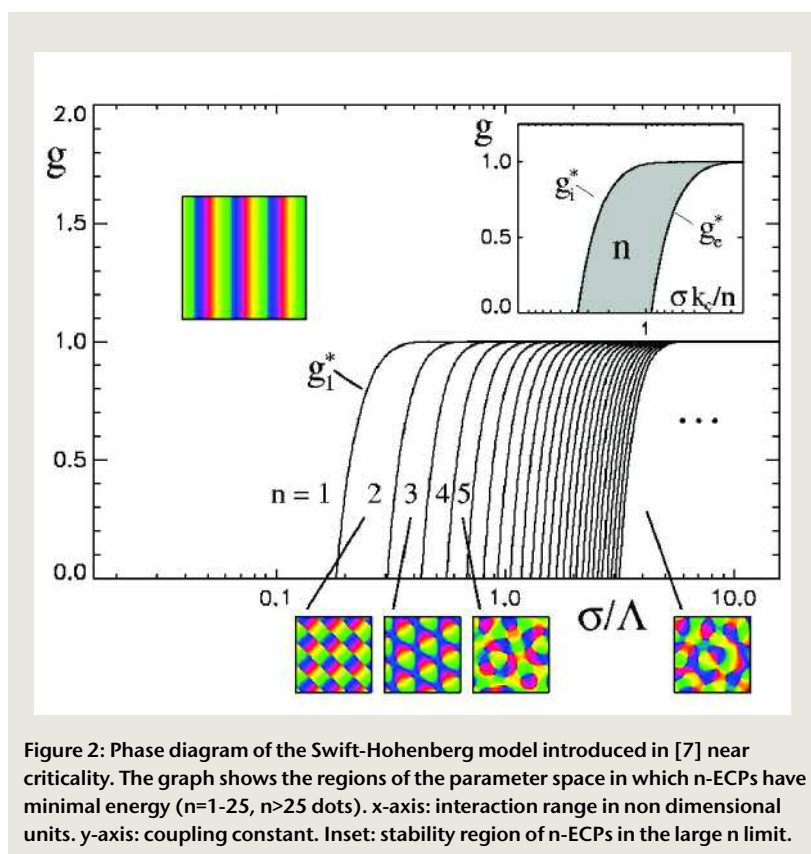


Figure 2: Phase diagram of the Swift-Hohenberg model introduced in [7] near criticality. The graph shows the regions of the parameter space in which n -ECPs have minimal energy ($n=1-25$, $n>25$ dots). x-axis: interaction range in non dimensional units. y-axis: coupling constant. Inset: stability region of n -ECPs in the large n limit.

Quantification of cortical column layout

Because these and related results indicate that the apparently complicated layout of visual cortical maps can be quantitatively ex-

plained by relatively simple model equations, substantial effort is dedicated to developing methods for the precise quantification of layout parameters from experimentally obtained brain imaging data. The layout of functional cortical maps exhibits a high degree of interindividual variability that may account for individual differences in sensory and cognitive abilities. By quantitatively assessing the interindividual variability of OPMs in the primary visual cortex using a newly developed wavelet based analysis method, we demonstrated that column sizes and shapes as well as a measure of the homogeneity of column sizes across the visual cortex are significantly clustered in genetically related animals and in the two hemispheres of individual brains [4,9]. Taking the developmental timetable of column formation into account, these observations indicate that essential control parameters of the dynamics of visual cortical pattern formation are tightly controlled genetically.

More recently, application of these methods led to the first demonstration of a dynamical rearrangement of cortical orientation columns

during visual development. In a study comparing the layout of orientation columns in two different visual cortical areas in kittens and cats we found that maps in the two areas exhibit matched column sizes at retinotopically corresponding positions in adult cats. In addition the data revealed that in kittens of various ages, column sizes progressively became better matched in the two areas over the course of visual cortical development [10].

Based on these methodological advances, we also started to characterize the statistics of pinwheel defects in collaboration with Len E. White (Duke University). Here it turned out that virtually all basic statistics of pinwheels in orientation maps are universal in a wide range of animals [11]. These findings are very surprising and beginning to shed a completely new light on the formation of cortical columns. Current model studies are addressing the conditions under which dynamical pattern formation can account qualitatively and quantitatively for the observed universal statistics.

- [1] M.C. Crair, *Curr. Opin. Neurobiol.* **9** (1999) 88.
- [2] L.C. Katz and J.C. Crowley, *Nat. Rev. Neurosci.* **3** (2002) 34.
- [3] F. Wolf and T. Geisel, *Nature* **395** (1998) 73.
- [4] M. Kaschube et al., *J. Neurosci.* **22** (2002) 7206.
- [5] H.Y. Lee, M. Yahyanejad and M.Kardar, *Proc. Natl. Acad. Sci.* **100** (2003) 16036.
- [6] P.J. Thomas and J.D. Cowan, *Phys. Rev. Lett.* **92** (2004) 188101.
- [7] F. Wolf, *Phys. Rev. Lett.* **95** (2005) 208701.
- [8] M. Schnabel et al., (in prep.).
- [9] M. Kaschube et al., *Eur. J. Neurosci.* **22** (2003) 7206.
- [10] M. Kaschube et al., (in prep.).
- [11] M. Kaschube et al., (in prep.).

2.1.3.2 Self-Organized Criticality in the Activity Dynamics of Neural Networks

J. Michael Herrmann

Anna Levina

U. Ernst (Bremen), M. Denker (Göttingen), K. Pawelzik (Bremen)

THE GUTENBERG-RICHTER law describes the relation between strengths and frequencies of earthquakes and thus an aspect of the complex processes in the upper terrestrial crust. It provides a precision which challenges the theoretical approaches to the statistics of events in other domains of the physics of complex systems including applications to finance as well as social and ecological systems. A neural system shares the characteristics of such systems in the sense that the extent of neural activities may span the full range from the level of single neural firing to the length scale of the whole nervous system. Most interesting are the cases where the events can be triggered by arbitrarily small driving forces or even by noise and spread in the system in an avalanche-like fashion.

The hallmark of criticality are power laws of the distribution of event sizes which indicate that large events occur much less frequently, but still sufficiently often in order to have a non-ignorable effect to the evolution of the system. In self-organized criticality the intrinsic dynamic of the system is such that the sys-

tem evolves into a state which is barely stable [1]. Small disturbances of the system will then lead to responses on all time and length scales and there is no need to fine-tune any parameters.

At least for a decade, theoretical neurophysics has aimed at describing the dynamics of the activity in the brain by models which show the effect of self-organized criticality [2], while at the same time maintaining a level of biological realism that supports the explanatory power of the approach.

The prediction of criticality in neural systems

Already for a globally coupled network of rather simple model neurons there are parameter values which give rise to a power-law distribution of the responses to a weak external stimulation. In Ref. [7] we have provided a finite-size analysis in order to be able to compare the theoretical results directly to the numerically obtained response distributions. The exact analytical treatment in that study, however, required a rather abstract neural

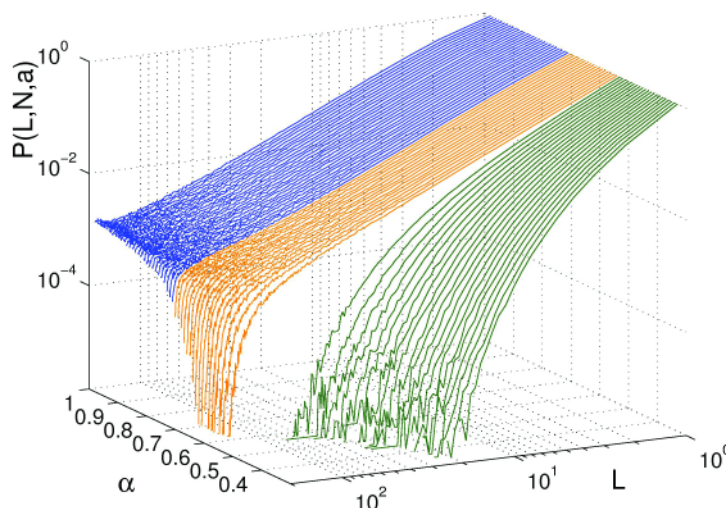


Figure 1: Probability distributions of avalanche sizes. With increasing maximal efficiency level we observe different regimes (a) in the subcritical, (b) the critical, $\alpha=0.53$, and (c) supra-critical regime, $\alpha=0.74$. Here the curves are temporal averages over 10^6 avalanches in a network of 100 neurons.

model. The more astonishing was the fact that about one year later an in-vitro experiments revealed (and acknowledged) a qualitatively identical picture for the local fields potential in rat cortex [4] and in a number of other cases in the following years.

The model lacked, however, the aspect of self-organization towards the critical case, but required rather a precise parameter tuning, while the real neurons returned to the power-law activity distribution even after strong changes in the biochemical milieu. A further elaboration in our modelling project demonstrated however that by an increase in biological detail the network easily achieved the required self-organizational capabilities. By the introduction of a realistic neurotransmitter dynamics [8] at the synapses the network exhibited a phase transition towards criticality and a very large range of the maximal synaptic efficiency where a nearly critical behaviour is present.

Towards a biological model

The biological function of self-organized criticality is much less understood than the physical mechanisms behind this phenomenon. Surely a stereotyped response to external stimuli would be less advantageous than a flexible reaction which may amplify barely noticeable events in the environment based on information which has been accumulated in the internal state of the brain. In addition such systems are expected to provide optimal capabilities for control and sequential information processing. A more simple explanation results from an effectiveness constraint. If the system adjusts its parameters such that each spike causes one of the target neurons to become consequently active and, on the other hand, the total activity is to remain bounded and stationary, then it can be proven within the framework of branching theory that the resulting activity distribution is indeed critical. Moreover from this a learning rule can be derived which controls the system towards criticality and which resembles biological learning rules [5].

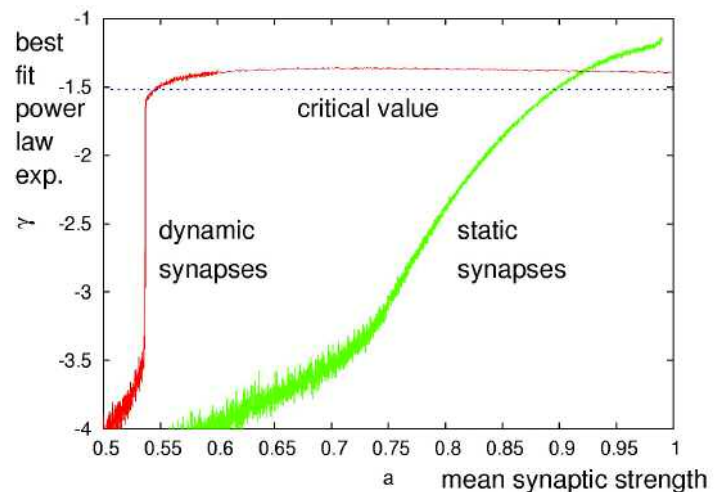


Figure 2: The best matching power-law exponent of the numerically obtained event size distribution. The red line represents the realistic model [6,8], while the green one stands for the abstract model [7]. Maximal synaptic efficiency α varies from 0.3 to 1.0 with step 0.001. The curves are temporal averages over 10^7 avalanches with $N=200$.

- [1] P. Bak, C. Tang, and K. Wiesenfeld, *Phys. Rev. Lett.* **59** (1987) 381.
- [2] A. Herz and J. J. Hopfield, *Phys. Rev. Lett.* **75** (1995) 1222.
- [3] Z. Olami, H. J. Feder and K. Christensen (1992). *Phys. Rev. Lett.* **68** (1992)1244.
- [4] J. Beggs and D. Plenz, *J Neurosci.* **23** (2003) 11167.
- [5] A. Levina, U. Ernst, and J. M. Herrmann, *Proceedings of Computational Neuroscience*, Edinburgh (2006).
- [6] A. Levina, J. M. Herrmann, and T. Geisel, *Advances in Neural Information Processing Systems* (2005).
- [7] C. W. Eurich, J. M. Herrmann, and U. Ernst, *Phys. Rev. E* **66** (2002).
- [8] M. Tsodyks, K. Pawelzik and H. Markram, *Neural Computation* **10** (1998) 821.

2.1.3.3 Dynamics of Action Potential Initiation in Cortical Neurons

Fred Wolf

Min Huang, Björn Naundorf, Andreas Neef
M. Volgushev (Bochum), M. Gutnick (Jerusalem, Israel)

NERVE CELLS COMMUNICATE with each other by sending out and receiving electrical impulses, called action potentials (APs). For a while it has become clear that the majority of these signals remain unanswered in the mammalian brain. Every second, a typical cell of the cerebral cortex receives thousands of signals from other nerve cells. In that same second, however, the cell only rarely decides – often not more than a dozen times – to send out an impulse itself.

Since the result of virtually all computational operations performed at the level of individual nerve cells are coded into sequences of action potentials, understanding the machinery that performs this encoding is of prime importance for deciphering the operation of cortical networks. To theoretically clarify how dynamical features of neuronal action potential generators shape the encoding properties of cortical neurons we are using concepts and methods from bifurcation theory and from the theory of stochastic processes. Quantifying key parameters of action potential initiation in cortical neurons in the living brain in collaboration with experimental neurophysi-

ologists, we recently discovered evidence for a cooperative activation of neuronal sodium channels. This non-canonical type of action potential initiation probably qualitatively expands the bandwidth of neuronal action potential encoding.

Dynamic response theory of fluctuation driven neurons

In the cerebral cortex, due to its columnar organization, large numbers of neurons are involved in any individual processing task. It is therefore important to understand how the properties of coding at the level of neuronal populations are determined by the dynamics of single neuron AP generation. To answer this question we studied how the dynamics of AP generation determines the speed with which an ensemble of neurons can represent transient stochastic input signals. Using a generalization of the θ -neuron, the normal form of the dynamics of Type-I excitable membranes, we calculated the transmission functions for small modulations of the mean current and noise amplitude.

Because of its qualitative dependence on modeling details previous theoretical studies focused mainly on the high frequency limit of these transmission functions [1-3]. Using a novel sparse matrix representation of the Fokker Planck equation to calculate the full transmission function we found that in the physiologically important regime up to 1 kHz the typical response speed is, however, independent of the high-frequency limit and is set by the rapidness of the AP onset [4] (see Fig. 1). In this regime modulations of the noise amplitude can be transmitted faithfully up to much higher frequencies than modulations in the mean input current, explaining recent experimental observations by Silberberg et al. [5].

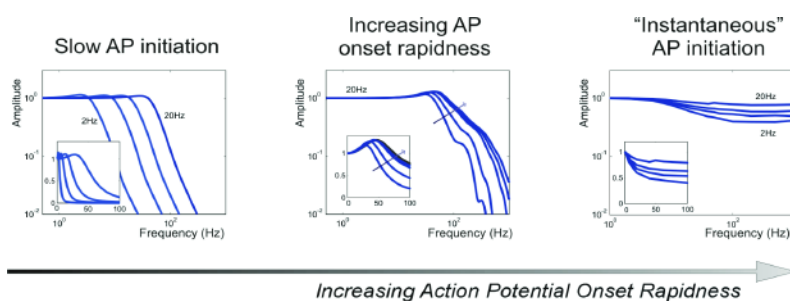


Figure 1: Effect of increasing the AP onset rapidness. With increasing onset rapidness, the transmission function shifts to larger values irrespective of the stationary firing rate. For the case of an instantaneous AP onset dynamics (fixed threshold), the transfer function remains finite in the high frequency limit. Curves are labelled for different stationary firing rates (modified from [4]).

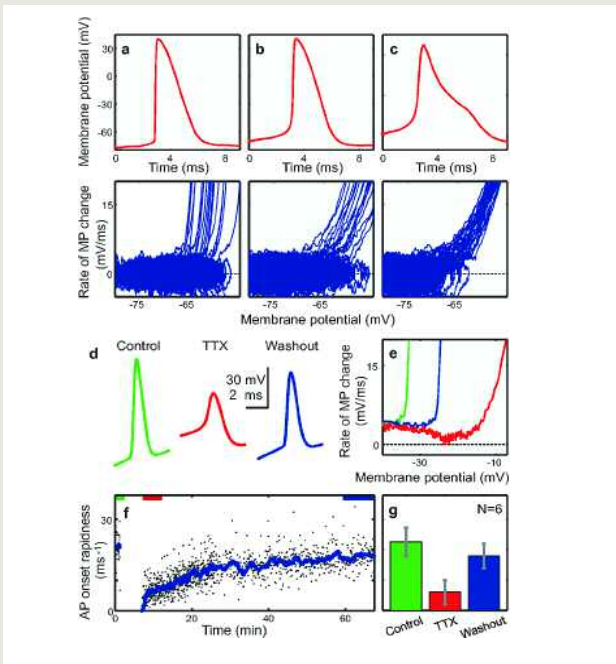


Figure 2: Cooperative activation of voltage-gated sodium channels can account for dynamics of AP initiation in cortical neurons. (a) Waveform (top) and phase plot (bottom) of APs elicited by fluctuating inputs in a conductance-based model incorporating cooperative activation of Na⁺ channels and closed-state inactivation. Both the AP onset potential variability and rapidness are comparable to in vivo recordings. (b) Same model, but without inter-channel coupling, and (c) with Hodgkin-Huxley-like channel activation. (d-g) Reducing the effective density of available Na⁺ channels by TTX application reversibly reduces the AP amplitude and onset rapidness in cortical neurons in vitro. AP waveforms (d) and phase plots of their initial parts (e). Time course of the AP onset rapidness (f) in a cortical neuron before, during and after the TTX application. (g) Reversible reduction of the AP onset rapidness by TTX in 6 neurons (error bars: s.e.m, modified from [6]).

The cooperative sodium channel activation hypothesis

As these results predict that apparently minor modifications of the AP generation mechanism can qualitatively change the nature of neuronal encoding an accurate quantitative description of the AP initiation dynamics operating in the intact brain became a focus of our research. In collaboration with Neurophysiologist Maxim Volgushev (Bochum University) we thus performed a quantitative analysis of the dynamics of action potential initiation in all major physiological classes of cortical neurons as observed in vivo and in brain slices. Unexpectedly, this study showed that key features of the initiation dynamics of cortical neuron action potentials – their very rapid initiation and the large variability of onset potentials – are outside the range of behaviors that can be modeled in the framework of the classical Hodgkin-Huxley theory [6]. To explore the possible origin of ‘anomalous’ action potential initiation dynamics we developed a new model based on the hypothesis of a cooperative activation of sodium channels. In this model, the gating of individual sodium

channels follows a scheme introduced by Aldrich, Corey, and Stevens [7]. It incorporates state-dependent inactivation from the open state and voltage-dependent inactivation from closed states. The key feature of our model is a coupling between neighboring channels: the opening of a channel shifts the activation curve of each channel to which it is coupled towards more hyperpolarized values, thus increasing its probability of opening. This model is able to reproduce the key features of cortical action potential initiation (Fig. 2). With strongly cooperative activation, voltage-dependent inactivation from closed states, and slow deinactivation (recovery from inactivation) of sodium channels, the simulated action potentials show both a large onset rapidness and large variability in onset potentials (Fig. 2a). Turning off the interchannel coupling made the onset dynamics much shallower, while leaving onset variability unaffected (Fig. 2b). Hodgkin-Huxley-type dynamics of action potential onset was recovered when inactivation and de-inactivation were set to be fast and voltage-independent (Fig. 2c). Figure 2 also shows results of a first

experimental test of the cooperative model. Assuming that channel interactions are distance-dependent in neuronal membranes, our model predicts that reducing the effective density of channels should weaken cooperativity, reduce the action potential onset rapidness and eventually lead to Hodgkin–Huxley type onset dynamics. We tested this prediction in vitro, recording action potentials while reducing the density of available sodium channels by the application of tetrodotoxin (TTX). As expected, TTX application led to a decrease in action potential amplitude (Fig. 2d). More importantly, it also led to a substantial reduction in the onset rapidness of action potentials (Fig. 2d, e) in all tested cortical neurons (Fig. 2g), as predicted by our

model. Current and planned studies are focusing on theoretically deriving critical predictions of the cooperative channel activation hypothesis to guide the next generation of neurophysiological experiments.

- [1] B. Lindner, L. Schimansky-Geier, *Phys. Rev. Letters* **86** (2001) 2934.
- [2] N. Brunel et al., *Phys. Rev. Lett.* **86** (2001) 2186.
- [3] N. Fourcaud-Trocme et al., *J. Neurosci.* **23** (2003) 11628.
- [4] B. Naundorf, T. Geisel, and F. Wolf, *J. Comput. Neurosci.* **18** (2005) 297.
- [5] G. Silberberg et al., *J. Neurophysiol.* **91** (2004) 704.
- [6] B. Naundorf, F. Wolf, and M. Volgushev, *Nature* **440** (2006) 1060.
- [7] R.W. Aldrich, D.P. Corey, and C.F. Stevens, *Nature* **306** (1983) 436.

2.1.3.4 Nonlinear Dynamics of Networks: Spatio-Temporal Patterns in Neural Activity

Marc Timme

Michael Denker, Markus Diesmann, Fred Wolf, Alexander Zumdieck
P. Ashwin (Exeter, UK)

New challenges for theory

SYNCHRONIZATION AND PRECISE spatio-temporal dynamics are ubiquitous in nature. Patterns of neural spikes that are precisely timed and spatially distributed constitute important examples: they have been observed experimentally in different neuronal systems [1,2] and are discussed as key features of neural computation. Their dynamical origin, however, is unknown. One possible explanation for their occurrence is the existence of feed-forward structures with excitatory coupling, so called synfire chains [3,4] which are embedded in otherwise random networks. Such stochastic models can explain the recurrence of coordinated spikes but do not account for the specific relative spike times of individual neurons.

As an alternative approach, we investigate how and under which conditions deterministic recurrent neural networks may exhibit pat-

terns of spikes that are precisely coordinated in time. Exact investigations of models for biological neural networks, however, require new mathematical tools for multi-dimensional systems, because neural systems exhibit several features that make them elude standard mathematical analysis. These features include e.g. network communication at discrete times only instead of continuously, as is the case in most systems of physics; significant delays in the interactions, which formally make the systems studied infinite-dimensional; complicated network connectivity where mean-field analyses fail; and strong heterogeneities, which require tools beyond those applicable to the homogeneous or close-to-homogeneous systems studied so far.

Time delays and unstable attractors

As a starting point towards addressing these challenges we investigated a very simple and

homogeneous neural network model, yet including interaction delays. We found the first example of a dynamical system that naturally exhibits *unstable* attractors, periodic orbits that are (Milnor) attracting and yet unstable [5]. They occur robustly in model neural networks which possess high symmetry and imply that the typical dynamics in such networks often is perpetual switching (Fig. 1) among states (periodic orbits) [6]. Given that the delayed interactions make this system formally infinite-dimensional, this problem also required mathematically rigorous analysis [7]. In systems similar to but less symmetric than the above we found that unstable attractors still exist, and moreover that they are the probable cause of another new phenomenon: long chaotic transients induced by dilution of the network connectivity [8]. This implies that in these neural networks, the transient phase and not the attractor dominate the dynamics. These studies also demonstrate an important fact commonly neglected in theoretical neuroscience: certain neural networks may not need to converge to stable state attractors in order to perform a computation, but computation might as well be performed in a transient phase, where it could be, moreover, much more flexible and more efficient. Therefore, in certain biological neural systems information processing might as well be based on unstable states [9].

**Networks of complicated connectivity:
Coexistence of states and their stability
problem**

It was widely believed that cortical networks with complicated (sparse random) connectivity necessarily also show complicated dynamics. In the same network, however, there can coexist a very different dynamical state [10], which despite irregular network connectivity displays very regular dynamics. For the case of completely regular (synchronous) dynamics we developed the first exact stability theory for networks of complex connectivities, where a novel multi-operator problem emerges that cannot be solved by standard methods. Developing new methods, partially

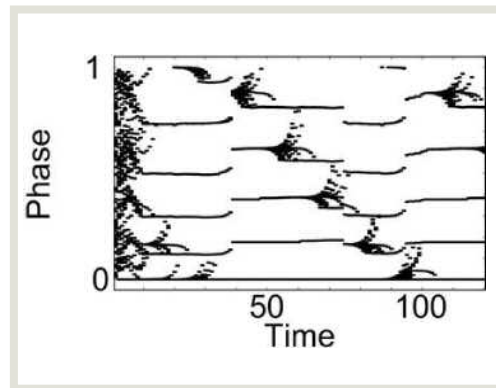


Figure 1: Perpetual switching in a system with unstable attractors. The figure shows the dynamics of the relative phases of $N=100$ neurons which are globally coupled in a homogenous network with time-delayed excitatory coupling. One finds a repetitive decay and regrouping of synchronized groups of neurons.

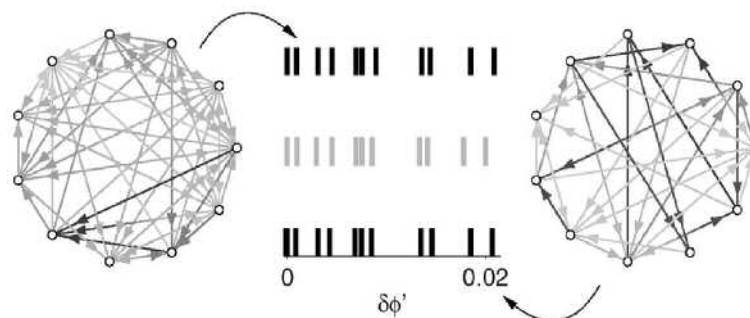
based on graph theoretical arguments, we could solve this multi-operator problem analytically for any given network.

**Strongly heterogeneous networks:
Do they still admit precise timing?**

As mentioned above, it is still an open question how spikes can be coordinated precisely in time into patterns that emerge in the dynamics of neural networks. The insights obtained in the above studies and the new methods that were stimulated have enabled us to address this question even for non-homogeneous systems: (i) We developed a method to predict short spike sequences from knowing the topology of the network and its inhomogeneous parameters [11]. The inverse problem was also solved: we designed networks which exhibit a prescribed spike sequence (Fig. 2). (ii) Recently we discovered a connectivity-induced speed limit to coordinating spike times in neural networks [12]. As expected, the speed of coordinating spike times – in the simplest case the speed of synchronization – increases with increasing coupling strengths. Surprisingly, however, these systems could not synchronize faster than at some speed limit (Fig. 3). We used Random Matrix Theory to derive an analytical prediction for the speed of the asymptotic network dynamics, explaining both the speed and its limit [13]. (iii) Very recently, we demonstrated that patterns of precisely timed spikes occur even in strongly heterogeneous networks with distributed delays and complicated connectivity [14].

In combination with many interesting studies

Figure 2: Designing inhomogeneous networks such that they exhibit prescribed patterns of spikes. One pattern of precisely timed spikes (center, grey) is prescribed; the task is to design networks that generate this pattern. The two statistically distinct networks shown on the left and on the right both exhibit such patterns (shown in black in the center panel). The networks have been calculated using a linear approximation in network space. The thickness of each connection indicates its strength of coupling.



of other research groups from all over the world these recent findings just constitute a few islands of knowledge contributing to a theory for the precise dynamics of spiking neural networks. For neural network dynamics it will be exciting to see the next steps towards uncovering the secrets that nature poses – and to further understand the distributed spatio-temporal code of the brain. More generally, interest in the dynamics of networks is currently growing and rapidly spreading into many fields of science. These activities are linked through their common mathematical foundations, which to a large extent are still to be developed. Non-standard features such as delays, complicated network connectivity, and heterogeneities will play a major role in many of the future investigations of network dynamics.

- [1] M. Abeles et al., *J. Neurophysiol.* **70** (1993) 1629.
- [2] Y. Ikegaya et al., *Science* **304** (2004) 559.
- [3] M. Diesmann, M.O. Gewaltig and A. Aertsen, *Nature* **402** (1999) 529.
- [4] Y. Aviel et al., *Neural Comput.* **15** (2003) 1321.
- [5] M. Timme, F. Wolf, and T. Geisel, *Phys. Rev. Lett.* **89** (2002) 154105.
- [6] M. Timme, F. Wolf, and T. Geisel, *Chaos* **13** (2003) 377.
- [7] P. Ashwin and M. Timme, *Nonlinearity* **18** (2005) 2035.
- [8] A. Zumdieck et al., *Phys. Rev. Lett.* **93** (2004) 244103.
- [9] P. Ashwin and M. Timme, *Nature* **436** (2005) 36.
- [10] M. Timme, F. Wolf and T. Geisel, *Phys.Rev.Lett.* **89** (2002) 258701.
- [11] M. Denker et al., *Phys.Rev.Lett.* **92** (2004) 074103.
- [12] M. Timme, F. Wolf, and T. Geisel, *Phys.Rev.Lett.* **92** (2004) 074101.
- [13] M. Timme, F. Wolf, and T. Geisel, *Chaos* **16** (2006) 015108.
- [14] R.-M. Memmesheimer and M. Timme, <http://arXiv.org: q-bio.NC/0601003> (2006).

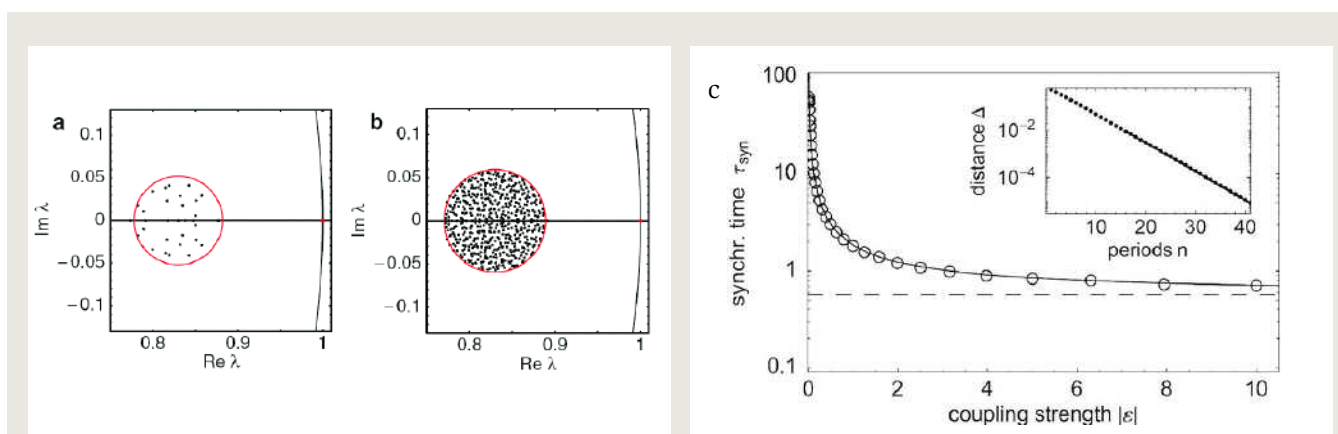


Figure 3: Speed limits to network synchronization. (a,b) The location of eigenvalues (black dots) in the complex plane of stability matrices of two networks agrees well with the prediction by Random Matrix Theory (circle). The rightmost point on the circle is an estimate for the second largest eigenvalue, determining the asymptotic speed of network synchronization. (c) Asymptotic synchronization time versus coupling strength (theory: solid line; numerical simulations: circles). The asymptote (dashed line) indicates a minimum characteristic synchronization time and thus a speed limit.

2.1.3.5 Quantum Graphs: Network Models for Quantum Chaos

Holger Schanz, Tsampikos Kottos

Marten Kopp, Mathias Puhlmann

G. Berkolaiko (Texas, USA), U. Smilansky (Rehovot, Israel)

IN QUANTUM CHAOS one tries to understand the implications of a chaotic classical limit for a quantum system. Despite the large variety of such systems, they have a number of universal physical properties in common. For example, a statistical analysis of the energy levels invariably shows striking similarities with the ›energies‹ obtained from the diagonalization of random matrices. For the Sinai billiard (left column of Fig. 1) this has been known for more than 20 years. Nevertheless, until recently no satisfactory explanation for this observation could be given. In the semiclassical approach to this problem the quantum density of states is expressed as a sum over classical periodic orbits by Gutzwiller's trace formula. One can then describe fluctuations in quantum spectra on the basis of information about the classical dynamics (sum rules and action correlations of periodic orbits).

Quantum graphs are minimal models which retain the trace formula and relevant properties of the contributing periodic orbits (Fig. 1, right). By contrast, other important features of classical chaos such as the deterministic nature of the dynamics and the generic coexistence of regular and chaotic trajectories are ignored by these models. In this way one gains numerical and analytical simplicity and can attack problems which are otherwise hard to solve. For example, the mentioned correlations between periodic orbits reduce to the simple fact, that on a graph different cycles can share the same length (Fig. 2) [1]. In the trace formula it is then necessary to sum the contributions from all these orbits coherently including all phases. We have developed methods to solve this combinatorial problem exactly for some simple networks [3] and approximately in a more general situation [5].

For the construction of a quantum graph one considers a network of B bonds which repre-

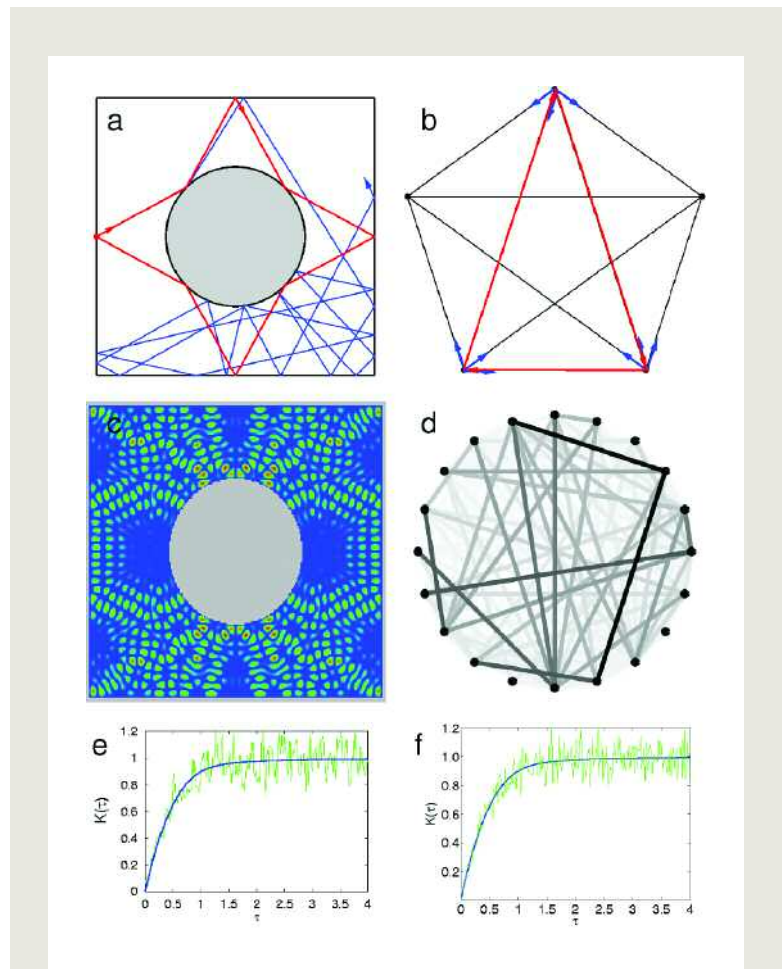


Figure 1: Comparison between the Sinai billiard (left) and a quantum graph (right). In a chaotic classical system all periodic orbits are unstable and small deviations in the initial conditions are amplified exponentially (a). The classical analogue of a quantum graph is a random walk on a network. Also in this case the probability to follow a given cycle decreases exponentially with the number of steps taken (b). Both models have stationary states with a discrete spectrum of allowed energies. For the Sinai billiard one finds these states by solving the Helmholtz equation in two dimensions (c). For the quantum graph diagonalization of a finite unitary matrix suffices. The resulting probability amplitudes to occupy a given bond are shown with a grey scale (d). The statistical properties of the quantum spectra are similar in both systems and follow closely the prediction of random-matrix theory (blue). This is shown in (e,f) for the spectral form factor (Fourier transform of the two-point correlation function).

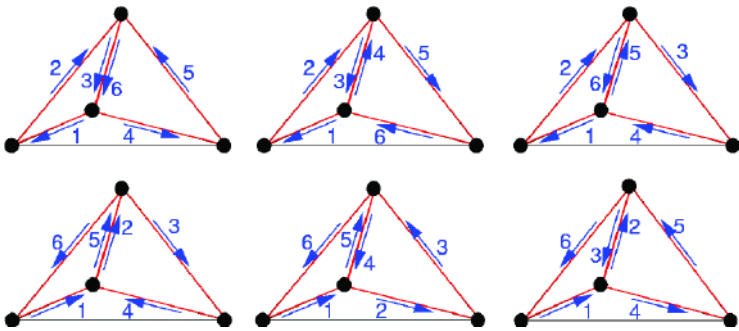


Figure 2: One can rearrange the itinerary of a periodic orbit on a network such that the new orbit passes through the same set of bonds in a different order. In the example shown here there are exactly six possibilities. In the trace formula the contributions from all these orbits must be added coherently when the spectral form factor or other quantum correlation functions are calculated [3,5,7,8].

sent the possible quantum states. Transitions can occur only between bonds which are connected at a vertex. The amplitudes of all possible transitions are collected in a B -dimensional matrix U which represents the time-evolution operator of the network. The classical version of the model is obtained when the elements of U are replaced by their modulus squared and interpreted as transition probabilities of a random walk. A statistical analysis of the spectrum of U yields results which are very similar to those found in chaotic systems if the underlying network is well connected and if there is some randomness in the phases of the transition amplitudes [1].

With a suitable choice for the transition amplitudes and the topology of the network the construction of a quantum graph is easily adapted to various physical situations. We have investigated the spectra and eigenfunc-

tions of isolated chaotic systems [1,5,6], the scattering properties of networks with attached leads [2,4,7,8] and also extended systems with disorder [3]. The questions addressed in these publications were quite diverse and included for example the semiclassical foundation of the universality in quantized chaotic systems [5], the quantum manifestation of substructures in the classical phase space [4] or the electronic transport through chaotic quantum dots [7]. Here we will discuss only one example in some detail, namely the phenomenon of ‘scarring’ in the wave functions of chaotic systems [6].

Fig. 1d shows one selected stationary state of a fully connected graph with 20 vertices (each pair of vertices is connected by one bond). Although there are some quantum fluctuations, the state essentially covers the whole network. However, this is not typical. Most eigenstates of the network live on a small

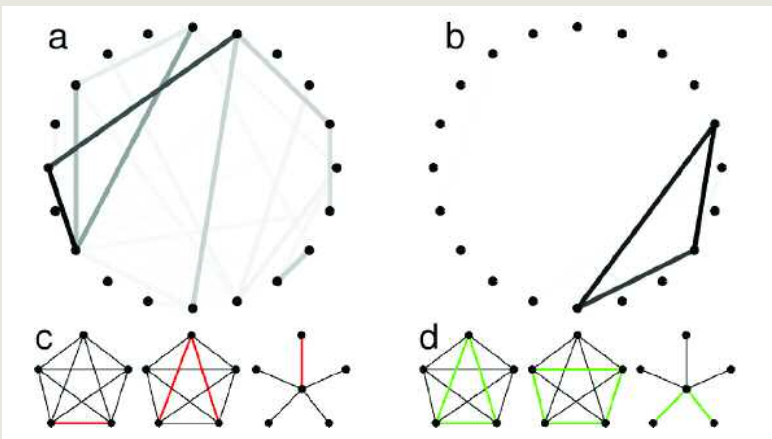


Figure 3: Most stationary states of a quantum graph occupy only a small fraction of the network. The majority of states are similar to the example shown in (a). Eigenstates which are restricted to a periodic orbit are called scars (b). The enhanced localization in (a) is due to the orbits shown in (c). These orbits are short and relatively stable. However, strong scarring is observed exclusively on the orbits shown in (d) although they are very unstable. Relevant is here that to each vertex along the orbit at least two scarred bonds are connected unless the vertex has degree one. Note that the v-shaped orbit falls into the first or the second group according to the topology of the network (fully connected vs. star graph).

fraction of the 380 available bonds and look similar to Fig. 3a. Sometimes one even observes states which are almost completely restricted to a triangle or some other short periodic orbit on the network. This phenomenon is not an artifact of quantum graphs. It had been observed before in many other chaotic quantum systems and is called scarring of wave functions by periodic orbits. The enhanced localization of eigenstates can also be seen in experiments. For example, scarring leads to strong fluctuations of the conductance of semiconductor quantum dots as a function of energy. The conventional theory of scarring predicts enhanced localization on short and relatively stable periodic orbits. However, this theory applies only to an average over a large number of states with similar energy while the properties of individual states remain unknown. Quantum graphs are no exception in this respect. The increased localization observed in the majority of states can be explained quantitatively by the influence of period-two orbits which bounce back and forth between two vertices. Therefore it was surprising that the states with the strongest localization correspond to triangu-

lar orbits while there are almost no states which are localized on a single bond. We have analyzed this behavior in detail and found a topological criterion for strong scarring in individual states which does not involve the stability exponent of the orbit (Fig. 3c-d). In this way we have demonstrated that enhanced average localization due to short orbits and strong scarring are two completely unrelated phenomena. Moreover, our theory allows to predict the energy and the location of strong scars in individual eigenstates of quantum graphs.

- [1] T. Kottos and U. Smilansky, *Phys. Rev. Lett.* **79** (1997) 4794.
- [2] T. Kottos and U. Smilansky, *Phys. Rev. Lett.* **85** (2000) 968.
- [3] H. Schanz and U. Smilansky, *Phys. Rev. Lett.* **84** (2000) 1427.
- [4] L. Hufnagel, R. Ketzmerick and M. Weiss, *Europhys. Lett.* **54** (2001) 703.
- [5] G. Berkolaiko, H. Schanz, and R. S. Whitney, *Phys. Rev. Lett.* **88** (2002) 104101.
- [6] H. Schanz and T. Kottos, *Phys. Rev. Lett.* **90** (2003) 234101.
- [7] H. Schanz, M. Puhlmann, and T. Geisel, *Phys. Rev. Lett.* **91** (2003) 134101.
- [8] M. Puhlmann et al., *Europhys. Lett.* **69** (2005) 313.

2.1.3.6 Random Matrix Theory and its Limitations

Tsampikos Kottos, Holger Schanz

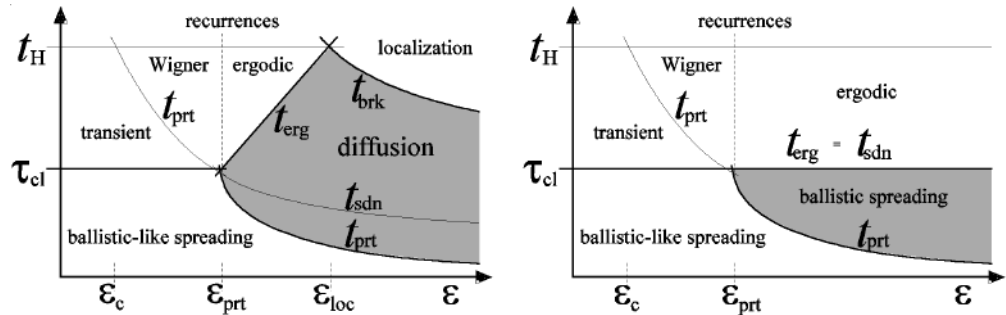
Moritz Hiller, Antonio Méndez-Bermúdez, Alexander Ossipov, Matthias Weiss
D. Cohen (Beer-Sheva, Israel), F. M. Izrailev (Puebla, Mexico), U. Smilansky (Rehovot, Israel)

RANDOM MATRIX THEORY (RMT) has become a major theoretical tool in so-called quantum chaos studies. In fact RMT has been applied fruitfully to other areas of physics ranging from solid-state to nuclear atomic and molecular physics [1] to neural networks [2]. The study of RMT models has been initiated by Wigner and it has almost become a dogma that this theory captures the *universal* properties of systems with underlying classical chaotic dynamics. However, the applicability of RMT is limited. What are these limitations and can we go beyond them? An answer to

this question is essential for any meaningful application of RMT regarding real physical systems such as driven quantum dots or mesoscopic open devices. Also, it should be remembered that RMT is commonly regarded as a reference case for comparison whenever an actual physical system is considered.

The past quantum chaos literature was strongly focused on understanding the interplay between universal (RMT-like) and non-universal (semiclassical) features as far as spectral properties are concerned. However, the study of spectral statistics is just the lower

Figure 1: A diagram that illustrates the various time scales in ›wavepacket dynamics‹ [3,4], depending on the strength of the perturbation ϵ . Here, ϵ_c is the perturbation needed to mix two nearby levels (hence related with Δ_b) while ϵ_{prt} is the perturbation needed to mix levels within the bandwidth Δ_b . The diagram on the left refers to an RMT model, while that on the right is for a quantized system that has a classical limit. The two cases differ in the non-perturbative regime (large ϵ): In the case of a quantized model we have a genuine ballistic behavior which reflects detailed Quantum Classical Correspondence, while in the RMT case we have a diffusive stage. In the latter case the timescale t_{sdn} marks the crossover from reversible to non-reversible diffusion.



level in the hierarchy of challenges to understand quantum systems. The two other levels are: studies of the shape of the eigenstates, and studies of the generated dynamics. The latter two aspects had been barely treated prior to our studies.

Recognizing this need, we have undertaken the task of investigating the validity of RMT in quantum dynamics studies. In this respect, a variety of dynamical scenarios has been investigated: wavepacket dynamics (see Fig. 1) [3,4], persistent driving [5], quantum dissipation due to interaction with chaos [6], and time reversal (fidelity) schemes [7]. In all these cases we have found that, depending on the driving strength, quantized chaotic systems have an adiabatic, a perturbative, and a non-perturbative regime. The distinction between these three regimes is associated with the existence of two energy scales: the mean level spacing $\Delta \sim \hbar^d$, and the bandwidth $\Delta_b \sim \hbar/\tau$ where τ is the classical correlation time that characterizes the chaotic dynamics and d is the dimension of the limit. In the $\hbar \rightarrow 0$ limit $\Delta \ll \Delta_b$. In the quantum chaos literature, Δ_b is known as the non-universal energy scale while in the context of ballistic quantum dots this energy scale is known as the *Thouless energy*.

We investigated the effects of Δ_b in the frame of quantum dynamics. We have found that while the dynamics in the former two regimes shows universal features which can be described by RMT models, the latter regime is non-universal and reflects the underlying semiclassical dynamics (see Fig. 1). Furthermore, for RMT models (suitable to describe disordered systems or many body interacting

fermions) we have found a ›strong‹ non-linearity in the response, due to a *quantal non-perturbative effect* [3,5]. Having established the limitations of RMT modeling our current efforts are threefold: (a) to create non-perturbative theories that go beyond RMT considerations (main emphasis to the problem of quantum dissipation) (b) to extend our dynamics studies for systems with classical phase space where chaotic and integrable components co-exist and (c) to investigate quantum dynamics of interacting (Bose) many body systems.

At the same time we have made important progress in understanding the applicability of RMT to describe the statistical properties of scattering in complex systems. Particular attention was given to the time dependent aspects of scattering (like current relaxation – see Fig. 2 – and delay times) and to the statistical properties of resonance widths. Our aim was to go beyond the universal RMT predictions [8,9] by taking into account specific properties of the system like localization [10], diffusion [11], fractality of the spectrum [12], or geometry of the sample [10]. This research is relevant not only for understanding electron transport in mesoscopic disordered solids but also to other areas such as quantum optics, microwave transport through random media, and atomic physics. As an example we refer to the ›random laser technology‹ which relies heavily on the properties of short resonances which determine the behavior of lasing thresholds.

Having acquired knowledge of the statistical properties of resonances and delay times for various cases, we have recently analyzed the

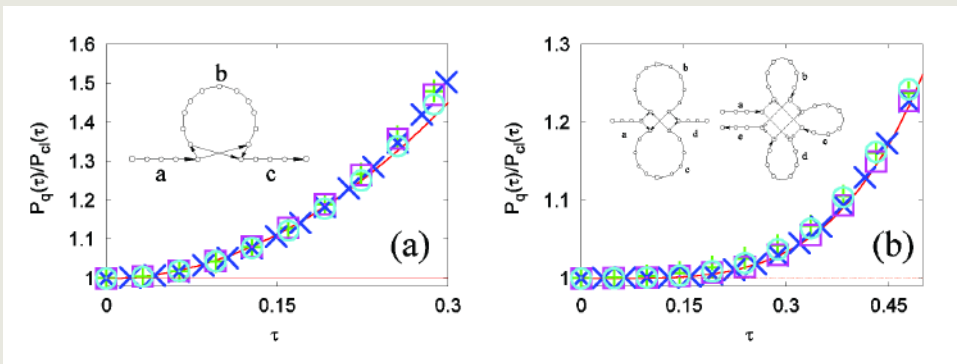


Figure 2: The ratio between quantum and classical survival probability has been computed for a ballistic quantum graph with $L=10$ attached decay channels and $G=500$ (+), 750 (x), 1000 (□), 2000 (o) internal states. It is shown as a function of the scaled time $\tau=t/G$. Quantum corrections are visible as deviations of the data from the horizontal line. For small τ they follow (a) $P(\tau)=[1+(L/2)\tau^2] P_{cl}(\tau)$ in the case with time-reversal symmetry and (b) $P(\tau)=[1+(L^2/24)\tau^4] P_{cl}(\tau)$ without as predicted by RMT. These semiclassical predictions account for the interference within the pairs of classical trajectories shown schematically in the insets. The two trajectories forming a pair are identical along the segments a,b,... but differ in the crossing regions (solid vs. dashed arrows) [9].

properties of random systems that exhibit a Metal-Insulator Transition (MIT) [10,13,14]. We showed that at the MIT both distributions are scale invariant, independent of the microscopic details of the random potential, and the number of channels. Theoretical considerations suggest the existence of a scaling theory for finite samples, and numerical calculations confirm this hypothesis [10,13].

Based on this, we gave a new criterion for the determination and analysis of the MIT (see Fig. 3) [10,13]. Recently, we have initiated a new research line [15], by studying the decay of the survival probability of a Bose-Einstein condensate which is periodically driven with a standing wave of laser light and coupled to a continuum. This study was performed in the frame of the nonlinear Gross-Pitaevskii

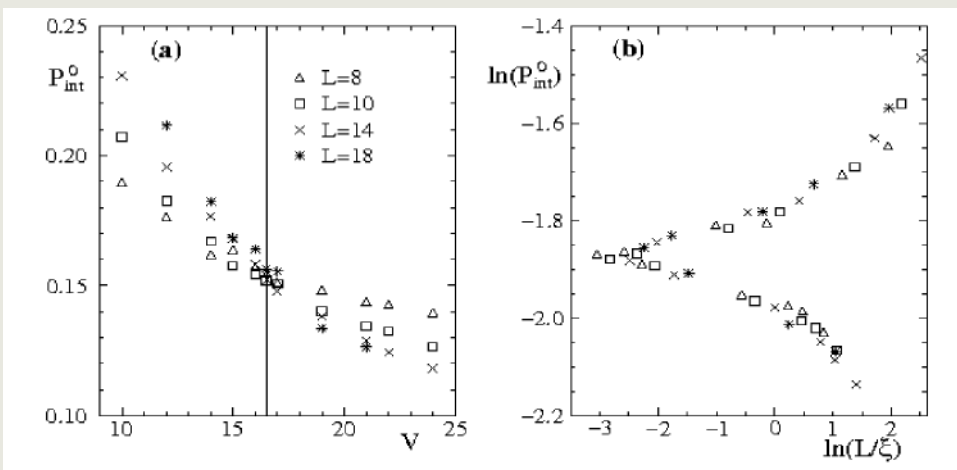


Figure 3: Integrated resonance width distribution $P_{int}(\Gamma_0) \equiv \int_{\Gamma_0}^{\infty} P(\Gamma) d\Gamma$, (here $\Gamma_0 \sim \Delta$, where Δ is the mean level spacing) as a function of the disorder strength V for different system sizes L provides a means to determine the critical point V_c where we have a MIT (vertical line at $V_c=16.5$). (b) The one-parameter scaling of $P_{int}(\Gamma_0) = f(L/\xi(V))$ is confirmed for various system sizes L and disorder strengths V ($\xi(V)$ is the localization length) using a box distribution for the on-site potential of a 3D Anderson model.

(GP) equation describing the mean-field dynamics of the open condensate. We have found that the survival probability decays as $P(t) \sim 1/t^\alpha$ with the power α being a scaling function of the ratio of the interaction strength between Bose particles and the localization properties of the corresponding linear system. Our next steps involve a full quantum mechanical study of such systems. We plan to

operate in the regime where the Bose-Hubbard Hamiltonian is applicable. In this respect, the study of small open quantum lattices (dimer or trimer) promises new exciting opportunities. These studies will be complemented with scattering analysis from non-linear quantum graphs where we will investigate the effect of non-linearity to chaotic scattering.

- [1] H.-J. Stöckmann, *Quantum Chaos: an Introduction*, Cambridge 1998
- [2] M. Timme, T. Geisel, and F. Wolf, *Chaos* **16** (2006) 015108.
- [3] M. Hiller et al., *Annals of Physics* **321** (2006) 1025.
- [4] D. Cohen, F. Izrailev, and T. Kottos, *Phys. Rev. Lett.* **84** (2000) 2052.
- [5] D. Cohen and T. Kottos, *Phys. Rev. Lett.* **85** (2000) 4839.
- [6] D. Cohen and T. Kottos, *Phys. Rev. E* **69** (2004) 055201 (R).
- [7] M. Hiller et al., *Phys. Rev. Lett.* **92** (2004) 010402.
- [8] T. Kottos and U. Smilansky, *Phys. Rev. Lett.* **85** (2000) 968.
- [9] M. Puhlmann et al., *Europhys. Lett.* **69** (2005) 313.
- [10] T. Kottos, *J. Phys. A: Math. Gen.* **38** (2005) 10761.
- [11] A. Ossipov, T. Kottos, and T. Geisel, *Europhys. Lett.* **62** (2003) 719.
- [12] F. Steinbach et al., *Phys. Rev. Lett.* **85** (2000) 4426.
- [13] T. Kottos and M. Weiss, *Phys. Rev. Lett.* **89** (2002) 056401.
- [14] Y. V. Fyodorov and A. Ossipov, *Phys. Rev. Lett.* **92** (2004) 084103.
- [15] T. Kottos and M. Weiss, *Phys. Rev. Lett.* **93** (2004) 190604.

2.1.3.7 From Ballistic to Ohmic Transport in Semiconductor Nanostructures

Ragnar Fleischmann, Holger Schanz

Kai Bröking, Jakob Metzger, Marc-Felix Otto, Manamohan Prusty
E. J. Heller (Harvard, USA), R. Ketzmerick (Dresden)

ACCORDING TO OHM'S law, the resistance of a wire is proportional to its length. This is a straightforward consequence of the diffusive motion of electrons in the disordered potential of a normal material. Today, unlike the time when Ohm arrived at his fundamental observation, conductors can be tailor-made with almost complete control over the microscopic structure. In semiconductors the residual impurities can be so weak that the average free electron path between two scattering events can exceed the typical system size on the nanometer scale. Then the motion of electrons is ballistic rather than diffusive and Ohm's law does not apply. For example, conduction measurements with almost perfect

semiconductor nanowires showed a resistance which was independent of the wire length.

Clearly it is a relevant question how the transition from ballistic to diffusive electron dynamics takes place and what replaces Ohm's law in such an intermediate situation. We are studying this question in various contexts and give only two examples here. First we show how the electron dynamics departs from a purely ballistic motion under the influence of the residual disorder which is present in a real two-dimensional electron gas (2DEG) at the interface between two semiconductors. Although the disorder is very weak it turns out to have a very strong effect on the distribution

of electrons inside the sample. In the second example we manipulate the electron dynamics such that it is ballistic or diffusive depending on the transport direction. We shall see how the resistance of such an unusual wire interpolates between the two extremes which are present simultaneously.

Influence of weak disorder: Branching of the electron flow

It has been known for a long time that impurity scattering in the high mobility two-dimensional electron-gas (2DEG) in semiconductor systems at low temperatures is dominated by small-angle scattering. The consequences of the small-angle scattering on length-scales short compared to the mean free path (MFP), however, come as a great surprise: instead of a fanning-out of the current paths it leads to a pronounced branching of the electron flow.

In an experiment performed in the Westervelt group at Harvard using scanning gate microscopy the current density exiting from a *quantum point contact* (QPC) into the 2DEG of a GaAs/AlGaAs heterostructure could be observed [1]. To theoretically validate the unexpected outcome of the experiment (Fig. 1B) as a consequence of impurity scattering it was necessary for us to model the disorder potential in the 2DEG in some detail [S. Shaw, R. Fleischmann, E. Heller in 1]. The disorder is mainly due to spatial fluctuations in the charge density of the donor-layer in the modulation-doped heterostructure. The resulting disorder potentials (Fig. 1A) turn out to have a variance on the order of a few percent of the Fermi-energy of the electrons (red plane in Fig. 1A) and to be smooth on length scales larger than the Fermi-wavelength of the electrons. Numerical simulations in these model potentials corroborate the experimental findings and show that the branching effect is basically a classical effect (Fig. 2). It is important to notice, that the formation of branches is not at all similar to the flow of rivers in valleys. In Fig. 2a the shadow of the classical current density cast over the disorder potential clearly shows that the branches do not flow

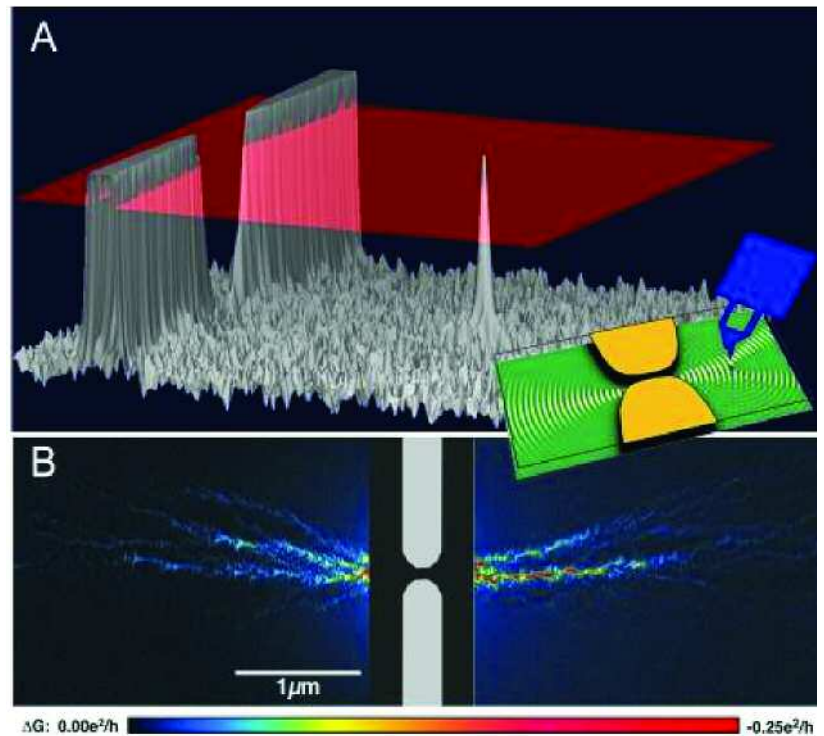
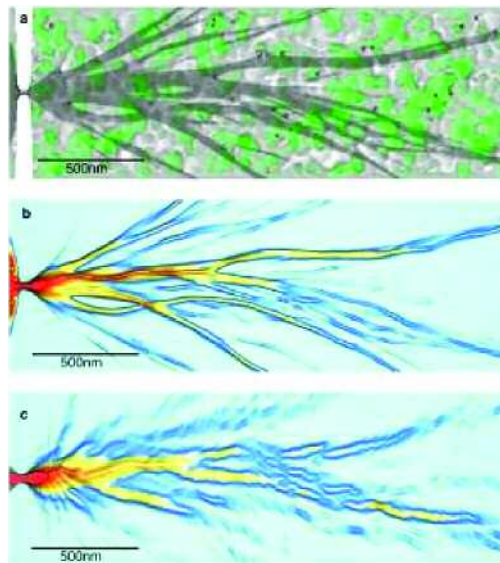


Figure 1: Model potential (A) of the experimental setup (sketched in the inset) that was used to image the current density emitting from a quantum point contact. The tip of a scanning probe microscope was used as a point scatterer. In first order it induces a change in the conductance proportional to the current density at the position of the tip. By scanning the tip over the sample and recording the conductance differences a map of the current density (B) could thus be measured. Here the gate voltage defining the QPC is adjusted so that only the first mode is propagating through it. The mean free path in the 2DEG is approximately $7 \mu\text{m}$; the experiment was performed at temperatures of 1.7 K.

along valleys but rather run equally over valleys and hills. This effect can not only be found in semiconductors, however, but is a very general phenomenon. Similar findings that have been described for the sound propagation in the ocean [2] on length-scales a trillion (10^{12}) times larger can be attributed to the same effect. In general, every two dimensional Hamiltonian system with weak correlated disorder should show the branching of the flow, even though the disorder potential is small compared to the kinetic energy and thus only allows for small changes in the velocities. But what is the mechanism behind the branching of the flow? While a satisfying quantitative analytical theory is still lacking and is the aim of ongoing work, we already can well demonstrate the origin of the branching numerically [3]. It is caused by the

Figure 2:
Numerical simulations of
the current density emitted
by the first mode of a
quantum point contact:
(a) False colour map of the
used potential
overshadowed by the
classical current density. (b)
Classical current density. (c)
Quantum mechanical
scattering wave function.



formation of caustics and the fact that in two dimensions caustics in general appear in pairs as illustrated in Fig. 3.

Competition of diffusive and ballistic transport

Figure 4 shows a model in which the electron dynamics is ballistic or diffusive depending on the transport direction. Under the influence of a transverse magnetic field an electron moves on a circular arc until it is reflected from one of the boundaries of the quasi one-dimensional wire. Due to the specific geometry there are regular and chaotic

trajectories. Some electrons simply skip along the straight boundary of the wire from right to left (green). The chaotic trajectories collide with the obstacles at the lower wall and frequently change their transport direction (red). In the limit where the size of the obstacles and their distance shrink to zero, the dynamics corresponds to biased diffusion with drift velocity v and diffusion constant D . We have shown in a more general context that the chaotic drift exactly compensates for the regular (skipping) transport [4]. In the present case the relevant parameters are the length scale $L = D/v$ and the relative weight c of the chaotic orbits in phase space. Both can be changed by tuning the magnetic field. For the resistance of a wire with length l we found the formula $R(l) = (1 - c \exp[-l/L]) / (1 - c)$ up to a constant prefactor and confirmed this numerically for a wide parameter range [5]. This expression interpolates in a non-trivial way between Ohm's law $R(l) \sim l$ for $c \rightarrow 1$ and the ballistic case $R(l) = \text{const}$ for $c \rightarrow 0$. The characteristic length scale L is a new feature and a qualitative difference to the two limiting cases. We continue to study models of this type because the intrinsic direction dependence of transport is an unusual and potentially useful effect. Currently we are interested in time-resolved transport properties and quantum effects.

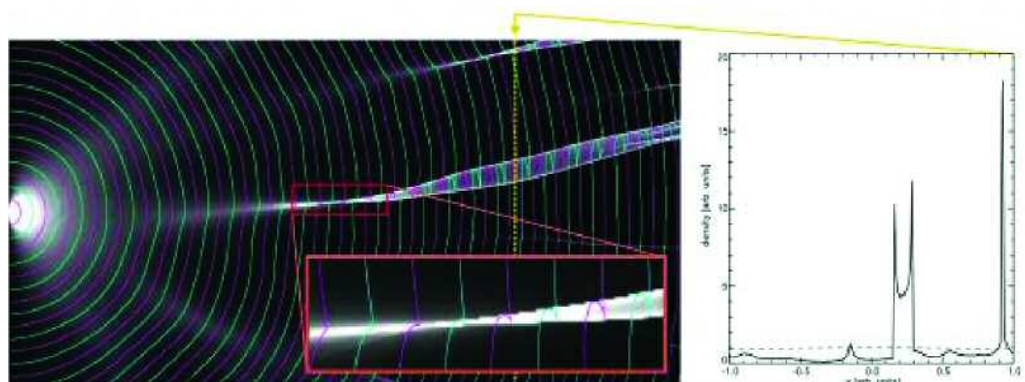


Figure 3: The time evolution of the initial manifold of a *point source* with cosine characteristic at fixed time intervals (turquoise and violet lines). The shadings represent the current density. The inset on the right shows a cut through the density (solid line) compared to the density in an idealized clean system (dotted line) and demonstrates that the branching is not necessarily a small effect and the rise in the density in the region between two sibling caustics due to the folding of the manifold.



Figure 4: Electrons move under the influence of a perpendicular magnetic field in a structure which is designed to allow for the simultaneous presence of ballistic and diffusive transport. The characteristic feature is that backscattering of electrons occurs only at one of the two boundaries of the channel. A periodic arrangement of large semicircular obstacles is shown here for clarity, but it could be replaced, e.g., by a boundary with a rough surface [5].

[1] M. A. Topinka et al., *Nature* **410** (2001) 183.
 [2] Michael A. Wolfson and Steven Tomsovic, *J. Acoust. Soc. Am.* **109** (2001) 2693.
 [3] R. Fleischmann et al., in preparation (2006).
 [4] H. Schanz et al., *Phys. Rev. Lett.* **87** (2001) 070601.
 [5] M. Prusty and H. Schanz, *Phys. Rev. Lett.* **96** (2006) 130601.

2.1.3.8 What are the Quantum Signatures of Typical Chaotic Dynamics?

Lars Hufnagel
 Matthias Weiss
 R. Ketzmerick (Dresden)

TYPICAL HAMILTONIAN SYSTEMS are neither integrable nor ergodic [1,2,3] but have a *mixed* phase space, where regular and chaotic regions coexist. Fig. 1b shows a phase space portrait of a typical mixed phase space of the well known kicked rotor, which is a paradigm for a generic Hamiltonian system. The regular regions are organized in a hierarchical way and chaotic dynamics is clearly distinct from the dynamics of fully chaotic systems. In particular, chaotic trajectories are trapped in the vicinity of the hierarchy of regular islands. The most prominent quantity reflecting this, is the probability $P(t)$ to be trapped longer than a time t , which decays as

$$P(t) \sim t^{-\gamma},$$

in contrast to the typically exponential decay in fully chaotic systems. While the power-law decay is universal, the exponent γ is system and parameter dependent [4,5]. The origin of

the algebraic decay is an infinite hierarchy of partial transport barriers [1,3], e.g., Cantori, surrounding the regular islands. Transport across each of these barriers is described by a turnstile, whose area is the flux exchanged between neighboring regions [14]. The fluxes deep in the hierarchy become arbitrarily small.

For mixed systems two types of eigenfunctions are well studied: There are ›regular‹ states living on KAM-tori of the regular islands and there are ›chaotic‹ states extending across most of the chaotic region as first described by Percival [6]. In addition, we were able to identify and quantify a third type of eigenstates (see Fig. 2). They directly reflect the hierarchical structure of the mixed phase space and are thus called *hierarchical states* [7]. These states are supported by the chaotic region but predominantly live in the vicinity of the regular islands with only a small contribution in the main part of the chaotic sea.

They are separated from the main chaotic sea by the partial transport barriers of the classical phase space.

The occurrence of the hierarchical states can be understood as follows: While the classical fluxes become arbitrarily small, quantum mechanics can mimic fluxes $\phi > \hbar$ only [8]. This leads to the concept of the flux barrier, which is defined to be the partial transport barrier in phase space with flux $\phi \approx \hbar$. This flux barrier divides the chaotic component of the phase space into two parts: Regions connected by fluxes $\phi > \hbar$ are strongly coupled and thus appear quantum mechanically as one part. They support the chaotic eigenstates. Regions connected by fluxes $\phi < \hbar$ couple only weakly to one another and support the hierarchical states. Thus the fraction of hierarchical states scales as

$$f_{\text{hier}} \sim \hbar^{-1/\gamma},$$

where the classical exponent determines the scaling. Not only has the existence of the flux barrier important consequences for eigenstates and eigenfunctions, it also limits quantum-classical correspondence and underlies a new type of conductance fluctuations, which was observed recently.

One of the central phenomena in mesoscopic

physics are conductance fluctuations [9]. They occur as a function of an external parameter, e.g., magnetic field or energy, when the phase coherence length exceeds the sample size. They can be measured, e.g., in semiconductor nanostructures at sub-Kelvin temperatures. For typical billiards, which exhibit a mixed phase space, the power-law decay of Eq. (1) led together with semiclassical arguments to the prediction of FCF [10]. They are characterized by a fractal dimension $D=2-\gamma/2, \gamma < 2$, of the conductance curve $g(E)$. A new type of conductance fluctuations has been observed for the cosine billiard with a mixed phase space [11]. In contrast to the previously found FCF, the conductance as a function of energy shows a smoothly varying background with many isolated resonances.

We have shown that both types are quantum signatures of the classical mixed phase space and in general appear simultaneously, but on different energy scales [12]. Furthermore, isolated resonances are caused by regions behind the flux barrier and are therefore scattering signatures of the hierarchical states. For open quantum systems the flux barrier introduces an important new time scale $t^* = \Omega_{n^*,n^*+1}/\Phi_{n^*,n^*+1}$. (Fig. 3) Beyond this time, regions behind the flux barrier are important and quantum dynamics differs from classical dynamics. Therefore the semiclassical derivation of FCF is only valid for energy scales $\Delta E > \Delta E' \equiv \hbar/t^*$.

We were able to calculate the scaling of this energy and the corresponding time scale, which nicely agrees with numerical simulations [12,13]. The coexistence of FCF and isolated resonances is illustrated in Fig. 4.

Although generic Hamiltonian systems possess a mixed phase space, classical properties of mixed systems and their quantum mechanical signatures are still only partly understood. In particular, we have shown recently that, for transporting islands, even the distinctions in regular and chaotic eigenstates fails [14].

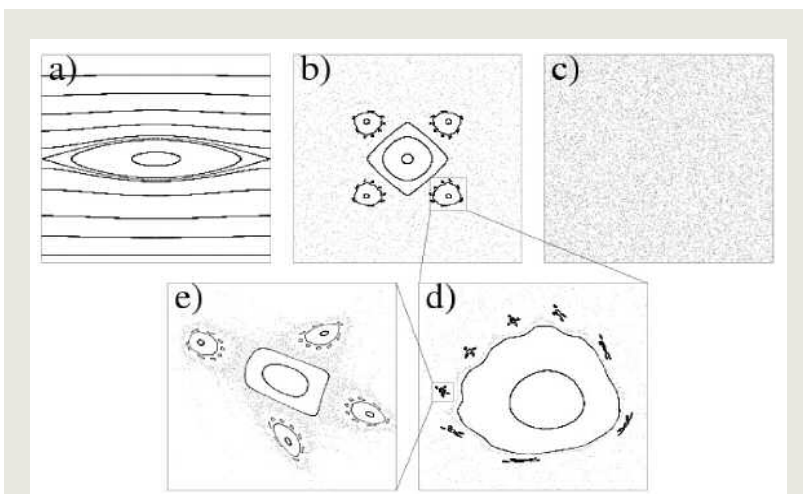


Figure 1: Phase space portraits of (a) mostly regular, (b) mixed, and (c) fully chaotic dynamics. The successive magnifications in (d) and (e) illustrate the hierarchical nature of mixed phase spaces.

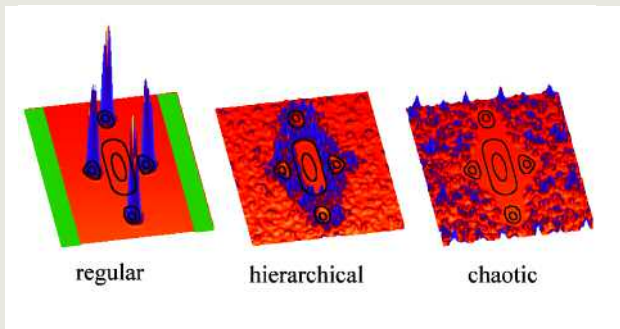


Figure 2 : Phase space representation of a regular, hierarchical, and chaotic eigenfunction. Solid lines indicate KAM tori of the classical phase space.

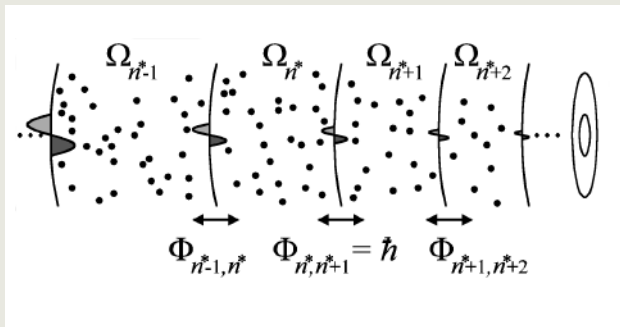


Figure 3: Sketch of the hierarchical phase space structure in the vicinity of a regular island. A linear infinite chain of phase space regions with volume Ω_{n+1} are separated by partial transport barriers. The flux $\Phi_{n,n+1}$ between two neighboring regions is given by the area of the turnstile. The quantum flux barrier at n divides the hierarchy into two regions.

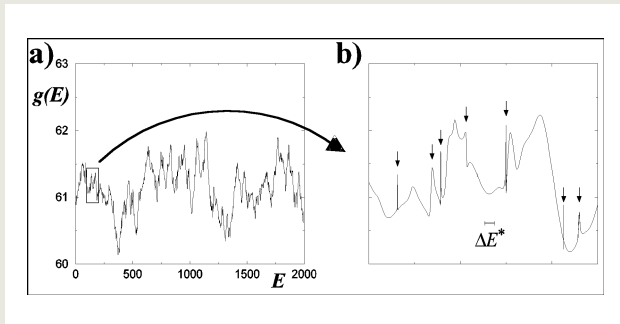


Figure 4: Dimensionless conductance as a function of energy showing the coexistence of fractal fluctuations on large energy scales (a) and isolated resonances on small scales (b).

[1] R. S. MacKay, J. D. Meiss, and I. C. Percival, *Physica D* **55** (1984) 13.
 [2] J. D. Meiss, *Rev. Mod. Phys.* **64** (1992) 795.
 [3] L. Markus and K. R. Meyer, in *Memoirs of the American Mathematical Society* **114** (American Mathematical Society, Providence, RI, 1974)
 [4] M. Weiss, L. Hufnagel, and R. Ketzmerick, *Phys. Rev. E* **67** (2003) 046209.
 [5] M. Weiss, L. Hufnagel, and R. Ketzmerick, *Phys. Rev. Lett.* **89** (2002) 239401.
 [6] C. Percival, *J. Phys. B: Atom. Molec. Phys* **6** (1973) L229.
 [7] R. Ketzmerick et al., *Phys. Rev. Lett.* **85** (2000) 1214.
 [8] O. Bohigas, S. Tomsovic, and D. Ullmo, *Phys. Rep.* **223** (1993) 45.
 [9] S. Datta, *Electronic transport in mesoscopic systems* (Cambridge University Press 1995).
 [10] R. Ketzmerick, *Phys. Rev. B* **54** (1996) 10841.
 [11] B. Huckestein, R. Ketzmerick, and C. Lewenkopf, *Phys. Rev. Lett.* **84** (2000) 5504.
 [12] R. Ketzmerick, L. Hufnagel, and M. Weiss, *Adv. Sol. St. Phys.* **41** (2001) 473.
 [13] L. Hufnagel, R. Ketzmerick, and M. Weiss, *Europhys. Lett.* **54** (2001) 703.
 [14] L. Hufnagel et al., *Phys. Rev. Lett.* **89** (2002) 154101.

2.1.3.9 Topological Superdiffusion – A New Theory for Lévy Flights in Inhomogeneous Environments

Dirk Brockmann

DIFFUSION PROCESSES ARE ubiquitous in nature. A freely diffusive particle is characterized by a relationship between the typical distance $|x(t)|$ it traveled and the time t that elapsed, i.e. $|x(t)| \sim t^{1/2}$. However, a variety of interesting physical systems violate this scaling behavior. For example, the distance of a superdiffusive particle from its starting point typically scales with time according to

$$|x(t)| \sim t^{1/\beta}$$

with $\beta < 2$. Superdiffusion has been observed in a number of systems ranging from early discoveries in intermittent chaotic systems [1], fluid particles in fully developed turbulence [2], and human eye movements [3] and most recently discovered, the geographic movement of bank notes [4]. Among the most successful theoretical concepts that have been applied to superdiffusive phenomena are random walks known as Lévy flights [5]

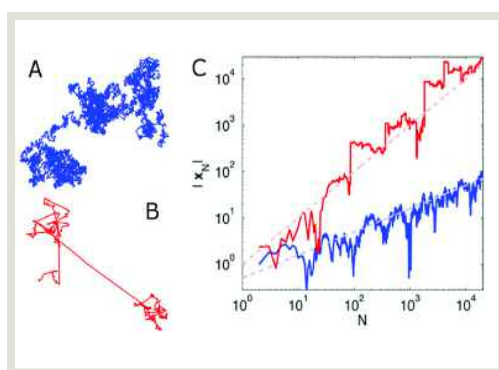
with an exponent $\beta < 2$ which is usually referred to as the Lévy index. Lévy flights have paved the way towards a description of superdiffusive phenomena in terms of fractional Fokker-Planck equations (FFPE). Since many of the aforementioned systems evolve in inhomogeneous environments, it is crucial to understand the influence of external potentials on the dynamics. While in ordinary diffusive systems an external force is easily incorporated into the dynamics by a drift term in the corresponding Fokker-Planck equation (FPE), the matter is subtler in superdiffusive systems due to the nonlocal properties of the fractional operators involved. Depending on the underlying physical model, different types of FFPEs are appropriate [6], therefore the ad hoc introduction of fractional operators may lead to severe problems.

In cases where the external inhomogeneity can be represented by an additive force, considerable progress has been made in a generalized Langevin approach, which led to an FFPE in which deterministic and stochastic motion, segregate into independent components. This approach, however, is suited only for systems in which such a segregation can be justified on physical grounds. For some reason though, it has been considered as the canonic theory for Lévy flights in external potentials.

One feature of generalized Langevin dynamics is its validity only for systems far from thermodynamic equilibrium. It fails in the large class of systems, which obey Gibbs-Boltzmann thermodynamics, e.g., where superdiffusion is caused by the complex topology on which the process evolves.

A good example is diffusion along rapidly folding heteropolymers [7] as depicted in Figure 2. A particle is attached to a heteropolymer and performs a random walk along the chain. The chain is flexible and rap-

Figure 1:
Ordinary random walks and Lévy flights. A) The two dimensional trajectory of an ordinary random walk resembles Brownian motion. B) The trajectory of a Lévy flight with Lévy index $\beta=1.0$. C) The distance $|x_n|$ from the origin of an ordinary random walk (blue) and a Lévy flight (red) as a function of the number of steps. The diffusive scaling $|x_n| \sim N^{1/2}$ is depicted by the blue dashed line, the superdiffusive scaling $|x_n| \sim N^{1/\beta}$ with $\beta=1.0$ by the red dashed line.



(see Fig.1). In contrast to ordinary random walks, the spatial displacements $\Delta \mathbf{x}$ of a Lévy flight lack a well-defined variance, due to a heavy tail in the single step probability density, i.e.

$$p(\Delta \mathbf{x}) \sim \frac{1}{|\Delta \mathbf{x}|^{1+\beta}}$$

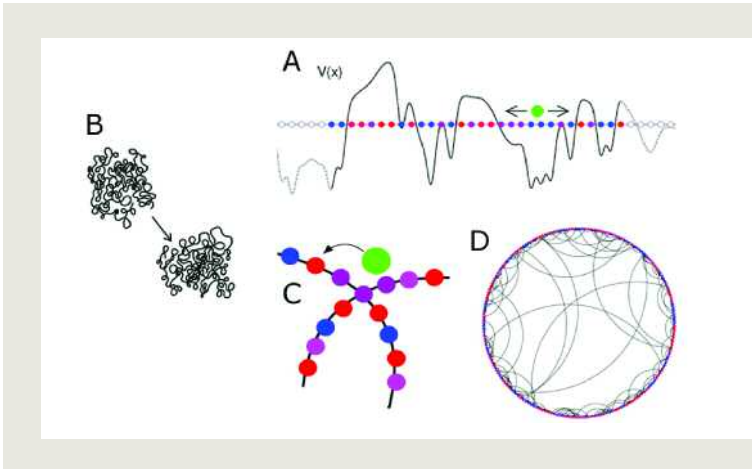


Figure 2: Topological superdiffusion A) A particle (green) performs a random walk on a polymer chain. Along the chemical coordinate x a potential is defined. B) The polymer is flexible and rapidly changes its 3-D conformation. C) Segments which are far apart along the chemical coordinate of the chain can come close and the hopping particle can perform intersegment transfer. D) effectively the random walk takes place on a complex network topology induced by the locations at which intersegment transfer can occur.

idly changes its conformational state. The heterogeneity of the chain is modeled by a potential V which is defined along the chemical coordinate of the chain and which specifies the probability of the particle being attached to a site. In a thermally equilibrated system this probability is proportional to the Boltzmann factor $e^{-V/k_B T}$. If the polymer is flexible and rapidly folding, the attached particle can perform intersegment transfer by virtue of segments which are close in Euclidean space but far apart along the chemical coordinate. The probability of observing a jump of length l in chemical coordinates depends on the folding dynamics of the polymer and generally decreases according to a powerlaw with distance. Effectively, the particle performs a Lévy flight along the chain in a heterogeneous environment imposed by the potential. However, superdiffusion is not caused by large fluctuations in stochastic forces but is rather a consequence of the topology of the system, the system is topologically superdiffusive.

We were able to show that systems of this type can be described by a novel type of FFPE of the form

$$\partial_t p = e^{-\beta V/2} \Delta^{\mu/2} e^{\beta V/2} p - p e^{\beta V/2} \Delta^{\mu/2} e^{-\beta V/2}$$

where β is the inverse temperature, μ the Lévy index, $\Delta^{\mu/2}$ the fractional generalization of the Laplacian and $p=p(x,t)$ the probability of finding the particle at a position x at time t . In⁸ we investigated the impact of external po-

tentials on this class of systems. Based on the paradigmatic case of a randomly hopping particle on a folded copolymer, we discovered a number of bizarre phenomena, which emerge when Lévy flights evolve in periodic and random potentials and showed that external potentials have profound effects on the superdiffusive transport. This is in sharp contrast to generalized Langevin dynamics, which displays trivial asymptotic behavior in these systems, a possible reason why Lévy flights in such potentials have attracted little attention in the past. We demonstrated that even strongly superdiffusive Lévy flights are highly susceptible to periodic potentials, as can be seen in the complexity of the eigenvalue band structure (Fig. 3).

The range of applications of this type of dynamics is wide. For instance the trajectories of human saccadic eye movements can be ac-

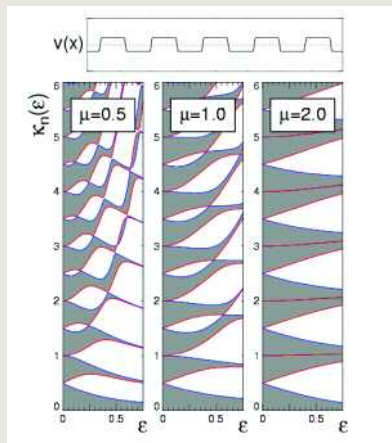


Figure 3: Eigenvalue bands for topologically superdiffusive processes in a smoothed box periodic potential. $\kappa_n(\epsilon) = E_n(\epsilon)^{1/\mu}$ denote the generalized chrysal momentum as a function of the inverse temperature $\epsilon = \beta/2$. Superdiffusive processes exhibit a rich behavior as opposed to the limiting case of ordinary diffusion, i.e. $\mu = 2$.

counted by a similar model [3] (Fig. 4). In this model the Boltzmann factor is identified with the visual salience, i. e. the attractivity, of a location in a scene: $s(\mathbf{x}) = \exp(-\beta V(\mathbf{x})/2)$. We were able to show that a process with intermediate Lévy index $\mu = 1$ is optimal for visual search tasks.

Most importantly, our theory can be applied in population dynamical contexts, particularly spatially extended models for the spread of infectious diseases. We are currently investigating the interplay of spatially variable population densities with scale free superdiffusive dispersal of individuals and paradigmatic

reaction kinetics for local outbreaks of infections. The combination of fractional Fokker-Planck equations mentioned above with local exponential growth due to the disease dynamics yields spatio-temporal patterns which differ vastly from those observed for ordinary diffusion (see Fig. 5). As our approach can be applied to realistic geographies we hope that it will serve as a starting point for the development of more realistic models for the spread of disease and that general containment strategies for emergent infections can be devised.

Figure 4:
Human saccadic eye-movements.
Left: A natural scene presented to two observers whose eye movements were recorded (middle). Very similar trajectories can be generated by a topologically superdiffusive process (right).

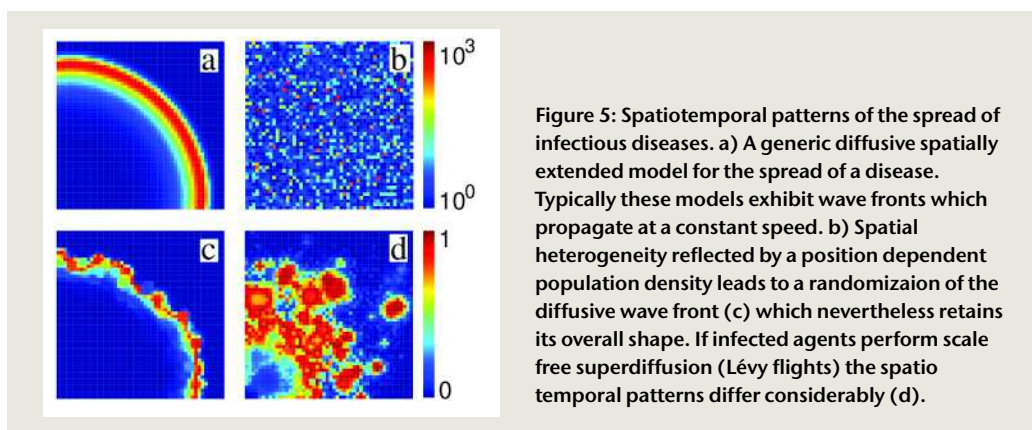
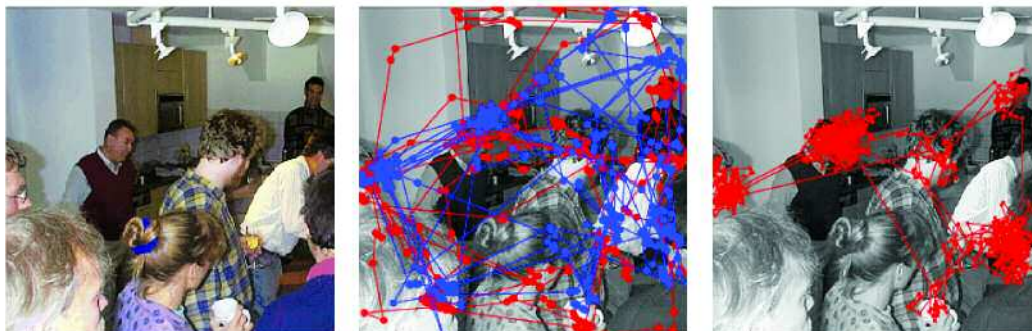


Figure 5: Spatiotemporal patterns of the spread of infectious diseases. a) A generic diffusive spatially extended model for the spread of a disease. Typically these models exhibit wave fronts which propagate at a constant speed. b) Spatial heterogeneity reflected by a position dependent population density leads to a randomization of the diffusive wave front (c) which nevertheless retains its overall shape. If infected agents perform scale free superdiffusion (Lévy flights) the spatio-temporal patterns differ considerably (d).

- [1] T. Geisel, J. Nierwetberg, and A. Zacherl, *Physical Review Letters* **54** (1985) 616.
 [2] A. La Porta et al., *Nature* **409** (2001) 1017.
 [3] D. Brockmann and T. Geisel, *Neurocomputing* **32** (2000) 643.
 [4] D. Brockmann, L. Hufnagel, and T. Geisel, *Nature* **439** (2006) 462.
 [4] Lévy flights and related Topics in Physics (eds.

- Shlesinger, M. F., Zaslavsky, G. M. & Frisch, U.) (Springer, Nice, France, 1994).
 [6] D. Brockmann and I. M. Sokolov, *Chemical Physics* **284** (2002) 409.
 [7] D. Brockmann and T. Geisel, *Physical Review Letters* **91** (2003) 048303.
 [8] D. Brockmann and T. Geisel, *Physical Review Letters* **90** (2003) 170601.

2.1.3.10 Human Travel and the Spread of Modern Epidemics

Dirk Brockmann, Lars Hufnagel

THE APPLICATION OF mathematical modeling to the spread of epidemics has a long history and was initiated by Daniel Bernoulli's work on the effect of cowpox inoculation on the spread of smallpox in 1760. Most studies concentrate on the local temporal development of diseases and epidemics. Their geographical spread is less well understood, although important progress has been achieved in a number of case studies. The key question, as well as difficulty, is how to include spatial effects and quantify the dispersal of individuals. Today's volume, speed, and globalization of traffic (Fig. 1), increasing international trade and intensified human mobility promote a complexity of human travel of unprecedented degree.

The severe acute respiratory syndrome (SARS) which spread around the globe in a matter of months in 2003 has not only demonstrated that the geographic spread of modern epidemics vastly differs from historic ones but also the potential threat of emergent infectious diseases such as Hanta, West Nile and Marburg fever which can be contained to their endemic region only with increasing difficulty. Particularly in the light of an imminent H5N1 influenza A pandemic the knowledge of dynamical and statistical properties of human travel is of fundamental importance and acute.

The spread of SARS on the global aviation network – a case study

The application of spatially extended models to the geographic spread of human infectious disease by means of reaction-diffusion equations has been motivated by the spread of historic pandemics such as the bubonic plague (1347–1350). A characteristic of the spread of the 'Black Death' was a wave front which propagated at a speed of approximately 4–5 km/per day, a direct consequence of the

local proliferation of the disease in combination with diffusive motion of infected individuals who could travel at most a few km/day at that time. In contrast, the rapid worldwide spread of the severe acute respiratory syndrome (SARS) in 2003 (Fig. 2), showed clearly that modern epidemics cannot be accounted for by conventional reaction diffusion models as humans can travel from any point on the globe to any other in a matter of days and no typical length scale for travel can be identified.

In a recent project [1] we focused on the key mechanisms of the worldwide spread of modern infectious diseases. In particular we investigated to what extent the worldwide aviation network plays a role in disseminating epidemics. To this end we compiled approximately 95% of the entire aviation traffic, which amounts to nearly 2 million flights per week between the 500 largest airports worldwide. Some of the questions we aimed to answer were: Is it possible to describe the worldwide spread of an epidemic based on a conceptionally lean model which incorporates the worldwide aviation network? If so,



Figure 1: The worldwide civil aviation network. Lines connect the 500 largest airports. Bright lines indicate high, dark lines low traffic between connected nodes. The entire depicted traffic comprises 95% of the worldwide traffic.

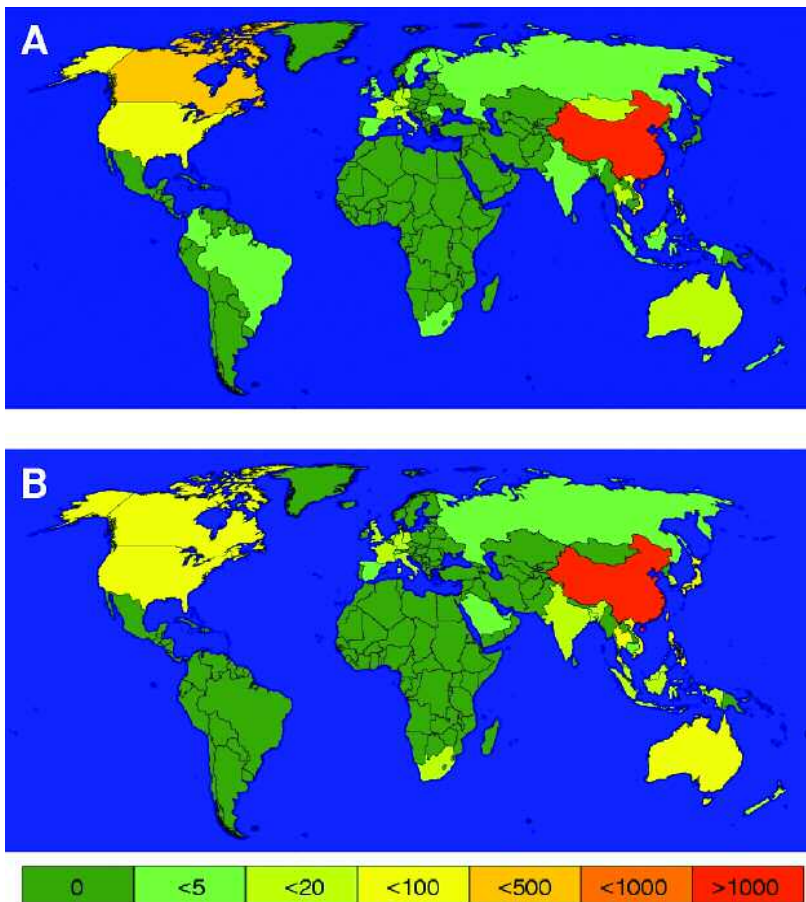


Figure 2: A) geographic spread of SARS in May 2003 as reported by the World Health Organization (WHO) and the Center for Disease Control and Prevention (CDC). The number of infecteds per country are encoded by color. B) The expected spread as predicted by the model after a time of 90 days. Depicted is the expectation value of the number of infecteds after 10000 simulations with an initial outbreak in Hong Kong.

namics of individuals. The local dynamics is described by the SIR reaction kinetic scheme in which individuals are initially susceptible (S), become infected (I) and recover (R) from the disease, become immune and cannot be infected a second time. The associated reaction kinetics



is defined by the two reaction rates α and β , the ratio of which is the basic reproduction number R_0 , which is the average number of secondary infections caused by one infected individual during the infectious period. If $R_0 > 1$, an epidemic outbreak occurs. For SARS, which spread around the world in 2003, a value $R_0 \approx 2-4$ was found. We assumed that the above SIR model governs the dynamics of the disease in each urban area surrounding an airport. Furthermore we assumed that the transport between urban areas is directly proportional to the traffic flux of passengers between them. Both constituents of our model are treated on a stochastic level, taking full account of fluctuations of disease transmission, latency, and recovery on the one hand and of the geographical dispersal of individuals on the other (Fig. 3). Furthermore, we incorporate nearly the entire civil aviation network.

how reliable are forecasts put forth by the model? How important are fluctuations? What facilitates the spread? And, last but not least, what containment strategies and control measures can be devised as a result of computer simulations based on such a model?

Our model consists of two part: a local infection dynamics and the global traveling dy-

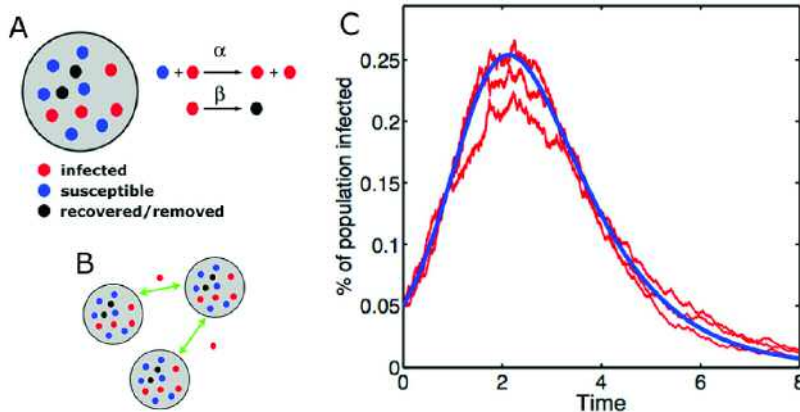


Figure 3: A) The SIR reaction kinetic model for the dynamics of local outbreaks. B) Dispersal between populations. C) The percentage of infected individuals in a population as a function of time for a basic reproduction number of $R_0=2$. The red curves are simulations of the full stochastic reaction kinetics, the blue curve depicts the mean field dynamics.

Fig2. depicts a comparison of the spread of SARS in May 2003 as reported by the World Health Organization and simulations of our model. Despite some differences the overall prediction of our model is surprisingly close to the observed global spread of SARS. The degree of agreement seems particularly surprising if one recalls the conceptual simplicity of our model and the fact that we incorporate fluctuations in the infection dynamics as well as the spatial dispersal. In² we investigated the reason why predictions based on the global travel on the aviation network is indeed possible. We were able to show that the strong heterogeneity of the network reflected by a wide range of airport capacities, fluxes between airports and particularly a wide range of connectivities decreases the effects of internal fluctuations. Furthermore, we were able to show that a containment strategy, which focuses on the most frequented connections, has practically no impact as opposed to a strategy which focuses on the most connected nodes in the network.

The scaling laws of human travel

Whereas the global aspects of disease dynamics can be accounted for by an comprehensive knowledge of the aviation network, such an approach is insufficient if a description for smaller length scales is required. In order to understand and predict the spread of disease on a wide range of length scales, we need to know the statistical rules that govern human travel from a few to a few thousands kilometers. Quantitative studies, however, prove to be very difficult, because people move over short and long distances, using various means of transportation (planes, trains, automobiles, etc.). Compiling a comprehensive dataset for all the means of transportation on extended geographical areas is difficult if not impossible.

In a recent project³ we approached the problem from an unusual angle. We evaluated data collected at the online bill tracking system *www.wheresgeorge.com* in order to assess the statistical properties of the geographic cir-

culatation of money with a high spatiotemporal precision. The idea behind this project was to use the dispersal of money as a proxy for human travel as bank notes are primarily transported from one place to another by traveling humans.

Wheresgeorge.com, which started in 1998 without any scientific motivation, is a popular US internet game in which participants can register individual dollar bills for fun and monitor their geographic circulation henceforth. Since its beginning a vast amount of data has been collected at the website, over 80 millions of dollar bills have been registered by over 3 million registered users.

Based on a dataset of over a million individual displacements we found that the dispersal of dollar bills is anomalous in two ways. First, the probability $p(\delta r)$ of traveling a distance δr in a short period of time $\delta T < 4$ days decays as a power law, i. e.

$$p(\delta r) \sim \frac{1}{\delta r^{1+\beta}}$$

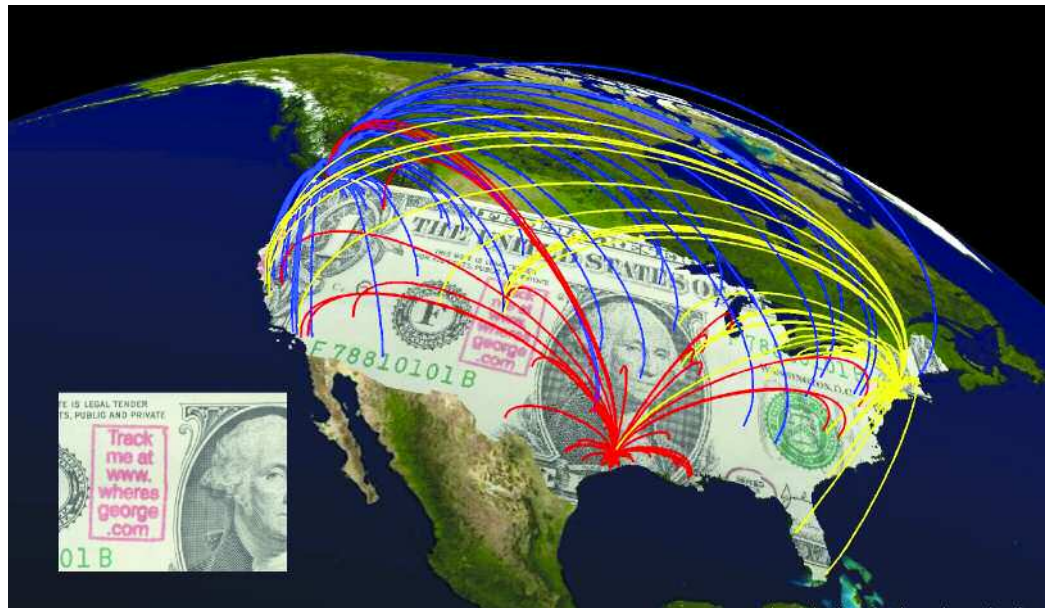
with an exponent $\beta \approx 0.6$. This exponent implies that no typical distance can be defined as mean as well as variance of the displacement are divergent. Surprisingly this behavior does not depend strongly on local properties such as the population density of the United States. Irrespective of the initial entry location, an asymptotic powerlaw was observed (see Fig. 5).

This observation lead us to conjecture that the trajectories of dollar bills are reminiscent of Lévy flights⁴, a superdiffusive random walk characterized by a power law in the single step distribution with an exponent $\beta < 2$. The position x_N of a Lévy flight scales with the number of steps according to

$$x_N \sim N^{1/\beta}$$

for $\beta < 2$ unlike the ordinary square root scaling $x_N \sim N^{1/2}$ exhibited by ordinary random walks. Employing the Lévy flight model we computed the time T_{eq} for an initially localized ensemble of dollar bills to redistribute

Figure 4:
Short time trajectories of individual dollar bills that were initially reported in Seattle (blue), New York (yellow) and Houston (red). Lines connect the initial entry location and the location where the bill was reported less than a week after initial entry.



equally within the United States and obtained $T_{eq} \approx 70$ days. However, the dispersal data showed clearly that even after one year, bills do not equilibrate within the United States and despite the clear evidence for the power law in the short time dispersal the Lévy flight picture seemed incomplete.

We thus developed the idea that the dispersal of money can be described by a process in which long jumps in space compete with long periods of rest at successive locations. We modeled the process as a continuous time random walk⁵ (CTRW) in which spatial displacements are interspersed with random periods of rest which are distributed according to a power law as well, i.e.

$$\phi(\delta T) \sim \frac{1}{\delta T^{1+\alpha}} \quad (2)$$

with an exponent $\alpha < 1$. A powerlaw in the waiting time usually leads to subdiffusive motion as the total time elapsed scales with the number of steps according to

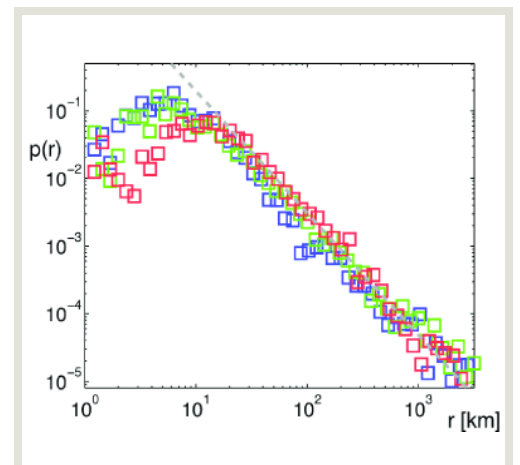
Figure 5:
Probability $p(r)$ of travelling a distance r in a short time $\delta T < 4$ days. In blue, green and red trajectories with initial entries in large cities, small cities and small towns respectively. Between 10 and 3500 km $p(r)$ is a powerlaw with an exponent $\beta \approx 0.6$.

$T_N \sim N^{1/\alpha} \mathbf{V}$ which implies that the number of steps increase sublineary with time, i.e. $N \sim T^\alpha$. In combination with the scaling of position with the number of steps such an ambivalent CTRW scales with time according to

$$x(t) \sim t^{\alpha/\beta}$$

This implies that the superdiffusive dispersal is attenuated by the long periods of rest. We were able to compute the asymptotics for the process which is given by

$$W_r(\mathbf{x}, t) = t^{-2\alpha/\beta} L_{\alpha,\beta}(x/t^{\alpha/\beta})$$



in which $L_{\alpha,\beta}$ is a universal scaling function of the process which depends on the two exponents only. Comparing to the data he found that for $\alpha=\beta=0.6$ the model agrees very well with the data (Fig. 6).

The dynamical equation for this ambivalent CTRW has the form

$$\partial_t^\alpha W(\mathbf{x},t) = D_{\alpha,\beta} \partial_{|\mathbf{x}|}^\beta W(\mathbf{x},t)$$

In which the ordinary derivatives ∂ and ∂_x^β are

replaced by fractional generalizations ∂_t^α and $\partial_{|\mathbf{x}|}^\beta$. These operators are nonlocal singular integral operators accounting for the spatial and temporal anomalies of the process. The dispersal of money is the first example of such a bifractional anomalous process in nature.

Existing models for the geographic spread of infectious diseases can now be checked for consistency with our findings and a new class of models for the spread of epidemics can be conceived which are based on our results.

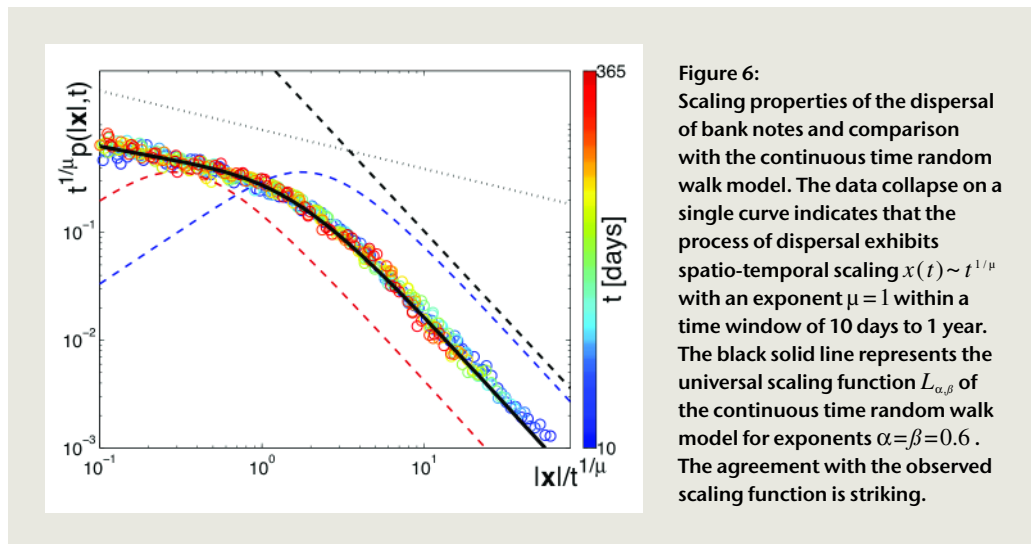


Figure 6: Scaling properties of the dispersal of bank notes and comparison with the continuous time random walk model. The data collapse on a single curve indicates that the process of dispersal exhibits spatio-temporal scaling $x(t) \sim t^{1/\mu}$ with an exponent $\mu = 1$ within a time window of 10 days to 1 year. The black solid line represents the universal scaling function $L_{\alpha,\beta}$ of the continuous time random walk model for exponents $\alpha=\beta=0.6$. The agreement with the observed scaling function is striking.

[1] L. Hufnagel, D. Brockmann, and T. Geisel, *Proceedings of the National Academy of Sciences of the United States of America* **101** (2004) 15124.
 [2] D. Brockmann, L. Hufnagel, and T. Geisel, in *SARS: A Case Study in Emerging Infections* A. McLean et al. eds. (Oxford University Press, Oxford, 2005) 81.

[3] D. Brockmann, L. Hufnagel, and T. Geisel, *Nature* **439** (2006) 462.
 [4] *Lévy flights and related Topics in Physics*, M.F. Shlesinger, G.M. Zaslavsky, and U. Frisch (Springer, Nice, France, 1994).
 [5] E. W. Montroll and G. H. Weiss, *Journal of Math. Physics* **6**, (1965) 167.

2.2 Dynamics of Complex Fluids

2.2.1 Overview

Stephan Herminghaus

A FLUID IS CALLED ›complex‹ if its constituents are complex systems on their own: the macromolecules in a polymer melt, the lamellae in a foam, the (dissipative) grains in the granulate, or the bio-molecules in the cytoplasm. Can one predict, on the basis of the properties of these building blocks, the dynamic behavior of the fluid (the liquid crystal, the polymer, the foam, the granulate, the biomaterial)? Are there general principles behind the emergence of large scale properties? Can the study of driven complex fluids yield deeper insight into the principles of systems far from equilibrium? These are just some of the questions which lead us in our studies of the dynamics of complex fluids.

Aside from such rather fundamental considerations, complex fluids have particularly strong importance to technological applications. Granular materials, for instance, cover the full range from toy model systems for irreversibility to practical applications like land slides, food technology and chemical engineering. Emulsions, similarly, may provide micro reactors for applications in ›discrete microfluidics‹, but the complex internal topology of lipid lamellae, which form between the droplets in a micro-channel, touches on yet unanswered questions in the mathematics of foam structures. Transformations in these topologies may be induced in a controlled

manner, if the lamellae consist themselves of complex fluids, such as liquid crystals or ferrofluids. Biological matter, like the actin in the cytoplasm, is further example of a complex fluid in confined geometry, where the mesoscale building blocks of the fluid interact strongly with the geometry of the confinement. This interaction can sometimes be described by means of surprisingly simple concepts.

The various mechanisms of self-assembly and self-organization, which drive the constituents of a complex fluid to arrange into structures on larger scale, are both interesting as genuinely non-equilibrium phenomena and promising as possible tools for generating novel systems by self-assembly. Once we understand the static and dynamic principles which are at work in these processes, the design of self-organized ›soft‹ nano-machines may come within reach, pointing to novel technologies for times to come.

2.2.2 People

**Prof. Dr. Stephan Herminghaus**

was born on June 23, 1959 in Wiesbaden, Germany. He received his PhD in Physics from the University of Mainz in 1989. After a post-doctoral stay at the IBM Research Center San José in California, he moved to the University of Konstanz, where he obtained his habilitation in 1994 and became a Heisenberg fellow in 1995. Later he started an independent research group at the Max Planck Institute for Colloids and Interfaces in Berlin (1996) and

launched a DFG Priority Program on Wetting Phenomena. He declined an offer of a full professorship at the Université de Fribourg, CH. In 1999, he was appointed as a full professor at the University of Ulm, where he also headed the Graduiertenkolleg 328. Since 2003 he is a Director at the Max Planck Institute for Dynamics and Self-Organization in Göttingen. In 2005, he was furthermore appointed as an adjunct professor at the University of Göttingen.

**Dr. Christian Bahr**

studied Chemistry at the Technical University Berlin and received his PhD in 1988. Research stays and postdoctoral work took place at the Raman Research Institute (Bangalore, India) and the Laboratoire de Physique des Solides of the Université Paris-Sud (Orsay, France). After his Habilitation for Physical Chemistry at the Technical University Berlin in 1992, he moved in 1996 to the Physical Chemistry Institute of the University

Marburg as a holder of a Heisenberg-Fellowship. 2001-2004 he worked as a software developer in industrial projects. In 2004 he joined the group of Stephan Herminghaus at the MPI for Dynamics and Self-Organization. Research topics comprise experimental studies of soft matter, especially thermotropic liquid crystals, phase transitions, structures of smectic phases, thin films, interfaces and wetting.

**Dr. Martin Brinkmann**

studied Physics and Mathematics at the Free University of Berlin between 1990 and 1998 where he received his Diploma in Physics. After an internship at the Dornier Labs (Immenstaad, Lake Constance) in 1999 he joined the theory group of Prof. Reinhard Lipowsky at the MPI of Colloids and Interfaces (Potsdam, Germany) to work on wetting of chemically patterned substrates. In 2003 he received his doctorate from the University of

Potsdam. During a postdoctoral stay in the Biological Nanosystems Group at the Interdisciplinary Research Institute in Lille (France) he explored wetting of topographic substrates as a possible way to manipulate small liquid droplets. Since the beginning of 2005 he investigates wetting of regular and random geometries in the department Dynamics of Complex Fluids at the MPI for Dynamics and Self-Organization.

**Dr. Manfred Faubel**

was born on 27.3.1944 in Alzey near Mainz. Physics studies at the University of Mainz (diploma 1969), and in Göttingen (PhD in 1976). Postdoctoral stays at the Lawrence Berkeley Laboratory, 1977, and in Okasaki at the Institute for Molecular Sciences in Japan, 1981. Employed by the MPI für Strömungsforschung since 1973. Molecular beams studies of rotational state resolved scattering cross sections for simple benchmark collision systems,

such as $\text{Li}^+\text{-H}_2$, He-N_2 and for reactive F-H_2 scattering. Since 1986 exploration of the free vacuum surface of liquid water microjets. Photoelectron spectroscopy of aqueous solutions with synchrotron radiation at BESSY/Berlin (1999 to present), and, by laser desorption mass spectrometry of very large ions of biomolecules from liquid jets in vacuum (in a collaboration with MPI-BPC).



Dr. Peter Heinig

studied physics at Leipzig University and received his Diploma in 2000. As a PhD student at the Max-Planck-Institute of Colloid and Interface Science in Golm he investigated the structure formation and wetting of two-dimensional liquid phases in Langmuir monolayers in the presence of long range interactions. After he received his PhD in 2003 from Potsdam University, and a postdoctoral stay at Florida State University in Tallahassee, he joined the

group of Dominique Langevin in Orsay as a postdoctoral fellow within the franco-german network »Complex Fluids from 3D to 2D«. During this time he studied the dynamics and rheology of free standing thin liquid films. Since September 2005 he is a Postdoc at the Max-Planck-Institute for Dynamics and Self-Organization.



Dr. Thomas Pfohl

studied Chemistry at the Johannes-Gutenberg University, Mainz, and received his doctorate in Physical Chemistry from the University of Potsdam in 1998. After his postdoctoral research at the Materials Research Laboratory, University of California, Santa Barbara, from 1998 to 2000, he became a research assistant at the Department of Applied Physics at the University of Ulm from 2000 until 2004. In 2001 he received a research grant to

lead his »Independent Emmy Noether Junior Research Group« by the DFG. Since 2004 he is project leader »Biological Matter in Microfluidic Environment« at the Department »Dynamics of Complex Fluids« at the Max-Planck-Institute of Dynamics and Self-Organization.



Dr. Ralf Seemann

studied physics at the University of Konstanz where he received his diploma in 1997. The diploma work was carried out at the Max Planck Institute of Colloids and Interfaces in Berlin-Adlershof. He received his doctorate in 2001 from the University of Ulm where he experimentally studied wetting and rheological properties of complex fluids. During a stay as postdoctoral researcher at the University of California at Santa Barbara, he explored techniques

to structure polymeric materials on the micro- and nano-scale. In 2002 he joined the group of Stephan Herminghaus at the University of Ulm. He received the science award of Ulm in 2003. Since 2003 he is a group leader at the Max Planck Institute for Dynamics and Self-Organization, Goettingen. Among others he is concerned with wetting of topographic substrates and discrete microfluidics.



PD Dr. Holger Stark

received his doctorate in theoretical physics from the University of Stuttgart in 1993. He pursued his postdoctoral research at the University of Pennsylvania in Philadelphia in 1994 to 1996 with a research fellowship from the Deutsche Forschungsgemeinschaft. After his habilitation at the University of Stuttgart in 1999, he received a Heisenberg scholarship in 2000. In the years 2001 to 2005, he was teaching and pursuing his research

at the University of Konstanz, where he also held a professorship during the summer semester 2004. He spent several research visits in the USA and Japan. Since 2006, Holger Stark is a group leader at the Max-Planck Institute for Dynamics and Self-Organization. He currently holds a professorship at the Ludwig-Maximilians University in Munich to deliver Sommerfeld Lectures during the summer semester 2006.

2.2.3 Projects

2.2.3.1 Wet Granular Matter and Irreversibility

Ralf Seemann, Martin Brinkmann

Axel Fingerle, Zoé Fournier, Klaus Röller, Mario Scheel, Vasily Zaburdaev

THE PHYSICAL PECULIARITIES of granular matter stem from its inherently dissipative nature. The grains in a slightly fluidized granulate, as in an hourglass, have an average center-of-mass kinetic energy corresponding to a few Giga-Kelvin or more. When two of them collide, part of the kinetic energy is transferred to their internal atomic degrees of freedom: the Giga-Kelvin heat bath is intimately coupled to the room-temperature bath of the atoms. This

a liquid, and the wet sand on the beach from which one may sculpture stable sand castles. Quite surprisingly, the yield stress of the wet material turns out to be remarkably independent of the liquid content. Detailed studies of this finding, including x-ray tomography (cf. Fig. 1) and numerical simulation of constant mean curvature structures between spheres, are described in the subsequent project (2.2.3.2).

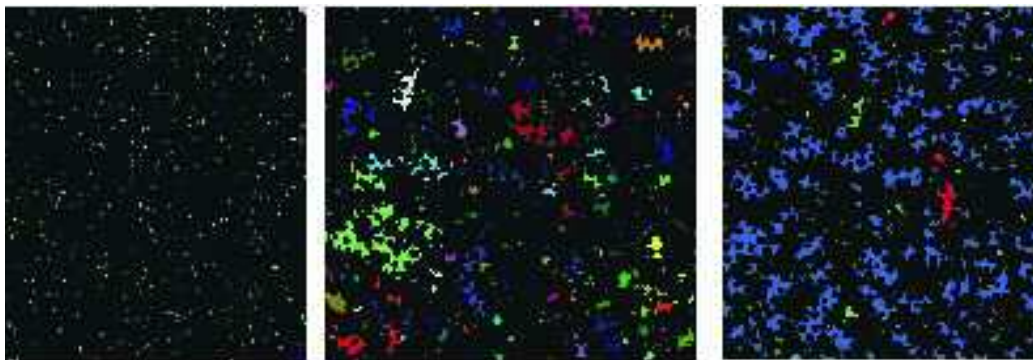


Figure 1: Distribution of liquid in a wet granular system, as seen by x-ray tomography. Shown are sections through a wet pile of glass beads at different water content. Left: 1%; center, 5.3%; right, 7.5%. Different colors indicate disjoint liquid clusters. At 5.3%, many liquid clusters are fully developed. At 7.5%, almost all liquid belongs to a single cluster which extends over the whole sample.

extreme non-equilibrium situation is at the heart of most of the intriguing features of granular matter.

In dry granulates, the dissipative processes are somehow ›hidden‹ in the momentary impact events. Wet granular matter, in contrast, provides its dominant dissipation by virtue of the hysteretic nature of the liquid bridges which form between adjacent grains: when two grains touch each other, a liquid bridge is formed and exerts an attractive force due to the surface tension of the liquid. However, for the bridge to disappear again, the grains must be withdrawn to a certain critical distance. That this dissipation can be dramatic is well known from the difference between the dry sand in the desert, which almost behaves like

A useful toy model of wet granular gases emerges if one considers just two-body hysteretic interactions between ideal hard spheres [1,2]. This simple model has proved quite successful in explaining most of the characteristic features of a wet granular pile. In simulations, we have established that many features of granular matter fluidized by vertical agitation may be recovered. Fig. 2 shows a simulation at three different times: at the very beginning, when the pile is still at rest (left), after some time, when the system is fully fluidized (center), and after an extended period of time when a quite interesting phenomenon, the granular Leidenfrost effect, has fully developed (right) [3]. This model system also exhibits surface melting

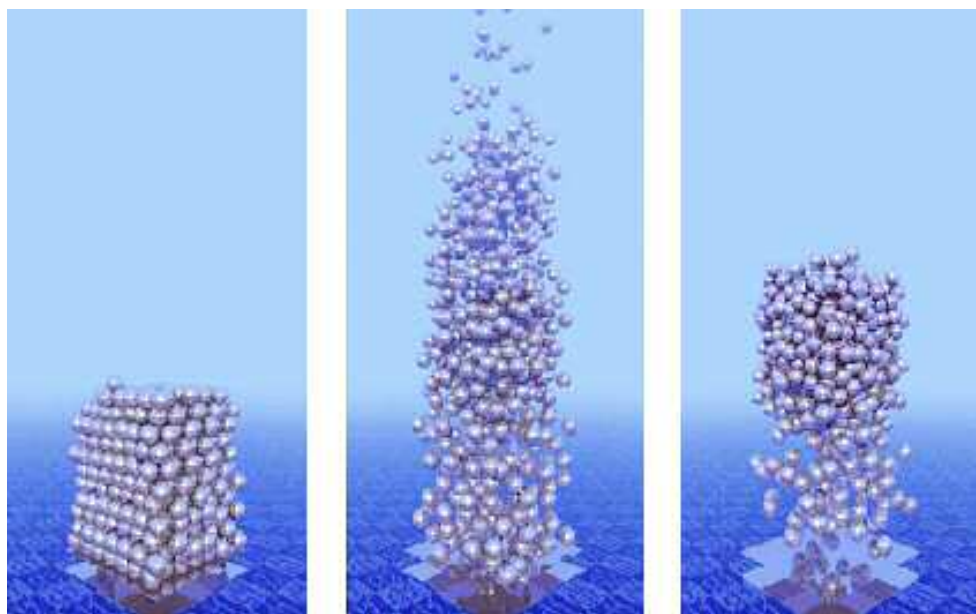


Figure 2 :
Granular dynamics simulation of a pile of spheres wetted by a liquid. At intermediate times (center), the pile is well fluidized. At large times (right), a Leidenfrost type phenomenon occurs, characterized by a solid plug hovering over a hot granular gas layer.

and other features analogous to phase transitions, which are also observed in experiments.

This model has a number of interesting properties. Its internal energy is a continuous function of time, and thus also its phase space trajectory is continuous, such that it can be dealt with using the extensive mathematical tools developed for dynamic systems [6]. In particular, it has been found that the recently developed fluctuation theorems seem to hold for granular systems, although the latter do not fulfill time reversibility as required by the standard formulations of fluctuation theo-

rems. In our system, we can follow in detail how dissipation takes place and try to alleviate the conditions for the fluctuation theorems such as to understand why they may apply at all to granular systems. Furthermore, wet granular materials provide a class of models general enough to cover standard granular physics as well as the dynamics of sticky gases, which serve as toy models for the formation of planetesimals from primordial clouds. We could show that at high attractive force, the limit of the sticky gas is reached, with all of the well-known scaling relations recovered. Our model may be more realistic, however, because impacts will never be perfectly sticky in reality.

At smaller attractive force, a wealth of new phenomena, including a symmetry-breaking phase transition, are found when merely observing the free cooling of this dissipative gas. This is shown in Fig.3, which shows the number of clusters as a function of simulation time for a one-dimensional wet granular gas. The dashed line represents the limit of the sticky gas, which approaches the well-known $-2/3$ scaling at large times. The solid line represents the simulation. It exhibits a condensation transition after a longer quiescent plateau phase. During the plateau, the system cools down until its granular temperature

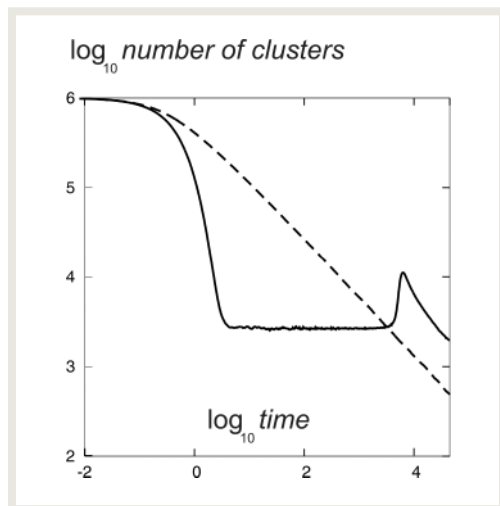


Figure 3:
The number of clusters (defined as grains connected by liquid bridges) in a freely cooling one-dimensional granular gas, as a function of simulation time. The characteristic peak corresponds to a phase transition which occurs when the granular temperature comes of the same order as the hysteretic energy loss scale.

comes within the energy scale of the capillary bridges. When this happens, the latter affect the dynamics strongly and lead to clustering. Finally, the sticky limit is approached from above. When one replaces the hysteresis in the interaction force by a fixed energy loss which is applied at each impact of two grains, the plateau and the peak vanish, thus demonstrating the importance of the hysteretic character of the force.

- [1] S. Herminghaus, *Advances in Physics* **54** (2005) 221.
- [2] M. Schulz, B. M. Schulz and S. Herminghaus, *Phys. Rev. E* **67** (2003) 052301.
- [3] K. Roeller, Diploma Thesis, Ulm 2005.
- [4] A. Fingerle, S. Herminghaus and V. Zaburdaev, *Phys. Rev. Lett.* **95** (2005) 198001.
- [5] G. Gallavotti and E. G. D. Cohen, *Phys. Rev. Lett.* **74** (1995) 2694.
- [6] C. Jarzynski, *Phys. Rev. Lett.* **78** (1997) 2690.
- [7] E. Ben-Naim et al., *Phys. Rev. Lett.* **83** (1999) 4069.

2.2.3.2 Statics and Dynamics of Wet Random Assemblies

Martin Brinkmann, Ralf Seemann

Mario Scheel, Zoé Fournier

K. Mecke (Erlangen), B. Breidenbach (Erlangen), W. Goedel (Chemnitz), M. DiMichiel (Grenoble, France), A. Sheppard (Canberra, Australia)

RANDOM ASSEMBLIES, SUCH as granular piles, textiles, fleece, or fur, are ubiquitous in nature, technology, and everyday life. They share the common feature of changing their mechanical properties dramatically in presence of a wetting liquid. Some of them such as the hairy cuticula of some plants (e.g. Mullein, *Verbascum Densiflorum B.*) are thus specially designed to avoid such moistening [1]. Most types of sand, the granular material par excellence, can be modeled as a random assembly of spherical particles. Other paradigmatic shapes like prolate ellipsoids or cylindrical rods describe larger classes of objects and may even serve for modelling fiber assemblies.

The astonishing stability of a sand-castle can be explained by the presence of numerous small water bridges in wet sand which span between adjacent grains [2]. The interfacial tension of the liquid-air interface and the negative Laplace pressure in these small liquid structures create a cohesive stress in the assembly. During shear, one observes discontinuous transitions between different capillary states of the liquid, in the simplest case the rupture and re-formation of bridges. This

mechanism opens up an additional path of energy dissipation during external agitation which, in a certain range of grain sizes, dominates over other dissipative mechanisms such as interparticle friction. The implications of the discrete amounts of energy lost in capillary transitions for the collective behaviour of wet granular material are discussed in the preceding project 2.2.3.1. In general, the mechanical behaviour of a wet random assembly

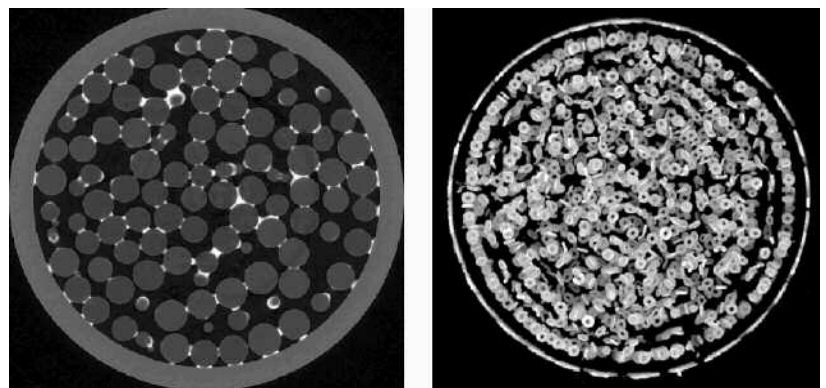


Figure 1: X-ray tomographies of wet assemblies of submillimetric glass spheres. The inner diameter of the glass tube containing the sample is about 9 mm. An aqueous NaI solution was used as the wetting liquid. The left image shows a slice through a sample, the right image is a projection of a three dimensional volume image (glass spheres and container are suppressed). Pendular bridges between adjacent spheres in contact appear as rings in the right image.

under a shear or compression will be linked to the local geometry of the assembly which governs the appearance of specific capillary states and the transitions between them.

Experimental techniques such as x-ray tomography or fluorescence microscopy can be utilized to image the liquid clusters in a three dimensional assembly. A wet random assembly of spheres can be easily prepared from slightly polydisperse, submillimetric glass beads and water. Figure 1 displays x-ray tomographies of such a wet assembly contained in a small glass tube. The most prominent structures at low water content are donut-shaped pendular bridges which grow and coalesce into larger liquid structures as the liquid content is increased [3]. Figure 2 illustrates experimentally observed pendular bridges (a,b) and the smallest type of liquid clusters (d,e) found between the glass beads. Surprisingly, this energetically driven reorganization of liquid does not lead to noticeable changes in the mechanical strength of the wet assembly. A beak-down of the shear resistance is observed beyond the percolation of liquid clusters [2,4].

If buoyancy is negligible, which typically holds for sub-milimetric liquid structures, the

shape of a pendular bridge between two spheres can be expressed in terms of analytic functions. All capillary states, however, which wet three or more spheres cannot be treated analytically and their study demands for numerical methods. The cluster shape and important physical quantities like the Laplace pressure of the cluster or the capillary forces acting on individual spheres can be obtained from a minimization of the interfacial energy, cf. Figure 2(c) and (f). All of the experimentally identified classes of liquid clusters resemble those found in regular packings. This can be explained by the remaining short range order in random assemblies of spheres. The question for the unexpected mechanical stability in the liquid cluster regime is linked to the evolution of the Laplace pressure during changes of the liquid content. The proposed qualitative dependence of the Laplace pressure on the cluster volume is depicted in Figure 3. Numerical minimizations provide an appropriate tool to find an answer to this open question.

Random assemblies of slender cylindrical rods typically exhibit a much smaller space filling when compared to assemblies of spherical particles. Other typical properties such as

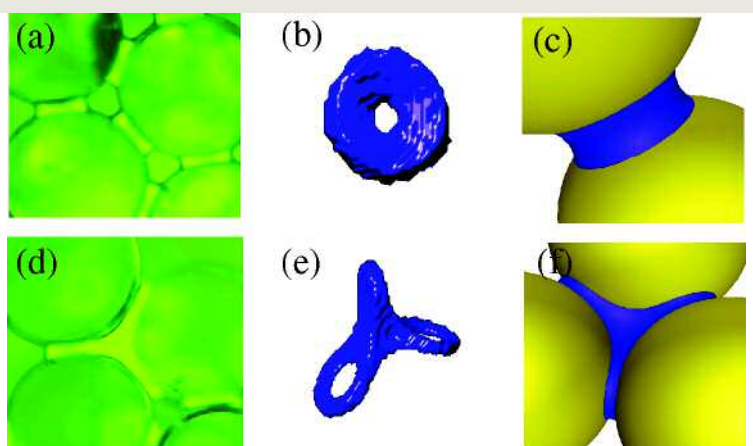


Figure 2: The series of images (a-c) show pendular bridges between spherical beads; images (d-f) display liquid clusters wetting three beads. Micrographs (a) and (d) are obtained by fluorescence microscopy. Three dimensional shapes in (b) and (e) are extracted from x-ray tomographies; the shapes depicted in (c) and (f) are the results of numerical minimization of the interfacial energy at fixed volume.

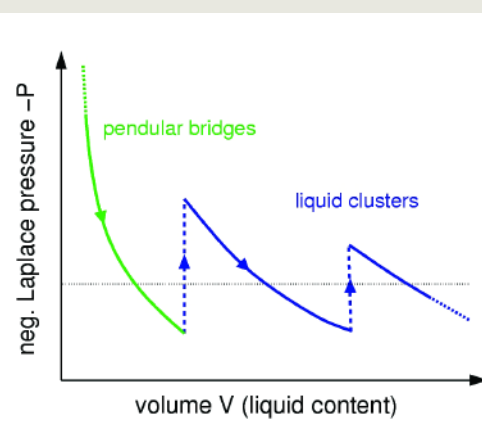


Figure 3: Schematic course of the Laplace pressure $-P$ of capillary states in an assembly of spheres for an increasing volume V . At small liquid volume only pendular bridges can be formed. Discontinuous transitions to larger liquid clusters occur at higher volumes. The Laplace pressure of these states, however, will fluctuate around a certain mean level (shown as the black dotted line).

a broad pore size distribution and the small correlation between contact points on a rod distinguishes them from random assemblies of spheres. The most important feature, however, is the anisotropic nature of the capillary interaction between cylindrical rods. In experiments, one observes a strong tendency of the wet rods to align and to form stable bundles. Numerical minimizations and analytical arguments show that the liquid can be found in localized, droplet-like states or in elongated droplets, which we call filaments, if the rods are close to parallel orientation. Similar droplet morphologies are found in the geometry of a rectangular slot [5]. The discontinuous transition between filaments and droplet states can be triggered by a change in the tilt angle and leads to a dissipation of energy

without breaking bridges. As outlined in the subsequent project 2.2.3.3 such transitions between elongated and localized liquid configurations are a generic feature of droplets wetting linear surface topographies [6,7].

- [1] A. Otten and S. Herminghaus, *Langmuir* **20** (2004) 2405.
- [2] S. Herminghaus, *Advances in Physics* **54** (2005) 221.
- [3] M. M. Kohonen et al., *Physica A* **339** (2004) 7.
- [4] Fournier et al., *J. Phys. Condens. Matter* **17** (2005) 477.
- [5] M. Brinkmann et al., *Appl. Phys. Lett.* **85** (2004) 2140.
- [6] M. Brinkmann and R. Blossey, *Eur. Phys. J. E* **14** (2004) 79.
- [7] R. Seemann et al., *Proc. Natl. Acad. Sci. USA* **102** (2005) 1848.

2.2.3.3 Wetting of Topographic Substrates

Ralf Seemann, Martin Brinkmann

Evgeny Gurevich, Krishnacharya Khare, Konstantina Kostourou

R. Lipowsky (Potsdam), J.-C. Baret (Eindhoven, The Netherlands), M. Decré (Eindhoven, The Netherlands), B. Law (Kansas, USA), E. Kramer (Santa Barbara, USA), F. Lange (Santa Barbara, USA)

ALTERNATIVELY TO CONVENTIONAL microfluidics, we consider systems with free liquid-liquid or liquid-vapor interfaces, which may therefore be called open microfluidic systems. An important advantage of open structures is that they are easy to clean and the liquid is freely accessible. The concept is to confine liquid to certain regions of the system, to keep it away from others, to transport it along pre-fabricated connection lines, and to mix it on demand. We do this by offering an appropriate surface topography to the liquid. In this approach, one takes advantage of the fact that the affinity of the liquid to corners and grooves is strongly different as compared to planar surfaces. If, for instance, the intrinsic contact angle between the liquid and the substrate material is sufficiently small, the liquid will strongly prefer to wet steps [1] or grooves

[2]. We explore the static wetting morphologies and their manipulation varying the wettability or geometry of the grooves.

Depending on control parameters such as the contact angle, the liquid volume, and the geometry of the grooves, a rich morphological behavior of liquid droplets of variable size (volume) can be found [2-4]. In case of rectangular grooves droplet like morphologies (D) can be found for large contact angles or shallow grooves. For decreasing contact angle or increasing aspect ratio liquid filaments with positive ($F+$) and liquid filaments with negative Laplace pressure ($F-$) can be found in experimental and numerical results as shown in Fig. 1. These liquid morphologies are in excellent agreement with the analytically derived morphology diagram, which is depicted in Fig. 2. Similar wetting morpholo-

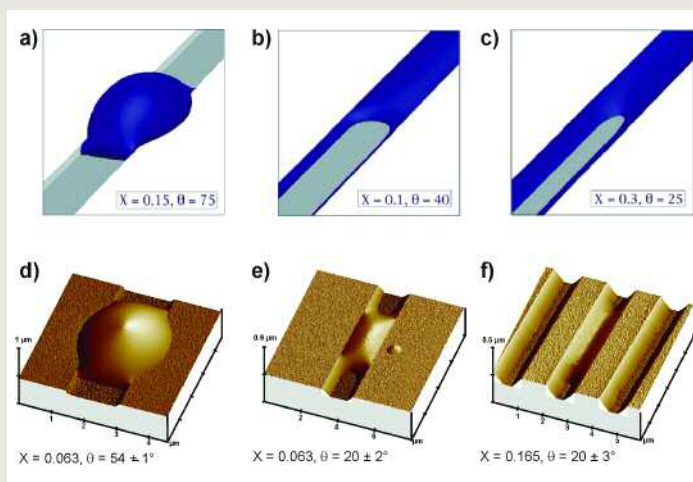


Figure 1: a) - c) Numerically generated wetting morphologies and d) - f) Scanning force micrographs of polystyrene droplets wetting a topographically structured substrate with rectangular cross section. a) + d) droplet morphologies (D). b) + e) liquid filaments, (F+), with positive Laplace pressure, $P_L > 0$. c) + f) liquid filaments, (F-), with $P_L < 0$. Liquid morphologies with $\theta < 45^\circ$ are in coexistence with liquid wetting the lower corner of the grooves.

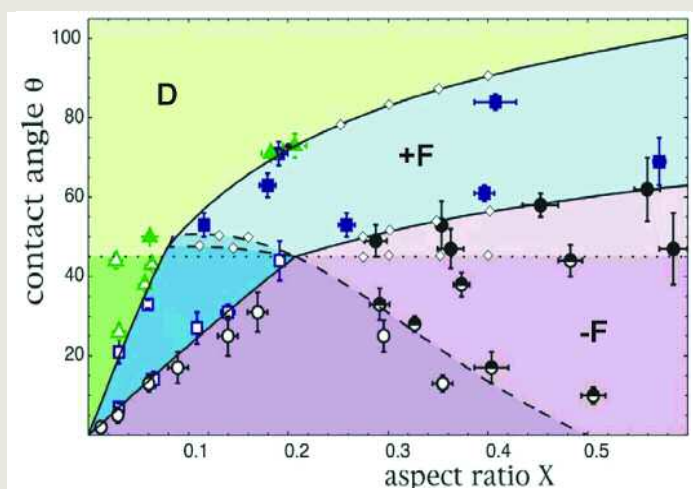


Figure 2: Analytically derived morphology diagram as a function of groove aspect ratio X and material contact angle θ . The solid line between the areas (F+) and (F-) denote liquid morphologies with zero mean curvature. The symbols denote experimental results from AFM scans. All experimental determined morphologies are fully consistent with the theoretical classification.

gies can be found for chemically structured, plane substrates where hydrophilic stripes are surrounded by a hydrophobic matrix [5] and for wetting morphologies on wet random assemblies as described in the preceding project. However, liquid morphologies on planar substrates always exhibit a positive Laplace pressure. This seriously restricts the applica-

bility of chemically patterned substrates to open microfluidics. As described in the following for rectangular grooves, topographic structures provide considerable advantages. To transport liquid along topographic grooves it is necessary to change the physical properties of these structures dynamically, such as to induce transitions between different liquid morphologies. This can result, if conceived properly, in controlled liquid transport. Moreover, electrowetting allows to reversibly change the apparent contact angle of an electrically conducting liquid on a solid substrate. The variation of the contact angle can be as large as several 10° . To minimize electrochemical effects we apply an ac-voltage. If one starts with a droplet like wetting morphology and increases the applied voltage, the length of the liquid filament shows a threshold behavior for the filling when the line of zero mean curvature in the morphological diagram is approached, c.f. Fig. 3. The finite lengths of the liquid filaments can be described by a voltage drop along the filament using an electrical transmission line model [6]. Moreover, the length of the liquid filament is sensitive to the chemical content of the liquid. This behavior gives us an easy handle to manipulate and transport liquid along grooves or sense the ionic content of a liquid and might enable the construction of complex and highly integrated open microfluidic devices.

In case of rectangular grooves, the liquid filaments reversibly grow and shrink in length as function of the applied voltage. The advancing and receding dynamics that defines the minimum switching time of the liquid filaments can be described exclusively by capillary forces, assuming the electrowetting-contact angle to vary along the liquid filaments according to the voltage drop along the filament [7].

Although it is easier to produce triangular grooves, they can not as easily be used to transport liquid reversibly along prefabricated grooves. Retracting an elongated liquid filament from a triangular groove into its reservoir by ramping down the applied voltage

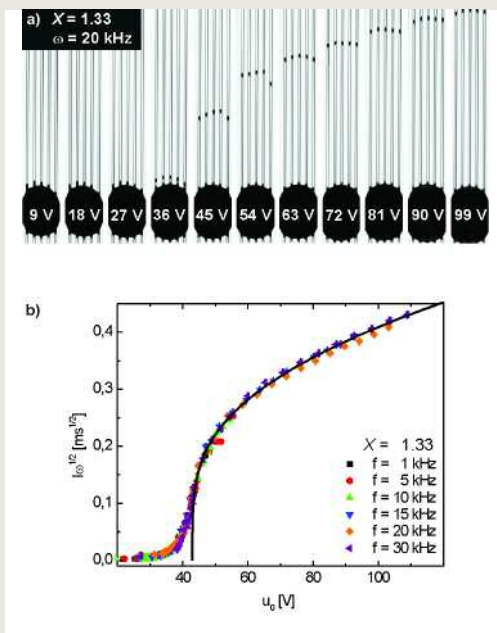


Figure 3: Spreading of liquid into grooves with rectangular cross section by electrowetting. Due to the slanted interface only the fronts of the liquid channels are visible in the optical micrographs. The dataset in b) shows the length of liquid filaments as function of the applied acvoltage for various frequencies, which collapse on a single master curve when scaled with the frequency of the applied ac-voltage. Fitting the theoretical model to the master curve yields the conductivity of the liquid.

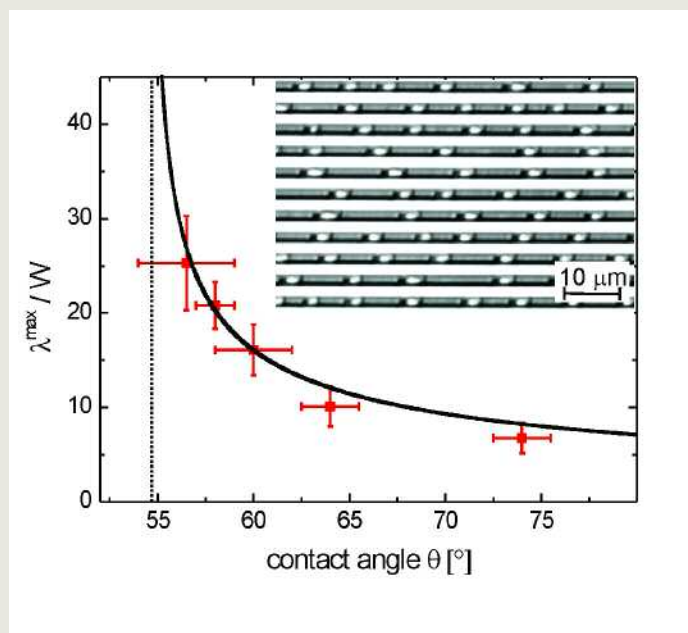


Figure 4: Preferred droplet distance resulting from the dynamic instability of liquid filaments with positive mean curvature in triangular grooves. The experimental data are shown as red squares whereas the solid line denotes the theoretical expectation. The wedge angle of the triangular groove is indicated as dotted line. *Inset*: Optical micrograph of polystyrene droplets with a well defined spacing in triangular grooves.

fails. When the contact angle of a liquid filament suddenly increases above the filling threshold, the liquid filament becomes dy-

namically unstable and decays into isolated droplets with well defined preferred distance [8].

- [1] M. Brinkmann and R. Blossey, *Eur. Phys. J. E* **14** (2004) 79.
- [2] R. Seemann et al., *PNAS* **102** (2005) 1848.
- [3] R. Seemann, E. J. Kramer and F. F. Lange, *New Journal of Physics* **6** (2004) 111.
- [4] T. Pfohl et al., *Chem. Phys. Chem.* **4** (2003) 1291.

- [5] M. Brinkmann and R. Lipowsky, *J. Appl. Phys.* **92** (2002) 4298.
- [6] J.-C. Baret, M. Décré, S. Herminghaus, and R. Seemann, *submitted to Langmuir*.
- [7] J.-C. Baret et al., *Langmuir* **21** (2005) 12218.
- [8] B. Law, E. Gurevich, M. Brinkmann, K. Khare, S. Herminghaus, and R. Seemann, *submitted to Langmuir*.

2.2.3.4 Discrete Microfluidics

Ralf Seemann

Craig Priest, Enkhtuul Surenjav, Magdalena Ulmeanu, Dmytro Melenevsky
T. Salditt (Göttingen), A. Griffith (Strasbourg, France)

WE EMPLOY MONODISPERSE emulsions to compartment liquids for microfluidic processing. Using this approach, some inherent problems of conventional microfluidic systems, where single phase liquids are transported through microchannel networks, can be circumvented [1]: for instance, axial dispersion can be suppressed entirely due to the nature of the droplets carrying various chemical contents as individual compartments. And second, mixing of two components can be

achieved within each droplet separately, and is found to proceed quite efficiently by the twisty flow pattern emerging within droplets when they are moved through a wavy channel system [2]. If the volume fraction of the continuous phase is reduced to a few percent only, the emulsion is called gel-emulsion due to its macroscopic rheological properties. Here, the dispersed droplets (compartments) assemble to a well-defined topology, analogous to foam. Accordingly, the position of a single droplet with a certain chemical content is fully determined within an ensemble of droplets while being transported through microfluidic channels.

To control the volume of the compartments precisely and to guarantee a well defined ›foam like‹ structure for a given confining channel geometry, it is mandatory to use droplets with excellent monodispersity. We developed a one-step, *in situ* method for the production of monodisperse gel emulsions, suitable for microfluidic processing [2], see Fig. 1. The to be dispersed phase is injected into the continuous phase where it is guided in a shallow channel and stabilized by the surrounding continuous phase and the channel walls. When the confining bottom wall ›vanishes‹ at a topographic step, the continuous stream of the phase to be dispersed decays into single droplets. This step-emulsification technique allows the *in situ* production of monodisperse gel-emulsions with volume fraction up to 96%. The mutual proximity of the single droplets, which follows from the small volume fraction of the continuous phase, allows for selectively induced coalescence to initiate chemical reactions between adjacent compartments. This can be done by applying a voltage pulse between two adjacent droplets via electrodes intergrated into a microfluidic channel, as shown in Fig. 2 [3]. For aqueous droplets on the micrometer

Figure 1: Fabrication of monodisperse (gel-) emulsions *in-situ* in a microfluidic device via step emulsification. a) The stream of the to be dispersed phase is stabilized between the coflowing continuous phase and the channel walls. At the topographic step, the confining bottom wall is ›removed‹ and the stream of the phase to be dispersed breaks up into monodisperse droplets. b) + c) *in-situ* fabricated gel-emulsion with 75% and 93% dispersed phase volume fraction, respectively.

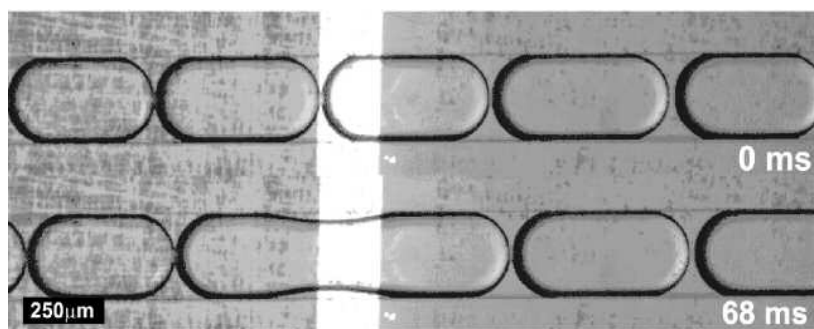
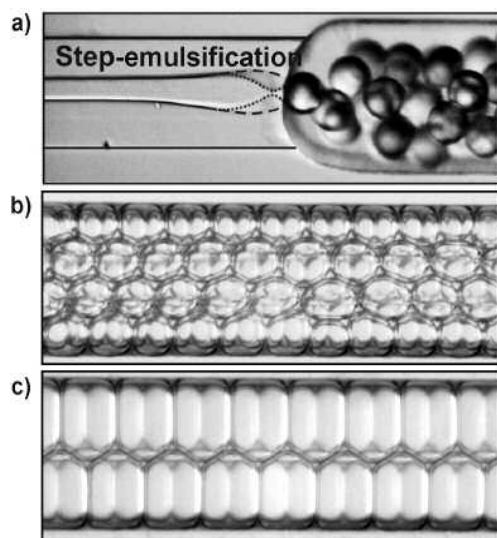


Figure 2: Emulsion droplets united in a bamboo structure selectively coalesced by applying a voltage between electrodes. The bright middle part shows the gap between the electrodes.

range, the diffusive mixing after coalescence will occur on a millisecond time scale leading to a well defined trigger for studying reaction kinetics.

The motion of a gel emulsion in a solid channel system is mainly governed by two physical aspects of the system. One is the dynamics of thin liquid films and three-phase contacts at solid surfaces, which has been investigated in many studies in recent years [4-9]. The other aspect concerns the mechanical properties of the gel emulsion itself. It is well known that for rather dry foams, which correspond to small continuous phase volume fraction in our case, move within pipes by plug flow. This is due to the finite threshold stress required to deform the foam network (e.g., the finite energy required for a T1-transition). The flow resistance of the foamy emulsion in a channel with spatially constant cross section is thus solely determined by the interaction of the contact lines and Plateau borders with defects at the walls, and by the flow resistance in the thin liquid films at the wall. However, when the channel (or pipe) geometry is temporarily changed, or when the foamy emulsion flows along a channel the

cross section of which varies along its axis, interesting topological transformations within the single compartments can be induced as depicted in Fig. 3. If the shape of the channel is tailored appropriately, controlled manipulation of the emulsion droplets by the channel geometry may be achieved, in order to position, sort, exchange, compile and redistribute liquid compartments, possibly with different chemical contents.

Besides the passive manipulation of foam like topologies by the channel geometries, we study the active manipulation of the resulting topology by external stimuli. Figure 4 shows the transition of a two row structure to a bamboo structure, and the selective guiding of droplets by applying a magnetic field using a ferrofluid as continuous phase, which is sensitive to magnetic fields. Replacing the ferrofluid by a liquid crystal, the emulsion is sensitive to temperature because the structure of the continuous phase is depending on temperature, as described in greater detail in the subsequent project.

Our approach may be called discrete microfluidics, and is well suited for extensive applications in combinatorial chemistry, DNA

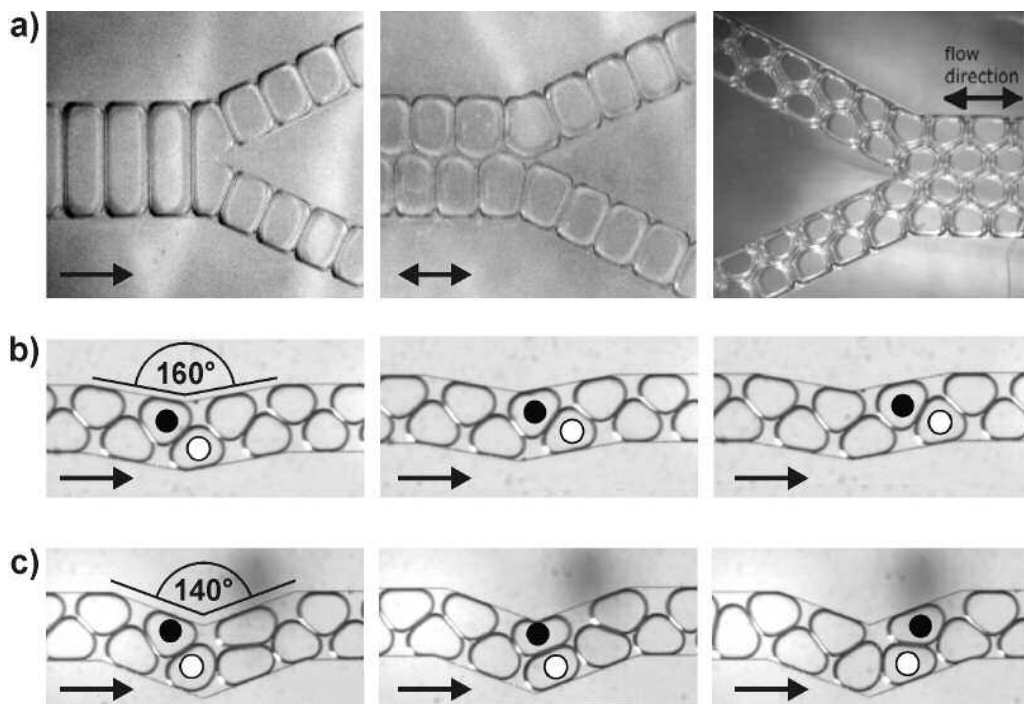


Figure 3: Interaction of mono-disperse gel-emulsions with a confining geometry. a) Depending on the ratio of channel to droplet size, the droplets are either split in half at the y-junction, or a foam like topology with two or more rows can be separated or assembled like a zipper. b) 160° corner: the sequence of droplets is not affected by the channel geometry c) 140° corner: the sequence of droplets of the top row is changed by one position relative to the bottom row.

sequencing, drug screening, and any other field where similar chemical reactions have to be induced with a large number of different molecules involved. Experiments to study the polymerization of e.g. collagen as a function of pH value are in preparation and explained in project 2.2.3.8.

Moreover, the lamellae can be used as confin-

ing geometry e.g. for lipids that form membranes in case the continuous phase volume fraction is minute. The usage of this well defined membrane topology in order to study the exchange of molecules between single compartments or for the analysis of the lipids by scattering techniques [10] is described in project 2.2.3.6.

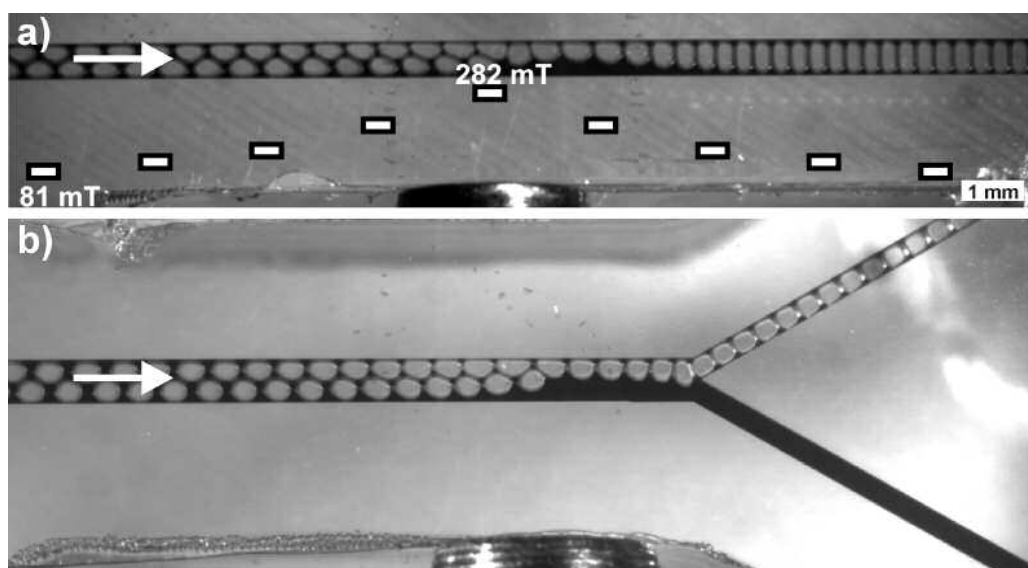


Figure 4:
Using a ferrofluid as continuous phase a) a two row topology can be switched to a bamboo structure by applying a magnetic field. The local field strength is indicated by the white bars. b) Using the same effect, droplets can be selectively guided to an outlet by applying a magnetic field.

- [1] K. Jacobs, R. Seemann, and H. Kuhlmann, *Nachrichten aus der Chemie* **53** (2005) 302.
 [2] C. Priest, S. Herminghaus and R. Seemann, *Appl. Phys. Lett.* **88** (2006) 024106.
 [3] C. Priest, S. Herminghaus and R. Seemann, submitted to, *Appl. Phys. Lett.*
 [4] R. Seemann, S. Herminghaus and K. Jacobs, *Phys. Rev. Lett.* **86** (2001) 5534.
 [5] R. Seemann, S. Herminghaus and K.

- Jacobs, *Phys. Rev. Lett.* **87** (2001) 196101.
 [6] S. Herminghaus, R. Seemann and K. Jacobs, *Phys. Rev. Lett.* **89** (2002) 056101.
 [7] J. Becker et al., *Nature Materials* **2** (2003) 59.
 [8] R. Seemann, et al., *J. Phys.: Condens. Matter* **17** (2005) S267.
 [9] C. Neto et al., *J. Phys.: Condens. Matter* **15** (2003) 3355.
 [10] T. Pfohl et al., *Chem. Phys. Chem.* **4** (2003) 1291.

2.2.3.5 Wetting and Structure Formation at Soft Matter Interfaces

Christian Bahr

Vincent Designolle, Wei Guo

THE STRUCTURE OF soft matter systems is easily influenced by external fields and forces. For example, a weak electric field is able to change the molecular alignment, and thus the optical properties, of a nematic liquid crystal phase. The presence of an interface may act on soft matter systems like a localized field and accordingly the structure near an interface often differs from the structure of the corresponding volume phase. In many cases, such as the free surface of thermotropic liquid crystals [1], this behaviour is especially pronounced near phase transitions, where one may observe a spatially differentiated coexistence of two phases, one of which being preferred by the interface. Understanding the behavior of soft matter at interfaces is important not only from the viewpoint of basic research but also for many applications; examples range from emulsion paint over printer ink and liquid crystal displays to membrane systems for drug delivery.

This project is concerned with soft matter systems containing thermotropic liquid crystals as one component. The liquid crystal component provides an «extra ingredient» to these systems namely the various phases and phase transitions that are present in these materials. One emphasis of the project is the study of the interface between liquid crystals and water or aqueous surfactant solutions near the phase transitions of the liquid crystal. The results will be of importance for basic aspects of wetting as well as for the development of new systems to be utilized in discrete microfluidics. A second focal point is the study of liquid crystal nanostructures which are generated by antagonistic boundary conditions and/or spatial confinements which are present in, e.g., open microfluidic channels.

For the study of liquid crystal/water interfaces a phase-modulated ellipsometer was constructed and a suitable sample cell was designed which enables the preparation of a planar interface between the two volume

phases. First measurements were conducted with the liquid crystal 8CB (octylcyano-biphenyl) at the interface to pure water and aqueous solutions of the surfactant CTAB (hexadecyltrimethylammonium bromide) in the temperature range around the nematic – isotropic transition of 8CB ($T_{NI} = 41^\circ\text{C}$). Our results [2] show, that at temperatures above T_{NI} the interface is covered by a nematic wetting layer provided that the aqueous phase contains CTAB with a concentration $c_a \geq 0.8 \mu\text{M}$. The thickness of the nematic layer shows a divergence-like increase when the volume transition temperature T_{NI} is approached from above and this behaviour becomes more pronounced with increasing surfactant concentration (Figure 1).

The experimental data were analyzed within the framework of a phenomenological model, in which the Landau-de Gennes theory of the nematic – isotropic transition is extended by a linear coupling of the nematic order parameter to an ordering surface field V . Data ob-

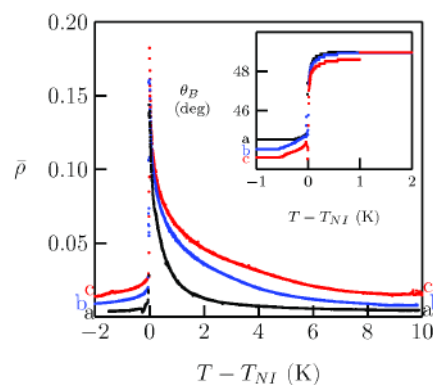


Figure 1: Temperature dependence of ellipticity coefficient $\bar{\rho}$ and Brewster angle θ_B at the interface between the thermotropic liquid crystal 8CB and aqueous CTAB solutions with concentrations $c_a = 0.8 \mu\text{M}$ (a), $3 \mu\text{M}$ (b), and $30 \mu\text{M}$ (c). T_{NI} designates the nematic - isotropic transition temperature of the volume liquid crystal phase.

tained for different c_a values could be described by the Landau model by adjusting the value of V only, with all other parameters remaining unchanged. In other words, the surfactant concentration can be used for a direct control of the ordering interface field V . The relation between V and c_a is clearly nonlinear (Figure 2) and can be described by a fitting function which has the form of a Langmuir

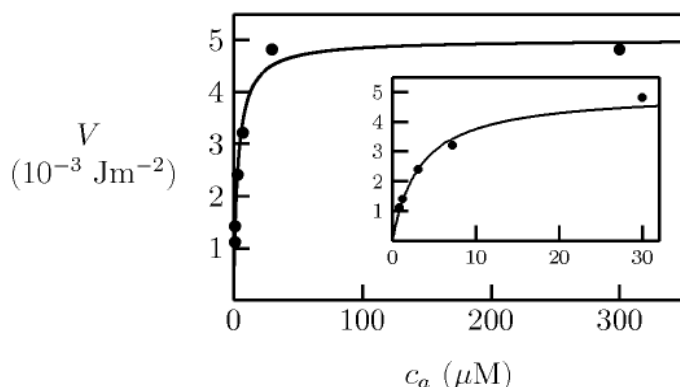


Figure 2:
Relation between interface potential V and CTAB concentration c_a in the aqueous volume phase. The solid line is a fit using a function possessing the form of a Langmuir adsorption isotherm.

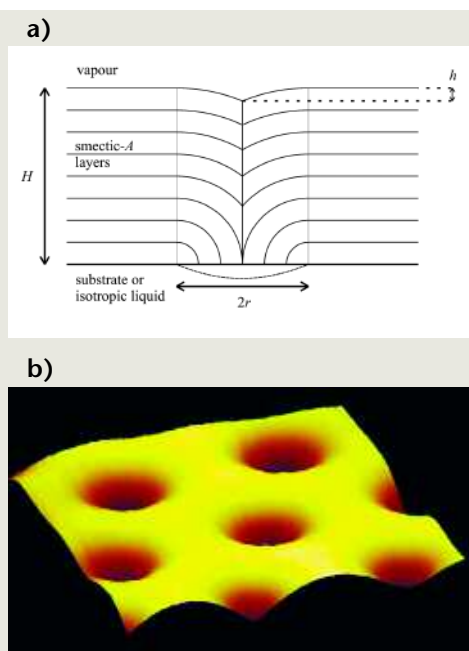
adsorption isotherm indicating that the magnitude of V is linearly related to the amount of adsorbed surfactant.

Temperature and surfactant concentration enable thus a comprehensive control of the structure of the liquid crystalline interface layer which separates the two isotropic volume phases. We will use this result for the development of new systems to be employed in discrete microfluidics applications (for details concerning discrete microfluidics see the previous project) in which liquid crystal compounds are used as continuous phase of gel emulsions. For example, a gel emulsion of water droplets in an isotropic liquid crystal could be prepared in which the lamellae separating the water cells can adopt an either liq-

uid crystalline or isotropic structure (depending on temperature and surfactant concentration); in this way even gel emulsions with smectic lamellae could be prepared although it is hardly possible to disperse water droplets in a smectic volume phase. Our results are also of relevance for basic aspects of wetting, recent theoretical work [3] on wetting layers in isotropic liquid crystals (described in more detail in project 2.2.3.10), and surfactant-induced interface transitions in other systems like n-alkanes [4].

Besides the study of liquid crystal/water interfaces we investigate structure formation in liquid crystal phases induced by antagonistic boundary conditions and/or spatial confinement. An example is the modulation of the smectic-A/air interface by focal conic defects in thin smectic films on silicon substrates. A focal conic defect, which is generated by opposite molecular alignment conditions at the smectic-A/air and smectic-A/substrate interface, consists of an arrangement of curved equidistant smectic layers and leads to a depression of the free surface (Figure 3). Using AFM we have measured the depression depth h as a function of temperature for different smectic compounds. Our results [5] show that the behaviour of h strongly depends on the type of the high-temperature phase above the smectic-A phase (nematic or isotropic) and on the nature of the corresponding phase transition (second-order or first-order).

Figure 3:
a) Schematic sketch of the smectic layer structure in a focal conic defect which is formed above a circular area with diameter $2r$ in which the molecules are aligned parallel to the substrate (at the air interface, the molecules align always perpendicular to the interface).
b) AFM image of defect-induced depressions in the smectic-A/air interface. The depth of the depressions amounts to 250 nm, the lateral dimension of the shown area is 25 μm .



- [1] R. Lucht and Ch. Bahr, *Phys. Rev. Lett.* **78** (1997) 3487; R. Lucht et al., *J. Chem. Phys.* **108** (1998) 3716; R. Lucht, Ch. Bahr and G. Heppke, *Phys. Rev. E* **62** (2000) 2324.
- [2] Ch. Bahr, *Phys. Rev. E* **73**(2006) 030702(R).
- [3] H. Stark, J. Fukuda and H. Yokoyama, *Phys. Rev. Lett.* **92** (2004) 205502; J. Fukuda, H. Stark and H. Yokoyama, *Phys. Rev. E* **69** (2004) 021714.
- [4] Q. Lei and C. D. Bain, *Phys. Rev. Lett.* **92** (2004) 176103; E. Sloutskin et al., *Faraday Discuss.* **129** (2005) 339.
- [5] V. Designolle et al., *Langmuir* **22** (2006) 363.

2.2.3.6. Membrane Assembly for Nanoscience

Peter Heinig, Ralf Seemann
Craig Priest, Magdalena Ulmeanu

IN BIOLOGICAL CELLS, membranes act as barriers between reaction compartments and control the transport of substances between cell organelles, the cytoplasm and the environment. The transport properties of biological membranes are highly specific and are controlled by a number of different parameters, as electric potentials or concentration gradients. The aim of this project is to make use of these membrane properties in order to control interactions between single reaction compartments, as for example water droplets in a water-in-oil (W/O) emulsion, fabricated using microfluidic devices. Furthermore, the potential of novel experimental methods for the analysis of objects immersed in membranes, such as transmembrane proteins or nanostructures, is investigated.

Gel-emulsions are emulsions with a small volume fraction of the continuous phase and form foam like structures with planar lamellae separating the emulsion droplets. A further decrease of the amount of continuous phase results in a thinning of the lamellae, possibly until a single bilayer of surfactant molecules remains (Fig. 1). In order to study single lamellae in microchannels under static and dynamic conditions, a microfluidic device has been used (Fig. 2): In a cross-junction of channels, water droplets in oily surroundings have been brought into contact such that a planar lamella is formed. The design allows to apply an electric potential across the lamella and to measure the film thickness by impedance measurement or the usage of voltage sensitive dyes. It was found that the thickness of the lamella depends on the substances used and on the applied pressure.

For this reason, the experimental conditions, under which black membranes are formed, were studied separately using the thin-film-technique developed by Scheludko. This

technique is commonly used to investigate free standing liquid films. The film is formed in a circular opening within a porous plate and a pressure between the film phase and surrounding phase is applied. The setup allows to observe the formation kinetics of thin films [1,2] and to precisely measure the film thickness in dependence of the disjoining pressure. Here, a Scheludko-setup has been built using a porous Teflon plate (porosity $\sim 10\mu\text{m}$) and the oily film has been observed in aqueous surroundings using optical mi-

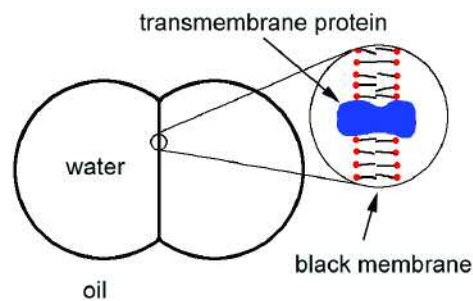


Figure 1: Sketch of two emulsion droplets of a water-in-oil emulsion forming a black membrane

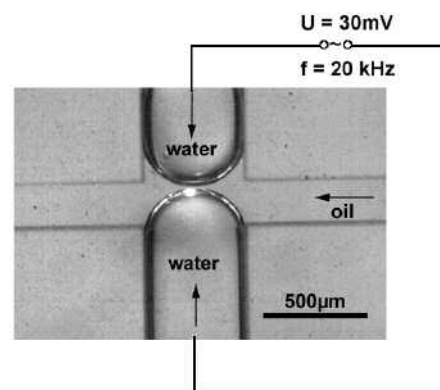


Figure 2: Microfluidic device for investigating single lamellae in microchannels.

croscopy. First experiments show that some systems, as for example tetradecane/monoolein/water, form stable black membranes. Closely packed monodisperse emulsions form crystalline structures and exhibit a high geometrical order. This property of 'emulsion crystals' can potentially be used for X-ray structure analysis of objects immersed in the lamellae between droplets or Plateau borders of the crystal. It is obvious that the monodispersity of the emulsion, as well as a precise control of the thicknesses of the lamellae, is of crucial importance. The fabrication of monodisperse emulsions with a low volume fraction of the continuous phase is subject of project 2.2.3.4. Here, the rotating cup technique has been applied (Fig. 3): The aqueous phase flows through a hydrophobized glass

capillary into a cup containing the oily phase and a surfactant. Rotating the cup with constant angular velocity exposes the water to shear flow and highly monodisperse emulsions can be created, reducing the polydispersity to less than 2% [3]. Oily phase from the generated emulsion was then removed by placing it on a porous Teflon plate and by applying an underpressure such that oil slowly flows out of the emulsion. Figure 4 shows the formation of planar lamellae in a regular emulsion structure using water/tetradecane/monoolein. The functionality of these lamellae will be tested by adding ion channel proteins, which penetrate the lamellae as soon as black membranes are formed. The lamellae then become permeable for specific ions, and ion transport can be detected for example utilizing fluorescent ion indicators also used in project 2.2.3.8. Other microfluidic devices which allow to create monodisperse emulsions and to precisely control the volume fraction of the continuous phase are under construction.

Figure 3: Rotating cup technique for the fabrication of monodisperse emulsions. Water flows through a capillary in a rotating cup containing the oily phase.

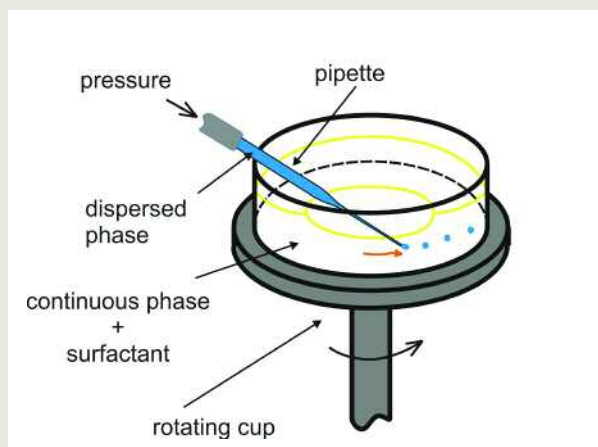
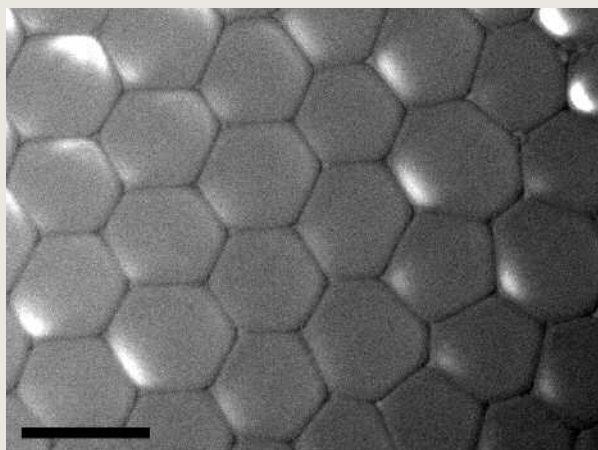


Figure 4: Planar lamellae in a water/tetradecane/monoolein emulsion. The bar represents 50 μm .



- [1] P. Heinig and D. Langevin, *Eur. Phys. J. E* **18** (2005) 483.
- [2] P. Heinig, C. Márquez Beltrán and D. Langevin, *Phys. Rev. E* in press.
- [3] P.B. Umbanhowar, V. Prasad and D.A. Weitz, *Langmuir* **16** (2000) 347.

2.2.3.7 Spectroscopy of Aqueous Surfaces

Manfred Faubel

B. Winter (Berlin), I.V. Hertel (Berlin), P. Jungwirth (Prag, Czech R.), S. Bradforth (Los Angeles, USA),
B. Abel (Göttingen), A. Charvat (Göttingen)

THE DISTINCT PHYSICAL properties and physico-chemical processes of liquid surfaces are determined ultimately by atomic phenomena and molecular forces in liquids. Yet, macroscopic measurements, even on scales ranging down to nanometers, provide only very indirect and averaged information on individual molecules in a liquid solution [1,2]. For atomistic studies of the state and of the arrangement of individual molecules in an aqueous surface we use photoelectron spectroscopy (Fig. 1a) which provides binding energies of individual atomic orbital energy levels for isolated molecules or solvated ions in the liquid from the analysis of the photoelectron kinetic energy spectra. In addition, the atomic or molecular density of molecules in a liquid solution can be determined by an intensity measurement of the atom-specific photoelectron emission lines. It has a surface layer probing depth of approximately 0.5 nm.

The photoelectron energy can be measured with high precision by deflecting the emitted photoelectrons in well defined electrostatic fields in a vacuum environment (Fig. 1b). This is in conflict with the notable, high water vapor pressure of aqueous liquids (~ 10 mbar) and, therefore, a very thin, fast flowing, liquid jet was developed as a vacuum exposed free liquid water surface. Sufficiently narrow liquid water jets, with diameters smaller than mean free path in water vapor, evaporate in vacuum without the occurrence of molecular collisions and/or electron scattering or soft x-ray photon absorption events in the emerging vapor cloud. Because the experimental free vacuum surface of liquid water can be only a few $10 \mu\text{m}$ wide, a photon source with high brilliance is required, which became available recently with modern synchrotron photon sources for the energy range of interest, between $15 \text{ eV} < h\nu < 1000 \text{ eV}$. The principal setup scheme for the liquid water jet photo-

electron spectroscopy is illustrated in Figure 1b [1].

Examples for synchrotron radiation photoelectron spectrum measurements on liquid water are presented in Figure 2 [3]. The neat water spectrum (bottom) is composed of the liquid water surface spectrum and of a contribution from the water vapor cloud evaporating from the room temperature liquid jet. It shows the four different valence bond elec-

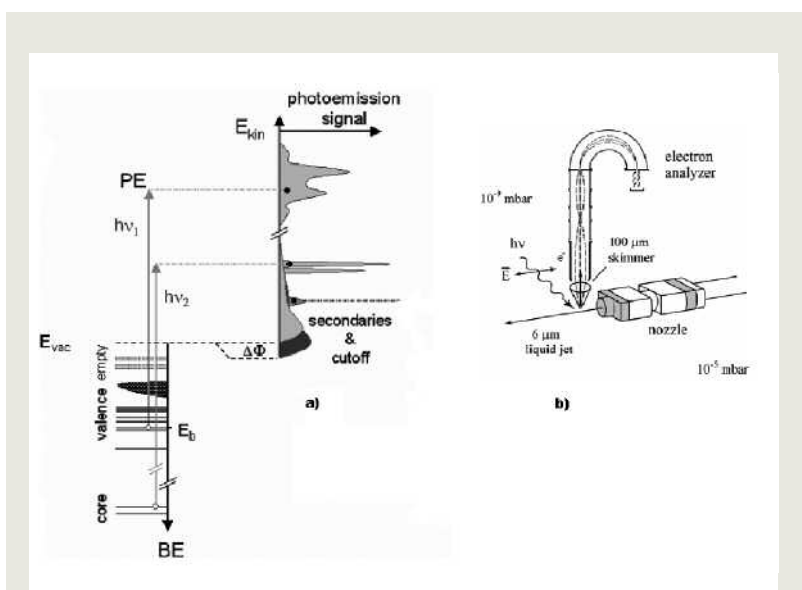
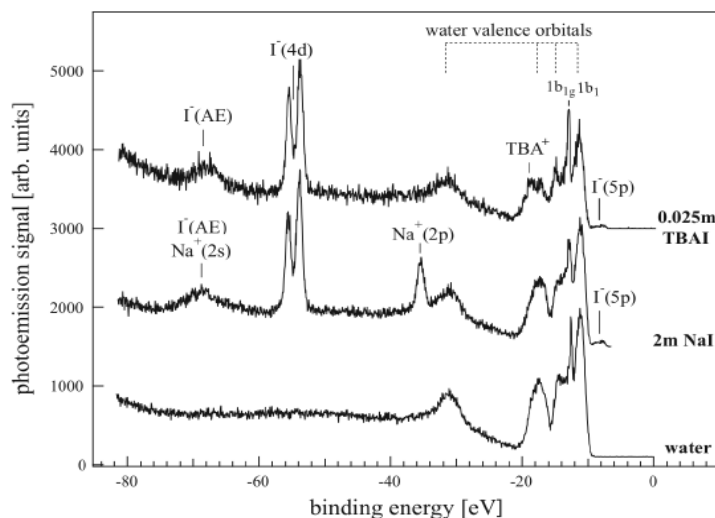


Figure 1: Photoelectron emission from valence bands of molecules or from inner core electron energy levels of atoms can be used to determine the binding energies and density of states distributions of all bound state electrons in a target (a). The electron binding energy is the difference between the incident photon energy and the observed photoelectron kinetic energy, $BE = h\nu - E_{kin}$. In chemically bonded atom states and in condensed matter electron binding energies show bonding specific energy shifts, called chemical shift or solvation shift. They are induced by the electronic nature of the molecular interaction forces. For measurements on liquid aqueous solutions with high vapor pressure (> 8 mbar for pure water at 0 °C) a liquid micro-jet with less than $10 \mu\text{m}$ diameter is used to maintain collision free molecular beam vacuum conditions in the vapor cloud emerging from the liquid surface (b). The kinetic energy spectrum of emitted photoelectrons is measured in ultrahigh vacuum by an electrostatic electron energy analyzer. Intense, focused, monochromatic synchrotron radiation with 30 eV to 1000 eV photon energy is used for the photoemission spectroscopy.

Figure 2: Photoemission spectra of (bottom) liquid water, and (middle) 2 m NaI and (top) 0.025 m TBAI aqueous solution measured at 100 eV photon energy. Ion emission is labeled. Electron binding energies are relative to vacuum, and intensities are normalized to the electron ring current. Nearly identical iodide signals are observed for the two salt solutions, even though the concentration of the surfactant is a factor 80 lower. Energy differences of $I^-(4d)$ peak positions for the two solutions are not observed.



tron energy levels of the H_2O molecule marked by the upper scale insert in Fig. 2. The narrow peak designated $1b_{1g}$ is a water vapor feature. A pure vapor phase spectrum is measured separately and can be subtracted. The liquid phase spectrum exhibits a considerable broadening of the four principal orbitals by the inhomogeneous molecular environment of the liquid water. In addition, the average liquid ionization peak energies are lowered by 1.6 to 1.9 eV with respect to the gas phase, which is theoretically understood as a consequence of the condensed phase surroundings with a high dielectric constant.

A more complex case for salt ion solvation in liquid water is investigated in Figure 2 (middle and top) in photoelectron spectra from a 2 mol solution of NaI, and for a 0.025 mol solution of the surface active tetra-butyl-ammonium iodide salt (TBAI)[3]. The latter is surface enriched by a factor of 80 as compared to the iodine in the «normal» salt aqueous NaI solution, and shows a very strong enhancement of the I^- anion photoelectron peak intensity in relation to the absolute salt concentration. A most remarkable and, still, unexplained experimental result is the independence of the observed electron binding energy of a given ion (Cl^- , Br^- , I^- , Li^+ , Na^+ , K^+ , Cs^+) with changing concentration of the solute salt in aqueous solution and with different counter-ions [4].

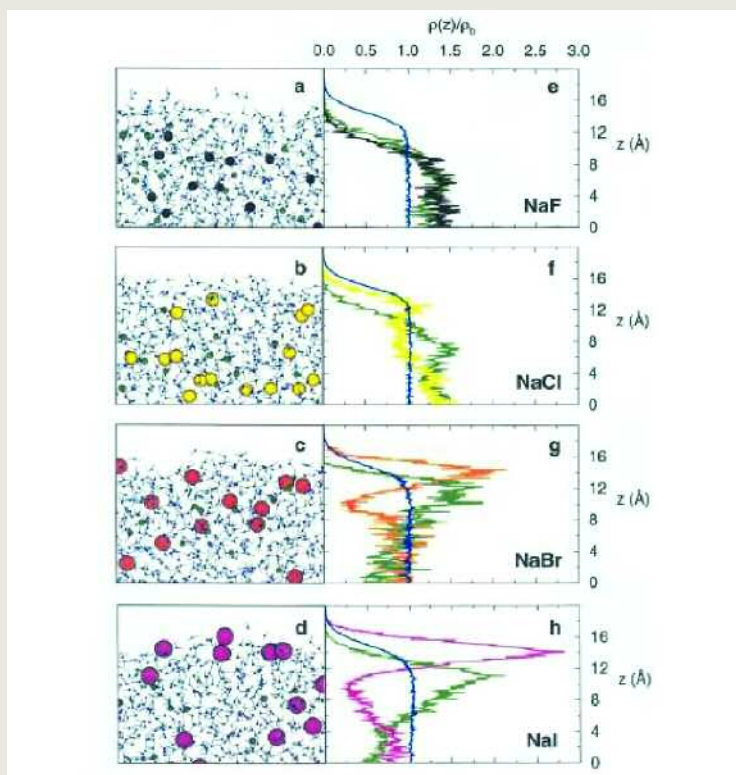


Figure 3 (Left): Snapshots from molecular dynamics simulations showing the interfacial distribution of sodium cations and halide anions for the alkali halide aqueous solutions. (Right) Plot of the respective number densities $\rho(z)$ of water oxygen atoms and ions vs distance z from the center of the slabs in the direction normal to the interface, normalized by the bulk water density, ρ_b . The colors of the curves correspond to the coloring of the atoms in the snapshots. Important to notice is that the small sodium cations are always depleted from the surface, as is also true for the small fluoride anions. However, for increasing anion size and hence polarizability, the propensity of anions to exist at the solution surface increases. For NaI solution, the two ion distributions are separated by ca. 3 Å.

Surface enrichment of solvate negative halogen ions was recently also investigated in an oceanographic context and is understood by new molecular computer simulations of liquid aqueous salt solutions including ion polarizability contributions to intermolecular forces in electrolyte solutions by Jungwirth [5].

Examples for computed salt ion distributions near the surface of a simulated liquid slab are presented in Figure 3 for several alkali-halide aqueous solution systems. Theoretical electron binding energies for individual anions and cation species, also, were derived from this liquid aqueous solution simulation. Thus far, these agree qualitatively with the liquid jet photoelectron spectroscopy experimental

data [6]. The ongoing analysis of the remaining discrepancies will lead to improvements in the understanding of the intermolecular potential models used in aqueous liquid solution modelling.

- [1] B. Winter and M. Faubel, *Chemical Reviews*, **2006**, Web release date: March 8, 2006 106, 1176.
- [2] D. Chandler, *Introduction to Modern Statistical Mechanics*, Oxford University Press, 1987.
- [3] B. Winter et al., *J. Phys. Chem. B* **108** (2004) 14558.
- [4] R. Weber et al., *J. Phys. Chem. B* **108** (2004) 4729.
- [5] P. Jungwirth and D. J. Tobias, *J. Phys. Chem. B* **105** (2001) 10468.
- [6] B. Winter et al., *J. Am. Chem. Soc.* **127** (2005) 7203.

2.2.3.8 Biological Matter in Microfluidic Environment

Thomas Pfohl

Rolf Dootz, Heather Evans, Sarah Köster, Alexander Otten, Dagmar Steinhauser
M. Abel (Potsdam), J. Kierfeld (Potsdam), S. Roth (Hamburg), B. Struth (Grenoble, France)
J. Wong (Boston, USA)

REMARKABLE PROGRESS HAS been achieved in the integration and analysis of chemical and biological processes on the nanoliter-scale by using microfluidic handling systems. Such systems require less reagent, resulting in a more efficient and cheaper experimental design, and have led to advances in the miniaturization of biological assays and combinatorial chemistry. Furthermore, due to the interesting physics of fluid flow on the micro- and nanoscale, microfluidics constitute a powerful tool in particular for the investigation of biological systems, whose dimensions are generally also on these length scales. Our experiments are focused on the flow behavior of individual macromolecules and the self-assembly of biological materials in micro- and nanochannels. These experiments enable studies of the influence of geometric confine-

ment on static as well as dynamic properties of biological materials [1,2].

Our examinations of the self-assembly of individual biomolecules and their dynamics in microflow environments aim to better understand a variety of molecular properties, such



Figure 1: Single fluctuating actin filaments confined in parallel straight microchannels (left, width of 6 μm) and curved microchannels (right, width of 2.5 μm).

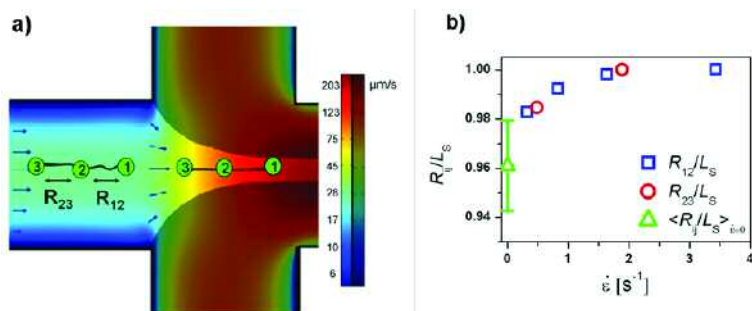


Figure 2: a) Overlay of the velocity field calculated by finite element method simulations and snapshots of an individual actin filament in elongational flow with endpoints and midpoints labeled 1,2,3 (channel width $40\mu\text{m}$). b) Normalized extension R_{ij}/L_S versus strain rate calculated combining experimental results and simulations.

as persistence length and bundle dimensions, in ambient conditions. Therefore, we analyze the influence of confining geometries on thermal fluctuations of actin by means of fluorescence microscopy. Actin is a semiflexible biological macromolecule found within eukaryotic cells, and is responsible for a variety of processes such as cellular motility and in particular cellular morphology, as actin is a primary component of the cytoskeleton. Fluorescence microscopy is particularly well suited, in combination with a pulsed laser illumination setup and CCD camera, for the collection of image sequences whereby the fluctuations of actin filaments can be quantified and subsequently analyzed. Furthermore, we observe the behavior of individual molecules (actin) and other objects (e.g. lipid vesicles) in specific flow fields which are generated by the geometries of the microfluidic devices. The flow fields of channels containing a variety of structures, for example hyperbolic or zig-zag geometries, can be precisely calculated using finite element method simulations [1,3]. Additionally, more complex mixing designs, for example a reagent gradient, can be generated by specific microfluidic designs. In cases where a reactant is added from the side channels, measurements along the main jet stream provide snapshots of the biomolecular interactions as a function of time. The dynamics of filament bundling and cytoskeletal network formation can be observed in situ, as a consequence of the well-defined addition of linker

proteins to individual actin filaments within microchannels.

The evolution and non-equilibrium dynamics of self-assembly processes of biological materials in microflow can be studied on the micro-, meso-, and nanoscale using characterization techniques such as fluorescence microscopy, as discussed previously, as well as other complementary methods such as confocal Raman microscopy and X-ray microdiffraction. [4,5] The latter technique is particularly advantageous in studies of biomolecules. Firstly, the X-ray beam is microfocused such that the beam is only $20\mu\text{m}$ in diameter at the sample. The small beam size permits the acquisition of X-ray patterns at specific spatial positions along and perpendicular to a microchannel. Secondly, improved diffraction signals are acquired owing to the increased flux of the X-ray beam as well as the orientation of the molecules within the microchannel. Finally, the collection of data in microflow conditions significantly reduces issues regarding radiation damage of the biomolecules.

DNA condensation is a topic of biological as well as physical interest, especially with respect to the hierarchical compaction of cellular DNA into chromosomes via histone proteins. Crossed microchannel devices are used to explore the interaction of DNA with histone-proteins as well as models for such moieties [6]. Hydrodynamic focusing of a stream

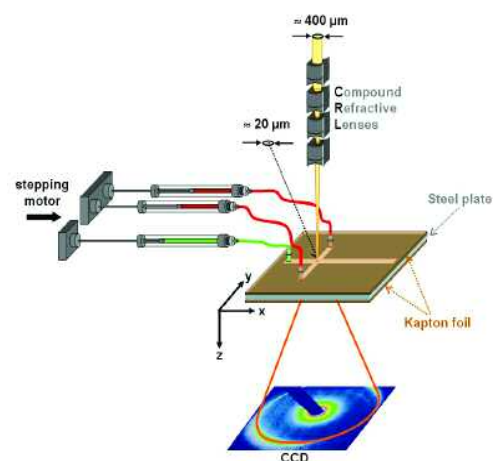


Figure 3: Schematic representation of the scanning X-ray microdiffraction setup.

of a semidilute DNA solution can predictably stretch and orient the biomolecules, enabling the study of the influence of confinement on static and dynamic properties of DNA [5]. The compaction of DNA is initiated via the addition of macroions (e.g. polyimine dendrimers) through the side channels, wherein these molecules diffuse into the focused stream at a rate proportional to their distance along the reaction channel. By varying the observation position along the microchannel, the evolution of the compaction process is observable. Using X-ray microdiffraction we are able to obtain data of DNA nanostructures with very high spatial resolution within a microfluidic device [4,5]. The comparison of the compaction of the DNA by histone-proteins with model-histone-proteins can help to clarify to what extent the wrapping of DNA around histones occurs ›actively‹ due to the special chemical structure of the histone-proteins, as opposed to the pure electrostatic interaction of negatively charged DNA with positively charged macroions.

Recently, we have extended our investigations to studies of collagen and fibrin, two ubiquitous extracellular filamentous proteins. A pH-gradient generated in microfluidic devices results in the hierarchical self-assembly of collagen, and the formation of collagen fibrils can be predicted as a function of pH values that are calculated using finite element modeling [7]. Using optimized microchannel geometries, it is possible to form droplets of aqueous materials in oil (see project 2.2.3.4). In the case of collagen, droplets of the protein in monotonically increasing pH concentra-

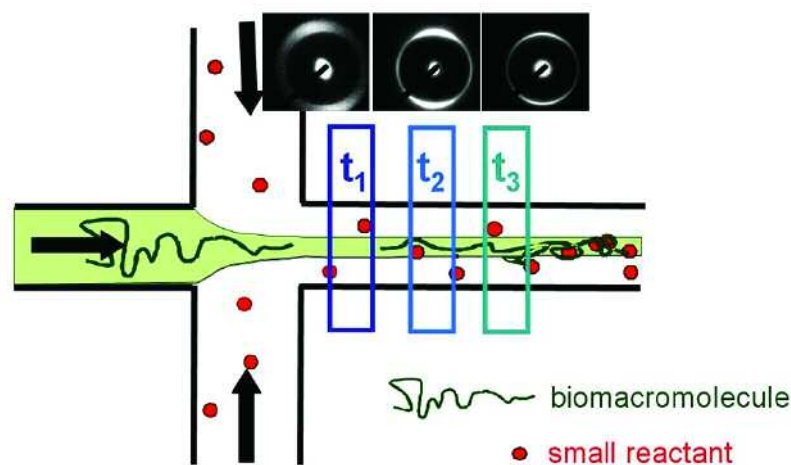


Figure 4: The hydrodynamic focusing enables a time resolved analysis of the non-equilibrium dynamics of DNA compaction induced by polyvalent ions. 2-D X-ray diffraction patterns of the evolution of DNA compaction can be obtained with a spatial resolution of 20 μ m.

tions can be formed in continuous flow conditions, permitting the controlled study of pH effects on collagen fibril formation in a particularly efficient design. Fundamental investigations of fibrin, the main protein in blood clotting or hemostasis, probe the dynamic assembly of the protein as a function of a variety of interaction parameters. The use of fibrin ›compartments‹ also has many advantages, principally to dramatically reduce the required volumes needed to extensively quantify effects of reactant concentrations on fibrin formation. The marriage of state-of-the-art microfluidic technologies with biological macromolecules provides a virtually endless supply of notable subjects and new opportunities to answer fundamental biophysical questions.

[1] T. Pfohl et al., *Chem. Phys. Chem.* **4** (2003) 1291.

[2] M. C. Choi et al., *Proceedings of the National Academy of Sciences of the USA (PNAS)* **101** (2004) 17340.

[3] S. Köster, D. Steinhauser and T. Pfohl, *Journal of Physics: Condensed Matter* **17** (2005) S4091.

[4] A. Otten et al., *Journal of Synchrotron Radiation* **12** (2005) 745.

[5] R. Dootz et al., *Journal of Physics: Condensed Matter* **18** (2006) 639.

[6] H. M. Evans et al., *Phys. Rev. Lett.* **91** (2003) 075501.

[7] S. Köster et al., *MRS Proceedings* **898E** (2005) 0989-L05-21.

2.2.3.9 Locomotion in Biology at Low Reynolds Number

Thomas Pfohl, Holger Stark

Erik Gauger, Michael Reichert, Eric Stellamanns

J. Bibette (Paris), M. Engstler (München)

WHEN WE THINK about locomotion, we are guided by our everyday experience in a macroscopic world. However, there exist much more organisms which move in the microscopic world in an aqueous environment; one prominent example is the *Escherichia Coli* (*E. coli*) bacterium in the human stomach. When we swim, we drift by inertia. However, these organisms do not know inertia. As soon as they stop their swimming stroke, they also stop moving. Due to the micrometer length scale, water appears very viscous to them; so Reynolds number is very small and micro-organisms had to invent mechanisms to move forward that might look rather strange to us [1]. Within the newly founded priority program SPP1207 of the Deutsche Forschungsge-

cells, e.g., use a beating elastic filament, called flagellum, to propel themselves. The paramecium possesses on its surface a whole carpet of shorter filaments, now called cilia, whose collective motion in the so-called metachronal waves pushes it forward. Cilia are also employed for fluid transport in the nose and lung, and to develop the left-right asymmetry of the embryo at an early stage. Certain bacteria, e.g., *E. coli*, move forward with the help of a bundle of helical filaments driven by a marvelous nano motor. The protozoan *African trypanosome* propels itself by a screwing motion of the whole chiral body.

The group of H. Stark has recently addressed the question where the bundling of the helical flagella of *E. coli* bacteria comes from [3]. As Fig. 1 illustrates, to form a bundle the rotations of the single helices must be highly synchronized. We investigated if hydrodynamic interactions, i.e., interactions due to the flow fields the rotating helices generate around themselves (see next project), could be the reason for such a synchronization. We therefore constructed two parallel rigid helices from a sequence of spheres and drove them by constant and equal torques. We indeed find that the helices synchronize to a phase difference zero as in Fig. 1. However, it is important that their orientations can jiggle around in space since strictly parallel helices do not synchronize. So synchronization is only achieved when the helices possess some flexibility. In our case, it might mimic the flexibility of the hook connecting the flagellum to the rotary motor.

The flagella of sperm cells or cilia are driven by internal motors [1]. The group of J. Bibette from the ESPCI in Paris has devised a biomimetic flagellum or cilium that is instead easily actuated by an external magnetic field [4]. They take superparamagnetic particles of micron size that form a chain in a magnetic field. They then link the particles together

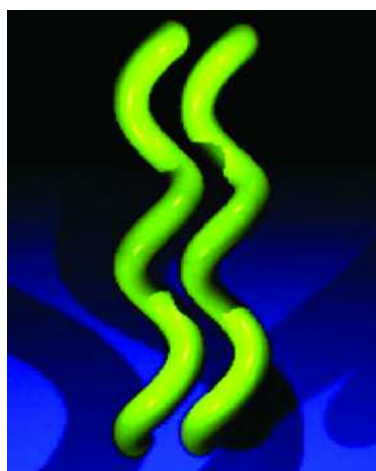


Figure 1:
Two rotating helices can only form a bundle when their rotations are highly synchronized.

meinschaft with the title *Strömungsbeeinflussung in Natur und Technik*, T. Pfohl, H. Stark, and their groups aim to contribute to the understanding of the principles governing the motion of micro-organisms, the fluid transport on a micrometer scale, and biomimetic materials.

According to Purcell [2], micro-organisms have to perform a periodic non-reciprocal motion in time to move forward at very low Reynolds numbers. This means, under time reversal the motion is not the same. Sperm

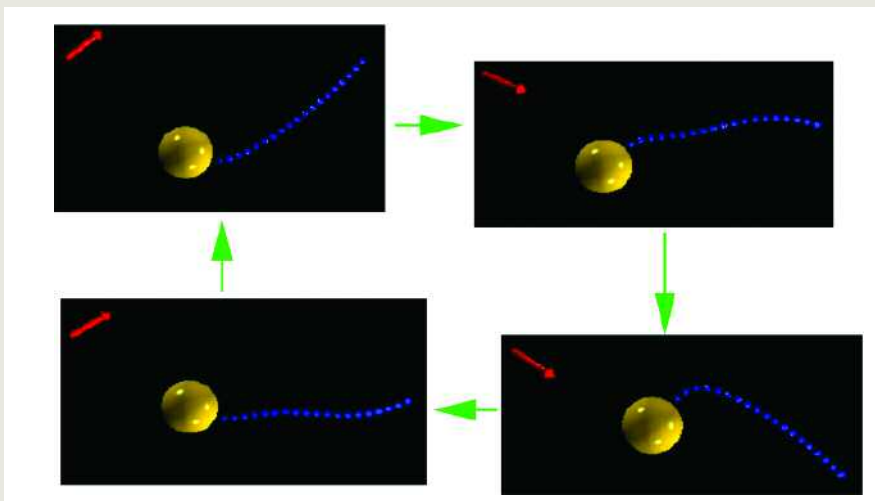


Figure 2: One actuation cycle of the simulated artificial swimmer. The superparamagnetic elastic filament (blue) tries to follow the oscillating magnetic field (red arrow). Due to the friction with the surrounding fluid, the filament bends and performs a ‘paddle’ motion. As a result, the load (yellow) is transported to the right.

with, e.g., double-stranded DNA to obtain an elastic filament. Attached to a blood cell, the resulting swimmer is actuated by an external magnetic field with oscillating direction. We have modeled this artificial swimmer using a bead-spring model that also possesses the bending energy of an elastic rod [5]. One actuation cycle is illustrated in Fig. 2. Our numerical study helps to identify the optimum swimming speed and efficiency as a function of magnetic field strength and frequency. The superparamagnetic elastic filament can also be attached to a surface and, with an appropriate time protocol of the magnetic field to create a non-reciprocal motion, used to transport fluid.

In collaboration with the geneticist Markus Engstler, LMU Munich, the group around T. Pfohl studies the influence of *African trypanosome* motility on the directional movement of proteins within its plasma membrane. *Trypanosomes* have ingeniously adapted to their extreme environment by actually exploiting for their survival the hostile flow conditions of the mammalian bloodstream. Evolution has provided these unicellular flagellates with a unique cell surface

coat consisting of a single type of variant surface glycoprotein (VSG). Host-derived antibodies are rapidly removed from the VSG coat. The Engstler group has shown that a coordinated action of directional cellular motility and plasma membrane recycling is necessary and sufficient for rapid removal of host-derived antibodies from the trypanosome cell surface. We found that immunoglobulins attached to VSG act as molecular sails. Hydrodynamic flow acting on the swimming cell selectively drags antibody-bound proteins within the plasma membrane towards the posterior pole of the cell, from where they are rapidly internalised by the localised and highly efficient endocytosis machinery [6]. Therefore, we develop microfluidic systems for mimicking the attack of host-derived antibodies as well as their removal in hydrodynamic flow. Surface protein movement and trypanosome motility are simultaneously visualized and measured using three-dimensional microscopy.

[1] D. Bray, *Cell Movements: From Molecules to Motility*, 2nd ed., Garland Publishing, New York (2001)

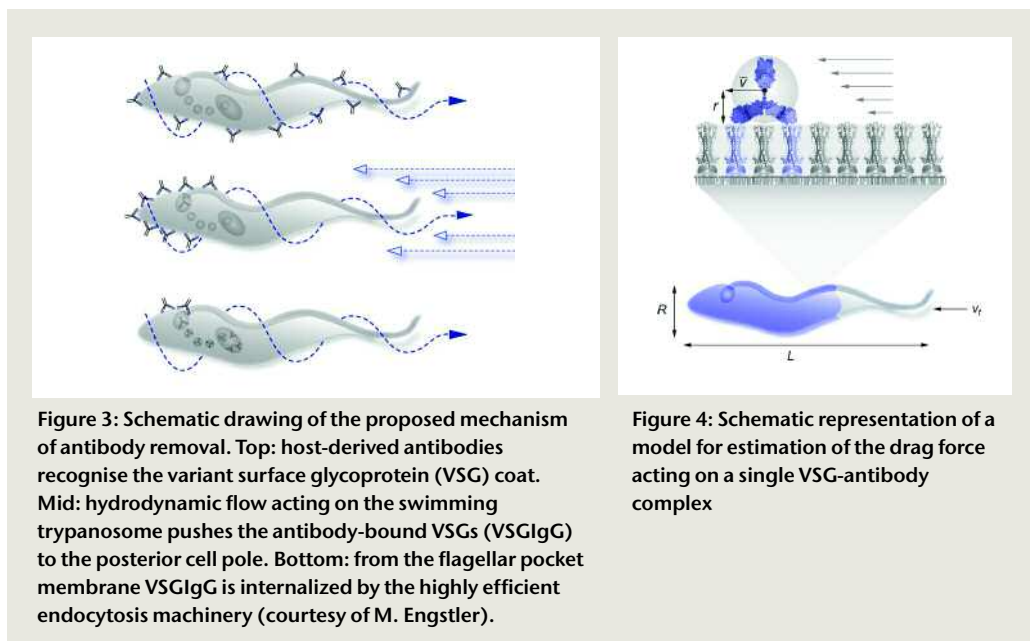


Figure 3: Schematic drawing of the proposed mechanism of antibody removal. Top: host-derived antibodies recognise the variant surface glycoprotein (VSG) coat. Mid: hydrodynamic flow acting on the swimming trypanosome pushes the antibody-bound VSGs (VSGIgG) to the posterior cell pole. Bottom: from the flagellar pocket membrane VSGIgG is internalized by the highly efficient endocytosis machinery (courtesy of M. Engstler).

Figure 4: Schematic representation of a model for estimation of the drag force acting on a single VSG-antibody complex

- [2] E. M. Purcell, *Am. J. Phys.* **45** (1977) 3.
 [3] M. Reichert and H. Stark, *Eur. Phys. J. E.* **17** (2005) 493.
 [4] R. Dreyfus et al., *Nature* **437** (2005) 862.

- [5] E. Gauger and H. Stark, submitted to *Phys. Rev. E*
 [6] M. Engstler, T. Pfohl, S. Herminghaus, M. Boshart, G. Wiegertjes, and P. Overath in preparation

2.2.3.10 Colloids In and Out of Equilibrium

Holger Stark

Andrej Grimm, Matthias Huber, Michael Reichert, Michael Schmiedeberg
 C. Bechinger, C. Lutz, J. Roth (Stuttgart), T. Gisler, S. Martin, G. Maret, K. Sandomirski (Konstanz),
 J. Bibette (Paris, France), J. Fukuda, H. Yokoyama (Tsukuba, Japan), T. Lubensky (Philadelphia, USA),
 A. Mertelj (Ljubljana, Slovenia), M.-F. Miri (Zanjan, Iran)

COLLOIDAL DISPERSIONS CONSIST of particles suspended in a liquid or gaseous environment. As milk, paint, fog, and drugs, they play an important role in our everyday life. Even the cell with its crowded constituents is regarded as a colloidal dispersion. A whole zoo of interactions like the electrostatic Yukawa potential or depletion forces whose properties can be fine-tuned and also the fact that colloids strongly interact with light fields, e.g., in optical tweezers, make them an ideal model system for statistical mechanics and to explore the non-equilibrium. Colloids dispersed in a complex fluid such as a nematic

liquid crystal experience new types of interactions that give rise to prominent structure formation into chains, hexagonal crystals, and cellular materials.

Hydrodynamic Interactions

Particles suspended in a liquid are in constant Brownian motion or they move under the influence of external forces. In both cases, they create a long-ranged flow field around themselves that in turn influences the motion of neighboring particles. These hydrodynamic interactions (a complicated many-body problem) constitute an inherent property of any

colloidal dispersion even of swarming bacteria. It is therefore of interest to explore their properties in detail.

Together with S. Martin and T. Gisler, our experimental colleagues from the University of Konstanz, we have devised a method to explore especially the hydrodynamic coupling of translating and rotating spheres [1,2]. Figure 1 illustrates the correlated translational and rotational motion of nearby birefringent particles trapped in optical tweezers. This experimental verification of our theoretical predictions [2] is the first explicit demonstration of hydrodynamic interactions between translating and rotating spheres.

Hydrodynamic interactions mediate collective motions that can be periodic or even transiently chaotic. To explore this property, we considered particles that circle on a ring driven by a constant force. A linear stability analysis reveals that regular clusters of these hydrodynamically interacting particles (e.g., three particles forming an equilateral triangle) exhibit a saddle-point instability, however only when they are allowed to make small excursions into the radial direction [3]. Three particles enter a characteristic limit cycle as illustrated in Fig. 2. Adding a strong enough sawtooth potential to the constant driving force creates a tilted potential landscape with potential wells [4]. Whereas a single particle now performs a ›stick-slip‹ motion, two neighboring particles use hydrodynamic interactions to move in a deterministic ›caterpillar-like‹ motion over the potential barriers that is initiated or terminated by thermal fluctuations. This illustrates that the system is an excellent model to study non-equilibrium processes.

Liquid-Crystal Colloids

Replacing the isotropic host liquid of colloidal dispersions by an anisotropic fluid such as a nematic liquid crystal (where rodlike molecules align on average along a common direction also called director) introduces an appealing system whose new phenomena have intensively been studied in recent years [5]. Together with colleagues from Japan, we

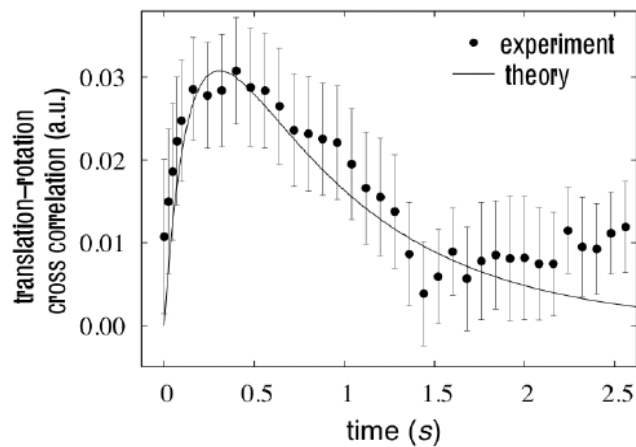


Figure 1: Translation-rotation cross correlation of two spherical birefringent particles trapped in optical tweezers. At equal times, the particles' positions and orientations are not correlated since there are no static interactions. With increasing time difference, correlations due to hydrodynamic interactions build up and ultimately decay to zero (experimental data, courtesy of S. Martin and T. Gisler, University of Konstanz).

used the Landau-Ginzburg-de Gennes free energy functional to demonstrate that wetting phenomena above the isotropic-nematic phase transition [6], as illustrated in project 2.2.3.5, also occur around colloidal particles [7]. They can even be used to construct tetravalent colloids that could arrange into colloidal crystals with diamond lattice structure known to possess a large photonic band gap [8].

Between two particles a bridge of condensed nematic phase forms close to the nematic-isotropic phase transition (see Fig. 3) [9]. These capillary bridges induce a very strong two-particle interaction, as verified by careful experiments of a group from Ljubljana. It also shows hysteresis similar to the one introduced in project 2.2.3.1. If the surfaces of the particles do not induce strong nematic ordering, theory and experiments demonstrate the occurrence of a weaker Yukawa interaction.

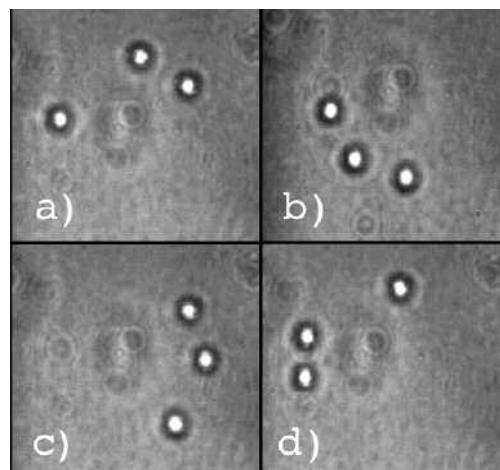


Figure 2: Characteristic limit cycle of three colloidal particles (bright) driven along a circular trap in counter-clockwise direction. The trap and the constant driving force are realized by a fast spinning optical tweezer (experimental data, courtesy of C. Lutz and C. Bechinger, University of Stuttgart).

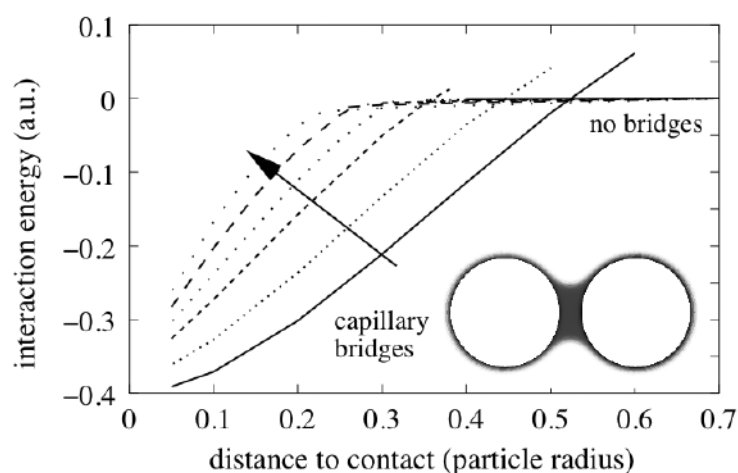


Figure 3: Two-particle interaction potential as a result of the formation of a bridge of condensed nematic phase (see inset) above the nematic-isotropic phase transition. A typical energy unit for 350 nm particles is 1500 thermal energies. Starting from the nematic-isotropic phase transition, temperature increases with the arrow.

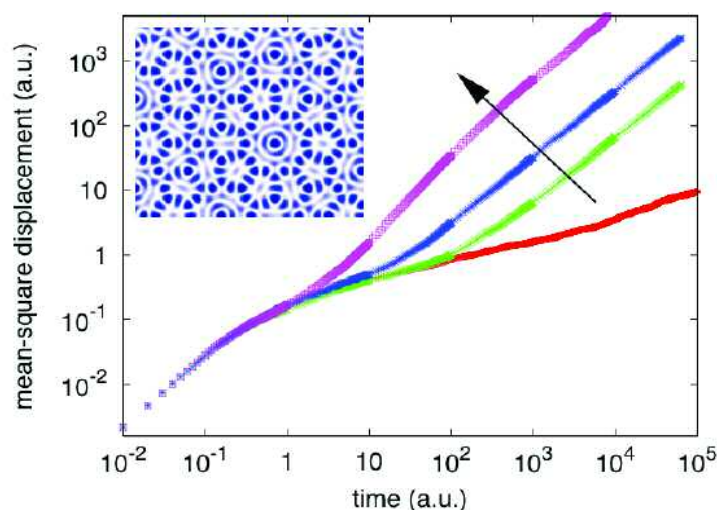


Figure 4: A Brownian particle in a two-dimensional quasicrystalline potential (created by the superposition of five plane waves along the edges of a pentagon, see inset) exhibits subdiffusion over several decades in time where it explores the complex potential landscape to reach thermal equilibrium (lower red curve). It then enters normal diffusion (not shown). With increasing phasonic drift velocity (indicated by the arrow), the subdiffusive regime vanishes and the particle assumes a normal diffusive regime with a much larger diffusion constant compared to the static potential.

Colloidal Adsorbates on Quasicrystalline Substrates

Together with colleagues from the University of Stuttgart [J. Roth (theory) and C. Bechinger (experiment)], we have proposed a project that uses colloids as model system to study how quasicrystalline substrates enforce the

controlled growth of quasicrystalline films. Quasicrystals possess a long-range positional order with a non-crystallographic point group symmetry such as a five-fold symmetry axis. Besides having been a subject of intense fundamental research that explores the new features of quasicrystals, they are also of techno-

logical importance due to their good corrosion resistance, low coefficient of friction, and good wear-resistance.

Based on the Alexander-McTague theory for melting and on Monte-Carlo simulations, we examined the influence of a one-dimensional quasicrystalline substrate potential on the structure of the ›adsorbed‹ colloids [10]. We find the following interesting but counterintuitive feature: a rhombic (distorted trigonal) phase that forms under the influence of the substrate potential melts again when the potential strength is further increased. Absolutely crucial for the melting is the quasi-periodicity of the substrate potential. Still the structure of the resulting ›modulated liquid‹ needs to be explored.

Besides phononic hydrodynamic modes (uniform translations for zero wave vector), quasicrystals also possess phasonic degrees of freedom. Due to a uniform ›phasonic drift‹ in a two-dimensional quasicrystalline potential (created by the superposition of five plane waves along the edges of a pentagon), local minima appear and vanish continuously. Figure 4 demonstrates how a Brownian particle in such a dynamic potential landscape behaves. The phasonic drift constantly pumps energy into the particle and keeps it far from equilibrium. We currently explore how this system can be used to study fundamental questions arising far from thermal equilibrium.

[1] A. Mertelj et al., *Europhys. Lett.* **59** (2002) 337; M. Schmiedeberg and H. Stark, *Europhys. Lett.* **69** (2005) 135.

[2] M. Reichert and H. Stark, *Phys. Rev. E* **69** (2004) 031407.

[3] M. Reichert and H. Stark, *J. Phys.: Condens. Matter* **16** (2004) S4085.

[4] C. Lutz et al., *Europhys. Lett.* **74** (2006) 719.

[5] H. Stark, *Phys. Rep.* **351** (2001) 387; P. Poulin et al., *Science* **275** (1997) 1770 .

[6] H. Stark, J. Fukuda and H. Yokoyama, *J. Phys.: Condens. Matter* **16** (2004) S1911.

[7] J. Fukuda, H. Stark and H. Yokoyama, *Phys. Rev. E* **69** (2004) 021714.

[8] M. Huber and H. Stark, *Europhys. Lett.* **69** (2005) 135.

[9] H. Stark, J. Fukuda and H. Yokoyama, *Phys. Rev. Lett.* **92** (2004) 205502.

[10] M. Schmiedeberg, J. Roth and H. Stark, submitted to *Phys. Rev. Lett.*

2.3 Fluid Dynamics, Pattern Formation and Nanobiocomplexity

2.3.1 Overview

Eberhard Bodenschatz

NONLINEAR OUT-OFF-EQUILIBRIUM SYSTEMS impact all levels of our everyday lives from ecology, sociology and economics, to biology, medicine, chemistry and physics. Typically these systems show self-organization and complex, sometimes unpredictable spatio-temporal dynamics. Although different in detail, the temporal and spatial structure of these systems can often be described by unifying principles.

Searching for and understanding these principles is at the center of our group's research. To achieve this goal, we are focusing on well-defined problems in the physics of fluid dynamics, of cellular biology, and of materials. Currently we are investigating experimentally and theoretically pattern formation and spatiotemporal chaos in thermal convection. In collaboration with researchers from the International Collaboration for Turbulence Research, we study particle transport in the fully developed turbulence of simple and complex fluids with its implication to fundamental theories, but also to practical issues like turbulent mixing and particle aggregation. We collaborate with cardiologists at the Veterinary School at Cornell University and the Heart Center at the University of Göttingen in the investigation of the dynamics of the mammalian heart at the cellular and organ scale. In collaboration with groups at the University

of California at San Diego, Cornell University, and Göttingen we conduct experiments in biophysics and nano-biocomplexity using micro-fluidic devices to probe and to understand the spatio-temporal dynamics of intra-cellular and extra-cellular processes. In material science/geophysics we are investigating within a wax-model spatio-temporal processes that resemble the dynamics of Earth's mid-ocean ridges.

Our research has been and will continue to be truly interdisciplinary from engineering, material science, geophysics, and applied mathematics, to chemistry, biology, and medicine. It fits well into the collaborative structure of the institute with Nonlinear Dynamics on the one side and Dynamics of Complex Fluids on the other.

On the following pages each individual topic will be shortly discussed to give a more detailed picture of the research programs of the Laboratory of Fluid Dynamics, Pattern Formation and Nanobiocomplexity.

2.3.2 People



Prof. Dr. Eberhard Bodenschatz

received his doctorate in theoretical physics from the University of Bayreuth in 1989. In 1991, during his postdoctoral research at the University of California at Santa Barbara, he received a faculty position in experimental physics at Cornell University. From 1992 until 2005, during his tenure at Cornell he was a visiting professor at the University of California at

San Diego (1999-2000). In 2003 he became a Scientific Member of the Max Planck Society and an Adjunct Director (2003-2005)/ Director (since 2005) at the Max Planck Institute for Dynamics and Self-Organization. He continues to have close ties to Cornell University, where he is Adjunct Professor of Physics and of Mechanical and Aerospace Engineering (since 2005).



Dr. Carsten Beta

studied Chemistry at the Universities of Tübingen and Karlsruhe and at the Ecole Normale Supérieure in Paris (France). In 2001, he joined the Department of Gerhard Ertl at the Fritz Haber Institute of the Max Planck Society in Berlin and in 2004 received his doctorate in Physical Chemistry from the Free University Berlin. He then moved to the USA as a

postdoctoral research fellow in the group of Eberhard Bodenschatz at Cornell University and as a visiting scientist at the University of California at San Diego. He is currently a group leader at the Max Planck Institute for Dynamics and Self-Organization in Göttingen.



Barbara Kasemann

Born in Schmallenberg, Germany. Professional training as biological technical assistant (BTA) at the Marine Fishery Regional Office in Albaum. Fabrication of monoclonal antibodies related to neuron degenerative diseases at Boehringer Mannheim. Subsequently, project manager for cell culture and animal experiment models at the Fraunhofer Inst. for Biomed. Engineering IBMT,

St. Ingbert. Research and development on CD 34 cells at a subsidiary of ASTA Medica, Frankfurt/M. Controlling and quality management (GMP) in a biotech. comp., focusing on the development of transplant techniques for blood stem cells. Research laboratory manager at the MPI for Dynamics and Self-Organization and deputy representative/coordinator for the institute's new building and research facilities.



Dr. Stefan Luther

received his doctorate in experimental physics from the University of Göttingen in 2000. From 2001-2004, he was a research associate at the University of Enschede, The Netherlands, where he worked on turbulent multiphase flow. Since 2004, he is group leader at the Max Planck Institute for Dynamics and

Self-Organization and visiting scientist at Cornell University, Ithaca NY, USA. In July 2006 he will move to Göttingen.



Dr.-Ing. Holger Nobach

received his doctorate in electrical engineering from the University of Rostock in 1997. During his postdoctoral research, between 1998 and 2000 on an industrial research program with Dantec Dynamics in Copenhagen and between 2000 and 2005 at the Technical University of Darmstadt, he developed measurement techniques for flow investigations. Since 2005 he

is a scientist at the Max Planck Institute for Dynamics and Self-Organization. He works on experimental investigation of turbulent flows with improved and extended optical measurement systems at the Cornell University. In July 2006 he will move to Göttingen.



Dr. Nicholas T. Ouellette

originally from Cambridge, Massachusetts, received his B.A. with High Honors in Physics and Computer Science from Swarthmore College in 2002. He did his graduate work in Physics at Cornell University working with Eberhard Bodenschatz studying Lagrangian particle tracking in intense turbulence, receiving his Ph.D. in 2006. He will continue to work on

Lagrangian turbulence in both Newtonian and dilute polymer solutions as well as the dynamics of heavy particles in turbulence at the Max Planck Institute for Dynamics and Self-Organization.



Dr. Gabriel Seiden

Born in Haifa, Israel. Earned his B.A. degree in physics in 2000 from the Technion-Israel Institute of Technology, where he also studied for his direct-track PhD in physics. His dissertation theme was the phenomenon of pattern formation in rotating suspensions. He is currently a postdoc researcher working with Eberhard Bodenschatz at the Max Planck

Institute for Dynamics and Self-Organization. His current research is on optical forcing in Rayleigh-Bénard convection and wax modeling of plate tectonics.



Dr. Dario Vincenzi

received his Ph.D in Physics from the University of Nice-Sophia Antipolis in 2003. His dissertation work dealt with turbulent transport. In 2004, he was lecturer at the Department of Mathematics of the University of Nice-Sophia Antipolis. In January 2005, he became a member of the Max Planck Institute for Dynamics and Self-Organization, Göttingen, and joined the

Bodenschatz group as a post-doctoral research associate in the Laboratory of Atomic and Solid State Physics at Cornell University. He is currently working on theoretical modeling of dilute polymer solutions and viscoelastic flows. In July 2006 he will move to Göttingen.



Dr. Haitao Xu

received his Ph.D in Mechanical Engineering from Cornell University in 2003. His dissertation work is on collisional granular flows. In September 2003, he joined Eberhard Bodenschatz group as a pos-doctoral research associate in the Laboratory of Atomic and Solid-State Physics at Cornell University and worked on experimental investigation of fluid turbulence.

In July 2006, he becomes a member of the Max Planck Institute for Dynamics and Self-Organization, Göttingen.

2.3.3 Projects

2.3.3.1 Particle Tracking Measurements in Intense Turbulence

Haitao Xu

Kelken Chang, Holger Nobach, Nicholas T. Ouellette

L. R. Collins (Cornell, USA), M. Kinzel (Darmstadt), Z. Warhaft (Cornell, USA)

International Collaboration for Turbulence Research

FROM SYSTEMS AS varied as the pumping of blood in the heart to the formation of clouds, to the dynamics of the interstellar medium, turbulence dominates fluid flow in the world around us. And yet, even though turbulence impacts a whole host of scientific fields, we lack a complete understanding of the subject. Fluid flow can be described in two complementary ways: the Eulerian perspective considers the motion of the fluid as it sweeps past a fixed point in the flow, while the Lagrangian perspective follows the motion of individual parcels of fluid. Eulerian measurements have been possible for many years, and have provided a great deal of insight into the structure of turbulence. On the basis of Eulerian measurements, a rich phenomenology of turbulence has been developed. The Lagrangian perspective, however, is more fundamental for many problems in turbulence, both practical and basic [1]. Relating Eulerian and Lagrangian measurements is currently an unsolved problem, in a large part because Lagrangian measurements have not been possible until very recently.

Our group has pioneered the use of high-speed particle tracking for Lagrangian measurements, first by adapting the silicon strip detector technology used in high-energy particle accelerators [2-4] and more recently by using high-speed commercial digital cameras [5,6]. We use these systems to track the simultaneous motions of hundreds of tracer particles added to a flow (Fig. 1). Under suitable conditions, these tracer particles are very good approximations to true fluid elements, giving us direct Lagrangian information. By analyzing the statistics of pairs of tracer particles, we have recently revisited the old

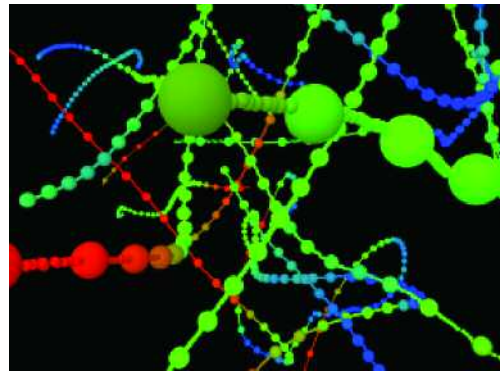


Figure 1: Particle tracks measured by our camera system in intense turbulence.

problem of pair dispersion in turbulence [6]. Pair dispersion is a fundamental component of turbulent mixing and transport. In turbulence the mean-square separation of a particle pair will grow faster than what would be ex-

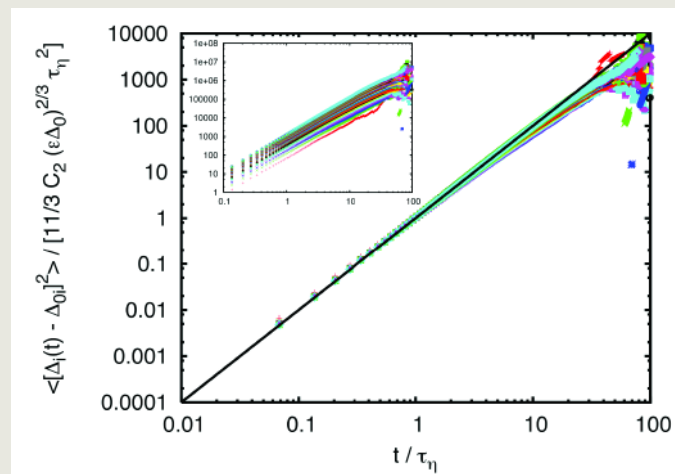


Figure 2: The time evolution of the mean-square particle separation. We observe clear power-law scaling. Data are shown for fifty different initial pair separations. When we simply plot the mean-square separation in time, we find many different curves (inset). When we scale by Batchelor's predicted t^2 power law, we find an excellent scale collapse.

pected from Brownian motion. Richardson famously predicted that, at small scales, it should in fact grow as the third power of time [7]; subsequently, Batchelor refined Richardson's work, identifying a regime in which the initial separation of the particle pair remains important and where the mean-square separation should grow as time squared [8]. In our

measurements in intense laboratory turbulence, we have found excellent agreement with Batchelor's t^2 law, with no hint of Richardson's law (Fig. 2). These results suggest that significantly more intense turbulence, perhaps more intense than exists anywhere naturally on Earth, would be required to observe a significant Richardson regime. Our results have important implications for designers of models of pollutant transport or weather modeling.

Turbulence is generally modeled as a cascade process, where energy is injected into the flow at large length and time scales and cascades down to smaller scales where it is converted to heat by molecular viscosity. In the intermediate range of scales where the energy loss is negligible, known as the inertial range, the statistics of the turbulence are expected to be universal for all turbulent flows, regardless of the large-scale forcing or geometry. Kolmogorov's phenomenological model, known simply as K41, has been very successful in explaining inertial range statistics [9], but in the past several decades strong discrepancies have been found with the K41 model for high-order Eulerian statistics. These discrepancies are attributed to the 'burstiness' of turbulence, a phenomenon known as intermittency. Deviations from the K41 model are typically measured from the statistics of the structure functions, namely the moments of the velocity increments. K41 predicts that the structure functions should scale as power laws in the inertial range; this behavior is reproduced in experiments and simulations, but the exponents of the power laws are significantly different from the K41 predictions. We have recently measured the Lagrangian structure function scaling exponents (Fig. 3), and have also found strong intermittency effects [10].

Many models have been proposed to account for intermittency. One of the most successful reinterprets the turbulent cascade as a multifractal process, implying that turbulent energy transfer has a fractal structure with a whole spectra of allowed fractal dimensions. Using our particle tracking system, we have

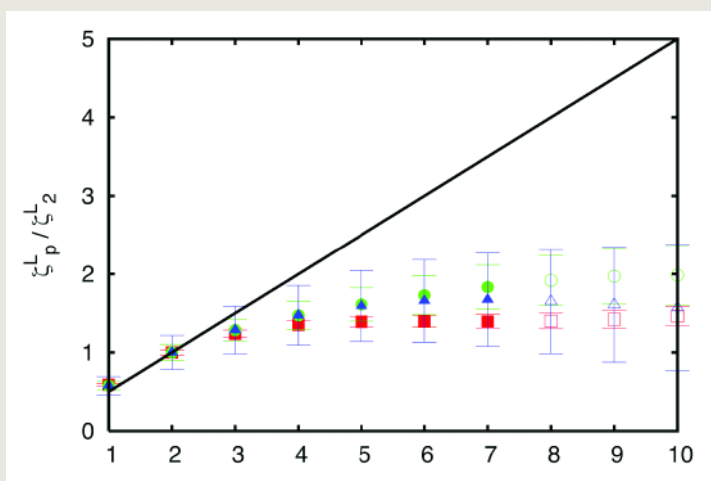


Figure 3: Scaling exponents of the Lagrangian structure functions in the inertial range as a function of structure function order. The solid line is the K41 prediction; the strong deviation of the measured scaling exponents from the K41 prediction shows the effects of intermittency. Data is shown for three different turbulence levels; open symbols denote data points that may not be fully statistically converged.

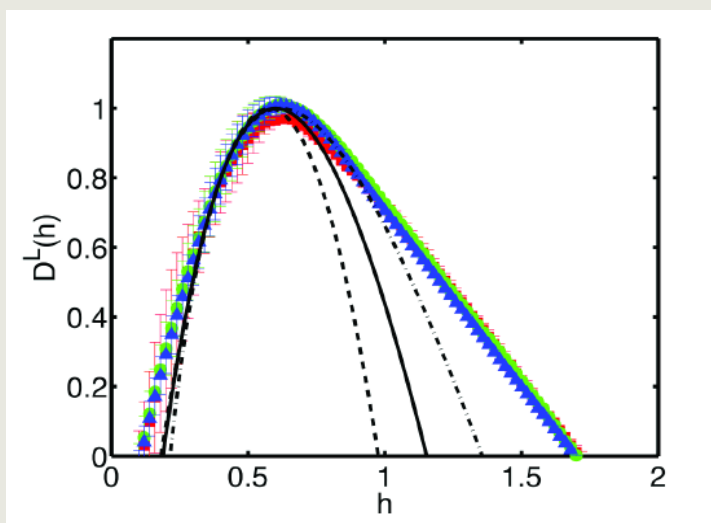


Figure 4: Directly measured multifractal dimension spectra shown for three different turbulence levels. The solid, dashed, and dot-dashed lines are previously-proposed models.

recently measured multifractal dimension spectra (Fig. 4), and have found more features in the dimension spectrum than were predicted [11].

In the future, we will extend our particle tracking techniques to new flows, such as the Göttinger Wind Tunnel, as well as to the tracking of heavy particles, of great interest to the cloud physics community. We are also studying the effects of long-chain polymers, known to reduce turbulent drag at boundaries, on bulk turbulence.

- [1] P. K. Yeung, *Annu. Rev. Fluid Mech.* **34** (2002) 115.
- [2] A. La Porta et al., *Nature* **409** (2001) 1017.
- [3] G. A. Voth et al., *Rev. Sci. Instr.* **12** (2001) 4348.
- [4] G. A. Voth et al., *J. Fluid Mech.* **469** (2002) 121.
- [5] N. T. Ouellette, H. Xu, and E. Bodenschatz, *Exp. Fluids* **40** (2006) 301.
- [6] M. Bourgoin et al., *Science* **311** (2006) 835.
- [7] L. F. Richardson, *Proc. R. Soc. Lond. A* **110** (1926) 709.
- [8] G. K. Batchelor, *Q. J. R. Meteorol. Soc.* **76** (1950) 133.
- [9] A. N. Kolmogorov, *Dokl. Akad. Nauk SSSR* **30** (1941) 301.
- [10] H. Xu et al., *Phys. Rev. Lett.* **96** (2006) 024503.
- [11] H. Xu, N. T. Ouellette, and E. Bodenschatz, *Phys. Rev. Lett.* **96** (2006) 114503.

2.3.3.2 Development of Fluid Dynamics Measurement Techniques

Holger Nobach

Kelken Chang, Nicholas T. Ouellette, Haitao Xu

S. Ayyalasomayajula (Cornell, USA), M. Kinzel (Darmstadt), C. Tropea (Darmstadt)

EXPERIMENTAL INVESTIGATIONS OF fluid mechanics and the verification of statistical turbulence models require measurement techniques that allow access to the fundamental flow quantities. Time series of the flow velocity can be measured with pressure tubes and hot-wire probes. To measure more quantities, like temporal or spatial derivatives, extended measurement probes are required. With a multi-hot-wire probe (five arrays with four hot-wires and one cold-wire each [1,2]) it is possible to measure the velocity fluctuation vector, all nine components of the spatial velocity gradient tensor and all three temporal velocity derivatives. However, these measurement techniques strongly affect the flow field due to the presence of measurement probes inside the flow.

Modern optical measurement techniques like Laser Doppler Velocimetry (LDV, Fig. 1) or Particle Imaging Velocimetry (PIV, Fig. 2) allow the access to flow quantities without disturbing the flow field. Based on the observation of small tracer particles, the LDV technique provides a time series of the velocity in a small measurement volume, while the PIV

technique yields an instantaneous, spatially resolved flow field. For both techniques there exist extensions of the basic principles that allow the measurement of all three velocity components, spatial derivatives or time-averaged, spatial statistics.

However, these techniques are restricted to measurements at fixed points in space (Eulerian measurements). To measure Lagrangian statistics, individual particle tracks must be followed in time and space simultaneously. This can be realized with a high-speed particle imaging and tracking systems, consisting of several digital high-speed cameras as employed in our laboratory ([3], Fig. 3).

Here we develop improved LDV and PIV systems to provide complimentary measurements to the hot-wire probes and the particle tracking measurements. For both techniques, LDV and PIV, recent developments [4-6] show that the measurement of particle acceleration as an additional quantity is possible. Main issues for both techniques are the improvement of the accuracy and the resolution (temporal, spatial as well as in signal amplitude).

In case of PIV, image deformation techniques

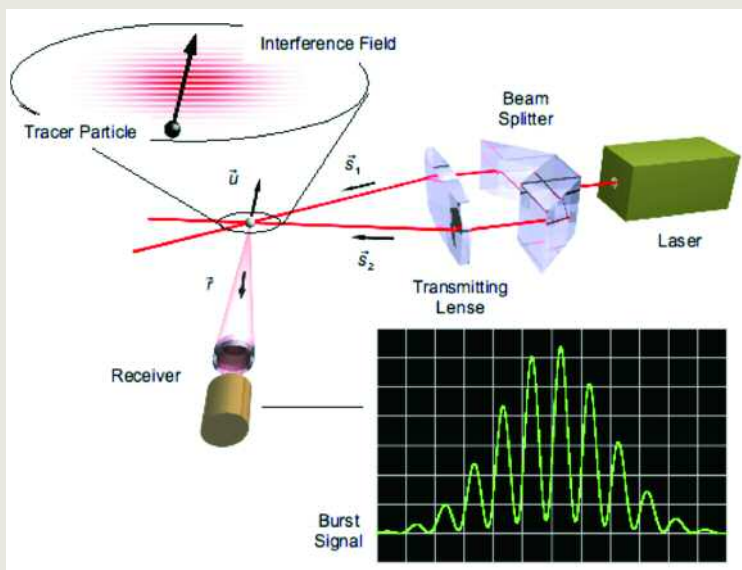


Figure 1: Laser Doppler Velocimetry

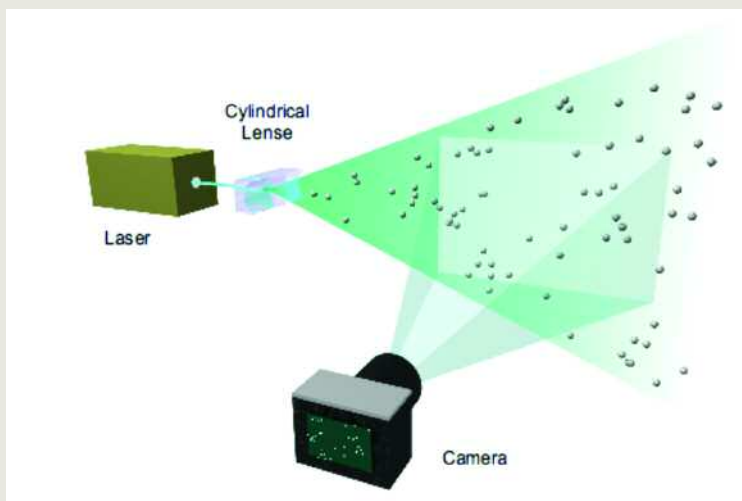


Figure 2: Particle Image Velocimetry

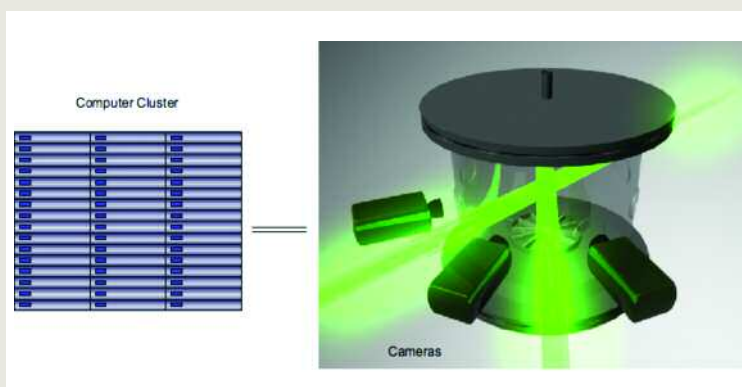


Figure 3: High-speed Particle Imaging and Tracking

have the potential to improve the spatial resolution [7-9]. Unfortunately, even with advanced windowing techniques that remove iteration instabilities [10], we recently found ambiguities that yield strong fluctuations of the estimated velocity field and, hence, limit the accuracy [11]. In order to overcome this limitation and to realize better spatial resolution of the PIV technique, the reason of this ambiguity must be identified and methods must be found, which are robust against this influence [12,13].

The laser Doppler measurement of particle acceleration would give a much-needed alternative to particle tracking techniques. In collaboration with the TU Darmstadt, we were able to successfully use a commercial LDV system to measure both, particle velocity and acceleration in backward scatter [14-16]. Because of the small measurement volume of an LDV system, the alignment procedures and the signal processing require the highest possible accuracies. Only this allows for acceleration measurement with sufficient resolution. Our first test measurement of the probability density of particle accelerations in a turbulence tank quantitatively agrees with the previous measurement of the Bodenschatz group using silicon strip detectors (Fig. 4). This new technique now provides an alternative measurement system, which can be used at smaller flow scales. Although the system performed well there is much room for improvements. In addition, the system needs to be modified so that it can be used inside the Göttinger High Pressure Turbulence Tunnel.

- [1] A. Tsinober, E. Kit, and T. Dracos, *J. Fluid Mech.* **242** (1992) 169.
- [2] A. Tsinober, L. Shtilman, and H. Vaisburd, *Fluid Dyn. Res.* **21** (1997) 477.
- [3] N.T. Ouellette, H. Xu, and E. Bodenschatz, *Exp. in Fluids* **40** (2006) 301.
- [4] B. Lehmann, H. Nobach, and C. Tropea, *Meas. Sci. Technol.* **13** (2002) 1367.
- [5] K.T. Christensen and R.J. Adrian, *In Proc. 4th Int. Symp. on PIV '01, Göttingen, Germany, paper 1080* (2001).
- [6] P. Dong et al., *Exp. in Fluids* **30** (2001) 626.
- [7] H. Nobach, N. Damaschke, and C. Tropea, *Exp. in Fluids* **39** (2005) 299.

- [8] H. Nobach et al., *In Proc. 6th Int. Symp. on PIV '05, Pasadena, California, USA* (2005).
- [9] H. Nobach and C. Tropea, *Exp. in Fluids* **39** (2005) 614.
- [10] J. Nogueira, A. Lecuona, and P.A. Rodriguez, *Exp. in Fluids* **27** (1999) 107.
- [11] H. Nobach and E. Bodenschatz, *Meas. Sci. Technol.* (submitted).
- [12] H. Nobach and E. Bodenschatz, *In Proc. 13th Int. Symp. on Appl. of Laser Techn. to Fluid Mech., Lisbon, Portugal, paper 26.3* (2006).
- [13] H. Nobach and E. Bodenschatz, *In Proc. 14. Fachtagung »Lasermethoden in der Strömungsmesstechnik«, Braunschweig, Germany, paper 4* (2006).
- [14] H. Nobach, M. Kinzel, and C. Tropea, *In Proc. 7th Int. Conf. on Optical Methods of Flow Investigation, Proc. SPIE 6262*, Moscow, Russia (2005).
- [15] M. Kinzel et al., *In Proc. 13th Int. Symp. on Appl. of Laser Techn. to Fluid Mech., Lisbon, Portugal, paper 17.4* (2006).
- [16] M. Kinzel et al., *In Proc. 14. Fachtagung »Lasermethoden in der Strömungsmesstechnik«, Braunschweig, Germany, paper 1* (2006).

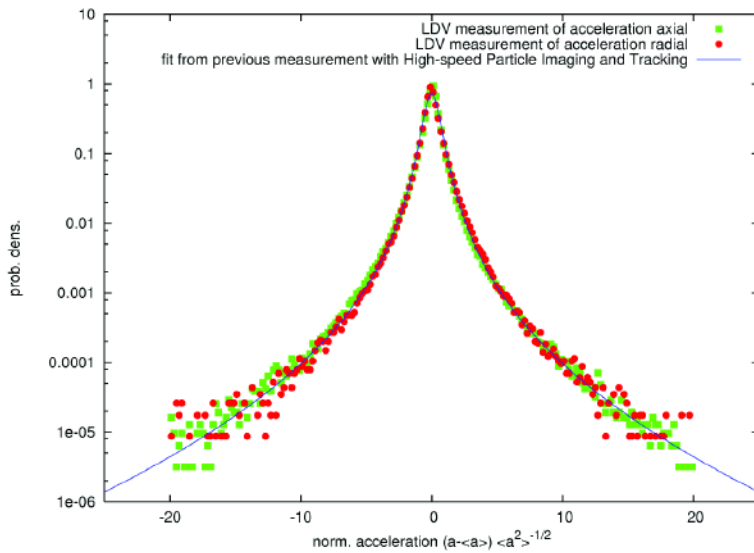


Figure 4: Probability density distribution of LDV acceleration measurements in a water tank at $Re = 500$

2.3.3.3 The Goettinger Turbulence Tunnel

Holger Nobach

Kelken Chang, Nicholas T. Ouellette, Haitao Xu
International Collaboration for Turbulence Research

THE INVESTIGATION OF fundamental principles of turbulent flows and the exploration of turbulence phenomena are major interests of the group. Important questions concern scaling and the validity of scale-independent constants. Computational fluid dynamics can substitute experiments only for small Reynolds numbers. Therefore, experimental facilities generating turbulent flow fields at high Reynolds numbers are essential for the research.

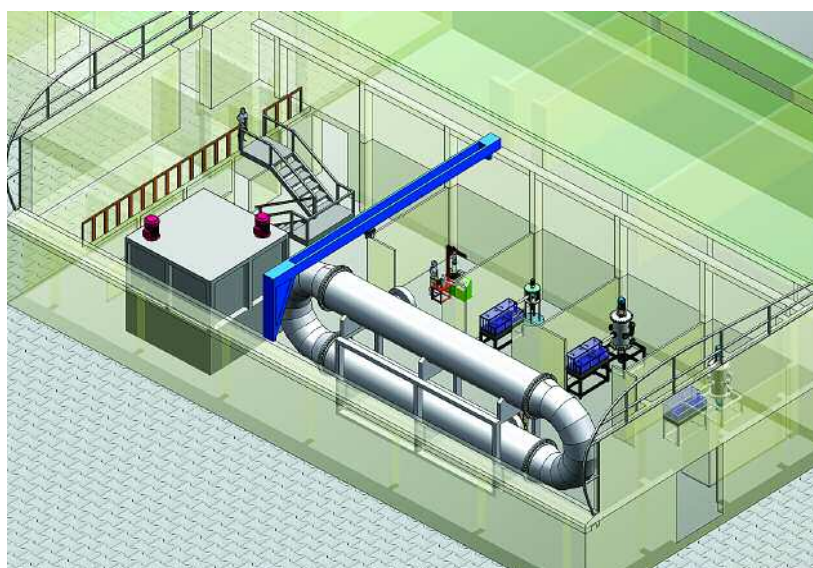


Figure 1:
Schematic of the
experimental hall

To achieve Reynolds numbers up to $Re_\lambda \sim 10,000$, which is close to the highest values on Earth, a wind tunnel with sulfur hexafluoride (SF_6) and air as working fluids, pressurized at 15bar, is being built in Göttingen. The wind tunnel is upright and consists of two measurement sections with a cross-sectional area of 2 m^2 and with lengths of 10 and 6m, respectively. The high turbulence levels are generated by active grids that will be installed at the beginning of each test section. The measurements will provide new insights into turbulence that will be indispensable for

understanding turbulent dispersion and related problems in the atmospheric and environmental sciences, micrometeorology and engineering.

Measurement techniques such as hot-wire anemometry, laser Doppler velocimetry and high-speed optical particle tracking will be implemented in the wind tunnel.

The hot-wire instrument consists of a multi-hot-and-cold-wire probe (five arrays with four hot-wires and one cold-wire each), allowing the measurement of the velocity fluctuation vector \vec{u}' , all nine components of the spatial velocity gradient tensor $\nabla \vec{u}'$ and all three temporal velocity derivatives $\partial \vec{u}' / \partial t$. The implementation of the hot-wire technique in the pressurized wind tunnel requires an automatic three-dimensional calibration inside the tunnel at the operation parameters of the tunnel.

The three-dimensional laser Doppler system can be used directly for three-dimensional particle (Lagrangian) acceleration measurements. The relatively small measurement volume yields a high spatial resolution and reduces systematic deviations due to temporal or spatial averaging. The limits of the achievable resolution, given by systematic deviations due to a divergence of the fringe system and random deviations due to signal noise, can be balanced by an accurate adjustment of the system (all optical components can be adjusted separately). The signals are recorded by high-speed AD-cards and processed offline in a computer using custom software. In test measurements a resolution of about 200 m/s^2 could be verified.

The optical particle tracking system consists of multiple high-speed cameras observing the three-dimensional traces of small particles in a certain fluid volume. The cameras take images at rate up to 37,000 fps at a resolution of 255×255 pixels. To extract the particle traces,

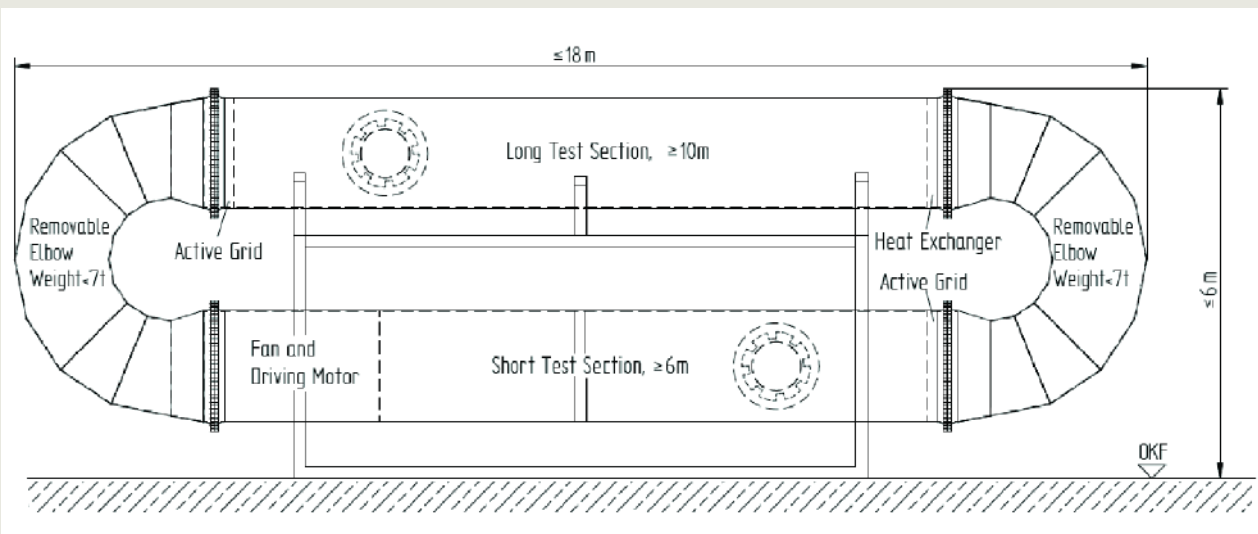


Figure 2: A sketch of the pressurized SF_6 wind tunnel.

the image sequences are processed in a computer cluster. The cameras can be mounted on a rail system, which is moving at the mean speed of the flow. This allows the observation of tracer particles over several meters, which increases the observation time significantly, independent of the mean velocity.

Other researchers from the International Collaboration for Turbulence Research (ICTR) will also use the tunnel. They will employ complimentary measurement technologies. ICTR is mainly an experimental group that uses a combination of proven and most modern technology to investigate problems of tur-

bulence. It was born out of the realization that progress in turbulence requires to go beyond the financial, technical, and manpower capabilities of a single researcher or a single research group. Very much analog to investigations in High Energy Physics, by joining forces the members of ICTR are providing access to shared facilities in measurement technology and a variety of turbulence generators. The MPIDS with the best facility worldwide will be a cornerstone of ICTR. We expect that 30% of the tunnel will be used by outside collaborators who will be housed during their stay in the guest apartments.

2.3.3.4 Polymer solutions and viscoelastic flows

Dario Vincenzi

L. R. Collins (Cornell, USA), Shi Jin (Cornell, USA)
International Collaboration for Turbulence Research

DILUTE POLYMER SOLUTIONS exhibit physical behaviors that distinguish them from ordinary Newtonian fluids. The elasticity of polymers, combined with fluid turbulence, produces very complex memory effects. Even small concentrations (a few parts per million of added polymers) can considerably change the large-scale behavior of a turbulent flow. One of the most striking effects is drag reduction: the injection of polymers in a turbulent flow can reduce the energy dissipation even by 80% [1]. Since the pioneering work of Toms [2], this technology is routinely used in oil pipelines to reduce pumping costs (<http://www.alyeska-pipe.com>).

The modeling of turbulent flows of polymer solutions represents a major challenge since it

couple hydrodynamic turbulence and polymer dynamics in solution, two problems that, even separately, are not fully understood.

A starting point for the theoretical description of dilute polymer solutions is the dynamics of isolated polymer molecules. While to date the stationary dynamics of a single, isolated polymer has received much attention [3], less is known about non-equilibrium dynamics. We have analytically solved the relaxation dynamics of a polymer molecule both in laminar and random flows [4–6]. By means of Fokker-Planck methods, we have computed the polymer relaxation time towards the stationary regime as a function of the velocity gradient. Our analysis brings to evidence an important slowdown of dynamics in the vic-

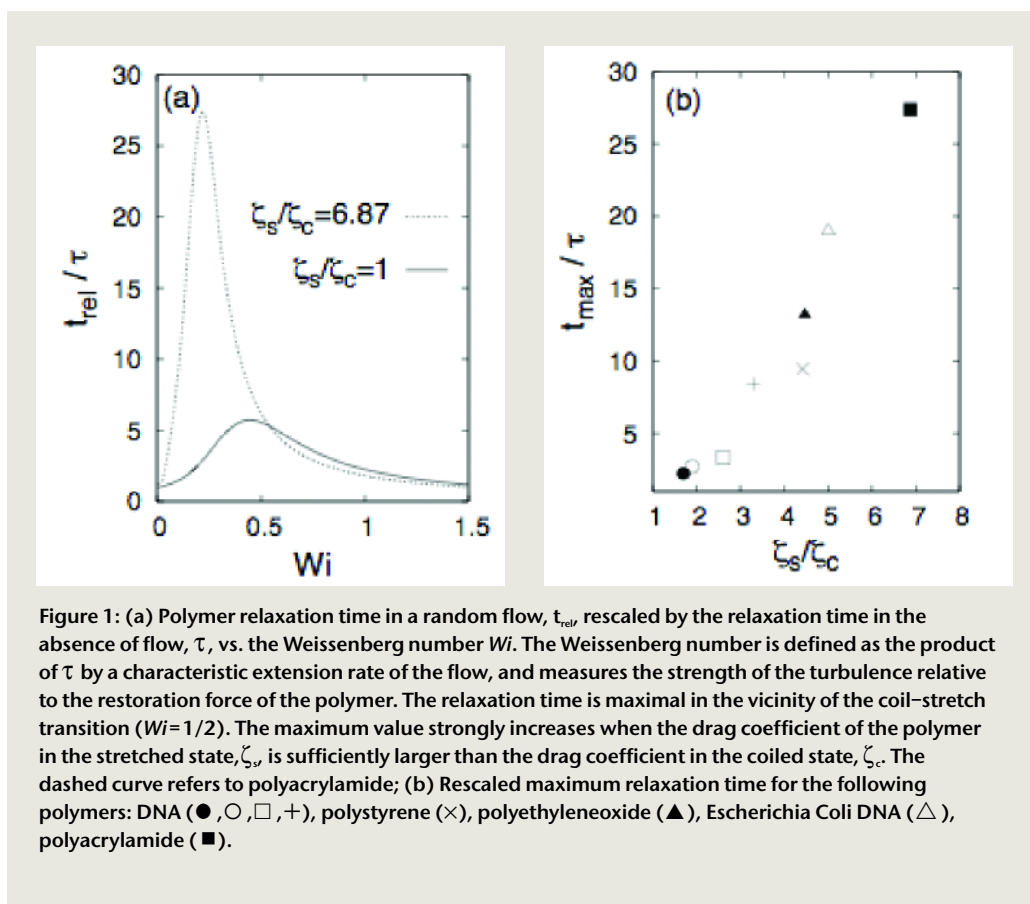


Figure 1: (a) Polymer relaxation time in a random flow, t_{rel} , rescaled by the relaxation time in the absence of flow, τ , vs. the Weissenberg number Wi . The Weissenberg number is defined as the product of τ by a characteristic extension rate of the flow, and measures the strength of the turbulence relative to the restoration force of the polymer. The relaxation time is maximal in the vicinity of the coil–stretch transition ($Wi=1/2$). The maximum value strongly increases when the drag coefficient of the polymer in the stretched state, ζ_s , is sufficiently larger than the drag coefficient in the coiled state, ζ_c . The dashed curve refers to polyacrylamide; (b) Rescaled maximum relaxation time for the following polymers: DNA (●, ○, □, +), polystyrene (×), polyethyleneoxide (▲), Escherichia Coli DNA (△), polyacrylamide (■).

nity of the so-called coil–stretch transition. For the elongational flow, this is related to conformation hysteresis [3]. For random flows, we have shown that hysteresis is not present. Nonetheless, the amplification of the relaxation time persists, albeit to a lesser extent, due to the large heterogeneity of polymer configuration. In both cases, the dependence of the drag force on the polymer configuration plays a prominent role (Fig. 1). This conclusion suggests that the conformation-dependent drag should be included as a basic ingredient of continuum models of polymer solutions.

The dynamics of an isolated polymer in a flow field forms the basis of constitutive models for numerical simulation of viscoelastic flows [3]. Direct numerical simulation (DNS) has recently emerged as an important tool for analyzing drag reduction in channel flows, boundary layers and homogeneous turbulence. In the context of two-bead models, the polymer conformation results from the counterbalance of the flow stretching and the action of entropic forces restoring extended polymers into the equilibrium configuration [7].

The advantage DNS has over laboratory experiments is that it yields information about the polymer orientation and the flow simultaneously, making it easier to understand the mechanism(s) of turbulent drag reduction and how they depend upon the polymer parameters. However, despite the successes of DNS, it is clear that it will not be a useful tool for designing large-scale systems, as the

Reynolds numbers that are required are much larger than can be achieved. A possible approach is to renounce resolving small scales and concentrate on the mean evolution. That approach leads to a closure problem since the stretching and restoration terms in the equations of motion cannot be expressed as explicit functions of the mean polymer conformation because of polymer-turbulence statistical correlations. In collaboration with engineers at the Sibley School of Mechanical and Aerospace Engineering at Cornell University, we have presented a systematic closure approximation for the *stretching* term in the evolution equation for the mean polymer conformation [8]. This term plays an important role in non-Newtonian turbulence by establishing the mean stretch of the polymer due to the background turbulent fluctuations. By assuming the velocity gradient in the frame of reference moving with the polymer is Gaussian and short-correlated in time, it was possible to derive an analytical closure for the stretching term. DNS were used to tune the coefficients appearing in the closure provided by the analytical work. The final closure with tuned coefficients is in excellent agreement with the simulations (Fig. 2). We presently are extending the model to homogeneous turbulent shear flow. Additionally, we are seeking a closure for the mean restoration term. In this case, knowledge of the distribution of stretch by the isolated polymer can be used to obtain an approximate closure in terms of the mean conformation tensor.

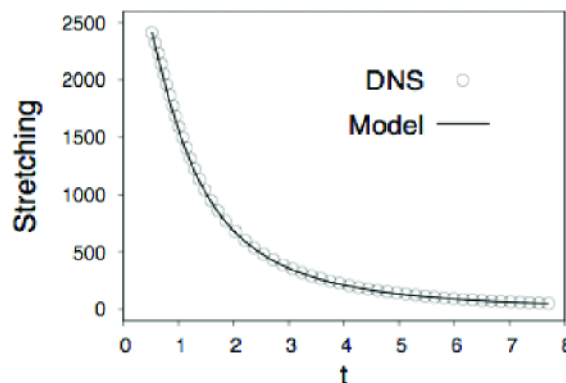


Figure 2: Left: Snapshot of the vorticity field from direct numerical simulations of 2D Navier–Stokes turbulence. Right: Plot of the stretching term vs. time. The points are from direct numerical simulations and the solid line is the theoretical prediction.

- [1] J.L. Lumley, *Annu. Rev. Fluid Mech.* **1** (1969) 367.
 [2] B. Toms, *Proc. Int. Rheo. Congress* **2** (1948) 135.
 [3] E.S.G. Shaqfeh, *J. Non-Newtonian Fluid Mech.* **130** (2005) 1.
 [4] M.M. Afonso and D. Vincenzi, *J. Fluid Mech.* **540** (2005) 99.
 [5] D. Vincenzi and E. Bodenschatz, *J. Phys. A: Math. Gen.* (2006), under review.
 [6] A. Celani, A. Puliafito, and D. Vincenzi, *Phys. Rev. Lett.* (2006), under review.
 [7] R.B. Bird et al., *Dynamics of Polymeric Liquids*, Wiley, New York (1987).
 [8] D. Vincenzi et al., *Phys. Rev. Lett.* (2006), under review.

2.3.3.5 Experiments on Thermal Convection

Gabriel Seiden

Will Brunner, Jonathan McCoy, Hélène Scolan, Stephan Weiß
 S. E. Lipson (Technion, Israel), W. Pesch (Bayreuth)

FLUID MOTION DRIVEN by thermal gradients (thermal convection) is a common and most important phenomenon in nature. Convection not only governs the dynamics of the oceans, the atmosphere, and the interior of stars and planets, but it is also important in many industrial processes. For many years, the quest for the understanding of convective flows has motivated many experimental and theoretical studies. In spatially extended systems convection usually occurs when a sufficiently steep temperature gradient is applied across a fluid layer. The convection structures appear often in regular arrangement, which we call a pattern. It is the investigation of such convection patterns that is at the center of this project. Pattern formation is common also in many other non-equilibrium situations in physics, chemistry, or biology. The observed patterns are often of striking similarity and indeed their understanding in terms of general, unifying concepts continues to be a main direction of research.

Many fundamental aspects of patterns and their instabilities have been studied intensively over the past 20 years in the context of Rayleigh-Bénard convection (RBC) [1]. In a traditional RBC-experiment a horizontal fluid layer of height d is confined between two thermally well conducting, parallel plates.

When the temperature difference between the bottom plate and the top plate exceeds a certain critical value the conductive motionless state is unstable and convection sets in. The most ideal pattern is that of straight, parallel convection rolls with a horizontal wavelength of $\sim 2d$. In the less well-known case of Inclined Layer Convection (ILC) the standard Rayleigh-Bénard cell is inclined at an angle with respect to the horizontal, resulting in a basic state which is characterized not only by heat conduction, but also by a plane parallel shear-flow with cubic velocity profile. This shear-flow not only breaks the isotropy in the plane of the layer, but also, at large angles and when inclined and heated from above, causes a transition from a thermal to a hydrodynamic shear-flow instability. For ILC we observed an intricate phase space, filled with nonlinear, spatio-temporally chaotic states [2].

In our experimental investigations we use a pressurized gas cell to study forcing and control of thermal convection in horizontal and inclined fluid layers. As explained in detail in [1], compressed gases have the advantage over other fluids in that they enable an experimental realization of large aspect-ratio samples (length/height < 150) with short relaxation times (< 2 sec). In addition, the Prandtl

number can be tuned from 0.17 to 150. The Prandtl number gives the relative importance of the nonlinearities in the heat conduction equation and the Navier-Stokes equation. Our current investigations are restricted to Prandtl numbers < 1.5 , where non-relaxational, spatio-temporally chaotic behavior can be observed very close to the onset of convection.

We use spatially periodic and spatio-temporal forcing schemes of various geometries to study the influence of modulations on pattern formation. We are particularly interested in investigating the spatio-temporal chaotic states like Spiral Defect Chaos [3] or undulation chaos [2]. Two types of forcing schemes are applied – one uses micro-machined surfaces, as shown schematically in Fig. 1, and the other uses a thermal imprinting technique that is improved but similar to the one pioneered by Busse and Whitehead [4]; we illuminate the cell with infrared light, which at a wavelength of $2.7 \mu\text{m}$ is absorbed by the CO_2 gas.

A considerable body of literature on time periodic forcing of hydrodynamic patterns, particularly convective patterns, has accumulated. Time periodic forcing can generate hexagons in a system where a roll pattern is expected; standing waves in a system where traveling waves are expected; and even four-mode superlattices. Spatially periodic forcing, on the

other hand, has received far less attention. In particular, there is no spatial counterpart to the extensive investigations of RBC subjected to time periodic forcing. Similarly, while temporal forcing of a spatiotemporally chaotic state has been investigated, the response of spatiotemporal chaos to spatial forcing remains an open question.

In one of our ongoing experiments we force with a parallel array of micromachined walls (see Fig. 1) a wavevector, which lies outside of the stability region for ideal parallel rolls, but still close to the critical wavenumber of the unforced system. Above onset with increasing temperature difference we first observe a pattern of ideal rolls, which give way to localized convection states consisting of kinks and anti-kinks, as shown in Fig. 2A. These are moving mostly along the rolls with kinks (or anti-kinks) rowing up or kink/antikink-pairs annihilating. As a function of temperature difference, there exist regions in parameter-space, where kinks (or antikinks) row up and generate a continuous oblique pattern, as shown in Fig. 2B. An analysis shows that a resonance triad of the forcing mode with two oblique modes that lie within the stability region generates these extended patterns.

Currently we use two apparatuses. The one with the micro-machined bottom plate is at

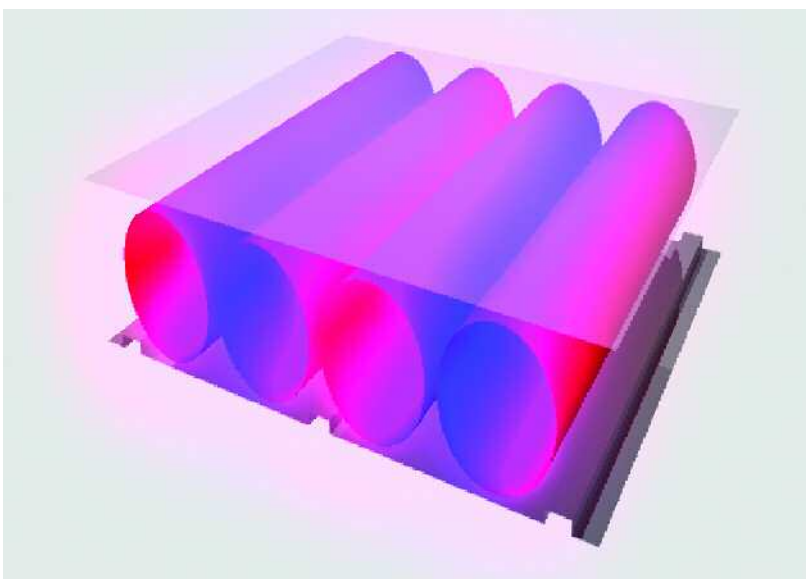
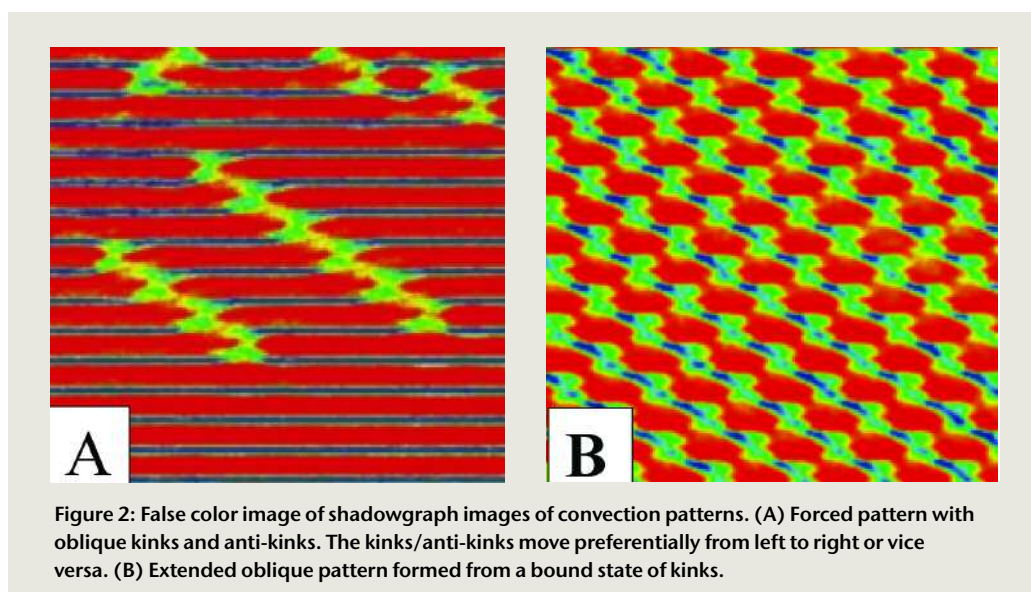


Figure 1: Schematic of the convection cell with micromachined bottom plate (to scale). The fluid height is typically 0.5 mm.

Cornell University and will move in Nov. 2006 to Göttingen after Jonathan McCoy graduates. The other has already been moved to Göttingen. It has been CE certified and also modified to allow for the optical forcing experiments.

- [1] E. Bodenschatz, W. Pesch, and G. Ahlers, *A. Rev. Fluid Mech.* **32** (2000) 709.
- [2] K.E. Daniels and E. Bodenschatz, *Phys. Rev. Lett.* **88** (2002) 4501.
- [3] K.E. Daniels, R.J. Wiener, and E. Bodenschatz, *Phys. Rev. Lett.* **91** (2003) 114501.
- [4] S.W. Morris et al., *Phys. Rev. Lett.* **71** (1993) 2026.
- [5] F.H. Busse and J.A. Whitehead, *J. Fluid Mech.* **47** (1971) 305.



2.3.3.6 Wax Modeling of Plate Tectonics

Gabriel Seiden

Will Brunner, Hélène Scolan, Stephan Weiß

THE TIME SCALE of plate tectonics is on the order of hundreds of millions of years, making it difficult to observe the dynamical processes involved. In addition, most of the interesting phenomena occur on the ocean-floors under 2 to 4 km of water. The only available means for studying the details of the dynamics are through numerical simulations and physical modeling. Current numerical simulations remain far from capturing the full complexity of the problem, which involves coupled multi-scale physical processes including fracture, phase transitions, and flow of complex fluids. This may leave physical modeling as an alter-

native. Physical models, in turn, may not capture every aspect of the physics (e. g., pressure, rheology, etc.) and often do not obey dynamic similarity in every detail. Our recent experiments [1] have shown that wax models may indeed be used to simulate certain universal features of mid-ocean ridge dynamics. At fast and intermediate spreading rate we observed behavior similar to that of Earth. We found transform faults, microplates and a similar across rift height variation. Our wax-analog experimental model simulates the divergence of two brittle lithospheric plates above a ductile mantle, exactly as it oc-

curs beneath the sea at the mid-ocean ridges. The experimental apparatus (Fig. 1) consists of a 1m long, 30 cm wide and 10 cm deep rectangular aluminum tank onto which two threaded rods are fastened. These rods carry two skimmers, which are partially immersed in the top layer of the wax and can be driven apart along the rods via a stepper motor. The tank is heated from below and from the sides in order to melt the wax in the interior of the tank, and cooled from above by a vent to allow for a thin crust to form. The experiment is initiated with a cut with a sharp knife to divide the wax surface into two plates. Activating the motor causes the skimmers to diverge, dragging with them the two wax plates and causing fluid wax from below to up-well into the rift between the plates, just as ductile mantle rock up-wells beneath a mid-ocean ridge.

Like oceanic microplates, wax microplates originate from *overlapping spreading centers*. Figure 2 depicts the nucleation of such a center on a spreading rift. A time series of the subsequent evolution of a wax microplate is shown in Fig. 3. The resemblance to the actual phenomenon is quite striking, as can be seen in Fig. 4 where we compare the topologically of the actual phenomenon with the wax microplate. Our wax-to-earth kinematic scaling relations indicate that the dimensions of the wax microplates are consistent with estimates for oceanic microplates [1,3], confirming the validity of the model. Moreover, close observation have enabled us to develop a theory for the nucleation of overlapping spreading centers and to further establish the geological model of microplates [1]. In particular, this formulation enables one to infer the time evolution of the pseudofaults, given the current phase-angle of its tip (see Fig. 4). Further results of our wax experiments compare favorably with other observations from mid-ocean ridges. The topography of mid-ocean ridges is known to vary with the spreading rate. Slower spreading rifts (< 25 mm/yr half spreading rate) form deep rift valleys (1-2 km deep), while faster spreading

rifts (> 40 mm/yr half spreading rate) form a small peak (axial high) at the rift axis. The topography at intermediate rates is a shallow valley within an overall axial high. All three types of behavior are observable in the wax with the same trend in spreading rates. For spreading rates $> 80 \mu\text{m/s}$ we found a shallow ridge with a height to width ratio of approximately 0.03. This ratio is very similar to the one reported for fast spreading oceanic rifts. The wax in the rift region was observed to be paste-like. If a hole was cut at the rift, the liquid wax would neither well up nor recede; the rift was at the same pressure as the liquid. Consequently, the across-rift topography can only be explained by a downward

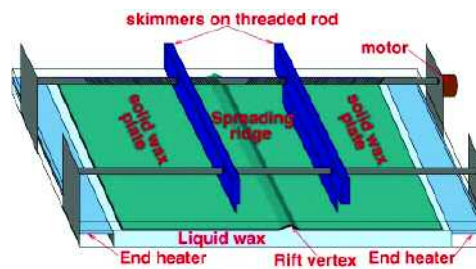


Figure 1: Scheme of experimental apparatus used in the investigation of the formation and evolution of wax microplates.

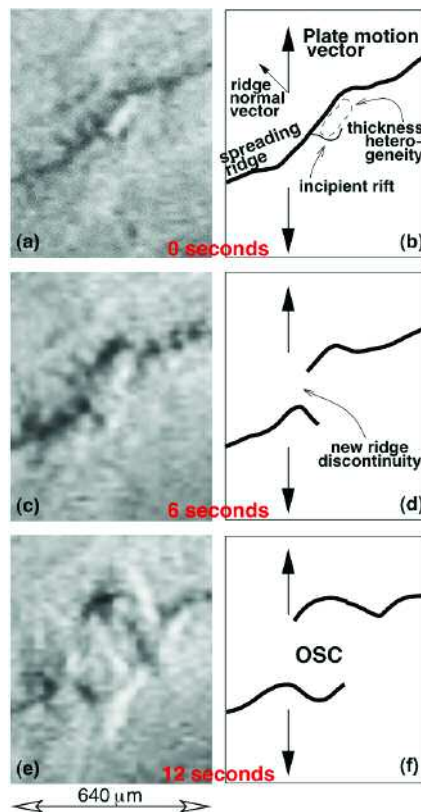


Figure 2: Nucleation of an overlapping spreading center, precursor of a wax microplate. The left column consists of a time series of images at high magnification. The right column consists of interpretive drawings of the evolution of the rift into an overlapping geometry.

Figure 3:
Time series of wax-microplate dynamical evolution. Interval between frames is 15 s. The spreading rate is $70 \mu\text{m s}^{-1}$. The left column consists of images of the microplates. The right column images are identical to the ones on the left, but with pseudofault pairs and spreading ridge overlaid in red.

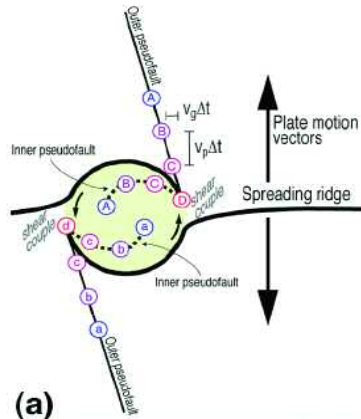
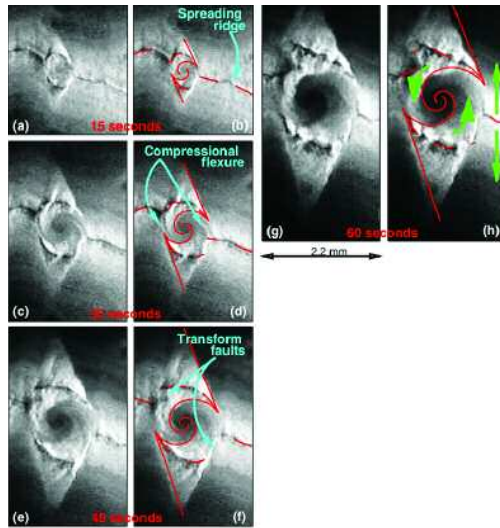


Figure 4:
Comparison between a wax-microplate and the Easter microplate.
(a) Schematic diagram illustrating the kinematics of microplates. The letters indicate points on the pseudofaults that were formerly at the rift tips, showing how the microplate grows with time. The current positions are marked as (d) and (D). (b) Image of a wax microplate with model fit and rift markers overlaid as in (a). (c) Bathymetry of the Easter microplate [4]. Colors denote elevation with respect to sea-level.

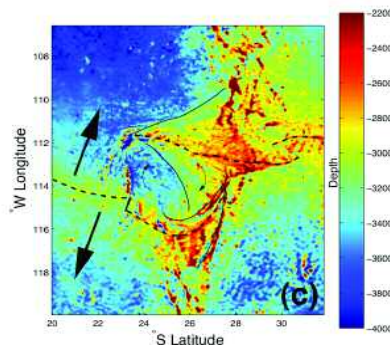
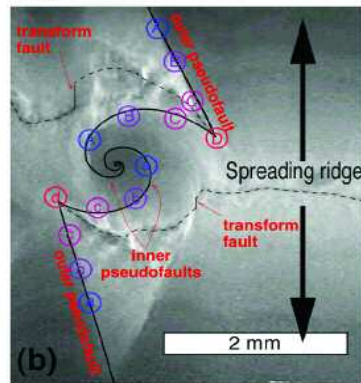


Figure 5. The experimental apparatus used for the measurement of the viscosity of the wax as a function of temperature. A small ball at the tip of a thin rod is immersed in the molten wax under constant load. The viscosity is calculated from the measured terminal velocity.

bending of the solidifying crust in the vicinity of the rift axis. For between $60 \mu\text{m/s}$ and $80 \mu\text{m/s}$ the rift was flat, and at lower spreading rates the rift formed a valley.

All the features described above are similar to that of Earth. However, at this point it is unclear what causes this behavior. The answer must lie in the rheological properties of the solidifying wax. These are very poorly known, a fact that hinders a more comprehensive and quantitative theoretical formalism. To this end we constructed an experimental apparatus (Fig. 4) designed to investigate the complex viscosity dependence of the different waxes used to model plate tectonics. These measurements, together with quantitative studies of the thermal and flow fields in a refined version of the wax-tectonics apparatus, will enable us to test numerical models that later, in a refined form, can be applied to Earth or other planets.

[1] H. Schouten, K.D. Klitgord, and D.G. Gallow, *J. Geophys. Res.* **98** (1993) 6689.
 [2] R.F. Katz, R. Ragnarsson, and E. Bodenschatz, *New J. Phys.* **7** (2005) 37.
 [3] R.L. Larson et al., *Nature* **356** (1992) 571.
 [4] W.F.H. Smith and D.T. Sandwell, *Science* **277** (1997) 1957.

2.3.3.7 Nonlinear Dynamics and Arrhythmia of the Heart

Stefan Luther

Michael Enyeart, Gisa Luther, Amgad Squires
R. Gilmour (Cornell, USA), B. Pieske (Göttingen)

HEART DISEASE IS one of the most prevalent diseases in the world and is the leading cause of death in industrialized countries. In Germany alone, heart rhythm disorders cause approximately 100,000 sudden deaths annually. Sudden cardiac death occurs unpredictably as a result of fast-developing electromechanical malfunctions of the heart. During normal functioning, the contraction of the heart is periodically triggered by planar electrical activation waves propagating across the heart followed by a refractory period. Numerical simulations and measurements suggest that during ventricular tachycardia (VT) the plane wave undergoes a transition to fast rotating, three-dimensional spiral waves (which are analogous to vortices in the Ginzburg-Landau model). Subsequently, spiral wave breakup results in a spatiotemporal chaotic state called ventricular fibrillation (VF, see Fig. 1). Ventricular fibrillation inhibits the synchronized contraction of the heart due to lack of spatiotemporal coherence. The blood flow stops and as a consequence the organism dies within minutes.

It is the topic of this research program to investigate the following questions: How is VT or VF created? Is there only one type of VT or VF? How can VT or VF be efficiently removed without harming the organism? What ionic channels can be identified/alterd that cause VT or VF? What treatment (medication, gene therapy) can be found to avoid VT or VF? Progress in this field requires a close interplay of time resolved three-dimensional measurements of wave propagation with mathematical modeling.

Numerical Simulations: Return Maps and Ionic Models

We have found evidence, both from experiments and from computer simulations, that the initiation and breakup of spiral waves in cardiac tissue is related to a period doubling

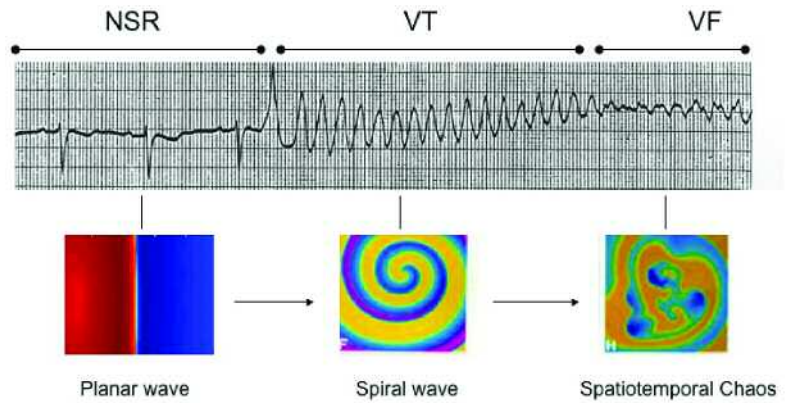


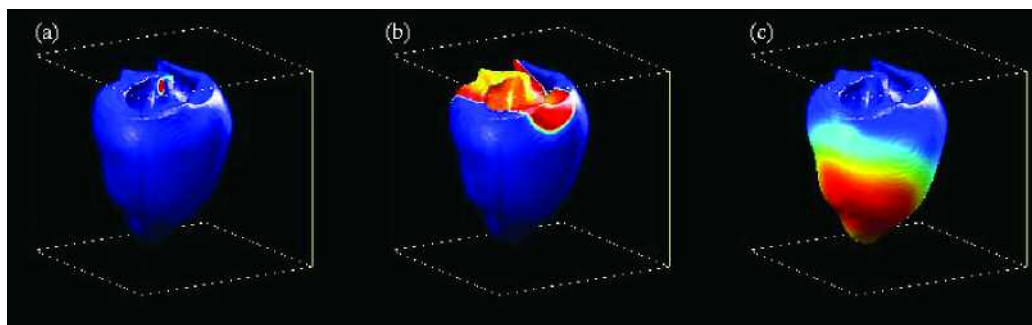
Figure 1: Onset of cardiac arrhythmia observed in an ECG recording (top). The normal sinus rhythm (NSR) undergoes a transition to ventricular tachycardia (VT) via a short episode of ventricular fibrillation (VF). Numerical simulations (bottom) show the corresponding hypothesized electrical activation patterns suggesting a transition from planar waves to spiral waves and spatiotemporal chaos.

bifurcation of cardiac electrical properties. At rapid heart rates, electrical *alternans* develops, a beat-to-beat long-short alternation in the duration of the cardiac action potential. In both the experiments and the computer models, rapid periodic pacing produced spatiotemporal heterogeneity of cellular electrical properties. These behaviors resulted from the interplay between local period two dynamics (alternans) and conduction velocity dispersion. This activity can be understood in terms of a period doubling bifurcation of a simple uni-dimensional return map (called the duration restitution relation) relating the duration of an action potential to the rest interval that preceded it [2]. In addition of simulating this simple model, we also investigate ionic models that produce a more detailed representation of cardiac action potentials. The ionic model is solved by taking into account a realistic heart geometry and tissue heterogeneity such as fiber orientation as shown in Fig.2. The model equations are solved numerically using finite differences and Cartesian coordinates. An auxiliary variable, the phase field, indicates the presence or absence of tissue at each grid point.

Experiment: Optical Mapping and Intramural Probes

The electrical activation of the heart surface can be measured optically using voltage sen-

Figure 2: Numerical simulation of the electrical activation of cardiac tissue using the canine ventricular model (CVM) and realistic geometry. Panels (a-c) show the time evolution of an excitation propagating across the ventricles. Blue indicates polarized tissue, red depolarized tissue.

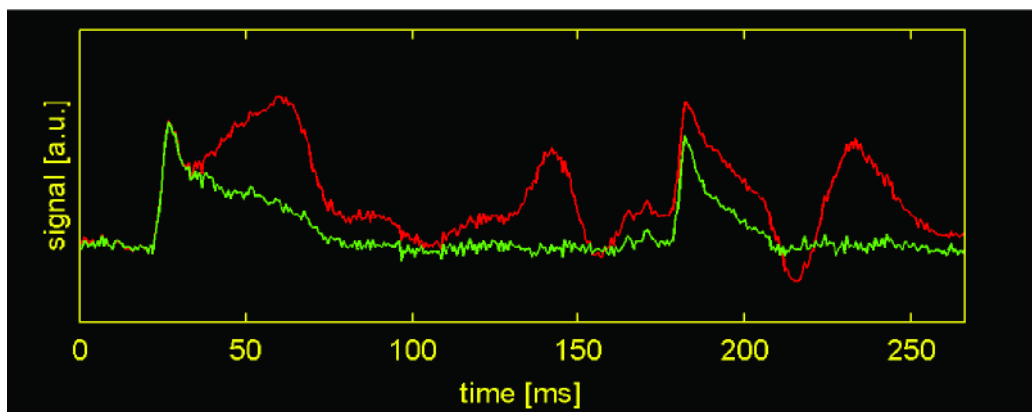


sitive dyes at high spatial and temporal resolution [3]. However, electrical activation triggers contractile motion, which in turn causes substantial distortions of the optical signal as shown in Fig. 3. These artifacts prevent an accurate measurement of the action potential duration and diastolic interval and thus bias the restitution relation. Hitherto approaches to prevent motion artifacts are based on mechanical or pharmacological immobilization of the tissue and are known to change its electrophysiological properties. Therefore, motion artifacts pose a severe limitation to the optical mapping technique. We have developed a numerical technique that reliably removes the effect of contractile motion from optical action potential measurements [4]. It is based on image registration using locally affine transformations that compensate motion and deformation effects. Figure 3 shows a time series with substantial motion artifacts and the corresponding restored signal. In addition, the measured displacement field provides valuable information on the surface strain. Our new technique removes a significant limitation to the optical mapping tech-

nique and provides the basis for studies of excitation-contraction coupling [5].

Optical mapping measures electrical activation of cardiac tissue on its surface. The main challenge is, however, to measure the three-dimensional propagation of the action potentials in the tissue. Currently, we are developing fiber optical probes that can be inserted into the heart wall. Up to 4 multimode fibers are bundled and provide optical measurement of cardiac action potentials at various tissue depths. During an experiment, several of these fibers are inserted into the ventricular wall. Data from the intramural and surface measurements are used to characterize cardiac activation during tachycardia and fibrillation. Wave breaks, spiral or scroll wave cores can be identified as phase singularities or defects. This approach is illustrated in Fig. 4. These phase singularities are the organizing structures of tachycardia and fibrillation. First encouraging experimental results indicate that our approach allows for locating scroll waves in the heart wall and to follow them in time. This new method can now be used to address the questions raised above.

Figure 3: Contractile motion of cardiac tissue results in substantial artifacts in action potential recordings (red trace). These distortions impede meaningful signal analysis such as action potential duration measurements. The green trace shows the corresponding restored times series with recovered action potential morphology.



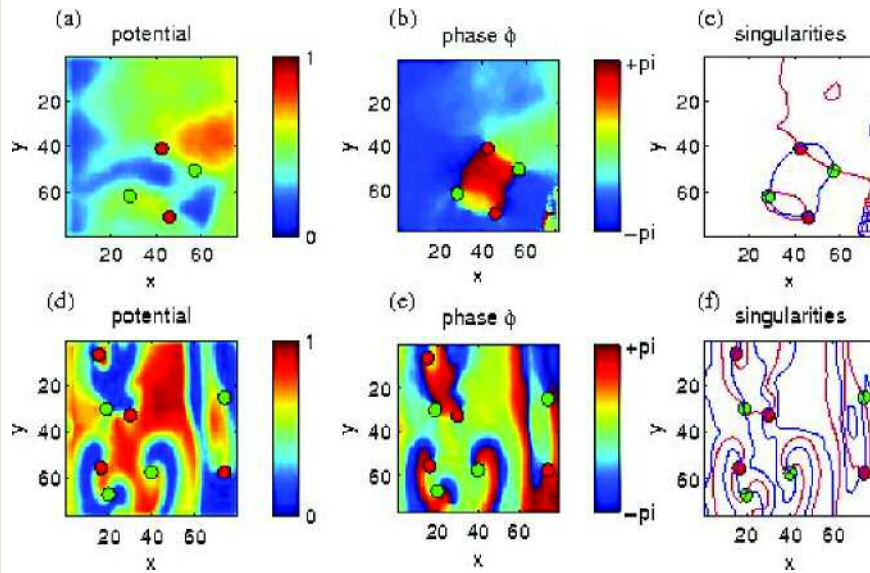


Figure 4: *Top row:* Experimental reentry pattern obtained during ventricular fibrillation using optical surface mapping with voltage sensitive dye. Field of view $2.5 \times 2.5 \text{ cm}^2$. (a) Normalized transmembrane potential. Color code same as panel (a). (b) Phase. (c) Position of phase singularities. The circles indicate the positions of phase singularities in all panels, where red and green indicate clockwise and counter clockwise rotation, respectively. *Bottom row:* Numerical example of a complex activation pattern in two-dimensional tissue of size $5.5 \times 5.5 \text{ cm}^2$. (d) Normalized transmembrane potential. Blue indicates polarized tissue, red depolarized tissue. (e) Phase. (f) Position of phase singularities given by the zero crossing of real (red) and imaginary part (blue) of the complex signal.

[1] J.F. Fox et al., *Circ. Res.* **90** (2002) 289.

[2] J.F. Fox, E. Bodenschatz, and R.F. Gilmour, *Phys. Rev. Lett.* **89** (2002) 138101.

[3] I.R. Efimov et al., *Circ. Res.* **95** (2004) 21.

[4] G.E. Luther et al., to be submitted to *Circ. Res.*

[5] D.M. Bers, *Nature* **418** (2002) 198.

2.3.3.8 Chemotaxis and Cell Migration

Carsten Beta

Albert Bae, Toni Fröhlich, Barbara Kasemann, Katharina Schneider, Danica Wyatt
H. Levine (UCSD, USA), W. F. Loomis (UCSD, USA), W.-J. Rappel (UCSD, USA)
C. Franck (Cornell, USA), G. Gerisch (MPIBC), H. Ishikawa (MPIBC)

CHEMOTAXIS – THE DIRECTED movement of a cell in response to chemical stimuli – is a fundamental phenomenon in many biological and medical processes including morphogenesis, immune response, and cancer metastasis. Over the past thirty years, major research efforts were undertaken to advance the understanding of how a cell senses, responds, and moves towards a chemical signal. In particular, the last decade has witnessed a rapid advance in deciphering the G-protein linked signaling pathways that govern the directional response of eukaryotic cells to chemoattracting agents [1,2]. However, for a thorough understanding of the complex phenomenon of chemotaxis the molecular details of intracellular signaling and the macroscopic migration of a cell have to be merged into an overall model.

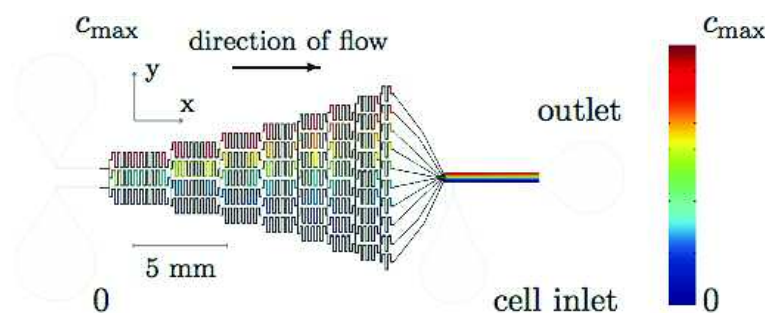
While many of the key components of intracellular biochemical networks could be identified in recent years, a complete picture of directional sensing and chemotaxis is mostly hampered by the lack of quantitative data. For the actual movement of a cell in gradients of chemoattractant as well as for the intracellular reaction networks almost none of the dynamical characteristics have been precisely determined. It is the aim of the *Chemotaxis and Cell Migration* project to provide quanti-

tative insight into the governing parameters of directional cell movement. A solid knowledge of the length and time scales for both cell migration and intracellular spatiotemporal dynamics of signaling networks is expected to considerably advance our understanding of a vast number of biological and medical processes that depend on chemotactic motion.

Our approach combines the work on a well-established model organism for chemotaxis with novel experimental techniques that allow the precise spatiotemporal addressing of this organism in easily tunable, highly controlled chemical environments. Chemotaxis has been studied for a large variety of biological systems ranging from prokaryotic cells to mammalian leukocytes and neutrophils. For our current projects we choose the eukaryote *Dictyostelium discoideum*, one of the most prominent biological model systems for chemotactic behavior [3].

Our experiments on *D. discoideum* are performed with microfluidic devices. Micrometer sized flow chambers combine a number of advantages that make them optimally suited for cell dynamics experiments: Due to strictly laminar flow conditions the chemical environment can be precisely controlled on the length scale of individual cells and arbitrary

Figure 1:
Layout of the microfluidic channel network used to generate a linear concentration gradient. The color coding displays the concentration from a 2-dimensional numerical simulation of the Navier-Stokes and drift-diffusion equation in the shown geometry using FEMlab 3.1. Black lines mark in- and outlets that were not part of the numerical simulation.



sequences of stimuli can be applied with high temporal resolution. Besides, only biocompatible materials are used, they are well suited for the combination with optical imaging techniques, and the microfabrication process follows well established and highly reproducible protocols.

As an example, Fig. 1 shows a microfluidic network for the built-up of a well-defined linear gradient between a minimal and a maximal concentration level. Through a cascade of successive dividing and remixing ten equidistant concentration levels are generated and united inside the main channel to form a linear concentration gradient. Compared to traditional chemotaxis assays like micropipette setups or diffusion chambers, a microfluidic device allows for a well defined and temporally stable concentration profile while a slow continuous fluid flow ensures that waste products and signaling substances released by the cells are washed away. In this setup, cell motility and chemotactic response can be systematically investigated as displayed in Fig. 2 for *D. discoideum* cells in linear gradients of the chemoattractant cAMP (cyclic adenosine 3',5'-monophosphate). The experiments show a chemotactic response and an increased motility for gradients between 10^{-3}

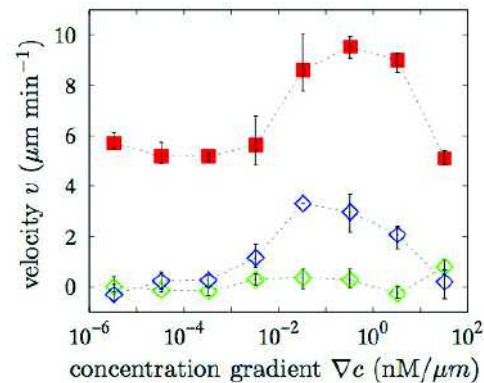


Figure 2: Average velocity components v_x (red diamonds) and v_y (= chemotactic velocity, blue diamonds) as well as motility (red squares) measured for different cAMP gradients.

and $10 \text{ nM}/\mu\text{m}$ [4]. Besides conventional microfluidic devices, we also combine micrometer sized flow channels with the use of caged substances. This approach leads to a highly versatile setup allowing for a wealth of new single cell experiments. An additional UV light beam is coupled into the imaging light path and allows to release caged chemoattractants by photoactivation inside a microfluidic chamber in the vicinity of a cell. In combination with differently shaped pin holes, the uncaging light spots can be individually tuned to generate arbitrary concentration profiles of released signaling substances, see e.g. Fig. 3. In this context, particular attention has to be paid to the deformation of the concen-

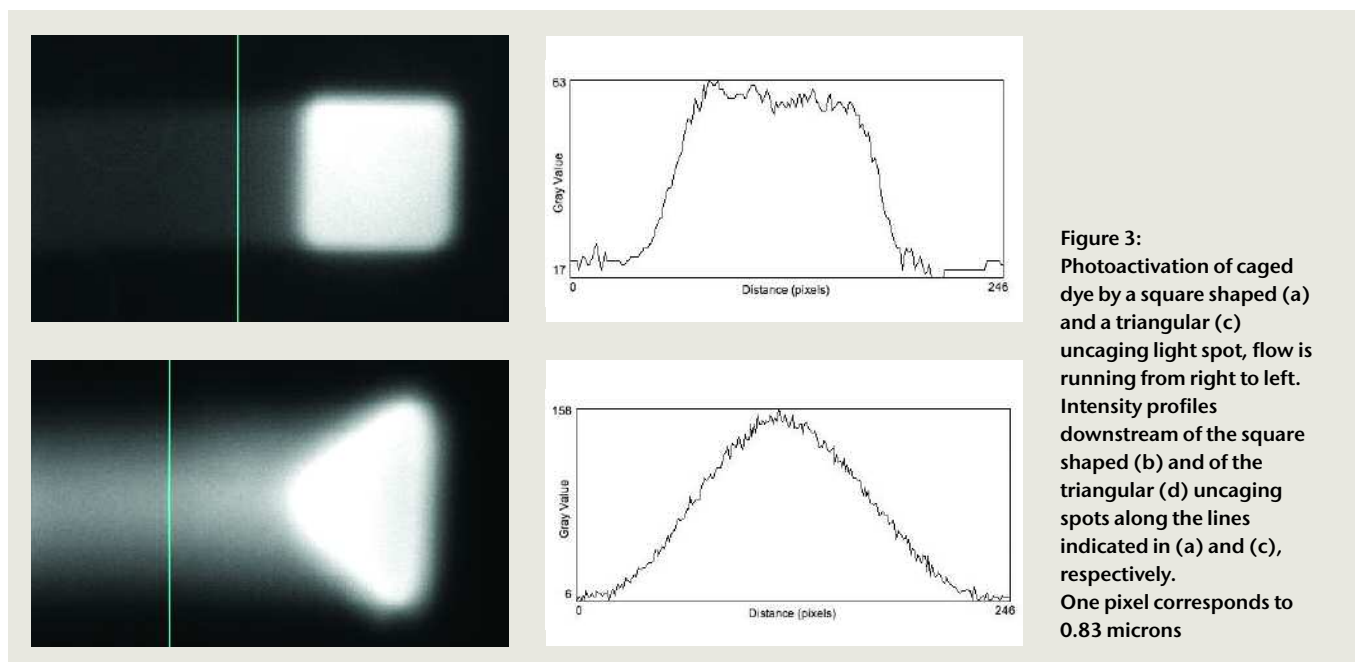
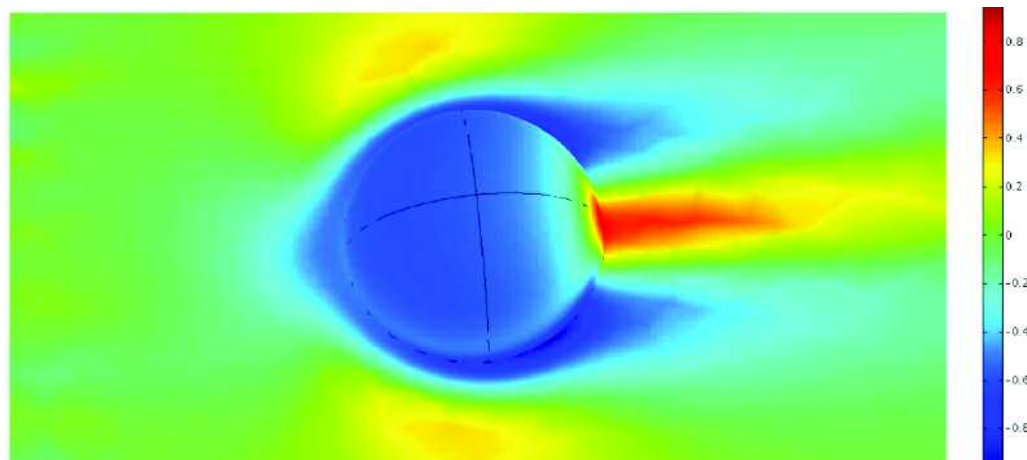


Figure 3: Photoactivation of caged dye by a square shaped (a) and a triangular (c) uncaging light spot, flow is running from right to left. Intensity profiles of the square shaped (b) and of the triangular (d) uncaging spots along the lines indicated in (a) and (c), respectively. One pixel corresponds to 0.83 microns

Figure 4:
Deviations from an ideal, unperturbed concentration gradient in the vicinity of a half-sphere in a microfluidic channel (from a numerical 3D finite element simulation using FEMlab 3.1) with a laminar flow. The Péclet number $Pe=200$.



tration distribution close to a cell. The interplay of flow profile and cell geometry can lead to nontrivial effects that are studied using both experimental 3D-imaging techniques and numerical finite element simulations (see Fig. 4).

A second focus of our project emphasizes the use of fluorescently labeled biomolecules in cell constructs to study the internal dynamics of chemotactic cells. In the framework of cooperations with the group of Prof. William F. Loomis (Division of Biological Sciences, University of California at San Diego) and the group of Prof. Günther Gerisch (MPI for Biochemistry, Martinsried), a library of cell lines is available in which different proteins, that

are known to be part of the chemotactic signaling pathways, are expressed together with a fluorescent marker. These constructs allow imaging of the spatiotemporal dynamics of protein distributions inside individual cells as they experience stimulation. As an example, Fig. 5 shows the uniform translocation of the GFP-marked Lim protein to the cell cortex in response to a uniform stimulus with $10\ \mu\text{M}$ cAMP. In these experiments, we use state-of-the-art fluorescence microscopy imaging techniques including a multi-channel laser scanning confocal microscope and total internal reflection fluorescence microscopy (TIRF).

Figure 5: Global translocation of the GFP-marked Lim protein to the cell cortex in response to a uniform stimulus with cAMP.

The bottom side length corresponds to 41.4 microns.



- [1] P.J.M. Van Haastert and P.N. Devreotes, *Nature Reviews* **5** (2004) 626.
- [2] C.A. Parent and P.N. Devreotes, *Science* **284** (1999) 765.
- [3] R.H. Kessin, *Dictyostelium: Evolution, Cell Biology, and the Development of Multicellularity*, Cambridge University Press (Cambridge, 2001).
- [4] L. Song et al., *Eur. J. Cell Biol.*, in press

2.3.3.9 The Cell Culture Laboratory – Myocardial Tissue Engineering

Barbara Kasemann

Stefan Luther, Katharina Schneider

Olympus Deutschland GmbH (Hamburg), B. Busse (Zell-Kontakt, Nörten-Hardenberg),
E.-K. Sinner (MPIPR, Mainz)

THE CELL CULTURE laboratory is one of the department's core research facilities. It provides expertise in diverse applications of cell characterization, diagnosis, and culturing. It offers extensive services and training to the research groups. The laboratory's interdisciplinary work focuses on the development of myocardial cell cultures. Applying principles of engineering and life science we are developing methods for two and three-dimensional aggregation of cardiomyocytes. The engineered myocardial tissue will allow for the investigation of fundamental mechanism of arrhythmia in a controlled physico-chemical environment. By combining cell culture experiments with biophysically realistic computer models we hope to gain further insight into cardiac cell and tissue function and pathology. The cell culture laboratory has been established in 2005. This report describes the equipment, the current research, and outlines the future work.

Equipment

The cell culture laboratory is a fully equipped research facility certified according to gene technology safety class S1. Our laboratory provides outstanding imaging facilities for diverse applications. A collaborative agreement with Olympus provides cutting edge microscope and imaging systems for research and training.

Our equipment includes a confocal and two epifluorescence microscopes, and two real time imaging and TIRFM systems (Olympus, Delta Vision). The confocal microscope offers several advantages over conventional optical microscopy, including controllable depth of field, the elimination of image degrading out-of-focus information, and the ability to collect serial optical sections from thick specimen. The TIRFM Systems allow for ultra sensitive

fluorescence microscopy at the cell surface, providing high contrast imaging with minimal background noise.

The cell culture laboratory comprises a class 2 microbiological cabinet including standard equipment such as UV illumination, vacuum pump, pipettors etc. The cell cultures are grown adherent to a surface or in suspension. An incubator provides a controlled CO₂ atmosphere at constant temperature. The cells are preserved and stored in liquid nitrogen and in a -80°C freezer. A laboratory dish washer, drying cabinet, and autoclave are available for cleaning and sterilization of glassware. The autoclave is also used for germicidal treatment of biological waste. For diagnosis and cell analysis an ELISA Reader and mycoplasma test are available.

Cardiac myocytes

Currently we are investigating and comparing various approaches to obtain and cultivate cardiomyocytes from embryonic chicken and the P19 cell line.

In order to obtain a primary cell culture from embryonic chicken, the heart is excised and dissected. The tissue is enzymatically dissociated into individual cardiac myocytes. For cultivation the cells are placed onto different substrates, e.g. glass or plastic. Cell adhesion is improved by covering the surfaces with proteins. After two days the cells begin to beat spontaneously. The properties of cell adhesion strongly depend on the substrate. We found that the cell adhesion is significantly improved on the semi-permeable membrane Lumox50. We have completed cell morphological tests, and electrophysiological characterization will follow.

Currently, we are evaluating the P19 cell line. This cell line was derived from an embryonal carcinoma induced in a C3H/He strain



Figure 1. Cell dissociation and preparation.



Figure 2: Cell diagnosis and characterization.

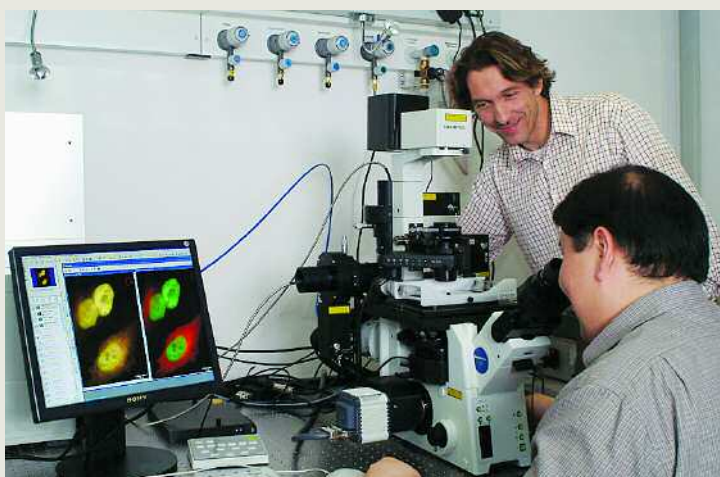


Figure 3: Training on the Olympus TIRFM System.

mouse. The pluripotent P19 cells can be induced to differentiate into neuronal, glial, skeletal, and cardiac cells. The first results with cardiac cells obtained from this cell line are very encouraging and further electrophysiological experiments are under way. This work is done in collaboration with Dr. Eva-Kathrin Sinner (Max Planck Institute for Polymer Research, Mainz).

Future Research

The successful development of cell cultures requires accurate control of the cells' physico-chemical environment. Lacking a microvascular structure, the growth of functional cell aggregates is limited by diffusion to a few cell layers. Microfluidic technology provides means to overcome this limitation. The goal of our research is the development of microfluidic two- and three-dimensional tissue scaffolds that provide a controlled mechanical and physico-chemical cellular environment. This challenging interdisciplinary project involves physics, engineering and life science in effort to affect the advancement of medicine.

When applied to cardiac myocytes, our approach will provide a simplified yet realistic model of cardiac tissue. By controlling the cell environment, such that regions are locally depleted from oxygen, we will obtain a model for diseased tissue such as myocardial infarct and ischemia and reperfusion damage. It will provide experimental insight into the role of dynamical vs. structural heterogeneities for the development and sustaining of cardiac arrhythmia.

2.4 Associated Scientists

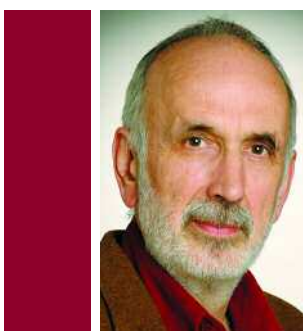
2.4.1 People



PD Dr. Folkert Müller-Hoissen

Folkert Müller-Hoissen received his doctorate in theoretical physics from the University of Göttingen in 1983. After postdoc positions at the MPI for Physics in Munich and the Yale University in New Haven, USA, he returned to the University of Göttingen as a Wissenschaftlicher Assistent, passed the Habilitation in 1993 and became a Privatdozent. Since 1996 he carries on his research in mathematical physics at the MPI for Fluid

Dynamics, which meanwhile evolved into the MPI for Dynamics and Self-Organization. Since 2000 he is also außerplanmäßiger Professor at the University of Göttingen.



PD Dr. Reinhard Schinke

Reinhard Schinke received his doctorate in theoretical physics from the University of Kaiserslautern in 1976. After a one year postdoctoral position at the IBM research laboratory in San Jose (Cal.) he took a position at the MPI für Strömungsforschung in the department for Atomic and Molecular Interactions in 1980. He received his habilitation in theoretical chemistry from the Technical University of Munich in 1988. His research

centers around the understanding of elementary processes in the gas phase like chemical reactions, photodissociation and unimolecular reactions. He is author of the monography »Photodissociation Dynamics« (Cambridge University Press, 1993) and received the Max-Planck research award in 1994 and the Gay-Lussac/Humboldt award in 2002.

2.4.2 Projects

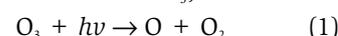
2.4.2.1 Elementary Gas-Phase Reactions

Reinhard Schinke

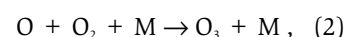
Sergei Y. Grebenshchikov, Mikhail V. Ivanov

THE INVESTIGATION OF elementary reactions in the gas phase (exchange reactions, photodissociation, unimolecular dissociation etc.) is important for understanding complicated processes, for example, in combustion and in the atmosphere. Theoretical studies aim at reproducing detailed experimental data by *ab initio* methods, explaining measured data on the basis of fundamental equations and making predictions for experiments, which are difficult to perform in the laboratory. The tools are global potential energy surfaces (PES's), calculated in the Born-Oppenheimer approximation by solving the electronic Schrödinger equation, and the solution of the nuclear Schrödinger equation for the intramolecular dynamics of the atoms on these PES's [1,2].

In recent years we concentrated on one particular molecule, ozone, which plays a central role in atmospheric chemistry. Both the photodissociation of O_3 ,



and the recombination



where M is necessary to carry away the excess energy, have been investigated. Although both processes appear to be seemingly simple, there are many open questions, which can be solved only by state-of-the-art quantum mechanical calculations.

The photoabsorption cross section of ozone in the wavelength region from the near ir to the uv shows four different bands: Wulf, Chappuis, Huggins and Hartley. Each band corresponds to one (or several) particular electronic states which are excited by the photon. Calculations have been completed or are in progress for all bands. The quantitative description of process (1) requires the calculation of PES's of all electronic states involved, each being a function of the three internal coordinates of O_3 . In addition, the non-Born-Oppenheimer coupling elements are required if more than one state is involved. Figure 1 shows one-dimensional cuts along the dissociation coordinate of all states of ozone, which possibly take part in the photodissociation [3,4]. For a total of 10 states global PES's have been determined. Quantum mechanical dynamics calculations, i.e., solving either the time-independent or the time-dependent Schrödinger equation, yield the absorption spectrum and the final rotational-vibrational product state distributions. In addition they reveal, in combination with classical mechanics calculations, the dissociation mechanisms and ex-

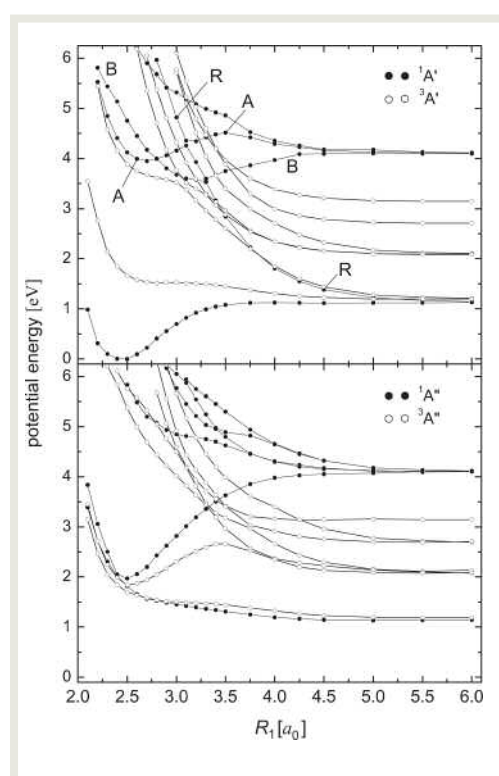


Figure 1: Potential cuts for the singlet and triplet A' (a) and the singlet and triplet A'' (b) states of ozone along the dissociation coordinate. From Zhu et al., Chem. Phys. Lett. 384, 45 (2004).

planations for certain prominent features like diffuse vibrational structures and predissociation lifetimes [5,6]. Figure 2 shows calculated rotational state distributions of O_2 for several vibrational states in comparison with measured results. Current work concerns the influence of spin-orbit coupling in the Wulf band and non-adiabatic coupling in the Hartley band and its influence on dissociation lifetimes.

The recombination of ozone in collisions of O atoms and O_2 molecules is a very complicated process and despite many experimental and theoretical efforts it is not yet fully understood. Questions concern the temperature dependence of the formation rate coefficient, and thus the formation mechanism (energy transfer or chaperon mechanism or both), and its surprisingly strong isotope dependence. The latter effect leads to a non-statistical distribution of isotopomers in the atmosphere as has been measured in the 1980'ies by means of balloon experiments [7]. The isotope dependence has created a great deal of interest among theorists because it seems to reveal a fundamental reaction mechanism. Up to now there is no satisfactory explanation on the basis of real *ab initio* calculations; a status report critically reviews all the dynamical calculations in the last decade to explain this effect [8]. The more realistic calculations, each of which however makes some model assumptions, hint at the difference of zero-point energies in the different channels in which the highly vibrationally excited ozone complexes can dissociate (Figure 3) [9]. In our current work we attempt to perform rigorous quantum mechanical calculations for state-specific lifetimes [2] of different isotopomers, which appear to be the key for the ozone isotope effect.

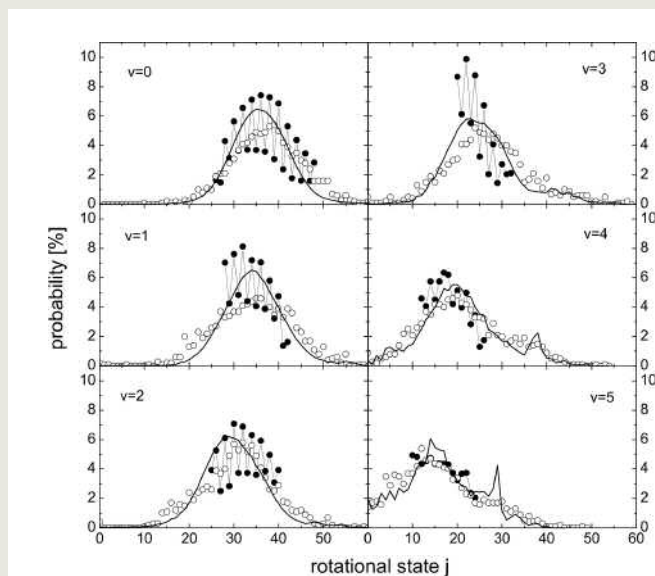


Figure 2: Comparison of experimental (●), classical (○) and quantum mechanical (—) rotational state distributions of O_2 for photolysis at 240 nm. From Qu et al., J. Chem. Phys. 123, 074305 (2005).

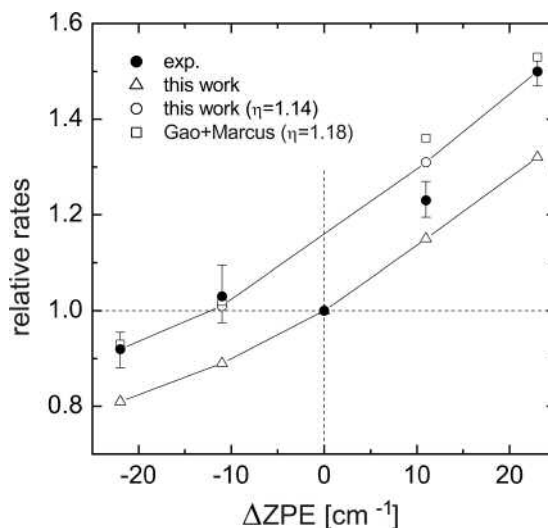


Figure 3: Comparison of relative formation rates as function of the zero-point energy difference between reactant and product channels, ΔZPE . The data points correspond to (from left to right): 8+66, 7+66, 6+66, 6+77, and 6+88. $T = 300$ K and low pressures. Δ unscaled trajectory results; \circ scaled trajectory results ($\eta = 1.14$); \bullet experimental results; \square statistical RRKM calculations ($\eta_{CM} = 1.18$). The scaled trajectory data for 8+66 and 6+88 agree with the experimental results and therefore are not discernable. From Schinke and Fleurat-Lessard, J. Chem. Phys. 122, 094317 (2005).

- [1] R. Schinke, *Photodissociation Dynamics*. Cambridge University Press, Cambridge, (1993).
- [2] S.Yu. Grebenshchikov, R. Schinke and W.L. Hase, in *Unimolecular Kinetics*, N. Green ed. (Elsevier, Amsterdam, 2003).
- [3] Z.-W. Qu, H. Zhu and R. Schinke, *Chem. Phys. Lett.* **377** (2003) 359.
- [4] H. Zhu et al., *Chem. Phys. Lett.* **384** (2004) 45.
- [5] Z.-W. Qu et al., *J. Chem. Phys.* **121** (2004) 11731.
- [6] Z.-W. Qu et al., *J. Chem. Phys.* **123** (2005) 074305.
- [7] K. Mauersberger et al., *Adv. At. Mol. Opt. Physics* **50** (2005) 1.
- [8] R. Schinke et al., *Ann. Rev. Phys. Chem.* **57** (2006) 625-661.
- [9] R. Schinke and P. Fleurat-Lessard, *J. Chem. Phys.* **120** (2005) 094317.

2.4.2.2 Mathematical Physics

Folkert Müller-Hoissen
A. Dimakis (Aegean, Greece)

Solitons and integrable systems.

CONTINUUM PHYSICS AND classical field theory is mathematically modelled with, typically nonlinear, partial differential equations (PDEs). These exhibit very peculiar phenomena, ranging from chaos to organizational behavior. The latter is typically related to the existence of symmetries of the respective PDE beyond those given by special groups of coordinate transformations. An extreme case is met if a PDE possesses an infinite number of (independent) symmetries, in which case the PDE extends to an infinite tower of compatible PDEs, a so-called hierarchy [1]. The most famous example is given by the Korteweg-deVries (KdV) equation which possesses multi-soliton solutions: an arbitrary number of solitary waves flow through each other and regain their initial form afterwards. By now quite a number of PDEs with properties similar to the KdV equation have been found and frequently recovered as certain limits of physical models. Several beautiful (including some rather miraculous) mathematical techniques have been developed to unravel the essential structure of such equations. All this is covered nowadays under the heading of integrable systems theory. For equations in this class there are typically methods to obtain exact solutions (e.g., via Bäcklund transformations, or the

powerful inverse scattering method). This is extremely important in particular in areas of physics where relevant exact solutions are extremely difficult to find and numerical methods difficult to apply, which is not only the case in general relativity.

Despite enormous progress, this field is still far from a kind of completion. Neither are there satisfactory integrability tests, nor do we understand well enough the relations between the various existing notions of integrability and the extent to which they can be applied and still generalized. On the other hand, it is quite natural that this field is not really bounded, but rather continues to extend into various directions, in particular towards handling equations which are not completely integrable.

Our project is not confined to a particular corner of this field. Presently particular emphasis is put on generalizations of integrable equations to the case of noncommutative dependent variables, like matrices of functions. This covers also the case of systems of coupled equations and thus achieves a certain unification. In the following we briefly describe three of our most recent research achievements.

The ubiquitousness of the famous Kadomtsev-Petviashvili (KP) hierarchy, which generalizes the KdV hierarchy, in mathematics

(in particular differential and algebraic geometry) and physics (from hydrodynamics to string theory) still remains a bit of a mystery. In a recent work [2] we showed that, for any *weakly nonassociative* algebra, generated by a single element, the KP hierarchy shows up in the algebraic structure of commuting derivations. As a consequence, any such algebra leads to a solution of the KP hierarchy, and in particular the multi-soliton solutions are obtained in this way. The essential and amazing point is that the nonassociative structure achieves to decouple the KP hierarchy of PDEs into a hierarchy of ordinary differential equations (though in a nonassociative algebra), which is easy to solve. Integrable models with dependent variables in *nonassociative* algebras of a special type already appeared in the work of Svinolupov [3] and collaborators.

Starting from work of Okhuma and Wadati [4], an analysis of the algebraic structure of the soliton solutions of the (noncommutative) KP hierarchy led us to the proof of a correspondence between its equations and a certain set of identities in an abstract algebra, carrying in particular a quasi-shuffle product [5,6]. This algebra expresses the building laws of the KP hierarchy equations. There are more identities in this algebra and it turned out that these correspond to extensions of the KP hierarchy in the case where the product between dependent variables is deformed in the sense of deformation quantization (see also [7,8] for explorations of deformed hierarchies). Soliton solutions of the deformed equations are deformations of ordinary solitons and the deformation parameters should be fixed in some physical model. So far objects of this type made their appearance only in the context of string theory. An independent motivation for further explorations of this framework stems from the fact that surprising relations between different integrable systems show up. For example, the simplest deformation equation of the (deformed) KdV equation has the form of the Heisenberg ferromagnet equation [7].

A central role in the mathematics of inte-

grable hierarchies is played by the Gelfand-Dickey formalism [1]. The latter, however, introduces an infinite number of auxiliary dependent variables and it is often desirable to turn the hierarchy equations into a form which only makes reference to the relevant dependent variables. We developed a convenient and unifying formalism to achieve this. The results are representations of hierarchies in terms of functional equations depending on auxiliary parameters [9,10]. In several cases of scalar equations (with commuting dependent variables), corresponding representations of hierarchies are available in terms of Hirota τ -functions (in particular as so-called 'Fay identities'). In contrast, our formalism also covers the noncommutative case. Furthermore, it provides bridges between the Gelfand-Dickey formalism and in particular approaches to integrable systems as formulated by Bogdanov and Konopelchenko [11], and Adler, Bobenko and Suris [12] (discrete zero curvature representation).

Development and applications of noncommutative geometry.

'Noncommutative geometry' is a mathematical framework which primarily aims at generalizations of concepts of differential geometry from a manifold (respectively, the algebra of smooth functions on it) to a (noncommutative) associative algebra [13]. In particular, it provides a setting for 'discrete geometry', based on directed graphs (digraphs). The latter play an important role in many areas of mathematics and applied sciences. In particular, they provide a framework for discretizations and discrete analogs of continuum models. The observation [14] that directed graphs are in correspondence with differential calculi on discrete sets set the stage for a formulation of discrete models in close analogy with continuum models, if the latter possess a convenient formulation in terms of differential forms. A differential calculus (more generally on an associative algebra) is an analog of the calculus of differential forms on a manifold. The

mentioned examples are ›noncommutative‹ in the sense that differentials and functions satisfy nontrivial commutation relations. The basic rules of the calculus of differential forms, i.e. the Leibniz rule and the nilpotency of the exterior derivative, are preserved, however. Illuminating examples of applications are the following.

- The Wilson action of lattice gauge theory results from the Yang-Mills action by deformation of the continuum differential calculus to a differential calculus associated with a hypercubic lattice graph [15, 16].
- Some discrete integrable models are obtained from continuum models via such a deformation of the continuum differential calculus, carried out such that certain ›integrability aspects‹ are preserved [17, 18]. The well-known integrable Toda lattice results in this way as a deformation of the linear wave equation in $1 + 1$ dimensions.

A differential calculus provides the basis for the introduction of geometric concepts, like metric, connection and curvature. In integrable systems theory, for example, the condition of vanishing curvature plays a crucial

role. Noncommutative geometry supplies us with corresponding generalizations (see also [19]), and thus new possibilities.

Over the years we further developed this formalism aiming at applications ranging from discretization (or rather discrete versions) of gauge theories and General Relativity to some kind of ›integrable‹ network models. More recent contributions to this project include the development of gauge theory and differential geometry on (bicovariant) group lattices [20, 21]. In the case of this special class of digraphs, we established a clear geometric interpretation of the a priori rather abstract algebraic generalizations of continuum geometric concepts. In particular, this framework allows the formulation of discrete analogs of differential geometric equations, including those of gravity theories.

A special class of differential calculi associated with automorphisms of the underlying algebra has been the subject of some other publications [22, 23]. This generalizes relevant examples like the differential calculus associated with a hypercubic lattice graph mentioned above, but even covers examples of bicovariant differential calculi on quantum groups.

- [1] L.A. Dickey, *Soliton Equations and Hamiltonian Systems*, World Scientific (2003)
- [2] A. Dimakis and F. Müller-Hoissen, nlin.SI/0601001
- [3] S.I. Svinolupov, *Theor. Math. Phys.* **87** (1991) 611.
- [4] K. Okhuma and M. Wadati, *J. Phys. Soc. Japan* **52** (1983) 749.
- [5] A. Dimakis and F. Müller-Hoissen, *J. Phys. A: Math.Gen.* **38** (2005) 5453.
- [6] A. Dimakis and F. Müller-Hoissen, *Czech. J. Phys.* **55** (2005) 1385.
- [7] A. Dimakis and F. Müller-Hoissen, *J. Phys. A: Math.Gen.* **37** (2004) 4069.
- [8] A. Dimakis and F. Müller-Hoissen, *J. Phys. A: Math.Gen.* **37** (2004) 10899.
- [9] A. Dimakis and F. Müller-Hoissen, nlin.SI/0603018
- [10] A. Dimakis and F. Müller-Hoissen, nlin.SI/0603048
- [11] L.V. Bogdanov and B.G. Konopelchenko, *J. Math. Phys.* **39** (1998) 4701.
- [12] V.E. Adler, A.I. Bobenko and Yu.B. Suris, *Comm. Math. Phys.* **233** (2003) 513.
- [13] [13] J. Madore, in *An Introduction to Noncommutative Differential Geometry and its Physical Applications*, (Cambridge University Press, Cambridge 1999)
- Applications, Cambridge University Press (1999)
- [14] A. Dimakis and F. Müller-Hoissen, *J. Math. Phys.* **35** (1994) 6703.
- [15] A. Dimakis, F. Müller-Hoissen and T. Striker, *J. Phys. A: Math. Gen.* **26** (1993) 1927.
- [16] A. Dimakis, F. Müller-Hoissen and T. Striker, *Phys. Lett. B* **300** (1993) 141.
- [17] A. Dimakis and F. Müller-Hoissen, *J. Phys. A: Math. Gen.* **29** (1996) 5007.
- [18] A. Dimakis and F. Müller-Hoissen, *Lett. Math. Phys.* **39** (1997) 69.
- [19] A. Dimakis and F. Müller-Hoissen, *J. Phys. A* **29** (1996) 7279.
- [20] A. Dimakis and F. Müller-Hoissen, *J. Math. Phys.* **44** (2003) 1781.
- [21] A. Dimakis and F. Müller-Hoissen, *J. Math. Phys.* **44** (2003) 4220.
- [22] A. Dimakis and F. Müller-Hoissen, *J. Phys. A: Math. Gen.* **37** (2004) 2307.
- [23] A. Dimakis and F. Müller-Hoissen, *Czech. J. Phys.* **54** (2004) 1235.

2.5 Publications

2.5.1 Nonlinear Dynamics (1996–2006)

1996

H.-U. Bauer, R. Der, and M. Herrmann, »Controlling the magnification factor of self-organizing feature maps«, *Neural Comp.* **8** (1996) 757.

H.-U. Bauer, M. Riesenhuber, and T. Geisel, »Phase diagrams of self-organizing maps«, *Phys. Rev. E* **54** (1996) 2807.

H.-U. Bauer et al., »Self-organizing neuronal maps«, *Bericht 102* (1996) 1.

H.-U. Bauer, and M. Riesenhuber, »Calculating conditions for the emergence of structure in self-organizing maps«, in *Proc. CNS 96* (1996).

H.-U. Bauer et al., »Selbstorganisierende neuronale Karten«, *Spektrum der Wissenschaft* **4** (1996) 38.

U. Ernst et al., »Identifying oscillatory and stochastic neuronal behaviour with high temporal precision in macaque monkey visual cortex«, in *Proc. CNS 96* (1996).

K. Pawelzik et al., »Orientation contrast sensitivity from long-range interactions in visual cortex«, in *Proc. NIPS 96* (1996).

R. Fleischmann et al., »Nonlinear dynamics of composite fermions in nanostructures«, *Europhys. Lett.* **36** (1996) 167.

F. Hoffmüller et al., »Sequential bifurcation and dynamic rearrangement of columnar patterns during cortical development«, in *Proc. CNS 96* (J. Bower ed.) (1996).

R. Ketzmerick, »Fractal conductance fluctuations in generic chaotic cavities«, *Phys. Rev. B* **54** (1996) 10841.

K. Pawelzik, J. Kohlmorgen, and K.-R. Müller, »Annealed Competition of Experts for a Segmentation and Classification of Switching Dynamics«, *Neural Comp.* **8** (1996) 340.

M. Riesenhuber, H.-U. Bauer, and T. Geisel, »Analyzing phase transitions in high-dimensional self-organizing maps«, *Biol. Cyb.* **75** (1996) 397.

M. Riesenhuber, H.-U. Bauer, and T. Geisel, »On-center and off-center cell competition generates

oriented receptive fields from non-oriented stimuli in Kohonen's self-organizing map«, in *Proc. CNS 96* (1996).

M. Riesenhuber, H.-U. Bauer, and T. Geisel, »Analyzing the formation of structure in high-dimensional self-organizing reveals differences to feature map models«, in *Proc. ICANN 96*, Springer Verlag (1996) 415.

J. H. Smet et al., »Magnetic focusing of composite fermions through arrays of cavities«, *Phys. Rev. Lett.* **77** (1996) 2272.

J. H. Smet et al., »Evidence for quasi-classical transport of composite fermions in an inhomogeneous effective magnetic field«, *Semicond. Sci. Technol.* **11** (1996) 1482.

F. Wolf et al., »Organization of the visual cortex«, *Nature* **382** (1996) 306.

1997

H.-U. Bauer, and T. Villmann, »Growing a hypercubical output space in a self-organizing feature map«, *IEEE Trans. Neur. Netw.* **8** (1997) 218.

H.-U. Bauer, D. Brockmann, and T. Geisel, »Analysis of ocular dominance pattern formation in a high-dimensional self-organizing-map model«, *Network* **8** (1997) 17.

H.-U. Bauer et al., »Analysis of SOM-based models for the development of visual maps«, in *Proceedings to the WSOM '97* (L. P. Oy ed.), Helsinki University of Technology (1997) 233.

H.-U. Bauer, and W. Schöllhorn, »Self-organizing maps for the analysis of complex movement patterns«, *Neural Processing Lett.* **5** (1997) 193.

D. Brockmann et al., »Conditions for the joint emergence of orientation and ocular dominance in a high-dimensional self-organizing map«, in *Proc. CNS 97* (J. Bower ed.) (1997).

D. Brockmann et al., »SOM-model for the development of oriented receptive fields and orientation maps from non-oriented ON-center OFF-center inputs«, in *Artificial Neural Networks - ICANN 97* (J.-D. Nicoud ed.), Springer (1997) 207.

K. Pawelzik et al., »Geometry of orientation preference map determines nonclassical receptive field properties«, in *Proc. ICANN 97* (1997).

M. Herrmann, H.-U. Bauer, and T. Villmann, »Topology preservation in neural maps«, in *ESANN 97* (1997) 205.

D. W. Hone, R. Ketzmerick, and W. Kohn, »Time Dependent Floquet Theory and Absence of an Adiabatic Limit«, *Phys. Rev. A* **56** (1997) 4045.

R. Ketzmerick et al., »What determines the spreading of a wave packet?« *Phys. Rev. Lett.* **79** (1997) 1959.

J. H. Smet et al., »Enhanced soft-wall effects for composite fermions in magnetic focusing and commensurability experiments«, *Physica E* **1** (1997) 153.

D. Springsguth, R. Ketzmerick, and T. Geisel, »Hall Conductance of Bloch Electrons in a Magnetic Field«, *Phys. Rev. B* **56** (1997) 2036.

1998

M. Bethge, K. Pawelzik, and T. Geisel, »Temporal Coding and Synfire Chains in Chaotic Networks«, in *Göttingen Neurobiology Report 1998, Proceedings of the 26th Göttingen Neurobiology Conference* (R. Wehner ed.), Thieme, **2** (1998) 757.

U. Ernst, K. Pawelzik, and T. Geisel, »Analysing the Context Dependence of Receptive Fields in Visual Cortex«, in *Perspectives in Neural Computing: ICANN 98* (T. Ziemke ed.), Springer-Verlag, **1** (1998) 343.

U. Ernst, K. Pawelzik, and T. Geisel, »Orientation preferences geometry modulates nonclassical receptive field properties«, in *New Neuroethology on the Move - Proceedings of the 26th Göttingen Neurobiology Conference* (R. Wehner ed.), Thieme (1998) 759.

U. Ernst, K. Pawelzik, and T. Geisel, »Delay-induced multistable synchronization of biological oscillators«, *Phys. Rev. E* **57** (1998) 2150.

U. Ernst et al., »Orientation contrast enhancement modulated by differential long-range interaction in visual cortex«, in *Computational Neuroscience: Trends in Research (CNS 97)*, Plenum Press (1998) 361.

J. Eroms et al., »Magnetotransport in large diameter InAs/GaSb antidot lattices«, *Physica B* **256-258** (1998) 409.

C. W. Eurich, U. Ernst, and K. Pawelzik, »Continuous Dynamics of Neuronal Delay

Adaption«, in *Perspectives in Neural Computing, International Conference on Artificial Neural Networks, ICANN 98* (T. Ziemke ed.), Springer-Verlag, **1** (1998) 355.

M. Herrmann, K. Pawelzik, and T. Geisel, »Self-Localization by Hidden Representations«, in *Proceedings for the 8th International Conference on Artificial Neural Networks, ICANN 98* (T. Ziemke ed.), Springer, **2** (1998) 1103.

M. Herrmann, K. Pawelzik, and T. Geisel, »Self-localization of a robot by simultaneous self-organization of place and direction selectivity«, in *Proceedings Second International Conference on Cognitive and Neural Systems, Boston 1998* (1998) 79.

R. Ketzmerick, K. Kruse, and T. Geisel, »Avoided Band Crossings: Tuning Metal-Insulator Transitions in Chaotic Systems«, *Phys. Rev. Lett.* **80** (1998) 137.

R. Ketzmerick et al., »A covering property of Hofstadter's butterfly«, *Phys. Rev. B* **58** (1998) 9881.

J. Lin et al., »Irregular synchronous activity in stochastically-coupled networks of integrate-and-fire neurons«, *Network* **9** (1998) 333.

S. Löwel et al., »The layout of orientation and ocular dominance domains in area 17 of strabismic cats«, *European Journal of Neuroscience* **10** (1998) 2629.

N. Mayer et al., »Orientation Maps From Natural Images«, in *Proceedings of the 26th Göttingen Neurobiology Conference* (R. Wehner ed.), Thieme, **2** (1998) 759.

N. Mayer et al., »A Cortical Interpretation of ASSOMs«, in *Proceedings of the 8th International Conference on Artificial Neural Networks, ICANN 98* (T. Ziemke ed.), Springer, **2** (1998) 961.

K. Pawelzik et al., »Orientation Preference Geometry Modulated Nonclassical Receptive Field Properties«, in *New Neuroethology on the Move - Proceedings of the 26th Göttingen Neurobiology Conference*, Georg-Thieme-Verlag (1998) 759.

H.-E. Plesser, »Noise turns Integrate-Fire Neuron into Bandpass Filter«, in *New Neuroethology on the Move, Proceedings of the 26th Göttingen Neurobiology Conference* (R. Wehner ed.), Thieme (1998) 760.

M. Riesenhuber et al., »Breaking Rotational Symmetry in a self-organizing map model for orientation map development«, *Neural Computation* **10** (1998) 717.

A. S. Sachrajda et al., »Fractal conductance fluctuations in a soft wall stadium and a Sinai Billiard«, *Phys. Rev. Lett.* **80** (1998) 1948.

- J. H. Smet et al., »Composite fermions in magnetic focusing and commensurability experiments«, *Physica B* **249** (1998) 15.
- T. Villmann, and M. Herrmann, »Magnification Control in Neural Maps«, in *European Symposium on Artificial Neural Networks, ESANN 98, D facto* (1998) 191.
- F. Wolf, and T. Geisel, »Spontaneous pinwheel annihilation during visual development«, *Nature* **395** (1998) 73.
- J. X. Zhong, and T. Geisel, »Level fluctuations in quantum systems with multifractal eigenstates«, *Phys. Rev. E* **59** (1998)
- 1999**
- H.-U. Bauer, M. Herrmann, and T. Villmann, »Neural Maps and topographic Vector Quantization«, *Neural Networks* **12** (1999) 659.
- D. Brockmann, and T. Geisel, »The Lévy-Flight Nature of Gaze Shifts«, in *Proceedings of the 27th Göttingen Neurobiology Conference* (U. Eysel ed.), Thieme, **1** (1999) 876.
- M. Diesmann, M.-O. Gewaltig, and A. Aertsen, »Stable Propagation of Synchronous Spiking in Cortical Neural Networks«, *Nature* **402** (1999) 529.
- T. Dittrich et al., »Spectral Statistics in Chaotic Systems with two Identical Connected Cells«, *J. Phys. A* **32** (1999) 6791.
- T. Dittrich et al., »Spectral correlations in Systems Undergoing a Transition from Periodicity to Disorder«, *Phys. Rev. E* **59** (1999) 6541.
- S. Dodel, J. M. Herrmann, and T. Geisel, »Components of brain activity - Data analysis for fMRI«, in *Proc. ICANN 99*, **2** (1999) 1023.
- B. Elattari, and T. Kottos, »One-dimensional Localization in the Presence of Resonances«, *Phys. Rev. B* **59** (1999) 5265.
- U. Ernst, »Struktur und Dynamik lateraler Wechselwirkungen im primären visuellen Kortex«, PhD thesis, MPI für Strömungsforschung, Göttingen (1999).
- U. Ernst, K. Pawelzik, and M. V. T. a. Sahar-Pikielny, »Relationships Between Cortical Maps and Receptive are Determined by Lateral Cortical Feedback«, in *Proceedings of the 27th Göttingen Neurobiology Conference*, Georg-Thieme-Verlag (1999) 168.
- U. Ernst et al., »Relation Between Retinotopical and Orientation Maps in Visual Cortex«, *Neural Computation* **11** (1999) 375.
- U. Ernst et al., »Theory of Nonclassical Receptive Field Phenomena in the Visual Cortex«, *Neurocomputing* **26-27** (1999) 367.
- J. Eroms et al., »Skipping orbits and enhanced resistivity in large-diameter InAs/GaSb antidotlattices«, *Phys. Rev. B* **59** (1999) 7829.
- C. W. Eurich, and U. Ernst, »Avalanches of Activity in a Network of Integrate-and-Fire Neurons with Stochastic Input«, in *Icann'99, Ninth International Conference on Neural Networks*, IEE Conference Publication No. 470 (1999) 545.
- C. W. Eurich et al., »Dynamics of Self-Organized Delay Adaptation«, *Phys. Rev. Lett.* **82** (1999) 1594.
- S. Grün et al., »Detecting Unitary Events without Discretization of Time«, *Journal of Neuroscience Methods* **94** (1999) 67.
- J. M. Herrmann, F. Emmert-Streib, and K. Pawelzik, »Autonomous robots and neuroethology: emergence of behavior from a sense of curiosity«, in *Proceedings of the 1st International Khepera Workshop* (U. Rückert ed.), HNI Verlagschriftenreihe, **64** (1999) 89.
- J. M. Herrmann, and K. Pawelzik, »Simultaneous self-organization of place and direction selectivity in a neural model of self-localization«, *Neurocomputing* **26-27** (1999) 721.
- J. M. Herrmann, K. Pawelzik, and T. Geisel, »Self-organization of predictive presentations«, in *Proc. ICANN 99* (1999) 186.
- W. Just, and H. Kantz, »Some Considerations on Poincaré Maps for Chaotic Flows«, *J. Phys. A* **33** (1999) 163.
- M. Kaschube et al., »The Variability of Orientation Maps in Cat Visual Cortex«, in *Proceedings of the International Conference on Artificial Neural Networks (ICANN99)* (A. Murray ed.), IEE, **1** (1999) 79.
- M. Kaschube et al., »Quantifying the Variability of Patterns of Orientation Columns in Cat's Area 17: Correlation-Lengths and Wavelengths«, in *Proceedings of the 27th Göttingen Neurobiology Conference*, Thieme, **1** (1999) 480.
- R. Ketzmerick, K. Kruse, and T. Geisel, »Efficient diagonalization of kicked quantum systems«, *Physica D* (1999) 247.
- T. Kottos, F. M. Izrailev, and A. Politi, »Finite-Length Lyapunov Exponents and Conductance for

- Quasi 1D disordered Solids«, *Physica D* **131** (1999) 155.
- T. Kottos, and U. Smilansky, »Periodic Orbit Theory and Spectral Statistics for Quantum Graphs«, *Annals of Physics* **274** (1999) 76.
- T. Kottos et al., »Chaotic Scattering of Microwaves«, *Radio Science* (1999)
- S. Löwel, and F. Wolf, »Pattern Formation in the Developing Visual Cortex«, in *Transport and Structure in Biophysics and Chemistry: Lecture Notes in Physics* (J. Parisi ed.), Springer Verlag (1999).
- N. Mayer, J. M. Herrmann, and T. Geisel, »Receptive field formation in BD cats depends on higher order statistics«, in *Proceedings of the 27th Göttingen Neurobiology Conference* (1999) 905.
- H.-E. Plesser, »Aspects of Signal Processing in Noisy Neurons«, PhD thesis, Universität Göttingen, Göttingen (1999).
- H.-E. Plesser, and T. Geisel, »Markov analysis of stochastic resonance in a periodically driven integrate-and-fire neuron«, *Phys Rev E* **59** (1999) 7008.
- H.-E. Plesser, and T. Geisel, »Bandpass Properties of Integrate-Fire Neurons«, *Neurocomputing* **26/27** (1999) 229.
- S. Rathjen et al., »Variability and Spatial Inhomogeneity of Patterns of Orientation Columns in Cat Striate Cortex«, in *Society for Neuroscience Abstracts* (1999) 278.
- S. Rotter, and M. Diesmann, »Exact Digital Simulation of Time-Invariant Linear Systems with Applications to Neuronal Modeling«, *Biol. Cyb.* **81** (1999) 381.
- O. Scherf, »Selbstorganisation neuronaler Strukturen durch Kooperation und Wettbewerb - Theorie der Bildung von Augendominanzmustern und Zeitreihenanalyse mit neuronalen Modellen«, PhD thesis, Johann-Wolfgang-Goethe-Universität, Frankfurt (1999).
- O. Scherf et al., »Theory of ocular dominance pattern formation«, *Phys. Rev. E* **59** (1999)
- F. Wolf, »Forschung und wissenschaftliches Rechnen«, (H. H. T. Plesser ed.), Gesellschaft für wissenschaftliche Datenverarbeitung, Göttingen (1999) 109.
- F. Wolf, and T. Geisel, »Pattern Formation in the Developing Visual Cortex: Topological Defects, their Generation, Motion, and Annihilation«, *Statistical Mechanics of Biocomplexity: Lecture Notes in Physics* **527** (1999) 174.
- 2000
- D. Bibitchkov, J. M. Herrmann, and T. Geisel, »Dynamics of associative memory networks with synaptic depression«, in *Proceedings of DYN 2000* (2000) 106.
- D. Bibitchkov, J. M. Herrmann, and T. Geisel, »Synaptic depression in associative memory networks«, in *Proceedings of the IJCNN 2000* (2000).
- D. Brockmann, and T. Geisel, »The ecology of gaze shifts«, *Neurocomputing* **32-33** (2000) 643.
- D. Cohen, F. Izrailev, and T. Kottos, »Wavepacket dynamics in energy space, RMT and quantum-classical correspondence«, *Phys. Rev. Lett.* **84** (2000) 2052.
- D. Cohen, and T. Kottos, »Quantum-mechanical non-perturbative response of driven chaotic mesoscopic systems«, *Phys. Rev. Lett.* **85** (2000) 4839.
- M. Diesmann, M.-O. Gewaltig, and A. Aertsen, »Analysis of spike synchronization in feed-forward cortical neural networks«, in *Society for Neuroscience Abstracts* (2000) 2201.
- T. Dittrich et al., »Classical and quantum transport in deterministic Hamiltonian ratchets«, *Ann.Phys., Leipzig* **9** (2000) 755.
- S. Dodel, J. M. Herrmann, and T. Geisel, »Comparison of temporal and spatial ICA in fMRI data analysis«, in *ICA 2000 Proceedings* (2000) 543.
- S. Dodel, J. M. Herrmann, and T. Geisel, »Localization of brain activity - blind separation for fMRI data«, *Neurocomputing* **32-33** (2000) 701.
- B. Elattari, and T. Kottos, »Effect of resonances on the transport properties of two-dimensional disordered systems«, *Phys. Rev. B* **62** (2000) 9880.
- U. Ernst et al., »Lateral Intracortical Interactions and Random Inhomogeneities: A Key to the Spontaneous Emergence of Cortical Maps in V1«, in *FENS Conference 2000* (2000).
- C. Eurich et al., »Delay Adaptation in the Nervous System«, *Neurocomputing* **32** (2000) 741.
- D. Fliegner, A. Retey, and J. A. M. Vermaseren, »A parallel version of form 3«, in *Proceedings of ACAT 2000* (2000).
- T. Geisel, R. Ketzmerick, and K. Kruse, »Quantum Chaos in Extended Systems: Spreading Wave Packets and Avoided Band Crossings«, in *New Directions in Quantum Chaos, Proceedings of Enrico Fermi School* (U. Smilansky ed.) (2000) 101.

- S. Grün, and M. Diesmann, »Evaluation of higher-order coincidences in multiple parallel processes«, in *Society for Neuroscience Abstracts* (2000) 2201.
- J. M. Herrmann, K. Pawelzik, and T. Geisel, »Learning predictive representations«, *Neurocomputing* **32-33** (2000) 785.
- B. Huckestein, R. Ketzmerick, and C. H. Lewenkopf, »Quantum transport through ballistic cavities: soft vs. hard quantum chaos«, *Phys. Rev. Lett.* **84** (2000) 5504.
- L. Hufnagel et al., »Metal-insulator transitions in the cyclotron resonance of periodic nanostructures due to avoided band crossings«, *Phys. Rev. B* **62** (2000) 15348.
- W. Just, »On the eigenvalue spectrum for time-delayed Floquet problems«, *Physica D* **142** (2000) 153.
- W. Just et al., »Influence of stable Floquet exponents on time-delayed feedback control«, *Phys. Rev. E* **61** (2000) 5045.
- M. Kaschube et al., »Building cortical architectures for peripheral and central vision«, in *Society for Neuroscience Abstracts*, **26** (2000) 1084.
- M. Kaschube et al., »Quantifying the Variability of Patterns of Orientation Domains in the Visual Cortex of Cats«, *Neurocomputing* **32-33** (2000) 415.
- M. Kaschube et al., »Cortical architectures for peripheral and central vision«, *European Journal of Neuroscience* **12** (2000) 488.
- R. Ketzmerick et al., »New class of eigenstates in generic Hamiltonian systems«, *Phys. Rev. Lett.* **85** (2000) 1214.
- R. Ketzmerick et al., »Bloch Electrons in a Magnetic Field - Why does Chaos send Electrons the Hard Way ?« *Phys. Rev. Lett.* **84** (2000) 2929.
- T. Kottos, and U. Smilansky, »Chaotic scattering on graphs«, *Phys. Rev. Lett.* **85** (2000) 968.
- K. Kruse, and F. Jülicher, »Actively contracting bundles of polar filaments«, *Phys. Rev. Lett.* **85** (2000) 1778.
- K. Kruse, R. Ketzmerick, and T. Geisel, »Quantum Chaos and Spectral Transitions in the Kicked Harper Model«, in *Statistical and Dynamical Aspects of Mesoscopic Systems. Proceedings of the XVI. Sitges Conference on Statistical Mechanics* (J. M. Rubi ed.), Springer, Berlin (2000) 47.
- S. Löwel et al., »Substantial genetic influence on visual cortical orientation maps«, in *Society for Neuroscience Abstracts*, **26** (2000) 820.
- S. Löwel et al., »Genetically controlled features of visual cortical orientation maps«, *European Journal of Neuroscience* **12** (2000) 127.
- N. Mayer, »Die Entwicklung rezeptiver Felder und neuronaler Karten im visuellen Kortex«, PhD thesis, Universität Göttingen, Göttingen (2000).
- N. Mayer, J. M. Herrmann, and T. Geisel, »The time course of the emergence of orientation selectivity«, in *European Journal of Neuroscience*, **12**, suppl. **11** (2000) 127.
- N. Mayer, J. M. Herrmann, and T. Geisel, »The Impact of Receptive Field Shape on Cortical Map Formation«, in *Proc. of the 7th Int. Conf. on Neur. Inf. Processing* (2000) 1443.
- N. Mayer, J. M. Herrmann, and T. Geisel, »Retinotopy and spatial phase in topographic maps«, *Neurocomputing 2000* **32-33** (2000) 447.
- A. Ossipov, T. Kottos, and T. Geisel, »Statistical properties of phases and delay times of the one-dimensional Anderson model with one open channel«, *Phys. Rev. B* **61** (2000) 11411.
- H. E. Plesser, and W. Gerstner, »Escape Rate Models for Noisy Integrate-and-Fire Neurons«, *Neurocomputing* **32-33** (2000) 219.
- H. E. Plesser, and W. Gerstner, »Noise in integrate-and-fire neurons: from stochastic input to escape rates.« *Neural Computation* **12** (2000) 367.
- A. Riehle et al., »Dynamical Changes and Temporal Precision of Synchronized Spiking Activity in Monkey Motor Cortex During Movement Preparation«, *Journal of Physiology (Paris)* **94** (2000) 569.
- H. Schanz, and U. Smilansky, »Periodic-orbit theory of Anderson localization on graphs«, *Phys. Rev. Lett.* **84** (2000) 1427.
- H. Schanz, and U. Smilansky, »Spectral Statistics for Quantum Graphs: Periodic Orbits and Combinatorics«, *Philosophical Magazine* **80** (2000)
- F. Schmüser, W. Just, and H. Kantz, »On the relation between coupled map lattices and kinetic Ising models«, *Phys. Rev. E* **61** (2000) 3675.
- M. Schnabel, and T. Wettig, »Fake symmetry transitions in lattice Dirac spectra«, *Phys. Rev. D* **62** (2000) 034501.
- D. Springsguth, »Spektrum und Transport für Bloch-Elektronen im Magnetfeld«, PhD thesis, Johann-Wolfgang-Goethe-Universität Frankfurt (2000).
- F. Steinbach et al., »Statistics of resonances and of delay times in quasiperiodic Schrödinger equa-

tions», *Phys. Rev. Lett.* **85** (2000) 4426.

T. Tetzlaff et al., »The prevalence of colinear contours in the real world«, *European Journal of Neuroscience* **12** (2000) 286.

M. Timme, T. Geisel, and F. Wolf, »System of unstable attractors induces desynchronization and attractor selection in neural networks with delayed interactions«, in *Society for Neuroscience Abstracts* (2000) 1969.

M. Timme, T. Geisel, and F. Wolf, »Unstable synchronization in networks of integrate-and-fire neurons«, *European Journal of Neuroscience* **12** (2000) 194.

M. Weiss, T. Kottos, and T. Geisel, »Scaling properties of one-dimensional Anderson models in an electric field: Exponential vs. factorial localization«, *Phys. Rev. B* **62** (2000) 1765.

M. Weiss, and T. Nilsson, »Protein sorting in the Golgi apparatus: A consequence of maturation and triggered sorting«, *FEBS Lett.* **486**, 2 **486** (2000) 2.

F. Wolf, and T. Geisel, »A general theory of pinwheel stability«, in *Society for Neuroscience Abstracts* (2000).

F. Wolf, and T. Geisel, »Are pinwheels essential?«, *European Journal of Neuroscience* **12** (2000) 75.

F. Wolf et al., »How can squint change the spacing of ocular dominance columns?«, *J. Physiol.* **94** (2000) 525.

2001

D. Bibitchkov, J. M. Herrmann, and T. Geisel, »Pattern and sequence storage with dynamic synapses«, in *28th Göttingen Neurobiology Conference, Göttingen*, Thieme Verlag (2001) 854.

D. Cohen, and T. Kottos, »Parametric dependent Hamiltonians, wavefunctions, random-matrix theory, and quantal-classical correspondence«, *Phys. Rev. E* **63** (2001) 36203.

M. Diesmann et al., »State Space Analysis of Synchronous Spiking in Cortical Neural Networks«, *Neurocomputing* **38-40** (2001) 565.

T. Dittrich, B. Mehlig, and H. Schanz, »Spectral Signatures of Chaotic Diffusion in Systems with and without Spatial Order«, *Physica E* **9** (2001) 494.

S. Dodel, J. M. Herrmann, and T. Geisel, »Emergent Neural Computational Architectures Based on Neuroscience - Towards Neuroscience-Inspired Computing. Lecture Notes in Computer

Science 2036«, (D. J. Willshaw ed.), Springer (2001) 39.

S. Dodel, J. M. Herrmann, and T. Geisel, »Temporal Versus Spatial PCA and ICA in Data Analysis for fMRI«, in *28th Göttingen Neurobiology Conference, Göttingen*, Thieme Verlag (2001) 897.

S. Dodel, M. Herrmann, and T. Geisel, »Is brain activity spatially or temporally correlated?«, *NeuroImage* **13** (2001) 110.

U. A. Ernst et al., »Intracortical Origin of Visual Maps«, *Nature Neuroscience* **4** (2001) 431.

M.-O. Gewaltig, M. Diesmann, and A. Aertsen, »Cortical Synfire-Activity: Configuration Space and Survival Probability«, *Neurocomputing* **38-40** (2001) 621.

M. O. Gewaltig, M. Diesmann, and A. Aertsen, »Propagation of cortical synfire activity: survival probability in single trials and stability in the mean«, *Neural Networks* **14** (2001) 657.

J. M. Herrmann, »Dynamical Systems for Predictive Control of Autonomous Robots«, *Theory in Biosciences* **120** (2001) 241.

L. Hufnagel, »Transport in Hamilton-Systemen: Von der Klassik zur Quantenmechanik«, PhD thesis, MPI für Strömungsforschung, Göttingen (2001).

L. Hufnagel et al., »Superballistic Spreading of Wave Packets«, *Phys. Rev. E* **64** (2001) 12301.

L. Hufnagel, R. Ketzmerick, and M. Weiss, »Conductance fluctuations of generic billiards: Fractal or isolated?«, *Europhys. Lett.* **54** (2001) 703.

M. Kaschube et al., »The prevalence of colinear contours in the real world«, *Neurocomputing* **38-40** (2001) 1335.

M. Kaschube et al., »2-D Analysis of Patterns of Ocular Dominance Columns in Cat Primary Visual Cortex«, in *28th Göttingen Neurobiology Conference, Göttingen*, Thieme Verlag (2001) 546.

M. Kaschube et al., »2-D Analysis of Ocular Dominance Patterns in Cat Primary Visual Cortex«, in *Society for Neuroscience Abstracts* (2001) 821.

R. Ketzmerick, L. Hufnagel, and M. Weiss, »Quantum Signatures of Typical Chaotic Dynamics«, *Adv. Sol. St. Phys.* **41** (2001) 473.

T. Kottos, and D. Cohen, »Failure of random matrix theory to correctly describe quantum dynamics«, *Phys. Rev. E* **64** (2001) 065202.

T. Kottos, and H. Schanz, »Quantum graphs: A

- model for Quantum Chaos«, *Physica E* **9** (2001) 523.
- K. Kruse, S. Camalet, and F. Jülicher, »Self-propagating Patterns in Active Filament Bundles«, *Phys. Rev. Lett.* **87** (2001) 138101.
- N. Mayer, J. M. Herrmann, and T. Geisel, »A Curved Feature Map Model of Visual Cortex«, in *28th Göttingen Neurobiology Conference, Göttingen*, Thieme Verlag (2001) 851.
- N. Mayer, J. M. Herrmann, and T. Geisel, »Signatures of Natural Image Statistics in Cortical Simple Cell Receptive Fields«, *Neurocomputing* **38-40** (2001) 279.
- A. Ossipov et al., »Quantum mechanical relaxation of open quasiperiodic systems«, *Phys. Rev. B* **64** (2001) 224210.
- K. Pichugin, H. Schanz, and P. Seba, »Effective Coupling for Open Billiards«, *Phys. Rev. E* **64** (2001) 056227.
- H. E. Plesser, and T. Geisel, »Stochastic resonance in neuron models: Endogenous stimulation revisited«, *Phys. Rev. E* **63** (2001) 031916.
- H. Schanz et al., »Classical and quantum Hamiltonian ratchets«, *Phys. Rev. Lett.* **87** (2001) 070601.
- M. Schnabel, F. Wolf, and T. Geisel, »Universal fine structure of orientation pinwheels«, in *Proceedings of the 28th Göttingen Neurobiology Conference*, Thieme, **1** (2001) 258.
- F. Steinbach, »Statistische Eigenschaften offener und geschlossener Quantensysteme: von Quantenchaos bis Quasiperiodizität«, PhD thesis, Georg-August-Universität, Göttingen (2001).
- T. Tetzlaff, T. Geisel, and M. Diesmann, »The ground state of synfire structures«, in *Proceedings of the 28th Göttingen Neurobiology Conference*, Thieme Verlag (2001) 260.
- M. Timme, T. Geisel, and F. Wolf, »Synchronization and Desynchronization in Neural Networks with General Connectivity«, in *Soc. Neurosci. Abstr.*, **27** (2001) 821.
- M. Timme, T. Geisel, and F. Wolf, »Mechanisms of synchronization and desynchronization in neural networks with general connectivity«, in *Proceedings of the 28th Göttingen Neurobiology Conference* (G. W. Kreuzberg ed.), **1** (2001) 595.
- M. Timme, F. Wolf, and T. Geisel, »Complex networks of pulse-coupled oscillators: Exact stability analysis of synchronous states«, in *WE-Heraeus Seminar »Synchronization in Physics and Neuroscience«* (2001).
- M. Timme, F. Wolf, and T. Geisel, »Unstable syn-
- chronization and switching among unstable attractors in spiking neural networks«, in *265. WE-Heraeus Seminar »Synchronization in Physics and Neuroscience«* (2001).
- M. Timme, F. Wolf, and T. Geisel, »Unstable attractors in networks of pulse-coupled oscillators«, in *Europhysics Conference Abstracts*, **25 F** (2001) 20.
- M. Timme, F. Wolf, and T. Geisel, »Unstable attractors in networks of biological oscillators«, in *European Dynamics Days 2001 - Book of Abstracts* (2001) 51.
- M. A. Topinka et al., »Coherent branched flow in a two-dimensional electron gas«, *Nature* **410** (2001) 183.
- M. Weiss, T. Kottos, and T. Geisel, »Taming chaos by impurities in two-dimensional oscillator arrays«, *Phys. Rev. E* **63** (2001) 056211.
- M. Weiss, T. Kottos, and T. Geisel, »Spreading and localization of wavepackets in disordered wires in a magnetic field«, *Phys. Rev. B* **63** (2001) R81306.

2002

- A. Bäcker et al., »Isolated resonances in conductance fluctuations and hierarchical states«, *Phys. Rev. E* **66** (2002) 016211.
- G. Berkolaiko, H. Schanz, and R. S. Whitney, »The Leading Off-Diagonal Correction to the Form Factor of Large Graphs«, *Phys. Rev. Lett.* **88** (2002) 104101.
- D. Bibitchkov, J. M. Herrmann, and T. Geisel, »Pattern storage and processing in attractor networks with short-time synaptic dynamics«, *Network: Comput. Neural Syst.* **13** (2002) 115.
- D. Bibitchkov, J. M. Herrmann, and T. Geisel, »Effects of short-time plasticity on the associative memory«, *Neurocomputing* **44-46** (2002) 329.
- D. Brockmann, and I. M. Sokolov, »Lévy Flights in External Force Fields: From Models to Equations«, *Chemical Physics* **284** (2002) 409.
- S. Dodel, J. M. Herrmann, and T. Geisel, »Functional Connectivity by Cross-Correlation Clustering«, *Neurocomputing* **44-46** (2002) 1065.
- C. W. Eurich, J. M. Herrmann, and U. A. Ernst, »Finite-size effects of avalanche dynamics«, *Phys. Rev. E* **66** (2002) 006137.
- R. Fleischmann, and T. Geisel, »Mesoscopic Rectifiers based on Ballistic Transport«, *Phys. Rev. Lett.* **89** (2002) 016804.

- S. Großkinsky, M. Timme, and B. Naundorf, »Universal Attractors of Reversible Aggregate-Reorganization Processes«, *Phys. Rev. Lett.* **88** (2002) 245501.
- S. Gruen, M. Diesmann, and A. Aertsen, »'Unitary Events' in Multiple Single Neuron Spiking Activity. II. Non-Stationary Data«, *Neural Computation* **14** (2002) 81.
- L. Hufnagel et al., »Eigenstates Ignoring Regular And Chaotic Phase-Space Structures«, *Phys. Rev. Lett.* **89** (2002) 154101.
- M. Kaschube et al., »Quantifying the Variability of Orientation Maps in Ferret Visual Cortex«, in *Society for Neuroscience Abstracts* (2002).
- M. Kaschube et al., »Building cortical architectures for central and peripheral vision«, in *FENS Abstr.*, **1** (2002) A051.13.
- M. Kaschube et al., »Genetic Influence on Quantitative Features of Neocortical Architecture«, *Journal of Neuroscience* **22** (2002) 7206.
- T. Kottos, and M. Weiss, »Statistics of Resonances and Delay Times: A Criterion for Metal-Insulator Transitions«, *Phys. Rev. Lett.* **89** (2002) 056401.
- K. Kruse, »A dynamic model for determining the middle of *Escherichia coli*«, *Biophys. J.* **82** (2002) 618.
- K. Kruse, and K. Sekimoto, »Growth of finger-like protrusions driven by molecular motors«, *Phys. Rev. E* **66** (2002) 031904.
- N. Mayer, J. M. Herrmann, and T. Geisel, »Curved Feature Metrics in Models of Visual Cortex«, *Neurocomputing* **44-46** (2002) 533.
- B. Naundorf, and J. Freund, »Signal detection by means of phase coherence induced through phase resetting«, *Phys Rev E* **66** (2002) 040901.
- A. Ossipov, T. Kottos, and T. Geisel, »Signatures of Prelocalized States in Classically Chaotic Systems«, *Phys. Rev. E* **65** (2002) 055209(R).
- M. Schnabel, T. Geisel, and F. Wolf, »Universal fine structure of orientation pinwheels«, in *Verhandlungen der Deutschen Physikalischen Gesellschaft* (2002).
- T. Tetzlaff, T. Geisel, and M. Diesmann, »The ground state of cortical feed-forward networks«, *Neurocomputing* **44-46** (2002) 673.
- M. Timme, F. Wolf, and T. Geisel, »Prevalence of Unstable Attractors in Networks of Pulse-Coupled Oscillators«, *Phys. Rev. Lett.* **89** (2002) 154105.
- M. Timme, F. Wolf, and T. Geisel, »Coexistence of Regular and Irregular Dynamics in Complex Networks of Pulse-Coupled Oscillators«, *Phys. Rev. Lett.* **89** (2002) 258701.
- M. Weiss, L. Hufnagel, and R. Ketzmerick, »Universal Power-Law Decay in Hamiltonian Systems?«, *Phys. Rev. Lett.* **89** (2002) 239401.
- F. Wolf et al., »Pronounced Variability of the Size of Cat Primary Visual Cortex«, in *Society for Neuroscience Abstracts* (2002).

2003

- G. Berkolaiko, H. Schanz, and R. S. Whitney, »Form Factor for a Family of Quantum Graphs«, *J. of Physics A* **36** (2003) 8373.
- D. Brockmann, »Superdiffusion in Inhomogeneous Scale-free Environments«, Where's George-August Universität, Göttingen (2003).
- D. Brockmann, and T. Geisel, »Particle Dispersion on Rapidly Folding Random Hetero-Polymers«, *Phys. Rev. Lett.* **91** (2003) 048303.
- D. Brockmann, and T. Geisel, »Lévy Flights in Inhomogeneous Media«, *Phys. Rev. Lett.* **90** (2003) 170601.
- D. Cohen, and T. Kottos, »Non-perturbative response: Chaos versus Disorder«, *J. of Phys. A: Math. and General* **36** (2003) 10151.
- S. Gruen, A. Riehle, and M. Diesmann, »Effect of cross-trial nonstationarity on joint-spike events«, *Biological Cybernetics* **88** (2003) 335.
- M. Kaschube et al., »Localizing the ticklish spots of cortical orientation maps«, in *2nd Symposium of the Volkswagen Stiftung »Dynamics and Adaptivity of Neuronal Systems - Integrative Approaches to Analyzing Cognitive Functions«* (2003).
- M. Kaschube et al., »The Pattern of Ocular Dominance Columns in Cat Primary Visual Cortex: Intra- and Interindividual Variability of Column Spacing and its Dependence on Genetic Background«, *European Journal of Neuroscience* **18** (2003) 3251.
- M. Kaschube et al., »Are orientation preference maps attractors of a developmental dynamics?« in *Society for Neuroscience Abstracts*, **29** (2003).
- T. Kottos, and D. Cohen, »Quantum irreversibility of energy spreading«, *Europhys. Lett.* **61** (2003) 431.
- T. Kottos, A. Ossipov, and T. Kottos, »Signatures of Classical Diffusion in Quantum Fluctuations of 2D Chaotic Systems«, *Phys. Rev. E* **68** (2003) 066215.

- T. Kottos, and U. Smilansky, »Quantum Graphs: A Simple Model for Chaotic Scattering«, *Journal of Physics A: Mathematical and General* **36** (2003) 3501.
- N. Mayer, J. M. Herrmann, and T. Geisel, »Shaping of Receptive Fields in Visual Cortex During Retinal Maturation«, *Journal of Computational Neuroscience* **15** (2003) 307.
- C. Mehring et al., »Activity dynamics and propagation of synchronous spiking in locally connected random networks«, *Biological Cybernetics* **88** (2003) 395.
- A. Ossipov, T. Kottos, and T. Geisel, »Fingerprints of classical diffusion in open 2D mesoscopic systems in the metallic regime«, *Europhys. Lett.* **62** (2003) 719.
- T. Prager, B. Naundorf, and L. Schimansky-Geier, »Coupled three-state oscillators«, *Physica A* **325** (2003) 176.
- H. Schanz, »Reaction Matrix for Dirichlet Billiards with Attached Waveguides«, *Physica E* **18** (2003) 429.
- H. Schanz, and T. Kottos, »Scars on Quantum Networks Ignore the Lyapunov Exponent«, *Phys. Rev. Lett.* **90** (2003) 234101.
- H. Schanz, M. Puhmann, and T. Geisel, »Shot noise in Chaotic Cavities from Action Correlations«, *Phys. Rev. Lett.* **91** (2003) 134101.
- M. Schnabel et al., »The ticklish spots of cortical orientation maps«, in *Proceedings of the 29th Göttingen Neurobiology Conference* (2003) 611.
- T. Tetzlaff et al., »The spread of rate and correlation in stationary cortical networks«, *Neurocomputing* **52-54** (2003) 949.
- M. Timme et al., »Pinwheel generation with shift-twist symmetry«, in *Society for Neuroscience Abstracts*, **29** (2003).
- M. Timme, F. Wolf, and T. Geisel, »Unstable attractors induce perpetual synchronization and desynchronization«, *Chaos* **13** (2003) 377.
- M. Weiss, L. Hufnagel, and R. Ketzmerick, »Can simple renormalization theories describe the trapping of chaotic trajectories in mixed systems?« *Phys. Rev. E* **67** (2003) 046209.
- F. Wolf, and T. Geisel, »Universality in Visual Cortical Pattern Formation«, *Journal of Physiology – Paris* **97** (2003) 253.
- 2004**
- D. Cohen, and T. Kottos, »Quantum dissipation due to the interaction with chaos«, *Phys. Rev. E* **69** (2004) 055201.
- M. Denker et al., »Breaking Synchrony by Heterogeneity in Complex Networks«, *Phys. Rev. Lett.* **92** (2004) 074103.
- M. C. Geisler et al., »Detection of a Landau Band-Coupling-Induced Rearrangement of the Hofstadter Butterfly«, *Phys. Rev. Lett.* **92** (2004) 256801.
- M. Hiller et al., »Quantum Reversibility: Is there an Echo«, *Phys. Rev. Lett.* **92** (2004) 010402.
- L. Hufnagel, D. Brockmann, and T. Geisel, »Forecast and Control of epidemics in a globalized world«, *PNAS* **101** (2004) 15124.
- M. Kaschube et al., »Sensitive locations in orientation preference maps«, in *Society for Neuroscience Abstracts*, **30** (2004).
- T. Kottos, and H. Schanz, »Statistical Properties of Resonance Width for Open Quantum Systems«, *Waves in Random Media* **14** (2004) S91.
- T. Kottos, and M. Weiss, »Current Relaxation in Nonlinear Random Media«, *Phys. Rev. Lett.* **93** (2004) 190604.
- K. Kreikemeier et al., »Large-scale reorganization of orientation preference maps in visual cortex (area 18) of adult cats induced by intracortical microstimulation (ICMS): an optical imaging study.« in *FENS Abstracts*, **2** (2004).
- K. Kreikemeier et al., »Space-time characteristics of orientation preference map (OPM) plasticity in visual cortex of adult cats induced by intracortical microstimulation (ICMS)«, in *Society for Neuroscience Abstracts*, **30** (2004).
- A. Ossipov, and T. Kottos, »Superconductor-proximity effect in hybrid structures: Fractality versus Chaos«, *Phys. Rev. Lett.* **92** (2004) 017004.
- K. F. Schmidt et al., »Plasticity of orientation preference maps in adult visual cortex: is there recovery?« in *FENS Abstracts*, **2** (2004).
- K. F. Schmidt et al., »Adult plasticity: long-term rearrangement of orientation maps in cat visual cortex«, in *Society for Neuroscience Abstracts*, **30** (2004).
- M. Schnabel et al., »Signatures of shift-twist symmetry in the layout of orientation preference maps«, in *Society for Neuroscience Abstracts*, **30** (2004).
- M. Timme, F. Wolf, and T. Geisel, »Topological

Speed Limits to Network Synchronization«, *Phys. Rev. Lett.* **92** (2004) 074101.

A. Zumdieck et al., »Long Chaotic Transients in Complex Networks«, *Phys. Rev. Lett.* **93** (2004) 244103.

2005

P. Ashwin, and M. Timme, »When instability makes sense«, *Nature* **436** (2005) 36.

D. Brockmann, L. Hufnagel, and T. Geisel, »Dynamics of Modern Epidemics«, in *SARS: A Case Study in Emerging Infections* (R. Weiss ed.), Oxford University Press (2005).

D. Cohen, T. Kottos, and H. Schanz, »Quantum pumping: The charge transported due to a translation of a scatterer«, *Phys. Rev. E* **71** (2005) 035202.

J. M. Herrmann, H. Schrobsdorff, and T. Geisel, »Localized activations in a simple neural field model«, *Neurocomputing* **65-66** (2005) 679.

M. Kaschube et al., »Orientation preference maps have sensitive spots«, in *Proceedings of the 30th Göttingen Neurobiology Conference* (2005).

M. Kaschube et al., »Interareal coordination of column development in cat visual cortex«, in *Society for Neuroscience Abstracts* (2005).

M. Kaschube et al., »Predicting sensitive spots in visual cortical orientation preference maps.« in *11th Magdeburg International Neurobiological Symposium »Learning and Memory: cellular and Systematic Views«* (2005).

K. Kreikemeier et al., »Space-time characteristics of orientation preference map (OPM) plasticity in visual cortex of adult cats«, in *Proceedings of the 30th Göttingen Neurobiology Conference* (2005).

A. Levina, J. M. Herrmann, and T. Geisel, »Dynamical Synapses Give Rise to a Power-Law Distribution of Neuronal Avalanches«, in *NIPS*2005* (2005).

A. Méndez-Bermúdez et al., »Trends in Electro-Optics Research«, Nova Science Publishers, Hauppauge (2005) 231.

B. Naundorf, T. Geisel, and F. Wolf, »Action potential onset dynamics and the response speed of neuronal populations«, *Journal of Computational Neuroscience* **18** (2005) 297.

B. Naundorf, T. Geisel, and F. Wolf, »Dynamical response properties of a canonical model for type-I membranes«, *Neurocomputing* **65** (2005) 421.

M. Puhmann et al., »Quantum decay of an open chaotic system: A semiclassical approach«, *Europhysics Letters* **69** (2005) 313.

H. Schanz, »Phase-Space Correlations of Chaotic Eigenstates«, *Phys. Rev. Lett.* **94** (2005) 134101.

H. Schanz, T. Dittrich, and R. Ketzmerick, »Directed chaotic transport in Hamiltonian ratchets«, *Phys. Rev. E* **71** (2005) 026228.

H. Schanz, and M. Prusty, »Directed chaos in a billiard chain with transversal magnetic field«, *Journal of Physics A: Mathematical and General* **38** (2005) 10085.

K. F. Schmidt et al., »Adult plasticity: Long-term changes of orientation maps in cat visual cortex«, in *Proceedings of the 30th Göttingen Neurobiology Conference* (2005).

K. F. Schmidt et al., »Adult plasticity: Activity-dependent short- and long-term changes of functional maps in cat visual cortex«, in *11th Magdeburg International Neurobiological Symposium »Learning and Memory: cellular and Systematic Views«* (2005).

M. Schnabel et al., »Signature of shift-twist Symmetry in the layout of orientation preference maps«, in *Proceedings of the 30th Göttingen Neurobiology Conference* (2005).

M. Schnabel et al., »Shift-twist Symmetry in natural images and orientation maps«, in *Society for Neuroscience Abstracts*, **31** (2005).

M. Voultzidou, S. Dodel, and J. M. Herrmann, »Neural Networks Approach to Clustering of Activity in fMRI Data«, *IEEE Trans. Med. Imaging* **12** (2005) 987.

M. Weiss, P. Ashwin, and M. Timme, »Unstable attractors: existence and robustness in networks of oscillators with delayed pulse coupling«, *Nonlinearity* **18** (2005) 2035.

F. Wolf, »Symmetry, Multistability, and Long-Range Interactions in Brain Development«, *Phys. Rev. Lett.* **95** (2005) 208701.

F. Wolf, »Symmetry Breaking and Pattern Selection in Visual Cortical Development«, in *École d'Été de Physique des Houches, 2003, Methods and Models in Neurophysics*, Elsevier, Amsterdam (2005) 575.

2006

D. Brockmann, L. Hufnagel, and T. Geisel, »The scaling laws of human travel«, *Nature* **439** (2006) 462.

M. Hiller et al., »Wavepacket Dynamics, Quantum

Reversibility and Random Matrix Theory», *Annals of Physics* **321** (2006) 1025.

J. A. Méndez-Bermúdez, T. Kottos, and D. Cohen, »Parametric invariant random matrix model and the emergence of multifractality«, *Physical Review E* **73** (2006) 036204.

B. Naundorf, F. Wolf, and M. Volgushev, »Unique features of action potential initiation in cortical neurons«, *Nature* **440** (2006) 1060.

M. Prusty, and H. Schanz, »Signature of Directed Chaos in the Conductance of a Nanowire«, *Phys. Rev. Let.* **96** (2006) 130601.

M. Schnabel et al., »Signatures of shift-twist symmetry in natural images and orientation maps«, in *FENS Abstracts* (2006).

M. Timme, T. Geisel, and F. Wolf, »Speed of synchronization in complex networks of neural oscillators: Analytic results based on Random Matrix Theory«, *Chaos* **16** (2006) 015108.

2.5.2 Dynamics of Complex Fluids (2003–2006)

2003

- J. Becker et al., »Complex dewetting scenarios captured by thin film models«, *Nature Materials* **2** (2003) 59.
- J. Buehrle, S. Herminghaus, and F. Mugele, »Interface profiles near three-phase contact lines in electric fields«, *Phys. Rev. Lett.* **91** (2003) 086101.
- H. M. Evans et al., »Structural polymorphism of DNA-dendrimer complexes«, *Phys. Rev. Lett.* **91** (2003) 075501.
- M.A.Z. Ewiss et al., »Molecular dynamics and alignment studies of silica-filled 4-pentyl-4'-cyanobiphenyl (5CB) liquid crystal«, *Liquid Crystals* **30** (2003) 1.
- D. Geromichalos et al., »Dynamic aspects of wetting in granular matter«, *Contact Angle Wettability and Adhesion* **3** (2003) 385.
- D. Geromichalos et al., »Mixing and condensation in a wet granular medium«, *Phys. Rev. Lett.* **90** (2003) 168702.
- S. Herminghaus, K. Jacobs, and R. Seemann, »Viscoelastic dynamics of polymer thin films and surfaces« *Eur. Phys. J. E* **12** (2003) 101.
- S. Herminghaus, »Harnessing the unstable«, *Nature Materials* **2** (2003) 11.
- A. Klingner, S. Herminghaus, and F. Mugele, »Self-excited oscillatory dynamics of capillary bridges in electric fields«, *Appl. Phys. Lett.* **82** (2003) 4187.
- C. Neto et al., »Satellite hole formation during dewetting: Experiment and simulation«, *J. Phys.: Condens. Matter* **15** (2003) 3355.
- C. Neto et al., »Correlated dewetting patterns in thin polystyrene films«, *J. Phys.: Condens. Matter* **15** (2003) 421.
- T. Pfohl et al., »Trends in microfluidics with complex systems«, *Chem. Phys. Chem.* **4** (2003) 1291.
- T. Pfohl and S. Herminghaus, »Mikrofluidik mit komplexen Flüssigkeiten«, *Physik Journal* **2** (2003) 35.
- M. Schulz, B. Schulz, and S. Herminghaus, »Shear-induced solid-fluid transition in a wet granular medium«, *Phys. Rev. E* **67** (2003) 052301.
- R. Seemann, »Zerreiprobe fr dnne Polymerfilme - Neue Erkenntnisse warum und wie dnne Flssigkeitsfilme aufbrechen«, *Chemie.de*, 19. August 2003.
- A. Thoss et al., »Kilohertz sources of hard x rays and fast ions with femtosecond laser plasmas.«, *Journal of the Optical Society of America - Optical Physics B* **20** (2003) 224.
- A.A.M. Ward et al., »Effect of cyclic deformations on the dynamic-mechanical properties of Silica-filled Butyl Rubber«, *Macromol. Mater. Eng.* **288** (2003) 971.
- A.A.M. Ward et al., »Studies on the dielectric behavior of Silica-filled Butyl Rubber Vulcanizates after cyclic deformation«, *J. of Macromol. Science B* **42** (2003) 1265.

2004

- B. Abel et al., »Characterization of extreme ultraviolet light-emitting plasmas from laser excited fluorine containing liquid polymer jet target« *J. Appl. Phys.* **95** (2004) 7619.
- A. Charvat et al., »New design for a time-of-flight mass spectrometer with a liquid beam laser desorption ion source for the analysis of biomolecules«, *Rev. Sci. Instrum.* **75** (2004) 1209.
- M. Chul Choi et al., »Ordered patterns of liquid crystal toroidal defects by microchannel confinement«, *Proceedings of the National Academy of Sciences of the USA (PNAS)* **101** (2004) 17340.
- S. Herminghaus, R. Seemann, and K. Landfester, »Polymer Surface Melting Mediated by Capillary Waves«, *Phys. Rev. Lett.* **93** (2004) 017801.
- M. Kohonen et al., »On Capillary Bridges in Wet Granular Materials«, *Physica A* **339** (2004) 7.
- A. Otten and S. Herminghaus: »How plants keep dry: a physicist's point of view«, *Langmuir* **20** (2004) 2405.
- M. Scheel, D. Geromichalos, and S. Herminghaus, »Wet granular matter under vertical agitation«, *J. Phys.: Condens. Matter* **16** (2004) 1.
- B. Struth et al., »Application of microfocussing at a none specific beamline«, *SRI 2003 Proceedings, AIP Conference Proceedings* **705** (2004) 804.

R. Weber et al., »Photoemission from aqueous alkali-iodine salt solutions, using EUV synchrotron radiation«, *J. Phys. Chem. B* **108** (2004) 4729.

B. Winter et al., »Full valence band photoemission from liquid water, using EUV synchrotron radiation«, *J. Phys. Chem. A* **108** (2004) 2625.

B. Winter et al., »Molecular structure of surface active salt solutions: photoelectron spectroscopy and molecular dynamics simulations of aqueous Tetrabutyl-Ammonium Iodide«, *J. Phys. Chem. B* **108** (2004) 14558.

M.A. Zaki Ewiss et al., »Wetting behaviour of 5CB and 8CB and their binary mixtures above the isotropic transition«, *Liquid Crystals* **31** (2004) 557.

2005

B. Abel et al., »Applications, features, and mechanistic aspects of liquid water beam desorption mass spectrometry«, *International Journal of Mass Spectrometry* **243** (2005) 177.

A. Ahmad et al., »New multivalent cationic lipids reveal bell curve for transfection efficiency versus membrane charge density: lipid-DNA complexes for gene delivery«, *Journal of Gene Medicine* **7** (2005) 739.

J.-C. Baret et al., »Electroactuation of Fluid Using Topographical Wetting Transitions«, *Langmuir* **21** (2005) 12218.

M. Brinkmann, J. Kierfeld, and R. Lipowsky, »Stability of liquid channels or filaments in the presence of line tension«, *J. Phys. Condens. Matter* **17** (2005) 2349.

T. v. Dorfmüller et al., Bergmann-Schaefer: *Lehrbuch der Experimentalphysik: Gase, Nanosysteme, Flüssigkeiten*, 2. Aufl, Hrsg. v. K. Kleineremanns, Walter de Gruyter -Verlagsgruppe, Berlin 2005.

K. Ewert et al., »Cationic lipid-DNA complexes for non-viral gene therapy: relating supramolecular structures to cellular pathways«, *Expert Opinion on Biological Therapy* **5** (2005) 33.

A. Fingerle, S. Herminghaus, and V. Zaboradaev, »Kolmogorov-Sinai Entropy of the Dilute Wet Granular Gas«, *Phys. Rev. Lett* **95** (2005) 198001.

Z. Fournier et al., »Mechanical properties of wet granular materials«, *J. Phys.: Condens. Matter* **17** (2005) S477.

P. Heinig and D. Langevin, »Domain shape relax

ation and local viscosity in stratifying foam films«, *Eur. Phys. J. E* **18** (2005) 483.

S. Herminghaus, »A Generic Mechanism of Sliding Friction between Charged Soft Surfaces«, *Phys. Rev. Lett.* **95** (2005) 264301.

S. Herminghaus (edtr.), *J. Phys.: Condens. Matter* **17** (2005) (special issue on wetting).

S. Herminghaus, »Dynamics of wet granular matter«, *Advances in Physics* **54** (2005) 221.

K. Jacobs, R. Seemann, and H. Kuhlmann« Trendbericht: Mikrofluidik« *Nachrichten aus der Chemie* **53** (2005) 302 (eingeladener Beitrag).

S. Köster et al., »Microaligned collagen matrices by hydrodynamic focusing: controlling the pH-induced self-assembly«, *MRS Proceedings* **898E** (2005) 0989-L05-21.

S. Köster, D. Steinhäuser, T. Pfohl, »Brownian motion of actin filaments in confining microchannels«, *J. Phys.: Condens. Matter* **17** (2005) S4091.

R. Lipowsky et al., »Droplets, bubbles, and vesicles at chemically structured surfaces«, *J. Phys. Condens. Matter* **17** (2005) S537.

R. Lipowsky et al., »Wetting, budding, and fusion-morphological transitions of soft surfaces«, *J. Phys. Condens. Matter* **17** (2005) S2885.

F. Mugele et al., »Electrowetting: A Convenient Way to Switchable Wettability Patterns«, *J. Phys.: Condens. Matter* **17** (2005) S559.

A. Otten et al., »Microfluidics of soft matter investigated by small angle x-ray scattering«, *Journal of Synchrotron Radiation* **12** (2005) 745.

R. Seemann et al., »Wetting morphologies at microstructured surfaces«, *Proc. Natl. Acad. Sci. USA* **102** (2005) 1848.

R. Seemann et al., »Dynamics and structure formation in thin polymer melt films«, *J. Phys.: Condens. Matter* **17** (2005) S267.

B. Winter et al., »Effect of bromide on the interfacial structure of aqueous tetrabutylammonium iodide: Photoelectron spectroscopy and molecular dynamics simulations«, *Chemical Physics Letters* **410** (2005) 222.

B. Winter et al., »Electron Binding Energies of Aqueous Alkali and Halide Ions: EUV Photoelectron Spectroscopy of Liquid Solutions and Combined Ab Initio and Molecular Dynamics Calculations«, *J. Am. Chem. Soc.* **127** (2005) 2703.

2006

S. Arscott et al., »Capillary filling of miniaturized sources for electrospray mass spectrometry«, *J. Phys.: Condens. Matter* **18** (2006) S677.

Ch. Bahr, »Surfactant-induced nematic wetting layer at a thermotropic liquid crystal/water interface«, *Phys. Rev. E* **73** (2006) 030702(R).

J.-C. Baret and M. Brinkmann, »Wettability control of droplet deposition and detachment«, *Phys. Rev. Letters* **96** (2006) 146106.

V. Designolle et al., »AFM study of defect-induced depressions of the smectic-A/air interface«, *Langmuir* **22** (2006) 362.

R. Dootz et al., »Evolution of DNA compaction in microchannels«, *J. Phys.: Condens. Matter* **18** (2006) S639.

R. Dootz et al., »Raman and surface enhanced Raman microscopy of microstructured PEI/DNA multilayers«, *Langmuir* **22** (2006) 1735.

K. Ewert et al., »A columnar phase of dendritic lipid-based cationic liposome-DNA complexes for gene delivery: hexagonally ordered cylindrical micelles embedded in a DNA honeycomb lattice«, *Journal of the American Chemical Society* **128** (2006) 3998.

M. Fischer, P. Heinig and P. Dhar, »The viscous drag of spheres and filaments moving in membranes or monolayers«, to appear in *J. Fluid. Mech* (2006).

C. Lutz et al., »Surmounting Barriers: The Benefit of Hydrodynamic Interactions«, *Europhys. Lett.* **74** (2006) 719.

C. Priest, S. Herminghaus, and R. Seemann, »Generation of monodisperse gel emulsions in a microfluidic device«, *Applied Physics Letters* **88** (2006) 024106.

M. Schmiedeberg and H. Stark, »Superdiffusion in a Honeycomb Billiard«, *Phys. Rev. E.* **73** (2006) 031113.

R. Seemann et al., »Freezing of Polymer Thin Films and Surfaces: The Small Molecular Weight Puzzle«, to appear in *J. Pol. Sci. B* (2006).

R. Seemann, S. Herminghaus, and K. Jacobs, »Structure Formation in thin Liquid Films: Interface Forces Unleashed«, to appear in *Springer, Heidelberg, New York* (2006)

B. Winter and M. Faubel, »Photoemission from liquid aqueous solutions«, *Chemical Reviews* **106** (2006) 1176.

B. Winter et al., »Electron binding energies of hydrated H₃O⁺ and OH⁻: Photoelectron spectroscopy of aqueous acid and base solutions combined with electronic structure calculations«, *Journal of the American Chemical Society* **128** (2006) 3864.

2.5.3 Fluid Dynamics, Pattern Formation and Nanobiocomplexity (2003–2006)

2003

A.M. Crawford, N. Mordant, and E. Bodenschatz, »Comment on Dynamical Foundations of Nonextensive Statistical Mechanics«, arXiv: physics/0212080 (2003).

K.E. Daniels and E. Bodenschatz, »Statistics of Defect Motion in Spatiotemporal Chaos in Inclined Layer Convection«, *Chaos* **13** (2003) 55.

K.E. Daniels, R.J. Wiener, and E. Bodenschatz, »Localized Transverse Bursts in Inclined Layer Convection«, *Phys. Rev. Lett.* **91**, (2003) 114501.

B.L. Sawford et al., »Conditional and Unconditional Acceleration Statistics in Turbulence«, *Phys. Fluids* **15** (2003) 3478.

2004

K.E. Daniels, C. Beck, and E. Bodenschatz, »Defect Turbulence and Generalized Statistical Mechanics«, *Physica D* **193** (2004) 208.

C. Huepe et al., »Statistics of Defect Trajectories in Spatio-Temporal Chaos in Inclined Layer Convection and the Complex Ginzburg-Landau Equation«, *Chaos* **14** (2004) 864.

S. Luther, J. Rensen, and S. Guet, »Aspect Ratio Measurement Using a Four-Point Fiber-Optical Probe«, *Exp. Fluids* **36** (2004) 326.

N. Mordant, A.M. Crawford, and E. Bodenschatz, »Experimental Lagrangian Acceleration Probability Density Function Measurement«, *Physica D* **193** (2004) 245.

N. Mordant, A.M. Crawford, and E. Bodenschatz, »Three-Dimensional Structure of Lagrangian Acceleration in Turbulent Flows«, *Phys. Rev. Lett.* **93** (2004) 214501.

D.S. Rhoads et al., »Using Microfluidic Channel Networks to Generate Gradients for Studying Cell Migration«, In *Cell Migration: Developmental Methods and Protocols* (J.-L. Guan, ed.), Humana Press, Totowa, NJ **294** (2004) 347.

E.A. Variano, E. Bodenschatz, and E.A. Cowen, »A Random Synthetic Jet Array Driven Turbulence Tank«, *Exp. Fluids* **37** (2004) 613.

C. Voelz and E. Bodenschatz, »Experiments with Dictyostelium Discoideum Amoebae in Different

Geometries«, in *Dynamics and Bifurcation of Patterns in Dissipative Systems* G. Dangelmayr and I. Oprea (eds.), World Scientific Series on Nonlinear Science **12**, World Scientific (Singapore) (2004) 372.

T. Walter, E. Bodenschatz, and W. Pesch, »Dislocation Dynamics in Rayleigh-Bénard Convection«, *Chaos* **14** (2004) 933.

2005

M.M. Afonso and D. Vincenzi, »Non Linear Elastic Polymers in Random Flow«, *J. Fluid Mech.* **540** (2005) 99.

J. Bluemink et al., »Asymmetry Induced Particle Drift in Rotational Flow«, *Phys. Fluids* **17** (2005) 072106.

A.M. Crawford, N. Mordant, and E. Bodenschatz, »Joint Statistics of the Lagrangian Acceleration and Velocity in Fully Developed Turbulence«, *Phys. Rev. Lett.* **94** (2005) 024501.

S. Guet, S. Luther, and G. Ooms, »Bubble Shape and Orientation Determination with a Four-Point Optical Fiber Probe«, *Exp. Therm. Fluid Sci.* **29** (2005) 803.

R.F. Katz, R. Ragnarsson, and E. Bodenschatz, »Tectonic Microplates in a Wax Model of Sea-Floor Spreading«, *New J. Phys.* **7** (2005) 37.

R.F. Katz and E. Bodenschatz, »Taking Wax for a Spin: Microplates in an Analog Model of Plate Tectonics«, *Europhysics News* **5** (2005) 155.

S. Luther et al., »Data Analysis for Hot-Film Anemometry in Turbulent Bubbly Flow«, *Exp. Therm. Fluid Sci.* **29** (2005) 821.

H. Nobach, K. Chang, and E. Bodenschatz, »Transformation von zeitlichen in räumliche Statistiken - zwei Alternativen zur Taylor-Hypothese«. Tagungsband 13. Fachtagung »Lasermethoden in der Strömungsmesstechnik«, 6.-8. Sept. 2005, Cottbus.

H. Nobach et al., »Full-Field Correlation-Based Image Processing for PIV«, Proc. 6th International Symposium on Particle Image Velocimetry, Pasadena, California, USA, September 21-23, 2005.

J. Rensen et al., »Hot-Film Anemometry in Two Phase Flows I: Bubble-Probe Interaction«,

- Int. J. Multiphase Flow* **31** (2005) 285.
J. Rensen, S. Luther, and D. Lohse, »The Effect of Bubbles on Developed Turbulence«, *J. Fluid Mech.* **548** (2005) 153.
- A.M. Reynolds et al., »On the Distribution of Lagrangian Accelerations in Turbulent Flows«, *New J. Phys.* **7** (2005) 58.
- B. Utter, R. Ragnarsson, and E. Bodenschatz, »Experimental Apparatus and Sample Preparation Techniques for Directional Solidification«, *Rev. Sci. Instr.* **76** (2005) 013906.
- B. Utter and E. Bodenschatz, »Double Dendrite Growth in Solidification«, *Phys. Rev. E* **72** (2005) 011601.
- T.H. van der Berg et al., »Drag Reduction in Bubbly Taylor-Couette Turbulence«, *Phys. Rev. Lett.* **94** (2005) 044501.
- H. Varela et al., »Transitions to Electrochemical Turbulence«, *Phys. Rev. Lett.* **94** (2005) 174104.
- H. Varela et al., »A Hierarchy of Global Coupling Induced Cluster Patterns? During the Oscillatory H₂-Electrooxidation Reaction on a Pt Ring-Electrode«, *Phys. Chem. Chem. Phys.* **7** (2005) 2429.
- T.H. van der Berg, S. Luther, and D. Lohse, »Energy Spectra in Microbubbly Turbulence«, *Phys. Fluids* **18** (2006) 038103.
- T.H. van der Berg et al., »Bubbly Turbulence«, *J. of Turbulence* **7** (2006) 1.
- H. Xu et al., »High Order Lagrangian Velocity Statistics in Turbulence«, *Phys. Rev. Lett.* **96** (2006) 024503.
- D. Vincenzi et al., »Statistical Closures for Homogeneous Shear Flow Turbulence of Dilute Polymer Solutions«, in *Progress in Turbulence 2 - Springer Proceedings in Physics* **109** (2006) in press.
- N.T. Ouellette et al., »An Experimental Study of Turbulent Relative Dispersion«, *New J. Phys.* (2006), in press
- H. Xu, N.T. Ouellette, and E. Bodenschatz, »Multifractal Dimension of Lagrangian Turbulence«, International Collaboration for Turbulence Research, *Phys. Rev. Lett.* **96** (2006) 114503.
- 2006**
- M. Bourgoin et al., »The Role of Pair Dispersion in Turbulent Flow«, *Science* **311** (2006) 835.
- A. Celani, A. Mazzino, and D. Vincenzi, »Magnetic Field Transport and Kinematic Dynamo Effect: A Lagrangian Interpretation«, *Proc. R. Soc. A* **462** (2006) 137.
- S. Luther and J. Rensen, »Hot-Film Anemometry in Two Phase Flows II: Local Phase Discrimination«, to appear in *Int. J. Multiphase Flow* (2006).
- N.T. Ouellette, H. Xu, and E. Bodenschatz, »A Quantitative Study of Three-Dimensional Lagrangian Particle Tracking Algorithms«, *Exp. Fluids* **40** (2006) 301.
- N.T. Ouellette et al., »Small-Scale Anisotropy in Lagrangian Turbulence«, *New J. Phys.* (2006) in press.
- L. Song et al., »Dictyostelium Discoideum Chemotaxis: Threshold for Directed Motion«, in press in *Eur. J. Cell Biol.* (2006).
- R. Toegel, S. Luther, and D. Lohse, »Viscosity Destabilizes Bubbles«, *Phys. Rev. Lett.* **96** (2006) 114301.

2.5.4 Associated Scientists

2.5.4.1 PD Dr. Reinhard Schinke (2003–2006)

2003

B. Abel et al., »Comment on 'Rate coefficients for photoinitiated NO₂ unimolecular decomposition: energy dependence in the threshold regime'«, *Chem. Phys. Lett.* **368** (2003) 252.

T. Azzam et al., »The bound state spectrum of HOBr up to the dissociation limit: Evolution of saddle-node bifurcations«, *J. Chem. Phys.* **118** (2003) 9643.

D. Babikov et al., »Quantum origin of an anomalous isotope effect in ozone formation«, *Chem. Phys. Lett.* **372** (2003) 686.

D. Babikov et al., »Metastable states of ozone calculated on an accurate potential energy surface«, *J. Chem. Phys.* **118** (2003) 6298.

D. Babikov et al., »Formation of ozone: Metastable states and anomalous isotope effect«, *J. Chem. Phys.* **119** (2003) 2577.

P. Fleurat-Lessard et al., »Theoretical investigation of the temperature dependence of the O + O₂ exchange reaction«, *J. Chem. Phys.* **118** (2003) 610.

P. Fleurat-Lessard et al., »Isotope dependence of the O + O₂ exchange reaction: Experiment and theory«, *J. Chem. Phys.* **119** (2003) 4700. [Erratum: **120** (2004) 4993].

S. Yu. Grebenshchikov, »Van der Waals states in ozone and their influence on the threshold spectrum of O₃(X¹A₁). I. Bound states«, *J. Chem. Phys.* **119** (2003) 6512.

S. Yu. Grebenshchikov, R. Schinke, and W. L. Hase, »State-specific dynamics of unimolecular dissociation«, in *Comprehensive Chemical Kinetics*, **39** Unimolecular Kinetics, Part 1. The Reaction Step, N. J. B. Green, ed. (Elsevier, Amsterdam, 2003).

M. V. Ivanov, and R. Schinke, »Two-dimensional neutral donors in electric fields«, *J. Phys.: Condensed Matter* **15** (2003) 5909.

V. Kurkal, P. Fleurat-Lessard, and R. Schinke, »NO₂: Global potential energy surfaces of the ground (²A₁) and the first excited (²B₁) electronic states«, *J. Chem. Phys.* **119** (2003) 1489.

L. Poluyanov, and R. Schinke, »Theory of Molecular Bound States including $\Sigma - \pi$ Vibronic Interaction«, *Chem. Phys.* **288** (2003) 123.

Z.-W. Qu, H. Zhu, and R. Schinke, »The ultra-violet photodissociation of ozone revisited«, *Chem. Phys. Lett.* **377** (2003) 359.

R. Schinke, P. Fleurat-Lessard, and S. Yu. Grebenshchikov, »Isotope dependence of the lifetime of ozone complexes formed in O + O₂ collisions«, *Phys. Chem. Chem. Phys.* **5** (2003) 1966.
R. Siebert, and R. Schinke, »The vibrational spectrum of cyclic ozone«, *J. Chem. Phys.* **119** (2003) 3092.

M. Tashiro, and R. Schinke, »The effect of spin-orbit coupling in complex forming O(³P) + O₂ collisions«, *J. Chem. Phys.* **119** (2003) 10186.

K.-L. Yeh et al., »A time-dependent wave packet study of the O + O₂ ($v = 0, j = 0$) exchange reaction«, *J. Phys. Chem. A* **107** (2003) 7215.

2004

S. F. Deppe et al., »Resonance spectrum and dissociation dynamics of ozone in the ³B₂ electronically excited state: Experiment and theory«, *J. Chem. Phys.* **121** (2004) 5191.

M. V. Ivanov, and R. Schinke »Two-dimensional analogs of the H₂⁺ ion in stationary electric fields«, *Phys. Rev. B* **69** (2004) 165308-1.

M.V. Ivanov, S. Yu. Grebenshchikov, and R. Schinke »Intra- and intermolecular energy transfer in highly excited ozone complexes«, *J. Chem. Phys.* **120** (2004) 10015.

M. Joyeux, R. Schinke, and S. Yu. Grebenshchikov »Semiclassical dynamics of the van der Waals states in O₃(X¹A₁)«, *J. Chem. Phys.* **120** (2004) 7426.

Z.-W. Qu et al., »The Huggins band of ozone: Unambiguous electronic and vibrational assignment«, *J. Chem. Phys.* **120** (2004) 6811.

Z.-W. Qu, »The Huggins band of ozone: A theo-

retical analysis», *J. Chem. Phys.* **121**, (2004) 11731.

R. Schinke, and P. Fleurat-Lessard »On the transition-state region of the $O(^3P) + O_2(^3\Sigma_g^-)$ potential energy surface«, *J. Chem. Phys.* **121** (2004) 5789.

R. Schinke, »Quantum mechanical studies of photodissociation dynamics using accurate global potential energy surfaces«, In *Conical Intersections: Electronic Structure, Dynamics and Spectroscopy*, W. Domcke ed. (2004) 473.

H. Zhu et al., »On spin-forbidden processes in the ultra-violet photodissociation of ozone«, *Chem. Phys. Lett.* **384** (2004) 45.

2005

L. Adam et al., »Experimental and theoretical investigation of the reaction $NH(X^3\Sigma) + H(^2S) \rightarrow N(^4S) + H_2(X^1\Sigma^+)$ «, *J. Chem. Phys.* **122** (2005) 114301-1.

W. L. Hase, and R. Schinke »Role of computational chemistry in the theory of unimolecular reaction rates«, In *Theory and Applications of Computational Chemistry: The first 40 years*, C.E. Dykstra et al. eds. (Elsevier, New York, 2005) 397.

M. V. Ivanov, and R. Schinke, »Temperature dependent energy transfer in Ar – O₃ collisions«, *J. Chem. Phys.* **122** (2005) 234318-1.

M. Joyeux et al., »Intramolecular dynamics along isomerization and dissociation pathways«, *Adv. Chem. Phys.* **130** (2005) 267.

K. Mauersberger et al., »Assessment of the ozone isotope effect«, *Adv. Atom. Mol. and Opt. Phys.* **50** (2005) 1.

Z.-W. Qu et al., »Experimental and theoretical investigation of the reactions $NH(X^3\Sigma) + D(^2S) \rightarrow ND(X^3\Sigma) + H(^2S)$ and $NH(X^3\Sigma) + D(^2S) \rightarrow N(^4S) + HD(X^1\Sigma^+)$ «, *J. Chem. Phys.* **122** (2005) 204313-1.

Z.-W. Qu. et al., »The photodissociation of ozone in the Hartley band: A theoretical analysis«, *J. Chem. Phys.* **123** (2005) 074305-1.

Z.-W. Qu, H. Zhu, and R. Schinke, »Infrared spectrum of cyclic ozone: A theoretical investigation«, *J. Chem. Phys.* **123** (2005) 204324-1.

Z.-W. Qu et al., »The triplet channel in the photodissociation of ozone in the Hartley band: Classical trajectory surface hopping analysis«, *J. Chem. Phys.* **122** (2005) 191102-1.

R. Schinke, and P. Fleurat-Lessard, »The effect of

zero-point energy differences on the isotope dependence of the formation of ozone: A classical trajectory study.

J. Chem. Phys. **122** (2005) 094317.

H. Zhu et al., »The Huggins band of ozone. Analysis of hot bands«, *J. Chem. Phys.* **122** (2005) 024310-1.

2006

S. C. Farantos et al., »Reaction paths and elementary bifurcation tracks: the diabatic 1B_2 -state of ozone«, *International Journal of Bifurcation and Chaos*, in press.

S. Yu Grebenshchikov et al., »Absorption spectrum and assignment of the Chappuis band of ozone«, submitted to *J. Chem. Phys.*, in press.

M. V. Ivanov, and R. Schinke, »Recombination of ozone via the chaperon mechanism«, *J. Chem. Phys.* **124** (2006) 104303-1.

L. Lammich et al., »Electron-impact dissociation and transition properties of a stored LiH_2^- beam«, *European J. Physics*, to be published.

R. Schinke et al., »Dynamical studies of the ozone isotope effect: A status report«, *Ann. Rev. Phys. Chem.* **57** (2006).

2.5.4.2 PD Dr. Folkert Müller-Hoissen (2003–2006)

2003

A. Dimakis, and F. Müller-Hoissen, »Riemannian geometry of bicovariant group lattices«, *J. Math. Phys.* **44** (2003) 4220.

A. Dimakis, and F. Müller-Hoissen, »Differential geometry of group lattices«, *J. Math. Phys.* **44** (2003) 1781.

A. Dimakis, and F. Müller-Hoissen, »Functional representations of integrable hierarchies«, Nlin.SI/0603018.

A. Dimakis, and F. Müller-Hoissen, »Functional representations of derivative NLS hierarchies«, Nlin.SI/0603048.

2004

A. Dimakis, and F. Müller-Hoissen, »Automorphisms of associative algebras and non-commutative geometry«, *J. Phys. A: Math. Gen.* **37** (2004) 2307.

A. Dimakis, and F. Müller-Hoissen, »Extension of noncommutative soliton hierarchies«, *J. Phys. A: Math. Gen.* **37** (2004) 4069.

A. Dimakis, and F. Müller-Hoissen, »Explorations of the extended ncKP hierarchy«, *J. Phys. A: Math. Gen.* **37** (2004) 10899.

A. Dimakis, and F. Müller-Hoissen, »Differential calculi on quantum spaces determined by automorphisms«, *Czech. J. Phys.* **54** (2004) 1235.

A. Dimakis, and F. Müller-Hoissen, »Extension of Moyal-deformed hierarchies of soliton equations«, in XI International Conference Symmetry Methods in Physics, C. Burdik, O. Navratil and S. Posta (eds.), *Joint Institute for Nuclear Research* (Dubna) (2004).

2005

A. Dimakis, and F. Müller-Hoissen, »An algebraic scheme associated with the noncommutative KP hierarchy and some of its extensions«, *J. Phys. A: Math. Gen.* **38** (2005) 5453.

A. Dimakis, and F. Müller-Hoissen, »Algebraic identities associated with KP and AKNS hierarchies«, *Czech. J. Phys.* **55** (2005) 1385.

A. Dimakis, and F. Müller-Hoissen, »Nonassociativity and integrable hierarchies«, Nlin.SI/0601001.

3. Services and Infrastructure

THE SERVICE GROUPS of the institute are headed by the Institute Manager relieving the Board of Directors and its Managing Director from a range of management tasks. The Institute Manager and her team are supporting the scientific departments and ensure that all staff and guests enjoy an excellent research environment. Next to financial affairs, human resources, grant administration, and coordination with the central administration, the Institute Management is in charge of the library, the information technology services, the facility management including machine and electronics shops, and all outreach activities.



Figure 1:
MPIDS at Bunsenstr.

3.1 Design and Engineering

BASED ON THE requests from scientific departments the mechanical design group develops and engineers solutions for scientific apparatuses. The group uses the most advanced software tools that allow the design of complex parts in three dimensions. This includes the three-dimensional assembly and simulation of the assembled components. Once the technical design has been finished, technical drawings are generated or the design is directly entered into the CAD engine that generates instruction sets that are understood by the CNC-machines.

The design group works in tight collaboration with the electronics shop that designs all electrical components including digital and analog electronics. The design group also certifies in collaboration with the mechanical and electronic shop the conformity of the apparatuses with the European and German laws.

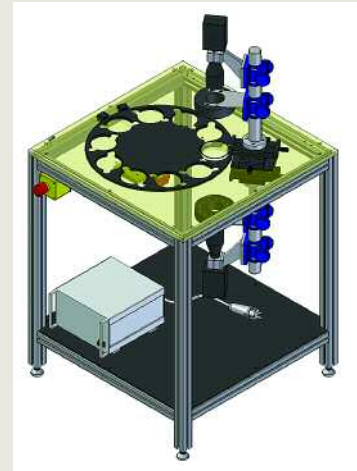
New parts and electronics are manufactured in the respective workshop. The machine shop also assembles components and appa-

tuses. It is equipped with conventional as well as computer controlled lathes, milling and EDM (electrical discharge) machines. The associated metalshop manufactures frames and other large metal parts, and it has state of the art welding equipment for handling steel and aluminum.

The machine and electronics shops are also responsible for the maintenance and repair of the existing machines and apparatuses. In addition, the staff provides a one-week course that trains graduate students and scientists in the safe use of the Research Shop. This ranges from basic tasks like drilling, cutting, tapping, or filing to the advanced use of modern machinery like that of milling machines, and a computer controlled lathe. Upon successful completion of the course the person may work independently in the Research Workshop. The institute is also training a total of six apprentices in the machine and electronics shop.



1. Design



2. Manufacturing



3. The apparatus



4. Installation



5. Ready for science

Figure 2: From Design to laboratory use.

3.2 Computing Facilities and IT-Services

THE CENTRAL IT service group maintains a variety of centralized resources and fulfills the IT needs of the institute. Examples are network infrastructure, user and security management, centralized software distribution and installation, and the implementation and management of high availability file servers. Each department operates their own computing facilities that are tailored to their specific applications and thus allow the flexibility of small organisational units and a rapid response to changing scientific needs. Furthermore information technology proliferates all areas, from administration and public relations, over the design and manufacture in the institute’s workshops, to teaching, communication, and outreach – computer based services and equipment are utilized throughout and need installation, integration and management.

A special focus of the IT service group is to maintain the IT infrastructure of tomorrow. The implementation of the most modern server technology often requires a tight col-



laboration with the software and hardware manufacturers. In addition, the thermal load from compute clusters is steadily increasing due to ever increasing densities of components. The IT-group is meeting this challenge by tailoring in collaboration with an outside company the next generation air-conditioned server racks.

Figure 3: 64bit HPC Linux cluster with HA AIX file server in air-conditioned racks. The systems shown provide 112 CPUs, 872GB RAM and more than 25TB disk space

3.3 Facility Management

THE MEMBERS OF the facility management team are in charge of all technical and infrastructural issues. They are supporting the departments during the installation of special experimental equipment or constructions and care for the unobstructed handling of all facilities. Special challenges on manpower arise from the fact that with the new experimental hall at the Fassberg additional maintenance is necessary until the move in 2009. In addition, the guesthouses will be renovated and modernized in the years to come.



Figure 4: Members of the MPIDS Facility Management Team

3.4 Administration



Figure 5: Members of the MPIDS Administration Team

THE ADMINISTRATION SUPPORTS all departments in performing their personal and financial management tasks. This includes: purchasing, accounting and bookkeeping, contract management, payroll accounting, calculation of travel expenses, administration of sponsored research and the management of 10 guest apartments and 14 guestrooms within 3 guesthouses. To perform these tasks the administration is using modern office tools such as SAP.

3.5 Library

THE LIBRARY OF the institute provides researchers, guests and visitors with all necessary printed and online accessible information focusing on the main research topics of

the institute. Due to the fact that the Max Planck Institute for Dynamics and Self-Organization has been founded only in November 2004 as the successor of the 80-year old Max Planck Institute for Flow Research, the existing inventory mainly contains literature from the former institute and some books even have antiquarian value. Due to the upcoming move of the institute the inventory of the library will be included into the Otto Hahn Library at the Max Planck Campus as soon as the Library extension of the Otto Hahn Library has been built.

Currently the institute library together with the library of the department »Nonlinear Dynamics« contains more than 7,700 volumes, subscribes to 24 printed research journals, and is part of the Max Planck electronic library system. The library is supported by a bookbinding shop.

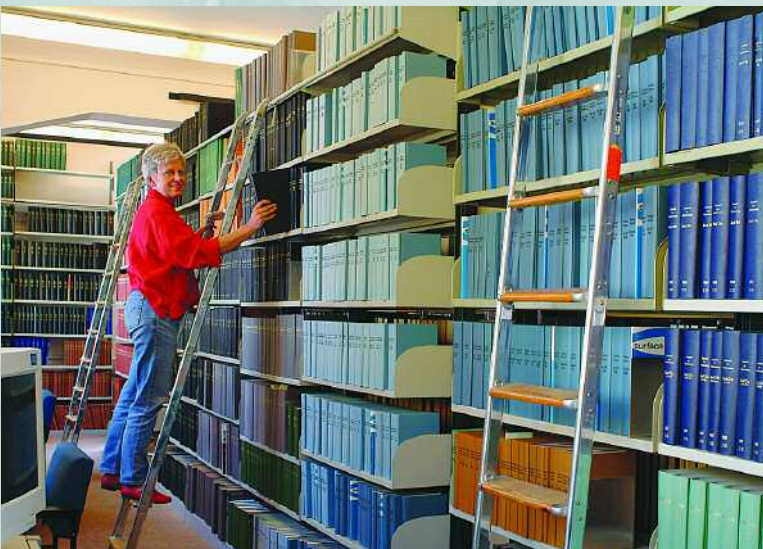


Figure 6: MPIDS Institute Library

3.6 Outreach Activities

ALL DEPARTMENTS OF the institute value highly the dissemination of their research results to the general public both locally and at the national/international level. Major findings are highlighted in internationally distributed press releases that are usually coordinated with the central press office of the Max Planck Society.

The answer is then published together with a picture and a short introduction of the corresponding scientist. Previous published »Frag' den Wissenschaftler« questions and answers can be found at the website of the journal <http://www.extratip-goettingen.de/fraeg-den-wissenschaftler.html> and that of the institute.

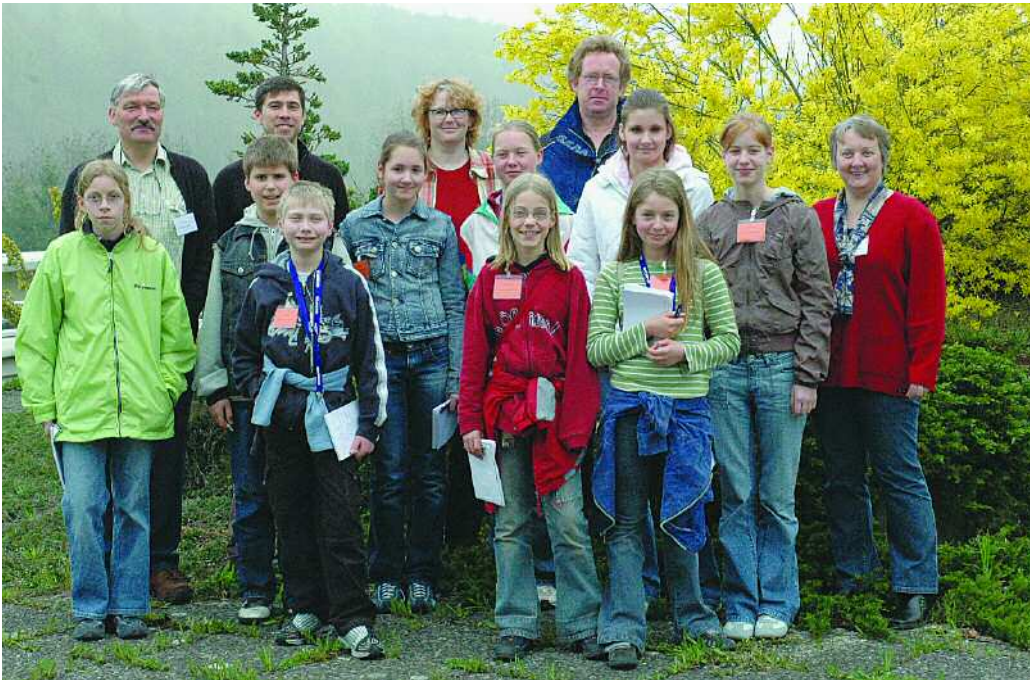


Figure 7:
MPIDS Girl's Days,
April 2006

The institute is also actively reaching out to the local community with multiple activities. We initiated the column »Frag' den Wissenschaftler« (Ask the Scientist) in cooperation with the weekly regional newsprint and advertising paper *Extra Tip*. The Extra Tip is distributed every Sunday free of charge to 190,000 households in the larger Göttingen area. Since January 2006 »Frag' den Wissenschaftler« has been published weekly. The general public (typically students from Grade 7–13) can ask questions about topics from science in general. A scientist from the institute (or other Göttinger research institutions) answers the question at a simple but precise

To better inform young people about science, the institute offers internships to students from local high-schools and to undergraduates that come from Germany and abroad. The institute also regularly participates in the worldwide initiative Girl's Day. In 2006 for the first time, a special one-day program had been offered and 10 girls and boys, mainly children of staff members, had the opportunity to inform themselves about different jobs within the machine shops, the bookbinding shop, the administration, and the research laboratories.

On an international level the institute is participating in the »Science Tunnel«, which is a travelling science exhibition about today's search for new knowledge. The show was developed by the Max Panck institutes under the leadership of the Max Planck Society. Two »identical« double pendula were built next to each other. To give the same initial conditions the pendula can be held by a magnetic switch and released. After they are released it is very simple to observe the difference in their motion and the chaotic behavior. The machine shop and the electronic shop built the apparatus that can be easily operated by the visitors of the show. In 2005 the Science Tunnel was exhibited in Miraka

(Japan, National Museum of Emerging Science and Innovation, September 16th to November 17th 2005) and now is displayed in Singapore (Singapore Science Center, March 24th to June 18th 2006) and later in Shanghai (Shanghai Science and Technology Museum, August 11th to October 8th 2006).

As international contacts and research stays at foreign institutions are an important part of the everyday life of today's scientist, »networking« is important. The MPIDS is part of an initiative that is establishing an ALUMNI network using the novel IT-tools of the public relation office of the Max Planck Society. This will allow an easier maintenance of the contacts to its former members.

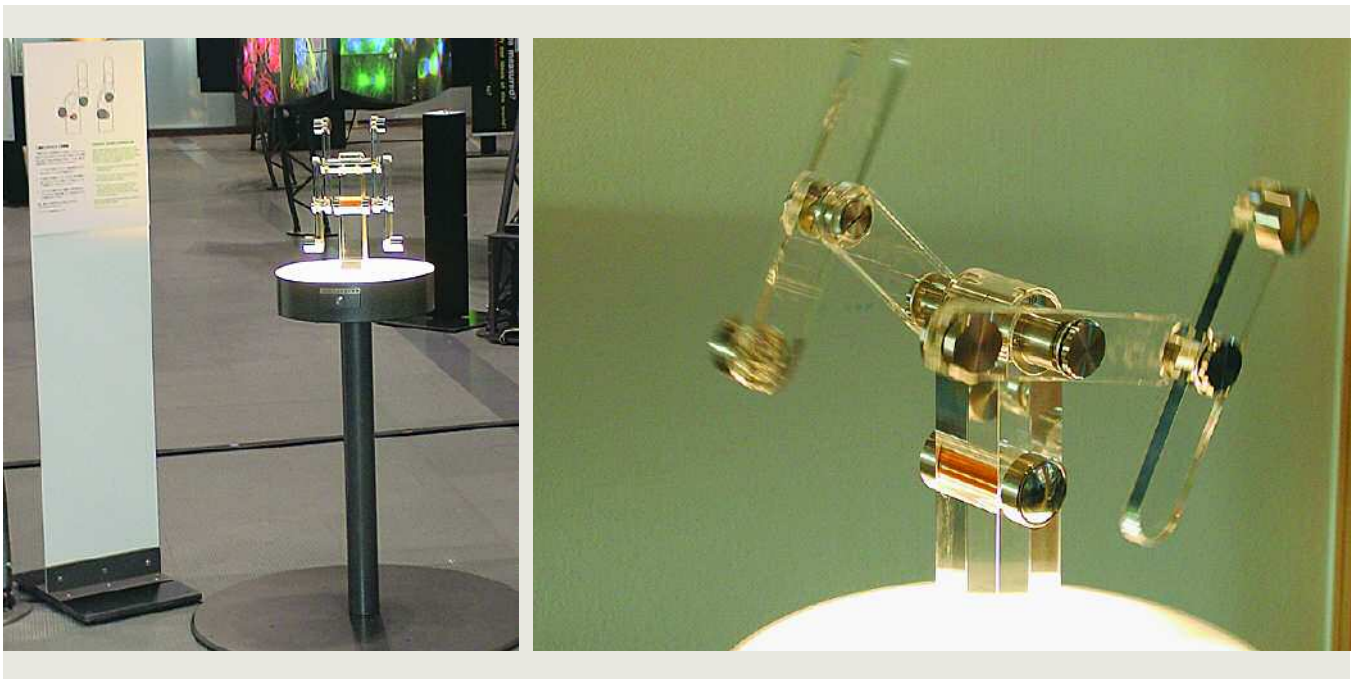


Figure 8 a,b:
»MPIDS - Double Pendula«
at the Science Tunnel
Exhibition 2005

How to get to the Max Planck Institute for Dynamics and Self-Organization

Location 1



Bunsenstraße 10
D - 37073 Göttingen

Departments: Nonlinear Dynamics (Prof. Geisel)
Dynamics of Complex Fluids (Prof. Herminghaus)

Services: Institute Management, Administration, Facility Management, Electronic and
Mechanic Workshop, IT-Services, Library, Outreach Office, Stock Rooms, Lecture
Hall, and Guest Houses.

By plane

From **Frankfurt am Main Airport** (FRA): Use the railway station at the airport. Trains to Göttingen (direct or via Frankfurt main station) leave twice an hour during daytime (travel time: 2 hours).

From **Hanover Airport** (HAJ): Take the suburban railway (S-Bahn) to the Central Station (»Hannover Hauptbahnhof«). From here direct ICE trains to Göttingen depart every 1/2 hour.

By train

Göttingen Station is served by the following ICE routes: Hamburg-Göttingen-Munich, Hamburg-Göttingen-Frankfurt, and Berlin-Göttingen-Frankfurt.

From Göttingen railway station:

From the Göttingen station you can take a Taxi (5 minutes) or walk (20 minutes). If you walk, you need to leave the main exit of the station and walk to the right. Follow the main street, which after the traffic lights turns into Bürgerstraße. Keep walking until you come to the Bunsenstraße. Turn right – you will reach the entrance gate of the MPIDS after about 300m.

By car

Leave the freeway A7 (Hanover-Kassel) at the exit »Göttingen«, which is the southern exit. Follow the direction »Göttingen Zentrum« (B3). After about 4 km you will pass through a tunnel. At the next traffic light, turn right (direction »Eschwege« B27) and follow the »Bürgerstraße« for about 600 m. The fourth junction to the right is the »Bunsenstraße«. You will reach the institute's gate after about 300m.

Location 2



Am Faßberg 17
D - 37077 Göttingen

Department: Fluid Dynamics, Pattern Formation and Nanobiocomplexity
(Prof. Bodenschatz)

Services: Experimental Hall, Clean Room, and Cell Biology Laboratories.

By plane

From **Frankfurt am Main Airport** (FRA): Use the railway station at the airport. Trains to Göttingen (direct or via Frankfurt main station) leave twice an hour during daytime (travel time: 2 hours).

From **Hanover Airport** (HAJ): Take the suburban railway (S-Bahn) to the Central Station (»Hannover Hauptbahnhof«). From here direct ICE trains to Göttingen depart every 1/2 hour.

By train

Göttingen Station is served by the following ICE routes: Hamburg-Göttingen-Munich, Hamburg-Göttingen-Frankfurt am Main, and Berlin-Göttingen-Frankfurt.

From Göttingen railway station:

On arrival at Göttingen station take a Taxi (15 minutes) or the bus (35 minutes). At platform A take the bus No. 8 (direction: »Geismar-Süd«) or No 13 (direction: »Weende-Ost/Papenberg«). At the second stop »Groner Straße« change to bus No. 5 (direction »Nikolausberg« and get off at the »Faßberg« stop, which is directly in front of the entrance of the Max Planck Campus (MPISDS and MPI for Biophysical Chemistry). Ask at the gate to get directions.

By car

Leave the freeway A7 (Hanover-Kassel) at the exit »Göttingen-Nord«, which is the northern of two exits. Follow the direction for Braunlage (B 27). Leave town – after about 1.5 km at the traffic light (Chinese restaurant on your right) turn left and follow the sign »Nikolausberg«. The third junction on the left is the entrance to the Max Planck Campus (MPIDS and MPI for Biophysical Chemistry). Ask at the gate to get directions.